



THE HONG KONG  
POLYTECHNIC UNIVERSITY

香港理工大學

Pao Yue-kong Library

包玉剛圖書館

---

## Copyright Undertaking

This thesis is protected by copyright, with all rights reserved.

**By reading and using the thesis, the reader understands and agrees to the following terms:**

1. The reader will abide by the rules and legal ordinances governing copyright regarding the use of the thesis.
2. The reader will use the thesis for the purpose of research or private study only and not for distribution or further reproduction or any other purpose.
3. The reader agrees to indemnify and hold the University harmless from and against any loss, damage, cost, liability or expenses arising from copyright infringement or unauthorized usage.

### IMPORTANT

If you have reasons to believe that any materials in this thesis are deemed not suitable to be distributed in this form, or a copyright owner having difficulty with the material being included in our database, please contact [lbsys@polyu.edu.hk](mailto:lbsys@polyu.edu.hk) providing details. The Library will look into your claim and consider taking remedial action upon receipt of the written requests.

**The Hong Kong Polytechnic University**

**Department of Building Services Engineering**

**Experimental and Simulation Study of Spatial  
Distribution of Human Respiratory Droplets under  
Typical Indoor Air Distribution Patterns**

**Li Xiaoping**

**A thesis submitted in partial fulfillment of the requirements for  
the Degree of Doctor of Philosophy**

**March, 2012**

## **Certificate of Originality**

I hereby declare that this thesis is my own work and that, to the best of my knowledge and belief, it reproduces no material previously published or written, nor material that has been accepted for the award of any other degree or diploma, except where due acknowledgement has been made in the text.

\_\_\_\_\_ (Signed)

Li Xiaoping (Name of student)

Department of Building Services Engineering

The Hong Kong Polytechnic University

Hong Kong SAR, China

March, 2012

## **Abstract**

Abstract of thesis entitled: Experimental and Simulation Study of Spatial  
Distribution of Human Respiratory Droplets under  
Typical Indoor Air Distribution Patterns

Submitted by : Li Xiaoping

For the degree of : Doctor of Philosophy

at The Hong Kong Polytechnic University in March, 2012.

The outbreaks of epidemic and pandemic viral infections, including severe acute respiratory syndrome (SARS) in 2003 and H1N1 during 2009 and 2010, create serious threats to human well-being both mentally and physically, and also result in huge economic losses throughout the world. It is reported that ventilation system processes strong relationships with the transmission and spread of some infectious diseases. Questions remain on whether the three typical air distribution methods, mixing ventilation (MV), under-floor air distribution (UFAD), and displacement ventilation (DV), can have significant differences in reducing the transmission of infectious diseases between occupants in a space.

This study therefore aims to develop some fundamental understandings on infection control in indoor environments with different air distribution systems. Dispersion of exhaled droplets released from normal breathing and coughing is investigated with

the intention to generalize the approaches in mitigating infectious diseases transmission for various breathing maneuvers. This work mainly consists of four parts: 1) an experimental study of distributions of artificially generated droplets in a DV ventilated full-scale chamber, 2) numerical estimations of droplet dispersion and co-occupant's exposure when human respiratory droplets are introduced into room air by nose-breathing or coughing at different intensities under MV, UFAD, and DV, 3) assessments of co-occupant's exposure level when the infected person coughs at different orientations to the co-occupant, including face-to-face, bending the head down, and turning the body around; and with two physical blockings, namely mouth covering and desk partition, under the three ventilation schemes, 4) numerical investigation on the performances of two types of personalized ventilation (PV) devices, i.e. a chair-based PV and a desk-mounted PV, on the co-occupant's exposure under MV and DV at different PV use conditions.

From the experimental study, it is found that the human related parameters, including breathing mode, breathing air temperature, and heat load of human body, play important roles on contaminant distribution and personal exposure for the exposed person. In order to ensure a lower exposure level, systematic and deliberate investigations must be conducted to fully assess the combined effects of these influencing parameters on contaminant distribution. The numerical study of nose-breathed droplets gives the same conclusion as the experiment that larger exhaled droplets under DV can travel farther horizontally and may pose higher risk for the co-occupant. However, lower inhaled fraction can be ensured for smaller droplets in

stratified ventilation system since the upward air movement can transport the exhaled droplets to the space above the breathing level.

The numerical study on coughed droplets reveals that there are two distinctive infection transmission stages, a first direct exposure stage initiated by the high momentum coughing jet and a second indirect exposure stage caused by indoor air movement. Sitting/standing in the traveling area of the coughing jet may result in higher direct exposure and higher total inhaled dose irrespective of the ventilation systems in place. Here, stratified ventilation does not help in lowering the first stage exposure. Coughing at a lower velocity, bending the head down, turning the body around, covering a cough, or blocking the coughed airflow by desk partition can all relieve the co-occupant from the direct exposure and consequently reduce the total inhaled dose. However, their effects in reducing personal exposure vary with ventilation systems. A preferred air distribution method in reducing infection transmission can not be easily identified, and detailed analysis is needed case by case. Overall, these personal and physical interventions have limited influences on the second stage exposure level under MV, while dramatic effects can be observed for stratified ventilation systems, especially for DV.

The numerical simulation on personalized ventilation (PV) system concludes that the type of PV device plays an essential role in indoor infection control. A well-designed PV system can ensure better inhaled air quality for all kinds of PV operation conditions, especially under stratified ventilation system, while higher

personal exposure may be induced if the PV supplying air enhances the mixing of exhaled droplets with room air. It is therefore important to conduct detailed analysis regarding to the effects of preferred PV system on infection transmission prior to implementation.

## **List of publications**

### **Journal publications**

1. Li X P, Niu J L, and Gao N P (2011) Spatial distribution of human respiratory droplet residuals and exposure risk for the co-occupant under different ventilation methods, HVAC&R Research, 17:4, 432-445.
2. Li X P, Niu J L, and Gao N P (2012) Co-occupant's exposure of expiratory droplets – effects of mouth covering, HVAC&R Research,18:4, 575-587
3. Li X P, Niu J L, and Gao N P (2012) Characteristics of physical blocking on co-occupant's exposure to respiratory droplet residuals, Journal of Central South University,19:3, 645-650
4. Li X P, Niu J L, and Gao N P (2012) Co-occupant's exposure with two types of personalized ventilation strategies under mixing and displacement ventilation systems, INDOOR AIR, DOI:10.1111/INA.12005

### **Conference publications**

1. Li X P, Niu J L, and Gao N P (2010) Respiratory Droplet Residual Distribution: Effects of Air Distribution Methods on Exposure. Proceedings of the Clima 2010 conference in Antalya. Antalya, Turkey.
2. Li X P, Niu J L, and Gao N P (2010) Particles Movement under Different Air Distributions - Impacts on Co-occupant's inhalation. ASHRAE IAQ 2010: Airborne Infection Control - Ventilation, IAQ & Energy. Kuala Lumpur, Malaysia.
3. Li X P, and Niu J L (2011) Effects of Mouth Coverings on Co-occupant's exposure under Different Ventilation Systems. 12<sup>th</sup> International Conference on Indoor Air Quality & Climate. Austin, Texas.
4. Li X P, and Niu J L (2011) Numerical Study of Physical Blocking's Performance on Occupant's Exposure to Respiratory Droplets under Mixing Ventilation System. ROOMVENT 2011. Trondheim, Norway.

## **Acknowledgements**

This project was partially funded by the Research Grants Council (RGC) of the Hong Kong SAR government under project No. PolyU5265/08E. The support from RGC is acknowledged.

Special acknowledgments should be given to my supervisor, Prof. Niu Jianlei, for his indispensable guidance, uncountable advices and invaluable opinions throughout the studies. I would also like to express my deep gratitude to Prof. Niu for his continuous support and kindness when I am pregnant, and making it possible for me to finish my studies in time. I feel lucky to be one of his Ph.D students.

I am particularly indebted to my co-supervisor, Dr. Gao Naiping, for his continuous encouragements and support throughout the course of my research work during the past three years for which I am very grateful.

I also wish to thank Mr. Hung Kit for his assistance in the using of measurement instruments, and Mr. Leung Chun-sing and Mr. Fung Wing-kwong for their help in the experimental work.

Thanks my group members: Dr. Liu Xiaoping, Mr. Cheng Yuanda, Mr. He Qibin, Mr. Huang Yu, Ms. Zhang Shuo, Ms. Xia Qian, and Ms. Hu Rong for many interesting discussions in studies and cheers they bring to my life.

Finally, I would like to dedicate this thesis to my husband, Dr. Zhang Weifeng of ICCAS, my daughter, Cheryl, and my parents.

## Table of contents

<b>Certificate of Originality .....</b>	<b>I</b>
<b>Abstract .....</b>	<b>II</b>
<b>List of publications .....</b>	<b>VI</b>
<b>Acknowledgements .....</b>	<b>VII</b>
<b>Table of contents.....</b>	<b>IX</b>
<b>List of Figures .....</b>	<b>XV</b>
<b>List of Tables.....</b>	<b>XXIV</b>
<b>Nomenclature.....</b>	<b>XXV</b>
<b>Chapter 1 Introduction .....</b>	<b>1</b>
<b>1.1 Background .....</b>	<b>1</b>
<b>1.2 Objectives .....</b>	<b>5</b>
<b>1.3 Structure of the thesis .....</b>	<b>5</b>
<b>Chapter 2 Literature Review.....</b>	<b>8</b>
<b>2.1 Introduction .....</b>	<b>8</b>
<b>2.2 Aerodynamics of breathing air.....</b>	<b>9</b>
<b>2.3 Properties of respiratory droplets.....</b>	<b>11</b>
2.3.1 Size distributions of respiratory droplets.....	12
2.3.2 Composition of respiratory droplets.....	15
2.3.3 Evaporation of respiratory droplets.....	16

2.3.4 Viability of pathogens in respiratory droplets .....	18
<b>2.4 Transmission modes of diseases via respiratory droplets.....</b>	<b>21</b>
<b>2.5 General routes to mitigate infectious disease transmission .....</b>	<b>25</b>
2.5.1 Antiviral drugs and vaccines .....	25
2.5.2 Physical interventions.....	25
2.5.3 Ultraviolet Germicidal Irradiation (UVGI) .....	28
2.5.4 Ventilation system.....	31
2.5.5 Personalized ventilation (PV).....	34
<b>2.6 Numerical simulation models .....</b>	<b>39</b>
2.6.1 Governing equations for indoor air movement .....	39
2.6.2 Governing equation for particle dispersion .....	41
2.6.3 Governing equation for particle deposition.....	45
<b>2.6.4 Evaluation indices.....</b>	<b>48</b>
<b>2.7 Importance of present study.....</b>	<b>50</b>
<b>2.8 Summary .....</b>	<b>51</b>
<b>Chapter 3 Experimental Studies of Droplet Dispersion in a Room</b>	
<b>with Displacement Ventilation System .....</b>	<b>53</b>
<b>3.1 Introduction .....</b>	<b>53</b>
<b>3.2 Material and methods .....</b>	<b>54</b>
3.2.1 Experimental chamber.....	54
3.2.2 Experimental equipments .....	56
3.2.3 Experimental design .....	59
<b>3.3 Results.....</b>	<b>61</b>

3.3.1 Air temperature distribution .....	61
3.3.2 Background particle concentrations .....	63
3.3.3 Horizontal dispersion of released particles.....	63
3.3.4 Vertical distribution of particles .....	66
3.3.5 Personal exposure for the co-occupant.....	74
<b>3.4 Summary .....</b>	<b>77</b>

## **Chapter 4 Numerical Studies of the Dispersion of Droplets**

### **Released during Nose-breathing and Coughing Processes .....80**

<b>4.1 Validation of numerical models .....</b>	<b>80</b>
4.1.1 Isothermal condition with an average particle size of 10 $\mu\text{m}$ .....	82
4.1.2 Non-isothermal condition with a mean particle size of 0.7 $\mu\text{m}$ .....	84
<b>4.2 Modeling of nose-breathing process .....</b>	<b>88</b>
4.2.1 Introduction .....	88
4.2.2 Case description.....	89
4.2.3 Airflow fields.....	92
4.2.4 Droplet dispersion .....	94
4.2.5 co-occupant's exposure .....	95
4.2.6 Summary.....	99
<b>4.3 CFD study of the dispersion of droplets released at different coughing velocities.....</b>	<b>100</b>
4.3.1 Introduction .....	100
4.3.2 Research method .....	101

4.3.3 Distribution of droplets generated at a higher coughing velocity of 22 m/s .....	101
4.3.4 Simulation of the distribution of droplets coughed at a low velocity of 6 m/s .....	115
4.3.5 Comparison of co-occupant's exposure at different coughing velocities.....	123
4.3.6 Summary.....	139

**Chapter 5 Effects of Coughing Orientations and Physical Blockings on Co-occupant's Exposure.....141**

<b>5.1 Numerical studies of droplet distribution at different coughing orientations.....</b>	<b>141</b>
5.1.1 Introduction .....	141
5.1.2 Case description.....	142
5.1.3 Co-occupant's exposure when the infected person coughs with the head down.....	143
5.1.4 Co-occupant's exposure when the infected person coughs with body turning around .....	149
5.1.5 Comparison of the co-occupant's exposure when the infected person coughs at different orientations .....	155
5.1.6 Summary.....	161
<b>5.2 Simulation of the performances of physical blockings on co-occupant's exposure.....</b>	<b>162</b>
5.2.1 Introduction .....	162

5.2.2 Case description.....	163
5.2.3 Effects of mouth covering .....	164
5.2.4 Effects of desk partition in between .....	175
5.2.5 Comparison of co-occupant’s exposure with different physical interventions .....	185
5.2.6 Summary.....	188
<b>Chapter 6 Airborne transmission with two types of personalized ventilation strategies under mixing and displacement ventilation schemes.....</b>	<b>190</b>
<b>6.1 Introduction .....</b>	<b>190</b>
<b>6.2 Cases description .....</b>	<b>190</b>
<b>6.3 Airflow fields.....</b>	<b>194</b>
<b>6.4 Co-occupant’s exposure under DV when the chair-based or the desk-     mounted PV is employed.....</b>	<b>195</b>
6.4.1 Droplet dispersion .....	195
6.4.2 Co-occupant’s exposure .....	199
<b>6.5 Co-occupant’s exposure under MV when the chair-based or the desk-     mounted PV is employed.....</b>	<b>203</b>
6.5.1 Droplet dispersion .....	203
6.5.2 Co-occupant’s exposure .....	206
<b>6.6 Summary .....</b>	<b>209</b>
<b>Chapter 7 Conclusions .....</b>	<b>211</b>
<b>7.1 Conclusions .....</b>	<b>211</b>

<b>7.2 Limitations and future work .....</b>	<b>214</b>
<b>References .....</b>	<b>216</b>

## List of Figures

Figure 2.1	Evaporation-falling curve of water droplets	18
Figure 2.2	Distribution of respiratory droplets under MV	32
Figure 2.3	Distribution of respiratory droplets under DV	33
Figure 2.4	Distribution of respiratory droplets under UFAD	34
Figure 2.5	Five types of desk-based PV system	37
Figure 2.6	Chair-based PV system	37
Figure 2.7	Map of regimes of interaction between particles and turbulence	44
Figure 2.8	A typical variation in measured deposition rate with particle relaxation time in fully developed vertical pipe flow	46
Figure 3.1	Schematic drawing of the experimental chamber	55
Figure 3.2	Arrangements during particle experiment	56
Figure 3.3	Particle generation system	57
Figure 3.4	Picture of the two employed manikins	58
Figure 3.5	Normalized air temperature distribution in line A (a) and line B (b)	62
Figure 3.6	Measuring points for particle horizontal dispersion	63
Figure 3.7	Horizontal distribution of particles with $D_p \leq 1.0 \mu\text{m}$ (a), $1.0 \mu\text{m} < D_p \leq 3.0 \mu\text{m}$ (b), $3.0 \mu\text{m} < D_p \leq 5.0 \mu\text{m}$ (c), $5.0 \mu\text{m} < D_p \leq 10.0 \mu\text{m}$ (d)	64
Figure 3.8	Particle distributions with breathing air heated to $32^\circ\text{C}$	66
Figure 3.9	Particle distributions with breathing air delivered at a temperature of $25^\circ\text{C}$	68
Figure 3.10	Particle distributions when breathing through nose	69
Figure 3.11	Particle distributions when breathing through mouth	71
Figure 3.12	Particle distributions with and without body heats for the two manikins	72

Figure 3.13	Personal exposure of the co-occupant at a face-to-face orientation with the polluting person	74
Figure 3.14	Personal exposure of the co-occupant with and without body heats	75
Figure 3.15	Personal exposure at different facing orientations for Case 1 (a), Case 2 (b), Case 3 (c), Case 4 (d), Case 5 (e), and Case 6 (f)	76
Figure 4.1	Geometry of the scaled chamber	80
Figure 4.2	Comparison of simulated and measured x-direction velocity	81
Figure 4.3	Comparison of simulated and measured normalized particle concentration	82
Figure 4.4	Configuration of the non-isothermal environmental chamber	83
Figure 4.5	Comparison of simulated and measured air velocity	84
Figure 4.6	Comparison of simulated and measured droplet concentration	86
Figure 4.7	Configuration of the simulated room	89
Figure 4.8	Airflow patterns and temperature distribution in the middle section ( $X=1.5\text{m}$ ) of the simulated room under MV (a), UFAD (b), DV (c), and the inhaled air path-line of the co-occupant under DV (d)	93
Figure 4.9	Normalized concentration distribution of $10\ \mu\text{m}$ droplets on the middle plane ( $X = 1.5\ \text{m}$ ) under MV (a), UFAD (b), and DV (c)	94
Figure 4.10	Average normalized concentration in the horizontal planes at different heights under MV (a), UFAD (b), and DV (c)	94
Figure 4.11	Inhaled fraction ( $IF$ ) of the co-occupant under different ventilation methods	96
Figure 4.12	Normalized concentration of $10\ \mu\text{m}$ droplets on the horizontal plane at breathing height ( $Y = 1.3\ \text{m}$ ) under MV (a), UFAD (b), and DV (c) plane at breathing height ( $Y = 1.3\ \text{m}$ )	97
Figure 4.13	Deposition rates on indoor surfaces	98

Figure 4.14	Distribution of CO <sub>2</sub> in the center plane of the room at the 0.5 <sup>th</sup> , 1.5 <sup>th</sup> and 5 <sup>th</sup> second under MV (a), UFAD (b) and DV (c)	102
Figure 4.15	Horizontal center (a) and vertical center (b) of droplet clouds varying with time under MV, UFAD, and DV	104
Figure 4.16	Cloud spatial volume of CO <sub>2</sub> , 5 μm and 10 μm droplets varying with time under MV (a), UFAD (b) and DV (c)	106
Figure 4.17	Cloud spatial volume of CO <sub>2</sub> , 5 μm and 10 μm droplets under MV (a), UFAD (b) and DV (c) during the first 10 seconds	107
Figure 4.18	Comparison of Cloud spatial volume for CO <sub>2</sub> (a), 5 μm (b) and 10 μm (c) droplets changing with time under MV, UFAD and DV	109
Figure 4.19	Normalized inhaled concentration of the co-occupant under MV, UFAD, and DV	110
Figure 4.20	Inhaled dose of the co-occupant under MV, UFAD, and DV	112
Figure 4.21	Cloud spatial volume of CO <sub>2</sub> under MV, UFAD, and DV during the first 10 seconds	113
Figure 4.22	Inhaled dose since the 10 <sup>th</sup> second	115
Figure 4.23	Dispersion of exhaled 10 μm droplets under MV (a), UFAD (b), and DV (c) when the infected person coughs at a low velocity of 6 m/s	116
Figure 4.24	Horizontal center (a) and vertical center (b) of droplet clouds varying with time under MV, UFAD, and DV	118
Figure 4.25	Cloud spatial volume of CO <sub>2</sub> (a) and 10 μm (b) droplets varying with time under MV, UFAD, and DV when the infected person coughs at 6 m/s	119
Figure 4.26	Normalized inhaled concentration of the co-occupant under different ventilation methods when the infected person coughs at a velocity of 6 m/s	120
Figure 4.27	Distribution of exhaled 10 μm droplets at the 50 <sup>th</sup> second (a), 100 <sup>th</sup> second (b), and 270 <sup>th</sup> second (c) under DV	121

	Inhaled dose of the co-occupant under different ventilation methods when the infected person coughs at a velocity of 6 m/s	122
Figure 4.28		
	Horizontal center (a) and vertical center (b) of droplet clouds varying with time under MV when the infected person coughs at different velocities	125
Figure 4.29		
	Cloud spatial volume of CO <sub>2</sub> (a) and 10 μm droplets (b) varying with time under MV when the infected person coughs at different velocities	126
Figure 4.30		
Figure 4.31	Normalized inhaled concentration of the co-occupant when the infected person coughs at 6 m/s and 22 m/s under MV	128
Figure 4.32	Inhaled dose ( <i>ID</i> ) of the co-occupant when the infected person coughs at 6 m/s and 22 m/s under MV	128
Figure 4.33	Comparison of the inhaled dose ( <i>ID</i> ) of the co-occupant at coughing velocities of 6m/s and 22m/s under MV	129
Figure 4.34	Horizontal center (a) and vertical center (b) of droplet clouds varying with time under UFAD when the infected person coughs at different velocities	130
Figure 4.35	Cloud spatial volume of CO <sub>2</sub> (a) and 10 μm droplets (b) varying with time under UFAD when the infected person coughs at different velocities	132
Figure 4.36	Normalized inhaled concentration of the co-occupant when the infected person coughs at 6 m/s and 22 m/s under UFAD	133
Figure 4.37	Inhaled dose ( <i>ID</i> ) of the co-occupant when the infected person coughs at 6 m/s and 22 m/s under UFAD	134
Figure 4.38	Comparison of the inhaled dose ( <i>ID</i> ) of the co-occupant at coughing velocities of 6m/s and 22m/s under UFAD	134
Figure 4.39	Horizontal center (a) and vertical center (b) of droplet clouds varying with time under DV when the infected person coughs at different velocities	135

Figure 4.40	Cloud spatial volume of CO <sub>2</sub> (a) and 10 μm droplets (b) varying with time under DV when the infected person coughs at different velocities	136
Figure 4.41	Normalized inhaled concentration of the co-occupant when the infected person coughs at 6 m/s and 22 m/s under DV	137
Figure 4.42	Inhaled dose ( <i>ID</i> ) of the co-occupant when the infected person coughs at 6 m/s and 22 m/s under DV	138
Figure 4.43	Comparison of the inhaled dose ( <i>ID</i> ) of the co-occupant at coughing velocities of 6m/s and 22m/s under DV	138
Figure 5.1	Configuration of the simulated room	143
Figure 5.2	Distribution of exhaled 10 μm droplets in the first 10 seconds under MV (a), UFAD (b), and DV (c) when the infected person coughs with the head bending down	144
Figure 5.3	Horizontal center (a) and vertical center (b) of droplet clouds varying with time under MV, UFAD, and DV when the infected person coughs with the head bending down	145
Figure 5.4	Cloud spatial volume of CO <sub>2</sub> (a) and 10 μm droplets (b) under MV, UFAD, and DV when the infected person coughs with the head bending down	146
Figure 5.5	Normalized inhaled concentration of the co-occupant under different ventilation systems when the infected person coughs with the head bending down	148
Figure 5.6	Inhaled dose of the co-occupant under different ventilation systems when the infected person coughs with the head bending down	149
Figure 5.7	Dispersion of exhaled 10 μm droplets in the first 40 seconds under MV (a), UFAD (b), and DV (c) when the infected person coughs with the body turning around	150
Figure 5.8	Horizontal center (a) and vertical center (b) of droplet clouds under MV, UFAD, and DV when the infected person coughs with the body turning around	151

Figure 5.9	Cloud spatial volume of CO <sub>2</sub> (a) and 10 μm droplets (b) under MV, UFAD, and DV when the infected person coughs with the body turning around	152
Figure 5.10	Normalized inhaled concentration of the co-occupant under different ventilation systems when the infected person coughs with the body turning around	154
Figure 5.11	Inhaled dose of the co-occupant under different ventilation systems when the infected person coughs with the body turning around	155
Figure 5.12	Comparison of the co-occupant's inhaled dose when the infected person coughs directly or with the head bending down	157
Figure 5.13	Comparison of the co-occupant's inhaled dose when the infected person coughs directly or with the body turning around	158
Figure 5.14	Comparison of the co-occupant's inhaled dose at the second indirect exposure stage under MV when the infected person coughs directly, with the head bending down, and with the body turning around	159
Figure 5.15	Comparison of the co-occupant's inhaled dose at the second indirect exposure stage under UFAD when the infected person coughs directly, with the head bending down, and with the body turning around	158
Figure 5.16	Comparison of the co-occupant's inhaled dose at the second indirect exposure stage under DV when the infected person coughs directly, with the head bending down, and with the body turning around	160
Figure 5.17	Configuration of the simulated room with physical blockings	164
Figure 5.18	Dispersion of exhaled 10 μm droplets during the first 10 seconds under MV when the infected person coughs with (a) and without (b) mouth covering	165

Figure 5.19	Dispersion of exhaled 10 $\mu\text{m}$ droplets under MV (a), UFAD (b), and DV (c) when the infected person coughs with mouth covering	166
Figure 5.20	Horizontal center (a) and vertical center (b) of droplet clouds under MV, UFAD, and DV when the infected person coughs with mouth covering	168
Figure 5.21	Cloud spatial volume of $\text{CO}_2$ (a) and 10 $\mu\text{m}$ droplets (b) under MV, UFAD, and DV when the infected person coughs with mouth covering	169
Figure 5.22	Normalized inhaled concentration of $\text{CO}_2$ under MV, UFAD and DV when the infected person coughs with and without mouth covering	171
Figure 5.23	Normalized inhaled concentration of 10 $\mu\text{m}$ droplets under MV, UFAD and DV when the infected person coughs with and without mouth covering	171
Figure 5.24	Inhaled dose of the co-occupant when the infected person coughs with and without mouth covering under MV, UFAD and DV	173
Figure 5.25	Comparison of the inhaled dose during the second stage (since the 10 <sup>th</sup> second) under MV when the infected person coughs with and without mouth covering	174
Figure 5.26	Comparison of the inhaled dose during the second stage under UFAD when the infected person coughs with and without mouth covering	175
Figure 5.27	Comparison of the inhaled dose during the second stage under DV when the infected person coughs with and without mouth covering	175
Figure 5.28	Dispersion of exhaled 10 $\mu\text{m}$ droplets during the first 10 seconds under MV when the infected person coughs with (a) and without (b) desk partition in between	176

Figure 5.29	Dispersion of exhaled 10 $\mu\text{m}$ droplets under MV (a), UFAD (b), and DV (c) when the infected person coughs with desk partition in between	177
Figure 5.30	Horizontal center (a) and vertical center (b) of droplet cloud under MV, UFAD, and DV when the infected person coughs with desk partition in between	179
Figure 5.31	Cloud spatial volume of CO <sub>2</sub> (a) and 10 $\mu\text{m}$ droplets (b) under MV, UFAD, and DV when the infected person coughs with desk partition in between	180
Figure 5.32	Normalized inhaled concentration for CO <sub>2</sub> under MV, UFAD and DV when the infected person coughs with desk partition in between	181
Figure 5.33	Normalized inhaled concentration for 10 $\mu\text{m}$ droplets under MV, UFAD and DV when the infected person coughs with desk partition in between	182
Figure 5.34	Inhaled dose of the co-occupant when the infected person coughs with and without desk partition in between under MV, UFAD and DV	183
Figure 5.35	Comparison of the inhaled dose during the second stage (since the 10 <sup>th</sup> second) under MV when the infected person coughs with and without desk partition in between	184
Figure 5.36	Comparison of the inhaled dose during the second stage under UFAD when the infected person coughs with and without desk partition in between	185
Figure 5.37	Comparison of the inhaled dose during the second stage under DV when the infected person coughs with and without desk partition in between	185
Figure 5.38	Comparison of the co-occupant's total inhaled dose under MV when the infected person coughs with mouth covering and desk partition in between	187

Figure 5.39	Comparison of the co-occupant's total inhaled dose under UFAD when the infected person coughs with mouth covering and desk partition in between	187
Figure 5.40	Comparison of the co-occupant's total inhaled dose under DV when the infected person coughs with mouth covering and desk partition in between	188
Figure 6.1	Configuration of the simulated room	192
Figure 6.2	Airflow patterns at $X = 2$ m and temperature distribution at $Z = 0.65$ m under MV (a) and DV (b)	195
Figure 6.3	Concentration distribution profiles of $10 \mu\text{m}$ droplets under DV when using the chair-based PV	197
Figure 6.4	Temperature contour and velocity vector (a), and concentration distribution profiles of $10 \mu\text{m}$ droplets (b) at the vertical plane of $X = 0.65$ m under DV when using the desk-mounted PV	199
Figure 6.5	Inhaled fraction of the co-occupant under DV using chair-based PV	201
Figure 6.6	Inhaled fraction of the co-occupant under DV using desk-mounted PV	202
Figure 6.7	Concentration distribution profiles of $10 \mu\text{m}$ droplets under MV when using the chair-based PV	204
Figure 6.8	Concentration distribution profiles of $10 \mu\text{m}$ droplets under MV when using the desk-mounted PV	205
Figure 6.9	Inhaled fraction of the co-occupant under MV when using chair-based PV	207
Figure 6.10	Inhaled fraction of the co-occupant under MV when using desk-mounted PV	208

## List of Tables

Table 2.1	Size distribution of expiratory droplets reported by Duguid (1946) and Chao et al. (2009)	14
Table 2.2	Concentration of several major substances in respiratory fluids	16
Table 2.3	Pooled estimation of personal protection effects to interrupt or reduce SARS spread	28
Table 2.4	Diffusion terms and source terms in the governing equations	42
Table 3.1	Heat loads for each segment of the manikin	59
Table 3.2	Description of the six experimental cases	60
Table 4.1	Inhaled dose of the co-occupant during the two stages	114
Table 8.1	Airflow rates served in different cases	193

## Nomenclature

Variable	Description	Unit
$C$	concentration	$\text{g/m}^3$
$C_{1\varepsilon}, C_{2\varepsilon}, C_{3\varepsilon}$	constants in the governing equation of $\varepsilon$	ND
$C_\mu$	model constant	ND
$C_C$	mass fraction of inhaled droplets for the co-occupant	ND
$C_I$	mass fraction of exhaled droplets for the infected person	ND
$C_i$	mass fraction of droplets in the $i^{\text{th}}$ cell	ND
CGC	cloud gravity center of droplets	ND
CSV	cloud spatial volume of droplets	ND
$d_p$	particle diameter	m
$D_p$	Brownian diffusivity	$\text{m}^2/\text{s}$
$g$	gravitational acceleration	$\text{m/s}^2$
$G_B$	generation of turbulence kinetic energy due to buoyancy	ND
$G_k$	generation of turbulence kinetic energy due to the mean velocity gradients	ND
$ID$	inhaled dose	ND
$IF$	inhaled fraction	ND
$k$	turbulent kinetic energy	$\text{m}^2/\text{s}^2$
$M$	number of particles	ND
$M_C$	mass flow rates of inhalation for the co-occupant	$\text{g/m}^3$
$M_I$	mass flow rates of inhalation for the co-occupant	$\text{g/m}^3$
$M_i$	air mass in the $i^{\text{th}}$ cell	g
$P$	pressure	Pa

Pr	Prandtl number	ND
$R_\varepsilon$	strain rate term in the $\varepsilon$ equation	ND
$S$	modulus of the mean rate-of-strain tensor	ND
$S_T$	source term in the energy equation	ND
$S_C$	source term in the concentration equation	ND
$S_{ij}$	mean rate-of-strain tensor	ND
$S_\phi$	source term of $\phi$	ND
t	time	s
T	temperature	°C
$u$	air velocity component in the x direction	m/s
$u^*$	friction velocity	m/s
$\vec{V}$	air velocity vector	m/s
$v$	air velocity component in the y direction	m/s
$V_d$	particle deposition velocity	m/s
$V_d^+$	dimensionless particle deposition velocity	ND
$V_s$	particle settling velocity	m/s
$V_s^+$	dimensionless particle settling velocity	ND
$V_p$	volume of particles	m <sup>3</sup>
$V$	volume occupied by particles and fluid	m <sup>3</sup>
$V_i$	volume of $i^{th}$ cell	m <sup>3</sup>
$w$	air velocity component in the z direction	m/s
$x, y, z$	coordinate	m
$X_i, Y_i, Z_i$	coordinate of the center of the $i^{th}$ cell	ND
$X_o, Y_o, Z_o$	coordinate of the nose-tip of the co-occupant	ND
$y^+$	Dimensionless normal distance between the wall and the center of first cell	ND

Greek  
symbols

$\alpha_k$	the inverse effective Prandtl numbers of $k$ equation	ND
$\alpha_\varepsilon$	the inverse effective Prandtl numbers of $\varepsilon$ equation	ND
$\beta_T$	thermal expansion coefficient	$\text{K}^{-1}$
$\rho$	air density	$\text{Kg/m}^3$
$\phi$	a general scalar quantity	ND
$\Phi_p$	volume fraction of particles	ND
$\varepsilon$	rate of dissipation of turbulent kinetic energy	$\text{m}^2/\text{s}^3$
$\varepsilon_p$	particle turbulent diffusivity	$\text{m}^2/\text{s}$
$\mu_{eff}$	effective viscosity	$\text{g/ms}$
$\mu$	molecular viscosity of air	$\text{g/ms}$
$\mu_t$	turbulent viscosity	$\text{g/ms}$
$\sigma_C$	turbulent Prandtl number for concentration	ND
$\sigma_T$	turbulent Prandtl number for temperature	ND
$\tau_p$	particle relaxation time	s
$\tau_K$	Kolmogorov time scale	s
$\tau^+$	Dimensionless particle relaxation time	ND
$\Gamma_\phi$	general form of diffusion coefficients	ND

# Chapter 1

## Introduction

### 1.1 Background

People with respiratory infectious diseases carry viruses or bacteria in their respiratory fluids, including saliva, sputum, and respiratory mucus. Their respiratory maneuvers, such as breathing, talking, coughing or sneezing, can disperse the carried viruses into external environments in the form of droplets. The susceptible person will catch the disease once those virus-carried droplets reach the mucous membrane. Since most people spend more than 90% of their time indoors (Jenkins et al. 1992; Klepeis et al. 2001; Robinson and Nelson 1995; Spengler and Sexton 1983), the control of respiratory infection transmission in built environments is extremely important.

A multi-disciplinary study reveals that ventilation system strongly influences air movement in built environments, and can be associated with the transmission and spread of some infectious diseases, such as measles, tuberculosis, chickenpox, influenza, smallpox, and severe acute respiratory syndrome (SARS) (Li et al. 2007). Mixing ventilation (MV), under-floor air distribution (UFAD) and displacement ventilation (DV) are three commonly employed ventilation schemes. Their specific air flow patterns will induce specific indoor contaminant distributions and

correspondingly specific exposure for occupants (Brohus and Nielsen 1996; Friberg et al. 1996; Gao et al. 2012; Hillerbrant and Ljungqvist 1990; Qian et al. 2008; Qian and Li 2010; Yin et al. 2009). Droplets released under DV can penetrate a farther distance and pose higher exposure for occupants sitting/standing near to the infected person because of the large vertical temperature gradient (Bjorn and Nielsen PV 2002; Qian et al. 2006). The well-mixed air movement of MV can evenly disperse the exhaled droplets indoors. This may result in almost the same exposure level for occupants locating at different positions. UFAD system, on the other hand, will present different infection transmission profiles with MV and DV due to its air mixing in the lower space and the mainly upward air movement in the whole space.

Besides ventilation system, non-pharmaceutical interventions are also believed to be effective approaches in mitigating the transmission of infectious diseases. One review by Jefferson et al. (2009) stated that high intervention effectiveness could be obtained when people with suspected symptoms were wearing face masks or gowns. Agah et al. (1987) also found that wearing a goggle and mask apparatus by healthcare workers could protect them from young children with respiratory syncytial virus and symptoms of respiratory tract disease. Another recent study by Aiello et al. (2010) confirmed that face masks alone could reduce influenza-like illnesses transmission apparently, especially in the combination with hand hygiene. However, the research of Tang et al. (2009) showed that the coughed air could exit from the edges of surgical masks, and Fabian et al. (2007) revealed that face mask could filter larger exhaled droplets efficiently, but no apparent effects were found on

fine droplets. Since smaller droplets can more easily reach the alveolar region and cause severe infection, it is necessary to investigate the performances of mouth covering on the dispersion of exhaled droplets and the co-occupant's exposure. The influences of desk partition will also be evaluated since this arrangement is commonly implemented in open-plan offices.

Furthermore, personalized ventilation (PV), as a complementary ventilation system to the total air distribution methods, offers an opportunity for each occupant to adjust the flow rate and direction of the fresh air supply to satisfy each individual's thermal requirements and improve the inhaled air quality (Cermak et al. 2006, Cermak and Melikov 2007, Gao and Niu 2008, Pantelic et al. 2009). There are still some concerns about whether the protecting PV devices, on the other hand, facilitate the dispersion of infectious agents generated by the PV user. The experimental study by Cermak and Melikov (2007) found that using computer monitor panel (CMP) PV device could promote the distribution of exhaled pollutants from the PV user under UFAD. The numerical investigation of He et al. (2011) concluded that the movable panel PV might induce a higher exposure for occupants under DV and UFAD. Stratified ventilation system, compared with MV, can generally provide a much cleaner micro-environment for occupants by forwarding the exhaled droplets to the space above the breathing level, but the aforementioned PV devices may weaken this advantage in the mitigation of infection spread by enhancing the dispersion of exhaled droplets in the breathing level. Other types of PV systems with the fresh air delivered in an upward direction may not only preserve the advantages of stratified

ventilation system but also assist it in transporting the exhaled droplets to the higher space and reducing the co-occupant's exposure.

Human respiratory droplets normally lies in the range of  $O(1 \mu\text{m})$  to  $O(1000 \mu\text{m})$  (Nicas et al. 2005). Smaller droplets shrink quickly to approximately half of their original size in less than 1 second due to evaporation (Nicas et al. 2005; Xie et al. 2007) and remain suspended for a long period, while larger ones will deposit onto indoor surfaces fast by gravitation (Xie et al. 2007). Among those suspended ones, droplets less than  $10 \mu\text{m}$  can more efficiently reach the alveolar region of human respiratory system and then pose higher health risk to the susceptible individuals (Guha 2008; Hinds 1999; Mangili and Gendreau 2005; Nardell et al. 1986).

Some experimental studies (Edwards et al. 2004; Papineni et al. 1997) have confirmed that normal breathing can produce respirable droplets, and the size of the majority of them is less than  $1 \mu\text{m}$  while some may be as large as several microns. Since the droplets from normal breathing are generated from the lower respiratory tract, the viruses carried will be more contagious. Meanwhile, its continuously happening characteristic makes it possible to account for a significant fraction of the droplets exhaled over the course of a day (Fiegel et al. 2006). Although coughing or sneezing does not happen frequently, these processes have been often investigated because they can generate much more droplets and pose higher health risk in seconds.

## **1.2 Objectives**

This study aims to develop a fundamental understanding of the influences of ventilation systems on the airborne transmission of respiratory diseases at various scenarios. Droplets released from normal breathing and coughing are considered separately to account for the low-velocity and high-velocity respiration processes.

The present study will focus on:

1. how the ventilation methods influence the distribution and dispersion of respiratory droplets and the corresponding exposure of occupants?
2. if a certain ventilation system always presents a better performance in mitigating the transmission of respiratory diseases over others?
3. if we can further reduce the occupant's exposure by adopting other physical interventions, such as mouth covering and desk partition, in conjunction with different ventilation schemes?
4. if the adoption of some PV devices by the infected person will result in higher exposure for the co-occupant under stratified ventilation system, and if there are any PV methods which can always ensure a better inhaled air quality for the co-occupant?

## **1.3 Structure of the thesis**

This thesis consists of seven chapters and the contents of each chapter are summarized as follows:

Chapter 1 states the background and objectives of this study, and provides an overview of the thesis.

Chapter 2 reviews the key characteristics of breathing air and respiratory droplets first. It is followed by a description of the transmission modes of diseases via respiratory droplets. The next part introduces some general routes in mitigating infectious disease transmission. The numerical simulation models employed in this thesis are then discussed. A closure of this chapter is made to summarize the section and to state the importance of this study.

Chapter 3 describes the experimental study of the dispersion of artificially generated droplets in a full scale DV ventilated chamber.

Chapter 4 investigates the dispersion of respiratory droplets and exposure level of the co-occupant under MV, UFAD, and DV when the infected person breathes via nose or coughs at different intensities.

Chapter 5 studies the influences of coughing orientations, including face-to-face, bending the head, and turning the body around, and two personal interventions, namely mouth covering and desk partition, on the distribution of exhaled droplets and personal exposure of occupants under different ventilation systems.

Chapter 6 evaluates the performances of two types of PV devices, a chair-based PV and a desk-mounted PV, on the co-occupant's exposure under MV and DV at varying PV use conditions.

Chapter 7 summarizes the conclusions of the present work and provides some recommendations for future work.

## **Chapter 2**

### **Literature Review**

#### **2.1 Introduction**

Transmission of infectious respiratory diseases may be influenced by many factors. Respiratory droplets, the virus carrier, are dispersed into room air by breathing air flowing over the liquid in the respiratory tract. Breathing maneuvers with different air speeds can strongly affect the distribution profiles of generated droplets and their origin in the respiratory system. In order to initiate an infection, pathogen-laden droplets must be transported to the breathing zone of the susceptible person by ventilation scheme or breathing air, or through direct contact with the contaminated surfaces. At the same time, pathogens in respiratory droplets have to remain their viabilities before being inhaled or reaching the mucous region. It seems that the inactivation of pathogens may be the most convenient way to mitigate infection transmission. However, it is impossible to build an environment which is suitable for the inactivation of all the pathogens. Some physical measures, including intervention and personalized ventilation (PV) system, may efficiently reduce the spread of infectious diseases and mitigate the occupants' exposure level.

Hence, the rest of this chapter presents a general review on the influencing factors for the spread of infectious respiratory diseases. The key characteristics of breathing

air are first introduced. It is then followed by an introduction of the properties of respiratory droplets. The third section describes the transmission modes of diseases via respiratory droplets. The next part introduces some general routes in mitigating infectious disease transmission. The numerical simulation models employed in this thesis is then discussed. A closure of this chapter is made to state the importance of this study and summarize the section.

## **2.2 Aerodynamics of breathing air**

To investigate the dispersion of expiratory droplets, a good understanding of their carrier, the breathing air, is very important. Several parameters are necessary to characterize the properties of expired air at different respiratory maneuvers, including velocity, flow rate, expelling direction, diameter of mouth or nose, and temperature. These parameters vary with respiratory maneuvers. Even for the same breathing activity, the respiratory parameters may change according to the age, height, weight, gender, body surface area, posture, and physical load of the target subject (Altman and Dittmer 1971; Handbook of Physiology 1986).

The airflow rate for normal breathing can be perfectly represented by a sine wave (Aranjo et al. 2004). It varies with the change of respiration frequency, minute volume, and tidal volume. Huang (1977) measured a breathing flow rate of 8.4 l/min with a frequency of 17 times per minute for human with light physical work. The early studies of Robison (1938) and Baldwin et al. (1948) stated that the minute volume for normal breathing followed a linear relationship with the body surface

area. The experimental study of Gupta et al. (2010) concluded a confidence interval for this relationship from 4.838 to 5.868 l/m<sup>2</sup> for male and 4.421 to 5.16 l/m<sup>2</sup> for female. Meanwhile, they found that the respiration frequency for both male and female varied with the height and weight of the investigated subjects. As to the direction of nose breathing jet, a side angle and a front angle were defined with a mean value of 60° and 69°, respectively, in a 95% confidence bound, while the spreading angles were 23° for side view and 21° for front view (Gupta et al. 2010). For mouth breathing, a horizontal airflow could be observed with a side-view spreading angle of 30° (Gupta et al. 2010). The measured average nose opening area by Gupta et al. (2010) during breathing was 0.71 cm<sup>2</sup> for male and 0.56 cm<sup>2</sup> for female, whilst 1.20 cm<sup>2</sup> for male and 1.16 cm<sup>2</sup> for female when mouth breathing.

As to the speaking process, a high airflow rate could be generated when spelling the alphabet 'F' loudly (Jennision 1942a). Duguid (1945) found that the air velocity when counting numbers could be as high as 16 m/s. Chao et al. (2009) measured the speaking velocity when the volunteers counted from 1 to 100 using PIV (Particle Image Velocimetry) techniques, and detected a maximum velocity of 4.6 m/s for male and 3.6 m/s for female, with an average velocity of 3.9 m/s. The experimental investigation from Gupta et al. (2010) reported expelled airflow rate for spelling alphabets, counting numbers and reading passages. Irregular flow rate over time was found for all of these three instances. The measured mean mouth opening area during talking was 1.8 cm<sup>2</sup> for both genders.

For the coughing activity, Zhu et al. (2006) measured a velocity in the range of 6 to 22 m/s with the most values being around 10 m/s using a digital PIV. Employing the same method, Chao et al. (2009) detected a maximum coughing velocity of 13.2 m/s for male and 10.2m/s for female, with an average velocity of 11.7 m/s. Different from Zhu et al. (2006) and Chao et al. (2009), Gupta et al. (2009) characterized a cough by mouth opening area, airflow rate, and direction of expelled air. The average mouth opening area when coughing was 4.00 cm<sup>2</sup> for male and 3.37 cm<sup>2</sup> for female with large variations. The cough peak flow rate changed from 3 to 8.5 l/s for male and 1.6 to 6 l/s for female. The expired volume during one cough lied in the range of 400-1600 ml for male and 250-1250 ml for female.

The temperature of exhaled air remained constant during the main part of expiration (Höppe 1981), although a rectangular function could be observed at the entrance of nose. This expiration temperature was rather sensitive to the ambient air temperature while no apparent variations could be observed with the changes of relative humidity. Meanwhile, Höppe (1981) found that the temperature of expired air through mouth was always higher than that through nose. For example, the expired temperature equaled 35°C when exhaling from mouth while 33°C when expelling from nose at an ambient air temperature of 20°C and a relative humidity of 50%.

### **2.3 Properties of respiratory droplets**

Respiratory droplets can be released in the passage of respiratory tract with a stream of air at a sufficiently high speed blowing over the surface of a liquid by wind shear

force, drawing toques of liquid out from the surface, pulling thin and breaking into columns of droplets (Hickey 1996). These processes result in droplets of different size and originating from different locations of respiratory system. Human respiratory activities such as breathing, talking, coughing or sneezing can generate droplets. The significance of each activity in the transmission of infectious diseases can be associated with several factors, including the number of droplets released, droplet size distribution profile, initial velocity of exhaled air, contents of virus or bacteria carried in the respiratory droplets, and the frequency of this activity.

### **2.3.1 Size distributions of respiratory droplets**

The number and size of droplets at different expiratory activities have been widely investigated (Duguid 1945 and 1946, Fairchild and Stamper 1987, Fennelly et al. 2004, Loudon and Roberts 1967, Papineni and Rosenthal 1997, Yang et al. 2007). Duguid (1945, 1946) measured a droplet distribution profile from 1 to 2000  $\mu\text{m}$  with 95% smaller than 100  $\mu\text{m}$  and the majority in 4 to 16  $\mu\text{m}$  while the droplet nuclei lied from 0.25 to 40  $\mu\text{m}$  with the majority being 1 to 2  $\mu\text{m}$ . Loudon and Roberts (1967) obtained droplets from 10 to 1473  $\mu\text{m}$  and droplet nuclei from 3 to 10  $\mu\text{m}$ . For these two experimental studies, droplet evaporation loss was considered by assuming the original size was four times larger than droplet nuclei by Duguid (1946), however no corrections were made by Loudon and Roberts (1967).

Since the measuring techniques during the earlier stage are based on counting large respiratory droplets after collection, the limited facilities confine the detection of

smaller droplets. Adopting optical particle detection techniques are capable of measuring micrometer or sub-micrometer particles. Fairchild and Stamper (1987) found that almost all droplets were smaller than 0.3  $\mu\text{m}$  by employing an optical particle counter. Using both optical particle counter and analytical transmission electron microscope, Papineni and Rosenthal (1997) measured the droplet size for breathing through nose or mouth, talking, and coughing. They found the exhaled droplets mainly lied in the range from 0.3 to 8  $\mu\text{m}$  with most of them smaller than 1  $\mu\text{m}$ , and larger droplets could be expelled during breathing. Fennelly et al. (2004) first investigated the size range of infectious droplets during coughing by patients with active tuberculosis using Andersen Cascade Impactor. The droplet size ranged from 2.1 to 3.3  $\mu\text{m}$ . Yang et al. (2007) measured both the dried droplet nuclei and the initial droplet size distribution produced during coughing process, and the experiment concluded that the size of dried droplets was 1 - 2  $\mu\text{m}$  and the initial size was in the range of 0.6 – 16  $\mu\text{m}$  with an average value of 8.35  $\mu\text{m}$ .

Since respiratory droplets will shrink quickly and be diluted once they are released into built environments, a delayed detection may introduce some errors in the measurements of droplet diameter and size distribution. Chao et al. (2009) measured the droplet size immediately at the mouth opening for coughing and speaking activities. The geometric mean diameter of the droplets expelled during coughing was 13.5  $\mu\text{m}$  and 6.0  $\mu\text{m}$  for speaking. It was also estimated that 947 - 2085 droplets were expelled for one cough and 112 - 6720 droplets were exhaled during speaking (counting 1 - 100 for 10 times). The diversities of these measured droplet size

profiles are mainly due to the rapid evaporation of droplets after generation and measuring techniques. The measured data of Duguid (1946) compensated droplets evaporation by assuming the original size was four times greater than measured droplet nucleus, and showed good consistency with the latest findings of Chao et al. (2009). Table 2.1 lists the size distribution of expiratory droplets reported by Duguid (1946) and Chao et al. (2009) during coughing and speaking for reference.

Table 2.1 Size distribution of respiratory droplets reported by Duguid (1946) and Chao et al. (2009)

Diameter (um)	Duguid (1946)		Chao et al. (2009)	
	Speaking (Counting 1-100 once)	Coughing (Once)	Speaking (Counting 1-100 averaged for 10 times)	Coughing (averaged for 50 times)
1-2	1	50		
2-4	13	290	1.7	4.0
4-8	52	970	26.8	55
8-16	78	1600	9.2	20.4
16-24	40	870	4.8	6.7
24-32	24	420	3.2	2.5
32-40	12	240	1.6	2.4
40-50	6	110	1.7	2.0
50-75	7	140	1.8	2.0
75-100	5	85	1.3	1.4
100-125	4	48	1.7	1.7
125-150	3	38	1.6	1.6
150-200	2	35	1.7	4.4
200-250	1	29	1.5	2.5
250-500	3	34	1.4	2.1
500-1000	1	12	0.5	1.4
1000-2000	0	2	0	0

Generally, nasal exhalation expels the least droplets with small diameters and speaking loudly can generate less than 300 droplets once. A cough disseminates almost 100,000 droplets and a sneeze can produce as many as two millions.

However, breathing or talking for two hours can exhale a total volume of air at the order of magnitude higher than 100 coughs (Gupta et al. 2010), although the peak flow rate during coughing is dramatically higher than breathing and talking. This may clearly imply that infection transmission through breathing and talking can not be neglected due to their higher event frequency.

### **2.3.2 Composition of respiratory droplets**

To investigate the evaporation process of expired droplets and survival of the carried pathogens, a well understanding of the composition of respiratory droplets is very important and necessary. Due to the varieties of human subjects and different originations of droplets in the respiratory system, there are great diversities on the composition of exhaled droplets. The early studies of Wells (1934) and Duguid (1946) stated that there were dissolved and suspended materials in the respiratory droplets besides a high percentage of water. Duguid (1946) found that the volume fraction of the solid substances contained was around 1.8%. The study of Manolis (1983) indicated that more than 200 volatile substances existed in the breathing air. Meanwhile, Griese et al. (2002, 2004) reported that several hundreds of substances were found in mucus, including glycoproteins, proteins, hormones, mineral, and buffer ions. A more detailed composition of some major ingredients was provided by Effros et al. (2002), who estimated the concentrations of solutes in the respiratory fluids by assuming the respiratory secretions were isosmotic with plasma. The concentration of several major components in the respiratory fluids is listed in Table 2.2 according to the data collected from Effros et al. (2002), which are important

factors in determining the evaporation rates and final diameter of respiratory droplets.

Table 2.2 Concentration of several major substances in respiratory fluids (data from Effros et al. 2002)

<b>Species</b>	<b>Molecular weight or atomic mass</b>	<b>Concentration</b>
Na <sup>+</sup>	23 g	91 ± 8 mM
K <sup>+</sup>	39.1 g	60 ± 11 mM
Cl <sup>-</sup>	35.5 g	102 ± 17 mM
Lactate	89 g	44 ± 17 mM
Protein	Not given	7.63 ± 1.82 g/dl

### **2.3.3 Evaporation of respiratory droplets**

Respiratory droplets are constituted of aqueous solution with inorganic and organic ions and proteins, in which pathogens are suspended. During the expiratory process, droplets are released into an environment generally with lower relative humidity and temperature than in the respiratory system. The contained water in droplet will evaporate and accordingly lead to the shrinkage of droplet size. According to the composition information of respiratory fluids in the literature (Effros et al. 2002), it is possible to make a reasonable estimation of evaporation rates and final size of the exhaled droplets.

Wells (1934) studied the evaporation process of free-falling water droplets and revealed the relationship among falling rate, evaporation, and droplet diameter. A reproduction of this classical curve is presented in Figure 2.1. According to Wells (1934), droplets smaller than 100 µm from a breathing person would dry out

completely before falling to the ground under normal air conditions, while larger droplets would settle down before complete evaporation of contained water.

Xie et al. (2007) conducted a further investigation on Wells' (1934) evaporation-falling curve mathematically when the water droplets were expelled at different initial velocities and into an indoor environment with different relative humidity. They found that more droplets would remain suspended in room air at a lower relative humidity because of increasing evaporation of water in the droplet, which could increase the probability of subsequent exposure for occupants. Employing the more sophisticated components of respiratory fluids from Effros et al. (2002), Nicas et al. (2005) developed two equations to estimate the equilibrium size of expiratory droplets for complete and incomplete desiccation. The estimated diameter of a completely evaporated droplet is about 0.44 times of its initial size. For incomplete evaporation under the typical range of indoor relative humidity from 30% to 70%, the equilibrium diameter would range from 0.47 times of original size for a relative humidity of 30% to 0.61 times for 70%. Meanwhile, the studies of droplets evaporation rates (Nicas et al. 2005, Xie et al. 2007) reported that the evaporation of droplets with initial diameter less than 20  $\mu\text{m}$  could be treated as instantaneous process due to the relatively short evaporation time scale.

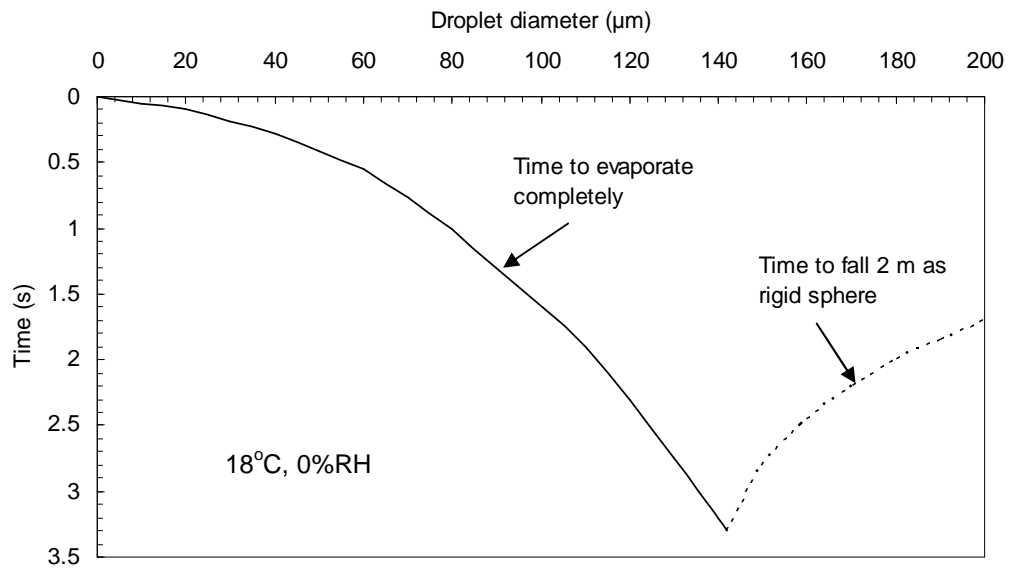


Figure 2.1 Evaporation-falling curve of water droplets (reproduced from Wells (1934))

### 2.3.4 Viability of pathogens in respiratory droplets

To initiate an infection, it is important for the pathogens in respiratory droplets remaining their viabilities before being inhaled by the susceptible person and reaching the mucus. The infection process for an animal is determined by the pathogen concentration, i.e. infective dose, and virulence which can enable an agent to overcome its physical and immunologic defenses. As to human beings, only small infective dose is possible to initiate some microbial diseases since the agents have affinity for specific tissue and possess potent virulence factors which render them resistant to inactivation (Cole and Cook 1998). It is reported that the infectious disease transmitted by airborne *Francisella tularensis* (the causative agent of tularemia) is resulted from a single micro-organism, whose virulence is related with

a cellular capsule (Cox 1987). The viability of pathogens therefore is undoubtedly noticeable for studying the transmission of infectious diseases. Cole and Cook (1998) reported that there were several factors influencing the infectivity of pathogens in respiratory droplets, such as generation process, and environmental conditions.

Aerosolization is an important and indispensable process to trigger the spread of infectious respiratory disease. Once the droplets are aerosolized from respiratory tract, a significant portion of carried pathogens will be destroyed or inactivated because of the effect of rapid dehydration of droplets when they are introduced to an environment with normally lower relative humidity and temperature (Marthi et al. 1990). Meanwhile, some water molecules may be bonded with the essential molecules of micro-organism, such as protein and DNA which maintain the biological integrity. Therefore, the rapid removal of water from droplets may destroy the structure of micro-organism and inactivate its infectivity (Zentner 1966).

Environmental conditions also affect whether a pathogen will remain its viability during its journey to a susceptible host after aerosolization. It is reported that micro-organisms generally survive better on hard surfaces than on porous surfaces or hands (Caroline 2007). Respiratory syncytial virus (RSV) can remain viable on counter for nearly 6 h, while only 20 to 30 min on gowns or paper tissues and less than 20 min on skins. Even for the shorter survival period, it is sufficient to cause infection when the contaminated hands touch the susceptible person's eyes or nose

(Hall et al. 1980). Influenza viruses have also been demonstrated to show the similar findings by Bean et al. (1982).

Temperature and relative humidity are two important environmental parameters affecting pathogen survival. Harper (1961) studied the survival ability of 4 viruses, vaccinia, influenza A, polio, and Venezuelan equine encephalomyelitis, after aerosolization into a dark environment with varying relative humidity and temperature. It was found that viruses survived better at lower temperature at different relative humidity. The more interesting finding was that vaccinia, influenza A, and Venezuelan equine encephalomyelitis exhibited better survival ability at lower relative humidity from 17% to 25%, while polio virus survived better at a higher relative humidity about 80%. Another experimental study conducted by Miller and Artenstein (1967) investigating the viability of 3 human respiratory viruses, adenoviruses 4 and 7, and parainfluenza 3, reported that adenoviruses were hardy survivors at a higher relative humidity of 80%, whilst parainfluenza 3 survived better at a lower relative humidity of 20%. The research of Ijaz et al. (1985) investigated the survival of human coronavirus 229E at air temperature of 6°C and 20°C, and relative humidity of 30%, 50%, and 80%. They found that maximum survival could be achieved at 80% relative humidity. These studies indicate that the effects of relative humidity and temperature on the survival of viruses are extremely complex. It is impossible to build an environment which is suitable for the inactivation of all the pathogens.

Besides the aforementioned physical factors, the structure of virus itself may also influence its viability. Generally, viruses without lipid envelope can remain viable for a longer period than viruses with lipid envelop, since enveloped viruses are more susceptible to degradation.

## **2.4 Transmission modes of diseases via respiratory droplets**

For a host with respiratory disease symptoms, pathogens will be contained in his/her fluids and mucus. During the host's respiration activities, droplets will be generated and the pathogens carried in can then be aerosolized into room air. If these pathogen-laden droplets are inhaled by the susceptible person or reach the mucous region via indirect contact, infections will be initiated. Generally, transmission of infectious diseases through respiratory droplets can be classified into three categories. They are airborne transmission, transmission by large droplets, and contact transmission.

Once aerosolized into room air, respiratory droplets will shrink rapidly because of the normally lower temperature and relative humidity in built environments. Smaller droplets will remain suspended for long periods of time, and air currents can distribute them to be widely dispersed according to the specific ventilation system employed. If these pathogen-laden droplets are inhaled and an infection is initiated, disease spread in this manner can be termed as airborne transmission (CDC 1996).

Large droplets primarily generated through sneezing, coughing, and talking, can be directly sprayed onto conjunctiva, nasal mucous membrane, or mouth, of the susceptible person to activate a new infection. The shedding distance of these large droplets is an essentially important factor in determining the influencing area of diseases transmitted through large droplets. The mathematical study of Xie et al. (2007) reported that large droplets could be carried more than 6 m away by the exhaled air at a sneezing velocity of 50 m/s, more than 2 m away at a coughing velocity of 10 m/s, and less than 1 m at a normal breathing velocity. It is clear that certain distance away from the infected person can safely avoid the exposure to infectious diseases transmitted via large droplets. Meanwhile, walking away or turning around are also feasible measures to escape this highly directional transmission mechanism.

Contact transmission occurs when the susceptible person touches the fomites on contaminated surfaces covered with settled pathogen-laden respiratory droplets or through physical contact with the infected individual (Garner 1996, Bonne and Gerba 2007). The general route of contact transmission involves three parts, droplet deposition onto surfaces, transfer of virus from surface to hand, and transfer from hand to conjunctiva or mucus. Virus inactivation on environmental surfaces and human skin are two major approaches to control disease transmission through contact. Viruses with lipid envelop such as parainfluenza virus have a very low chance to survive on hands (Sattar et al. 2002). The similar phenomenon can also be observed for influenza A virus as well (Bean et al. 1982). For inanimate surfaces,

micro-organisms generally survive better on hard surfaces than on porous surface (Caroline 2007). The research of Bean et al. (1982) indicated that influenza A virus could survive for more than 24 - 48 h on stainless steel and plastic surfaces, while could not be detected after 8 - 12 h on porous surfaces such as paper tissue, and pajamas. It was possible to transfer viable influenza A virus from paper or tissue to hands within 15 min, but almost 24 h for virus transfer from stainless steel to hands. The estimated inactivation rates of viruses are approximately  $24 \text{ day}^{-1}$  on porous surfaces and  $2.9 \text{ day}^{-1}$  on stainless steel. Another study on Swiss banknotes reported that influenza A virus with the subtypes of H1N1 and H3N2 presented very low inactivation rates (Thomas et al. 2008). No significant decay was observed for H3N2 influenza A virus even after 10 days. The possible reason might be that nasal mucus had a strong survival-enhancing effect because of the stabilization of proteins and salts carried in (Schaffer et al. 1976). This especially low inactivation rate might explain why influenza A virus could be widely detected in indoor environments. These researches indicated that the infection risk through contact transmission may be considerable if non-porous surfaces are extensively adopted.

As mentioned in section 2.3, the size of respiratory droplets has a wide spectrum from  $O(1 \mu\text{m})$  to  $O(1000 \mu\text{m})$ . During the infected person's respiration process, droplets will be released at varying velocities. This momentum can drive large droplets with high inertia to approach the susceptible person directly and cause infection transmission through large droplets. Larger droplets, on the other hand, will settle down onto the indoor surfaces quickly. Before the decaying of the viruses

or bacteria carried in, infectious diseases can be transmitted to the susceptible person by indirect surface contact if he/she contacts the contaminated surfaces and then touches his/her mouth, nose or eyes. Differently, smaller droplets can dry out very quickly and form droplet nuclei. The nuclei can remain suspended in room air for a longer period and spread infection by airborne transmission. The distribution of these droplet nuclei are mainly related to the ventilation system employed. For a room with MV system, these droplets will be evenly distributed, while concentration stratification can be observed under DV and UFAD systems (Gao et al. 2008; Qian et al. 2006; Li et al. 2011).

It is necessary to emphasize that which of the three transmission modes is responsible for the spread of infectious diseases remains highly controversial. The initial dominant opinion claimed by Chapin (1910) stated that communicable respiratory infection was transmitted by routes of large droplets over short distance or through indirect contact with contaminated surfaces. The pioneering study by Wells and Brown (1936) produced challenge against the infection spread modes of large droplets and contact transmission. Their experimental research (Wells and Brown 1936) provided evidence for the existence of droplet nuclei as one means spreading respiratory disease by airborne transmission. During the later several decades from the later 1930s to the early 1980s, extensive researches have been conducted on airborne route. But for the later many years, no noteworthy attention was paid on airborne infection any more. The emergence of severe acute respiratory syndrome (SARS) in 2002 and 2003 triggered intensive study on respiratory disease

transmission through droplet nuclei again. A review on viral infections reported that airborne transmission was possible for many types of viruses (Sattar and Iljaz 1987). Although the importance of airborne transmission is debatable, there appears to be an agreement that it is at least possible.

## **2.5 General routes to mitigate infectious disease transmission**

### **2.5.1 Antiviral drugs and vaccines**

Antiviral prescribing and vaccines seem to be the mainstay in the campaign with pandemic infections, especially against the seemingly mild disease such as influenza. Even in the recommendations from WHO (World Health Organization), vaccines and antivirals were mentioned 24 and 18 times respectively, while some non-pharmaceutical interventions were seldom cited with twice for hand-washing and mask, and once for gloves and gowns (WHO 2009). However, antiviral drugs might be limited and vaccines would not be available early for a new-coming disease, for example, the influenza (H1N1) pandemic (Aiello et al. 2010). Non-pharmaceutical interventions then play an important role in the prevention and reduction of infectious disease transmission for the whole pandemic period, especially at the beginning.

### **2.5.2 Physical interventions**

For new respiratory diseases, including severe acute respiratory syndrome (SARS) in 2003 caused by coronavirus and H1N1 pandemic influenza from 2009 to 2010, antiviral prescribing is limited and vaccines are not available at the beginning of

viral infection outbreaks. Non-pharmaceutical interventions, on the other hand, are feasible measures to mitigate infectious disease transmission (Aiello et al. 2010, Del Valle et al. 2010, Jefferson et al. 2009, Weber and Stilianakis 2009). There are many physical interventions that are possible to interrupt or reduce the spread of infectious respiratory viruses, including isolation, distancing, barriers, personal protection, and hygiene.

During the outbreak of SARS, isolation or quarantine was employed as one public health tool to prevent the spread of SARS in Taiwan, Canada, Singapore, Hong Kong, and Mainland China (CDC 2003, Poutanen et al. 2003, Twu et al. 2003, Yu et al. 2004). In Taiwan, the effects of two types of quarantine (level A and level B) were assessed, in which level A focused on persons who had close exposure to persons infected with SARS in health care facilities, other community, and domestic areas, and level B included travelers sitting within 3 rows of the infected person or returning from areas affected by SARS as designated by WHO (Twu et al. 2003). This study concluded that the isolation of those with known or suspected exposure to the infected person could have reduced the quarantined people by 64%. One study in Beijing stated that the isolation of cases during the SARS epidemics could limit infection transmission from those who had close exposure to people showing SARS symptom (Qu et al. 2003).

As to the effects of distancing, the mathematical study by Xie et al. (2007) indicated that human expelled droplets could penetrate a distance more than 6 m with a 50 m/s

sneezing velocity, more than 2 m at a 10 m/s coughing velocity, and 1 m at a 1 m/s normal breathing velocity. When the susceptible person is in a face-to-face orientation with the infected person, exhaled droplets can be delivered to the co-occupant's breathing zone directly by breathing jet and pose higher exposure in seconds (Gao et al. 2008, Li et al. 2011, Zhu et al. 2006). These findings imply that certain distance away from the polluting source is a feasible way to reduce the transmission of respiratory diseases.

Personal protection is also one effective approach to mitigate the spread of respiratory viruses. Table 2.3 shows some pooled estimation of effects from case-control studies of public health interventions to interrupt or reduce SARS transmission (Jefferson et al. 2009). It could be concluded that dramatic reduction of infectious disease transmission could be achieved through some personal behaviors, including frequent hand-washing, face masks, gloves and gowns. The research of Tang et al. (2009) demonstrated that wearing a surgical mask would redirect and decelerate exhaled airflows from the infected individuals and might minimize the pathogen-laden viruses entering the breathing zone of others. Another recent study by Aiello et al. (2010) showed that face masks alone could reduce influenza-like illnesses transmission apparently, especially in the combination with hand hygiene. One study also found that wearing a goggle and mask apparatus could protect healthcare workers from young children infected with respiratory syncytial virus and symptoms of respiratory tract disease (Agah et al. 1987). Two reports (Kitamura et al. 2007, Satomura et al. 2005) suggested that gargling with water might attenuate

the symptoms of the disease, and was effective against mild forms of acute respiratory tract.

Table 2.3: Pooled estimation of personal protection effects to interrupt or reduce SARS spread (Jefferson et al. 2009)

Intervention	Intervention effectiveness (%)
Frequent handwashing(>10 times daily)	55
Wearing mask	68
Wearing N95 mask	91
Wearing gloves	57
Wearing gown	77
Handwashing, mask, glove, and gown combined	91

### 2.5.3 Ultraviolet Germicidal Irradiation (UVGI)

UVGI is to disinfect biological contaminant in air or on surfaces by adopting UV radiation. UV radiation is a portion of electromagnetic spectrum with wavelengths ranging from 100 to 400 nm (CDC, 2005), and can be classified as: UVA with a wavelength from 315 to 400 nm, UVB from 280 to 315 nm, and UVC from 100 to 280 nm (ISO 2007). The one used in germicidal irradiation is UVC which has maximum effect at a wavelength of 260 nm (Sharp 1937). The UV lamps, mainly available as low-pressure mercury vapor lamps, emit radiation at a wavelength of 253.7 nm (IESNA 2000), and can be used in room to irradiate the air in the upper

part, installed in air ducts to irradiate air passing through the duct, or incorporated into room air handling units. It should be reminded that direct irradiation to the occupied zones should be avoided since it might be harmful to occupants.

The effectiveness of UVGI system is related with the exposure of infectious pathogens to a sufficient dose of UV light to ensure inactivation (CDC 2005), since its function is determined by the ability to deliver sufficient irradiance for a long time to achieve certain irradiation dose in order to inactivate the pathogens. Regarding the limited exposure time of organisms contained in airborne droplets, it will be essential to maintain sufficient irradiance to achieve the necessitated dose. Meanwhile, the efficacy of UVGI appliance can be influenced by the mixing of room air, air velocity, relative humidity, UVGI intensity, and the configuration of UV lamps.

Researches (Riley and Permutt 1971, Riely and Kaufman 1971) have demonstrated that enhancing the mixing of room air by ceiling fans could double the efficiency of UVGI system in inactivating an organism which is highly sensitive to UV lights. The study of Ko et al. (2002) reported that employing a mixing fan could apparently improve the effectiveness of UVGI by 16% at 2 ACH and 33% at 6 ACH. It is clear that the enhancement of air mixing in built environments can raise the efficacy of UVGI system. Meanwhile, some experimental studies in chambers found that the ability of UVGI in killing or inactivating organisms decreased substantially once the air relative humidity was above 60% (Ko et al. 2000, Peccia et al. 2001, Riley and

O'Grady 1961, Riley and Kaufman 1972). The corresponding results have also been reported in room studies at high relative humidity (Riley and Permutt 1971, Riley et al. 1976). However, the study of Riley and Permutt (1971), and Miller and Macher (2000) indicated the increase of relative humidity from 25% to 67% had no apparent influences on UVGI levels. The actual reason for the reduced efficiency of UVGI at higher relative humidity is still unknown. For the optimum application of UVGI system, the recommended relative humidity should be less than 60% (CDC 2005). The study on air flow rates showed that ventilation rates usually had no adverse effect on the efficacy of upper-air UVGI. Furthermore, an airflow rate of 6 ACH in a well-mixed room when combined with UVGI could achieve a comparative efficiency in inactivating pathogens as a ventilation rate larger than 12 ACH when employing solely mechanical ventilation (Riley and Permutt 1971). Ventilation rate higher than 6 ACH would, however, increase the air velocity and then reduce the time the air is irradiated. This will hamper the killing of pathogens (Collins 1971, Kethley and Branch 1972).

UVGI intensity is the primary factor influencing the performance of upper-air UVGI system, and can be affected by the lamp wattage, distance from the lamp, surface area, and the presence of reflective surfaces. Therefore, the designing of UVGI system should consider room geometry, ventilation, fixture (lamp plus housing and louvers) layout, and the expected level of equivalent ACH in determining the parameters of UVGI to achieve the desired irradiance levels.

#### **2.5.4 Ventilation system**

It has been demonstrated that air distribution methods strongly influence the airflow patterns in buildings, and can be associated with the transmission and spread of some infectious diseases (Li et al. 2007). MV, UFAD, and DV are the three commonly employed air-distribution strategies in buildings. The specific airflow patterns and temperature distribution of each ventilation system may induce specific contaminant dispersion profiles and specific exposure for occupants.

The conventional mixing system delivers conditioned air at a velocity much higher than the acceptable one for indoor occupants, and with a temperature greatly higher or lower than the designed indoor air temperature according to the heating or cooling load. The high speed incoming air rapidly mixes with indoor air and forms a relatively strong turbulent airflow environment in the entire space. Because of the entrainment of room air into fresh air, the conditioned air temperature will reach the designing level and air speed will decrease to an acceptable level (no higher than 0.25m/s) before entering the occupied zone (ASHRAE 2001). This method of air distribution creates a relatively uniform environment in the whole conditioned area. Results of some laboratory experiments and numerical simulations found that this system could widely disperse the emitted contaminants being quite evenly distributed in the conditioned space with no regards to the source locations (Chao and Wan 2004, Gao and Niu 2007, Gao et al. 2008, Li et al. 2011). Figure 2.2 presents the distribution of human respiratory droplets under MV (Li et al. 2011). Generated droplets are driven upward immediately after exhalation because of the

higher temperature differences between the exhaled air and ambient air. Due to the well-mixed air movement of MV, the exhaled droplets are much uniformly distributed with lower concentration for larger ones because of deposition mechanism.

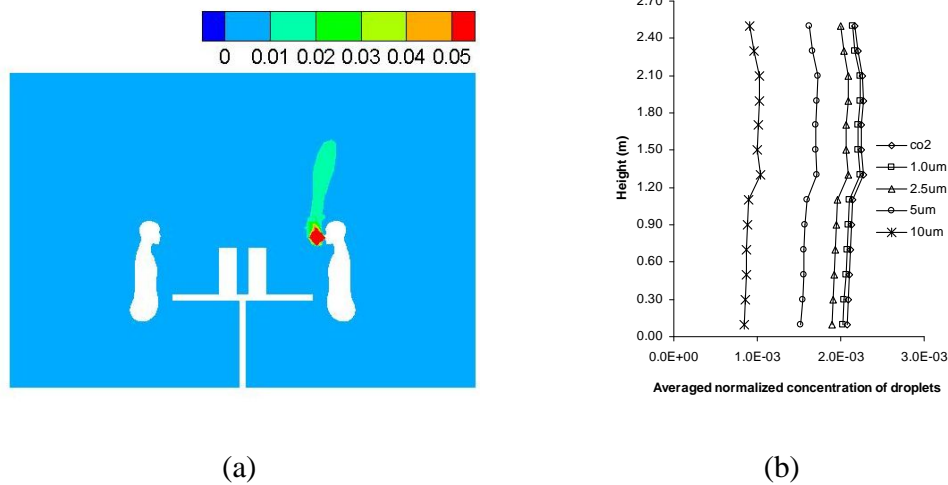


Figure 2.2: Distribution of respiratory droplets under MV (normalized concentration of 10  $\mu\text{m}$  droplets in the center plane (a); average normalized concentration profiles in the horizontal planes at different heights (b))

Compared with MV, low level supply systems such as DV and UFAD are more effective when contaminant removal effectiveness is considered (Akimoto 1999, Matsunawa 1995) and possess a potential to achieve better inhaled air quality by supplying the conditioned fresh air near the occupants. Although there are some similarities, differences still exist between these two low-level supply systems. The primary difference lies in the manner in which the air is delivered into the space.

DV system imparts conditioned air at a quite lower velocity to maintain the generally laminar air movement, while UFAD system employs higher velocity diffuser to achieve greater mixing in the occupied region. This will result in different contaminant distribution profiles as presented in Figure 2.3 for DV and Figure 2.4 for UFAD.

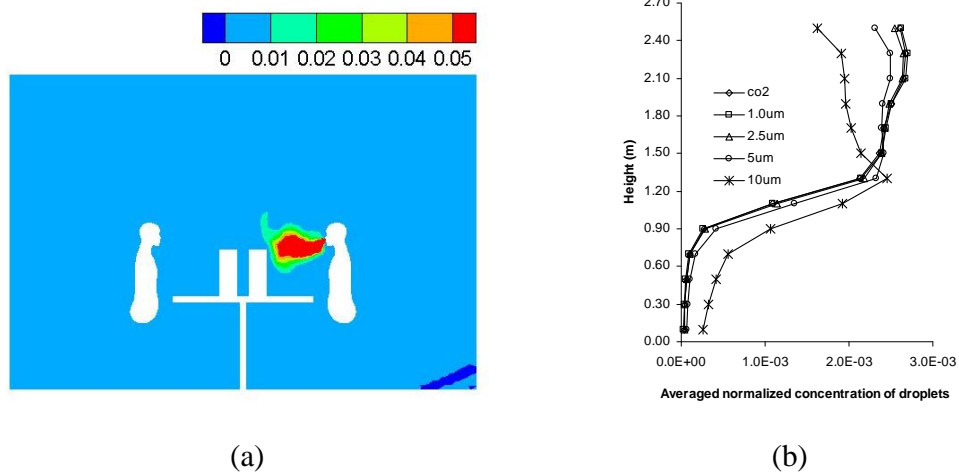


Figure 2.3: Distribution of respiratory droplets under DV (normalized concentration of 10 µm droplets in the center plane (a); average normalized concentration profiles in the horizontal planes at different heights (b))

Different from MV, exhaled droplets can travel a relatively longer distance horizontally under DV and UFAD because of temperature stratification. This may lead to higher exposure level when the susceptible person sits/stands close to the infected person (Nielsen et al. 2002; Qian et al. 2006). However, lower exposure can still be achieved when the susceptible person locates at a certain distance away from

the infected one, since the upward air movement of UFAD and DV can drive the exhaled droplets to the higher space (Li et al. 2011). Although stratified distribution of respiratory droplets can be observed in the two ventilation systems, there are some distinct differences in the dispersion of droplets with varying diameters, especially in the lower region of room. Droplet concentration decreases with increasing diameter under UFAD because of the higher deposition rates, while it increases with droplet size under DV due to the mainly upward air flow which can hamper the deposition of larger droplets and facilitate the extraction of smaller droplets.

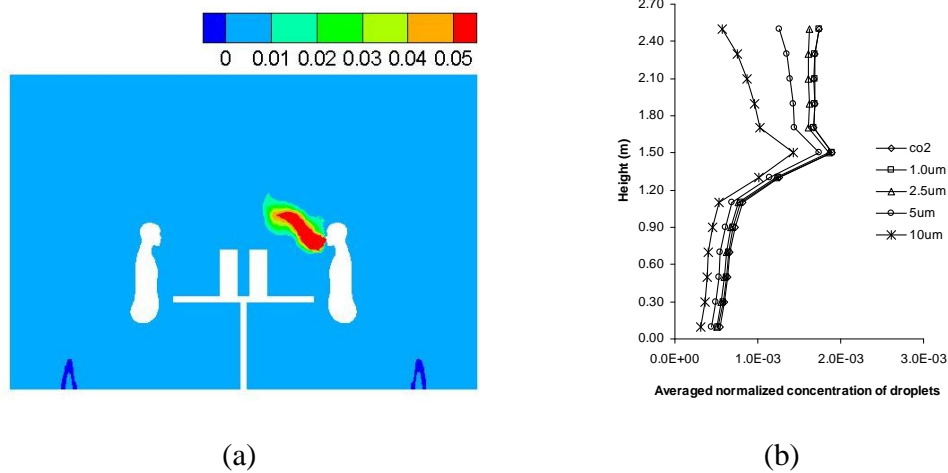


Figure 2.4: Distribution of respiratory droplets under UFAD (normalized concentration of 10  $\mu\text{m}$  droplets in the center plane (a); average normalized concentration profiles in the horizontal planes at different heights (b))

### 2.5.5 Personalized ventilation (PV)

The traditional total ventilation systems, such as MV, UFAD, and DV, can only guarantee the thermal comfort of a large percentage of occupants. Personalized ventilation (PV) system offers the opportunity for each occupant adjusting the flow rate and direction of personalized fresh air to satisfy his/her own requirements, since occupants' physiological and psychological responses to the indoor thermal environments are different due to the variances in clothing, activity, individual preferences on room air temperature and movement, etc. ASHRAE (2001) reported that the thermal insulation of occupants' clothing level might range from 0.4 clo to 1.2 clo, and the metabolic rate might vary from 1 met to 2 met because of the differences in occupant's individual activities. The preferred air temperature can be as great as 10 °C different (Grivel and Candas 1991), and the optimum air velocity may have a four times difference (Melikov et al. 1994). Meanwhile, the fresh air diffusers of total ventilation system are equipped far from the occupants to avoid draught sensation. The fresh air will be more or less polluted and warmed by the time it is inhaled. Although it is generally believed that DV can provide more fresh air to the occupants compared with MV and UFAD, the field studies found that almost half of occupants in rooms with DV were dissatisfied with the air quality (Melikov et al. 2004, Naydenov et al. 2002). PV, on the other hand, can directly deliver the conditioned fresh air to the occupants' breathing zone and improve the inhaled air quality.

According to the position of personalized air diffuser, PV system can be mainly classified into three types. They are desk-based PV, partition-based PV, and chair-

based PV systems. Figure 2.5 presents five desk-based PV systems with different positions investigated by Melikov et al. (2002). Two small personal environment module (PEM) diffusers can be placed at two sides of computer monitor to generate two symmetrical air jets. The horizontal desk grill (HDG) can horizontally deliver fresh cooling air toward the occupant's body, while vertical desk grill (VDG) supplies conditioned air to the occupant vertically. Computer monitor panel (CMP) represents a PV device mounted on the top of computer monitor allowing the change of airflow direction vertically, and a flexible movable panel (MP) diffuser is mounted on a movable duct to facilitate the change of airflow rates and the distance between the PV diffuser and the user. Partition-based PV system is the one with personalized air diffusers mounted on the partitions in modern offices, in which the conditioned fresh air can be delivered toward the breathing zone of the occupant (Hiwatashi et al. 2000, Jeong 2003), or supplied upward and falls down over the user's body due to the density difference between the conditioned air and room air (Yang et al. 2004). The third type of PV system is the chair-based one with adjustable personalized air diffusers (Niu 2005; Nobe et al. 2003). The chair-based PV system developed by Niu (2005) is illustrated in Figure 2.6 with air supplying diffuser being mounted right below the chin of the user, which can impart conditioned fresh air to the breathing zone of the occupants as more as possible. Since the location of this chair-based PV may hamper the activity of the user, this device seems more suitable for prolonged seating conditions, such as in theatres, cinemas, lecture halls, commercial airplanes, and for bus drivers. If the user needs to

move around, the ventilation nozzle connected with flexible support can be conveniently moved aside.

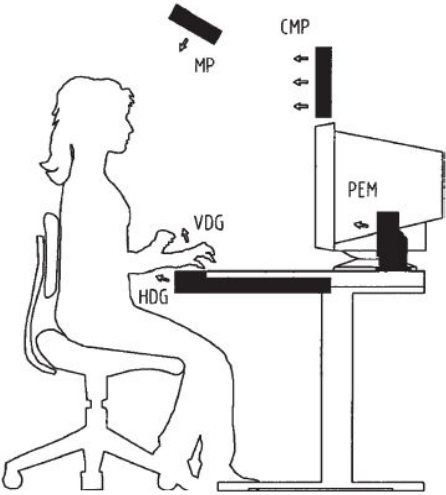


Figure 2.5: Five types of desk-based PV system. PEM - personal environment module, HDG - horizontal desk grill, VDG - vertical desk grill, CMP – computer monitor panel, MP – movable panel. (Melikov 2004)

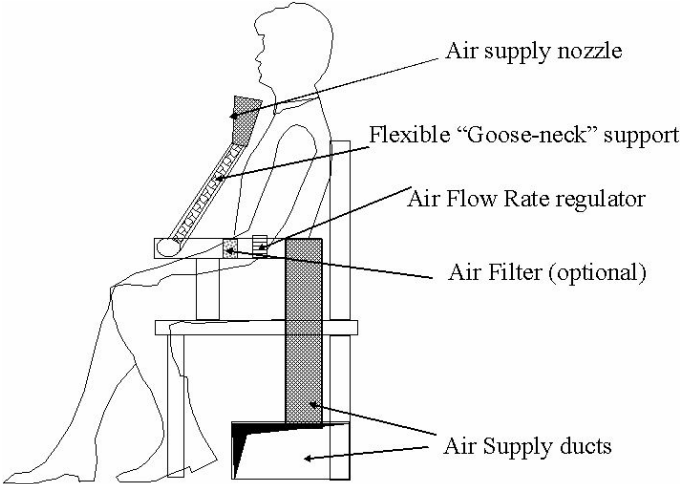


Figure 2.6: Chair-based PV system. (Niu 2005)

The most important advantage of PV is to provide clean and cool air to each occupant to achieve higher inhaled air quality (Melikov 2004). Extensive researches have been conducted numerically and experimentally. Melikov et al. (2003) stated that personalized airflow transverse to the free convection flow around the human body presented the highest potential to deliver clean air to the breathing zone. Directing personalized air toward the face with a mean velocity of 0.3 m/s was possible to deliver 100% fresh air to the breathing zone of the occupant (Bolashikov et al. 2003). Cermak et al. (2006) experimentally demonstrated that PV could always improve the user's inhaled air quality under MV and DV when the contaminant was released from the floor level or with regard to human body. Another study by Cermak and Melikov (2007) under UFAD found that using PV as a complementary ventilation system could provide excellent protection to the seated occupants from any pollution. Numerical study by Gao and Niu (2009) in commercial airplane concluded that employing chair-based PV could shield up to 60% of air pollutants. The experimental study of Pantelic et al. (2009) reported that employing the desk-based PV could not only reduce the peak aerosol concentration levels in the occupant's breathing zone, but also shorten the exposed period.

Although many studies demonstrate that PV system in conjunction with total ventilation system can improve the inhaled air quality for the user, concerns still exist about whether this protecting PV device, on the other hand, facilitate the dispersion of infectious agents generated by the PV user. The experimental study by Cermak and Melikov (2007) found that using RMP PV device under UFAD could

promote the distribution of exhaled pollutants from the PV user. The performances of another desk-mounted PV, i.e. MP, were numerically investigated under MV, UFAD, and DV by He et al. (2011). They found that this type of PV system might enhance the mixing of exhaled pollutants with room air under DV and UFAD, and increase the exposure level of occupants.

The dilemma of using PV in improving the inhaled air quality and promoting the distribution of exhaled pollutants brings concerns and uncertainties in air ventilation system design. There are many factors which may influence the performances of PV devices, including the installed position, conditioned air injecting direction, delivering velocity, temperature difference with ambient air, PV airflow rates, and size of target area (Faulkner et al. 1999; Melikov et al. 2002). The well-designed PV system should not only improve the thermal sensation for occupants but also preserve the advantages of the adopted total-volume ventilation system in the control of infection transmission at varying PV use scenarios.

## **2.6 Numerical simulation models**

Numerical simulations will be conducted in the following chapters to investigate the dispersion of human respiratory droplets and co-occupant's exposure under different ventilation systems. This part describes the employed numerical models for indoor air movement, droplets transportation and deposition.

### **2.6.1 Governing equations for indoor air movement**

The governing equations for indoor air flow are based on the Eulerian framework, and the mass, momentum and energy equations are solved in a finite-volume method. The renormalization group (RNG)  $k-\varepsilon$  model (Choudhury 1993) is adopted to simulate the indoor air turbulence considering that it can predict indoor air flow patterns reasonably (Zhang et al. 2007). Standard logarithmic law wall functions (Launder 1974) are chosen to bridge the solution variables at the near-wall cells and the corresponding quantities on the adjacent wall. Boussinesq assumption is adopted to account for the change of air density due to temperature variation in the momentum equations. The SIMPLE algorithm is employed to couple the pressure and velocity fields.

The governing equations are as follows:

$$\frac{\partial \rho}{\partial t} + \text{div}(\bar{V}) = 0 \quad (2.1)$$

$$\frac{\partial(\rho\phi)}{\partial t} + \text{div}(\rho\bar{V}\phi) = \text{div}(\Gamma_\phi \text{grad}\phi) + S_\phi \quad (2.2)$$

where  $\phi$  is a general scalar quantity which can represent U, V, W,  $k$ ,  $\varepsilon$ , T, and tracer gas concentration. The diffusion coefficient and source term for each scalar are listed in Table 2.4. The specialties of RNG  $k-\varepsilon$  model are the derivation of effective viscosity  $\mu_{eff}$  and strain rate term  $R_\varepsilon$  in the  $\varepsilon$  equation.  $\mu_{eff}$  is calculated by the below differential equation:

$$d\left(\frac{\rho^2 k}{\sqrt{\varepsilon\mu}}\right) = 1.72 \frac{\bar{v}}{\sqrt{\bar{v}^3 - 1 + C_v}} d\bar{v} \quad (2.3)$$

where  $\hat{\nu} = \mu_{eff} / \mu$ ,  $C_v = 100$ . This equation allows the  $k - \varepsilon$  model to better predict the low-Reynolds-number flows and near-wall flows for the reason that the indoor airflow is not fully turbulent. The strain rate term  $R_\varepsilon$  allows the RNG  $k - \varepsilon$  model more responsive to the effects of rapid strain and streamline curvature than the standard  $k - \varepsilon$  model.

### 2.6.2 Governing equation for particle dispersion

As to the interaction between particles and turbulence, particle-laden turbulent flows are classified into different regimes as shown in Figure 2.7, where  $\Phi_p$  refers to volume fraction of particles with  $\Phi_p = MV_p / V$ ;  $M$  is the number of particles;  $V_p$  is the volume of particles;  $V$  is the volume occupied by particles and fluid;  $\tau_p$  is particle response time; and  $\tau_k$  is Kolmogorov time scale.

For very low values of  $\Phi_p (< 10^{-6})$ , the particles have negligible effect on turbulence, and the interaction between the particles and turbulence is termed as one-way coupling. This implies that the particle dispersion depends on the state of turbulence in this regime, but the momentum transfer from the particles to the turbulence has an insignificant effect on the flow because of the low concentration of the particles. When  $\Phi_p$  is in the region from  $10^{-6}$  to  $10^{-3}$ , the momentum transfer from the particles is large enough to alter the turbulence structure. This interaction is called two-way coupling. In the third regime, due to the increased particle loading,  $\Phi_p > 10^{-3}$ , flows are referred to as dense suspension. In addition to the two-way

coupling between the particles and turbulence, particle to particle collision takes place, which can be termed as four-way coupling.

Table 2.4 Diffusion terms and source terms in the governing equations

Variable	$\phi$	$\Gamma_\phi$	$S_\phi$
x velocity	U	$\mu_{eff} = \mu + \mu_t$	$-\frac{\partial P}{\partial x} + \frac{\partial}{\partial x} \left( \mu_{eff} \frac{\partial u}{\partial x} \right) + \frac{\partial}{\partial y} \left( \mu_{eff} \frac{\partial u}{\partial x} \right) + \frac{\partial}{\partial z} \left( \mu_{eff} \frac{\partial u}{\partial x} \right)$
y velocity	V	$\mu_{eff} = \mu + \mu_t$	$-\frac{\partial P}{\partial y} + \frac{\partial}{\partial x} \left( \mu_{eff} \frac{\partial u}{\partial y} \right) + \frac{\partial}{\partial y} \left( \mu_{eff} \frac{\partial u}{\partial y} \right) + \frac{\partial}{\partial z} \left( \mu_{eff} \frac{\partial u}{\partial y} \right) - \rho g$
z velocity	W	$\mu_{eff} = \mu + \mu_t$	$-\frac{\partial P}{\partial z} + \frac{\partial}{\partial x} \left( \mu_{eff} \frac{\partial u}{\partial z} \right) + \frac{\partial}{\partial y} \left( \mu_{eff} \frac{\partial u}{\partial z} \right) + \frac{\partial}{\partial z} \left( \mu_{eff} \frac{\partial u}{\partial z} \right)$
Kinetic energy	k	$\alpha_k \mu_{eff}$	$G_k + G_B - \rho \varepsilon$
Dissipation rate	$\varepsilon$	$\alpha_\varepsilon \mu_{eff}$	$C_{1\varepsilon} \frac{\varepsilon}{k} (G_k + C_{3\varepsilon} G_B) - C_{2\varepsilon} \rho \frac{\varepsilon^2}{k} - R_\varepsilon$
Temperature	T	$\frac{\mu}{Pr} + \frac{\mu}{\sigma_T}$	$S_T$
Concentration	C	$\frac{\mu}{S_C} + \frac{\mu}{\sigma_C}$	$S_C$

where,  $G_k = \mu_t S^2$ ,  $S = \sqrt{2S_{ij}S_{ij}}$ ,  $S_{ij} = \frac{1}{2} \left( \frac{\partial u_j}{\partial x_i} + \frac{\partial u_i}{\partial x_j} \right)$ ,  $G_B = \beta T_g \frac{\mu_t}{\sigma_T} \frac{\partial T}{\partial y}$ ,

$\mu_t = \rho C_\mu \frac{k^2}{\varepsilon}$ ,  $C_\mu = 0.0845$ ,  $C_{1\varepsilon} = 1.42$ ,  $C_{2\varepsilon} = 1.68$ ,  $C_{3\varepsilon} = \tanh \left| \frac{v}{\sqrt{u^2 + w^2}} \right|$ ,

$\sigma_T = 0.85$ ,  $\sigma_C = 0.7$ ,

$$\alpha_k = \alpha_\varepsilon \text{ is calculated by equation } \left| \frac{\alpha - 1.3929}{\alpha_0 - 1.3929} \right|^{0.6321} \left| \frac{\alpha + 2.3929}{\alpha_0 + 2.3929} \right|^{0.3679} = \frac{\mu}{\mu_{eff}}$$

in which,  $\alpha_0 = 1.0$ . If  $\mu \ll \mu_{eff}$ , it can be concluded that  $\alpha_k = \alpha_\varepsilon \approx 1.393$

$$R_\varepsilon = \frac{C_\mu \rho \eta^3 (1 - \eta/\eta_0)}{(1 + \beta \eta^3)} \times \frac{\varepsilon^2}{k}, \text{ where } \eta = Sk/\varepsilon, \eta_0 = 4.38, \beta = 0.012$$

For droplets generated during respiratory activities, the diameter mainly falls in the range of O(1  $\mu\text{m}$ ) to O(1000  $\mu\text{m}$ ) (Nicas et al. 2005) and rapidly shrinks by approximately 50% when exposed to indoor air by evaporation. Most droplet nuclei lie in the region of O(1~10  $\mu\text{m}$ ) (Morawska et al. 2008). The estimated total number of droplets expelled ranges from 947 to 2085 per cough and 112 to 6720 for speaking (Chao et al. 2009). Assuming three consecutive coughs happened in a office with a volume of 32  $\text{m}^3$ , the estimated concentration of droplets would ranges from  $10^{-9}$  to  $10^{-7}$ . This demonstrates that it is fairly reliable to employ one-way coupling approach in simulating the dispersion of respiratory droplets indoor.

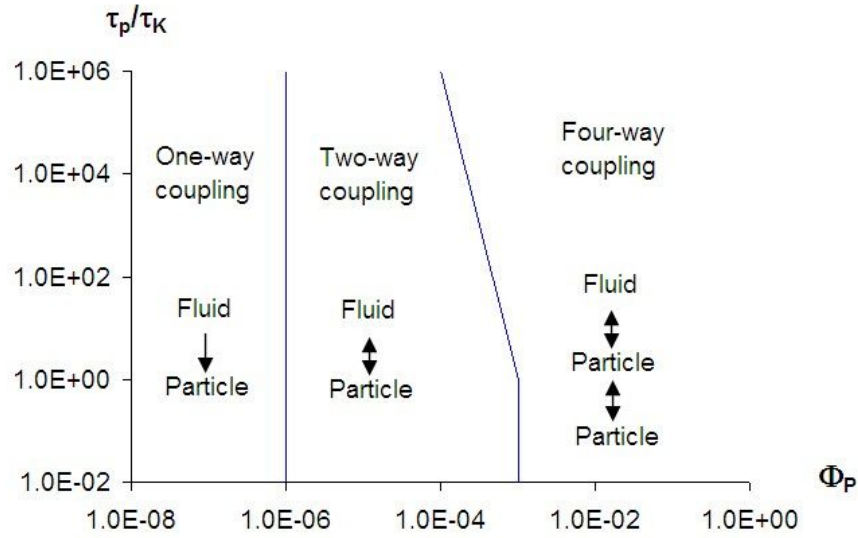


Figure 2.7 Map of regimes of interaction between particles and turbulence

(Reproduced from S. Elghobashi, 1994)

With regard to the distribution of exhaled droplets in one-way coupling regime, a commonly used simplified Eulerian drift-flux model can be employed (Chen et al., 2006, Lai and Chen 2006). The term ‘drift-flux’ stands for particle flux caused by effects other than convection, such as gravitational settling, Brownian, and turbulent diffusion. The advantage of this approach is the feasibility of incorporating other external forces. The governing equation of particle concentration is similar to Navier-Stokes equations, except that it integrates the gravitational settling effect of particles into the convection term:

$$\frac{\partial(\rho C)}{\partial t} + \nabla \cdot (\rho(\vec{V} + \vec{V}_s)C) = \nabla \cdot \left( \frac{\mu_{eff}}{\sigma_C} \right) + S_C \quad (2.4)$$

where,  $\rho$  is the density of the air,  $C$  is particle mass concentration,  $\vec{V}$  is vector of air velocity,  $\vec{V}_s$  is vector of particle settling velocity,  $\mu_{eff}$  is effective viscosity,  $\sigma_c$  is a non-dimensional number.

The gravitational settling velocity of particles ( $\vec{V}_s$ ) is calculated by Stokes equation (Hinds 1999). Here  $\sigma_c$  is set as 1.0. The term  $\mu_{eff} / \partial_c$  can also be written as  $D_p + \varepsilon_p$ , in which  $D_p$  is Brownian diffusivity and  $\varepsilon_p$  is turbulent viscosity. The equation above is discretized directly into algebraic equation by the finite volume method, not like the other numerical treatments in which the settling term  $\rho \vec{V}_s C$  is moved into the source term. The drift-flux model is not a fully-coupled multi-fluid model, and in the progress of CFD calculation the indoor flow field and temperature field are solved firstly.

### **2.6.3 Governing equation for particle deposition**

Particles deposit onto surfaces from turbulent flows by a variety of mechanisms. Factors known to influence deposition rates include particle size, surface roughness, airflow near surfaces, particle spatial distribution, and the orientation of the deposition surface with respect to gravity. Many experiments have been conducted to investigate the effects of various parameters on the deposition of suspended particles (Liu 1974, McCoy 1977, Wells 1967). Although the obtained data are considerably scattered, they illustrate the basic characteristics of particle deposition,

as shown in Figure 2.8, where  $V_d^+$  refers to the dimensionless particle deposition velocity and  $\tau^+$  is the dimensionless particle relaxation time.

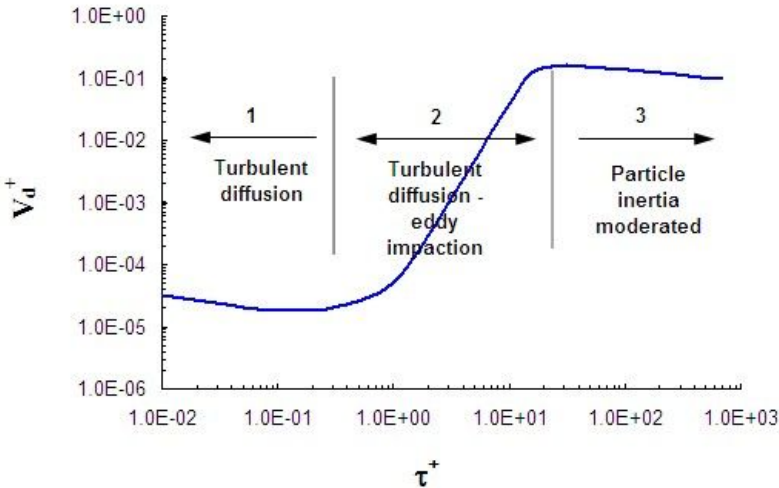


Figure 2.8 A typical variation in measured deposition rate with particle relaxation time in fully developed vertical pipe flow (From Guha, 2009)

As illustrated in Figure 2.8, the variation of particle deposition falls into three distinct categories. In the first region, the deposition velocity decreases with particle diameter. This is the so-called turbulent diffusion regime. The striking feature of the next zone, the eddy diffusion-eddy impaction regime, is that the deposition velocity increases by three to four orders of magnitude. The third regime, usually termed as the particle inertia moderated regime, results in an eventual decrease in the deposition velocity for large particles.

For indoor air movement, the friction velocity is usually in the range of several centimeters per seconds (0.1-3.0 cm/s) (Lai 1999). Regarding the human respiratory droplets studied, their diameters range from  $O(1 \mu\text{m})$  to  $O(1000 \mu\text{m})$  with majority of them less than  $100 \mu\text{m}$  (Nicas 2005). The corresponding dimensionless relaxation time is around 0.17 for  $100 \mu\text{m}$  droplets assuming the friction velocity equals 3.0 cm/s. This implies that Fick's law of diffusion can be safely employed to estimate the deposition of respiratory droplets indoor.

One commonly employed deposition model is from Lai and Nazaroff (1999) for indoor low velocity environments. This semi-empirical model links the air velocity to the macro-deposition velocity with no consideration given to the effect of spatial distribution of particles. Besides Brownian and turbulent diffusion mechanisms, this model also account for the effect of gravitational settling for horizontal surfaces. With the assumption that the deposition flux is one-dimensional and constant in the concentration boundary layer, and the particle eddy diffusivity equals the fluid turbulent viscosity ( $\varepsilon_p = \nu_t$ ), the dimensionless deposition velocity can be expressed by the following equation:

$$V_d^+ = \frac{V_s^+}{\exp(V_s^+ I) - 1}, \text{ downward surface,} \quad (2.5)$$

$$V_d^+ = \frac{1}{I}, \text{ vertical surface,} \quad (2.6)$$

$$V_d^+ = \frac{V_s^+}{1 - \exp(-V_s^+ I)}, \text{ upward surface,} \quad (2.7)$$

where,  $V_s^+ = V_s / u^*$  ,  $V_d^+ = V_d / u^*$  ,  $I = \int_{r^+}^{30} (\frac{v}{\varepsilon_p + D_p}) dy^+$  ,  $y^+ = y u^* / \nu$  ,  
 $r^+ = (d_p / 2)(u^* / \nu)$ ,  $V_s$  refers to particle settling velocity,  $V_d$  is particle deposition velocity,  $\nu$  means kinetic air viscosity,  $D_p$  is Brownian diffusivity,  $y$  refers to the normal distance between the wall and the first cell center,  $d_p$  is particle diameter,  $u^*$  refers to friction velocity

#### 2.6.4 Evaluation indices

To compare the influences of different ventilation methods on the co-occupant's exposure, the index inhaled fraction ( $IF$ ) (Nazaroff 2004) is adopted and a new index, inhaled dose ( $ID$ ), is defined. The inhaled fraction is defined as the proportion of emitted pollutant mass flow rate from the infected person which is inhaled by the co-occupant, and the inhaled dose is defined as the fraction inhaled by the co-occupant of the total pollutant mass exhaled. For steady respiratory process, the two indices will be the same and adopting inhaled fraction is more convenient, while the coughing maneuver is not continuous and inhaled dose can more accurately quantify the co-occupant's exposure for this transient process. The two indices can be stated as the following two equations:

$$IF = \frac{C_c M_c}{C_I M_I} = \frac{C_c}{C_I} \quad (2.8)$$

$$ID = \frac{\int_0^t C_c M_c dt}{\int_0^T C_I M_I dt} \quad (2.9)$$

Here,  $C_c$  is the inhaled droplet mass fraction for the co-occupant and  $C_I$  is the exhaled fraction from the infected person.  $M_c$  and  $M_I$  are the mass flow rates of inhalation for the co-occupant and exhalation for the infected person respectively.  $T$  refers to the time interval for a respiratory activity.  $IF$  can be best applied for assessing exposure to a constant emission source, while  $ID$  for a instantaneous source.

For a transient coughing process, droplet dispersion is subjected to the high momentum coughing jet at first and indoor air movement later. In order to characterize the effects of ventilation methods on droplets distribution, two indices, including droplets cloud gravity center (CGC) and droplets cloud spatial volume (CSV), are employed to capture the dynamic dispersion course of human respiratory droplets. The two equations are defined as:

$$CGC_h = \frac{\sum C_i M_i (Y_i - Y_o)}{\sum C_i M_i} \quad (2.10)$$

$$CGC_v = \frac{\sum C_i M_i \sqrt{(X_i - X_o)^2 + (Z_i - Z_o)^2}}{\sum C_i M_i} \quad (2.11)$$

Here,  $CGC_h$  and  $CGC_v$  represent horizontal center and vertical center of droplet cloud respectively.  $C_i$  refers to droplet mass concentration in the  $i^{th}$  cell, and  $M_i$  is air mass in the  $i^{th}$  cell.  $X_o$ ,  $Y_o$  and  $Z_o$  are the coordinates of the co-occupant's nose-tip, while  $X_i$ ,  $Y_i$  and  $Z_i$  represent the center position of the  $i^{th}$  cell.

$$CSV = \sum V_i (NC \geq NC_{set}) \quad (2.12)$$

In which,  $V_i$  means the volume of the  $i^{th}$  cell.  $NC$  equal to  $C/C_i$  refers to the normalized droplet concentration in each cell. This equation implies that  $CSV$  only counts the cell when the normalized concentration in this cell ( $NC$ ) is not less than the set concentration ( $NC_{set}$ ).

## **2.7 Importance of present study**

The dispersion of human respiratory droplets in built environments has been widely investigated both numerically and experimentally. However, the research in this area is far from sufficient. Gravitation greatly influences the distribution of exhaled droplets. Droplets with larger diameters preserve higher potential to deposit onto indoor surfaces and maintain lower suspended concentration. It is therefore important to account the effects of gravitational forces in studying the transportation of exhaled droplets and evaluating the occupant's exposure. Meanwhile, the convective airflow around human body can transport the contaminants in the lower level to occupant's breathing zone and being inhaled, at the same time it may also protect occupants from the horizontal dispersion of pollutants. Including an exposed person in the research domain can present a more reliable exposure level. Furthermore, assessing the occupant's exposure to the coughed/sneezed droplets during the first several seconds can not illustrate the whole picture of disease transmission. With the dissipation of the high momentum coughing jet, air distribution system can gradually disperse the exhaled droplets to be widely distributed in room and induce a long-term exposure for occupants. The last but not least, a systematic research on the effects of the three commonly employed

ventilation systems can build a general understanding on the designing of air distribution methods with the intention to reduce infection transmission. The performances of various complementary approaches, including coughing orientations, physical interventions, PV devices, are also discussed under different ventilation schemes in order to generalize some personal protection strategies.

## **2.8 Summary**

This chapter reviews the characteristics of human respiratory activities and exhaled droplets, and also discussed transmission modes of infectious diseases and general approaches in mitigating infection spread. Larger respiratory droplets will settle down very quickly after generation, while smaller droplets can remain suspended for a long period of time. Among these, droplets smaller than 10  $\mu\text{m}$  can be readily inhaled, reach the alveolar region of respiratory system, and cause severe damages. Meanwhile, researches show that non-pharmaceutical interventions, including personal protection, PV, and air distribution system, play an important role in the prevention and reduction of infectious disease transmission for the whole pandemic period, especially at the beginning. This thesis therefore aims to investigate the influences of ventilation system and various personal protection strategies on the dispersion of human respiratory droplets, especially for droplets less than 10  $\mu\text{m}$ , and occupant's exposure.

This thesis also gives a review on the numerical simulation models used for indoor air movement and droplet dispersion. In the following numerical simulation chapters,

the renormalization group (RNG)  $k-\varepsilon$  model is employed to simulate indoor air movement. Standard logarithmic law wall functions are adopted to bridge the solution variables at the near-wall cells and the corresponding quantities on the adjacent wall. Boussinesq assumption is chosen in the momentum equations to account for the change of air density due to temperature variation. The SIMPLE algorithm is employed to couple the pressure and velocity fields. A simplified Eulerian method, drift-flux model, is adopted to calculate the dispersion of respiratory droplets. To account for droplets deposition onto indoor surfaces, a semi-empirical model is adopted with the assumption that the deposition flux is one-dimensional and constant in the concentration boundary layer.

## **Chapter 3**

# **Experimental Studies of Droplet Dispersion in a Room with Displacement Ventilation System**

### **3.1 Introduction**

In contrast to MV and UFAD, DV can deliver more conditioned fresh air to occupants' breathing zone directly by serving at floor level and improve the quality of inhaled air (Gao et al. 2008; Li et al. 2011; Qian et al. 2006). The temperature stratification pattern however may facilitate the transportation of exhaled contaminants in breathing height and increase personal exposure for occupants close to the source. It has been reported that a distance of 1.2 m away from the source can prevent the exposed person from direct exposure to respiratory droplets during normal breathing process (Björn and Nielsen 2002). Suspended droplets can still be transmitted to the breathing zone of occupants through airborne transmission and pose significant health risk. Up to now, many experimental studies have been conducted to investigate the dispersion of respiratory droplets or particles in mechanical ventilated environments (Chao and Wan 2004; Chao et al. 2008; Lai and Wong 2010; Qian et al. 2006 and 2008, Zhang and Chen 2006).

Research shows that human respiratory droplets can travel a longer distance horizontally in breathing level and then pose higher health risk for the susceptible

person (Mui et al. 2008; Qian et al. 2006). Droplets with large diameters present different traveling trajectories as tracer gas. Understanding the horizontal transportation of exhaled droplets is extremely important for developing approaches to mitigate infection transmission. Qian et al. (2006 and 2008) has reported that droplets breathed through mouth or nose may present different traveling trajectories and pose different health risk for the susceptible person (Qian et al. 2006 and 2008). Breathing air temperature varies with indoor environment (Höppe 1988), which will also exert some influences on the dispersion of carried droplets. Furthermore, the body heat of occupant may influence the transportation of human respiratory droplets due to the convective airflow around the body and the formation of thermal plume.

These factors affecting the spatial distribution of human respiratory droplets in a size range from 0.8  $\mu\text{m}$  to 10  $\mu\text{m}$  are experimentally investigated, and the personal exposure of the co-occupant in a full-scale DV ventilated room is evaluated.

## **3.2 Material and methods**

### **3.2.1 Experimental chamber**

Figure 3.1 presents a schematic drawing of the full-scale experimental chamber. The dimensions of this room are 4.0 m long, 2.7 m wide and 2.4 m high. A wall-mounted diffuser (1.0 m  $\times$  0.6 m) is installed at floor level to supply conditioned air at a low speed. Return grille (0.3 m  $\times$  0.3 m) responsible for circulating about 60% airflow rates is mounted in the ceiling level, while the exhaust air is extracted from

the ceiling gaps and through the ceiling-mounted lamps. Two thermal manikins, a source manikin and an exposed manikin, are placed in the chamber to represent two working people, the polluting person and the co-occupant, with the original setting displayed in Figure 3.1.

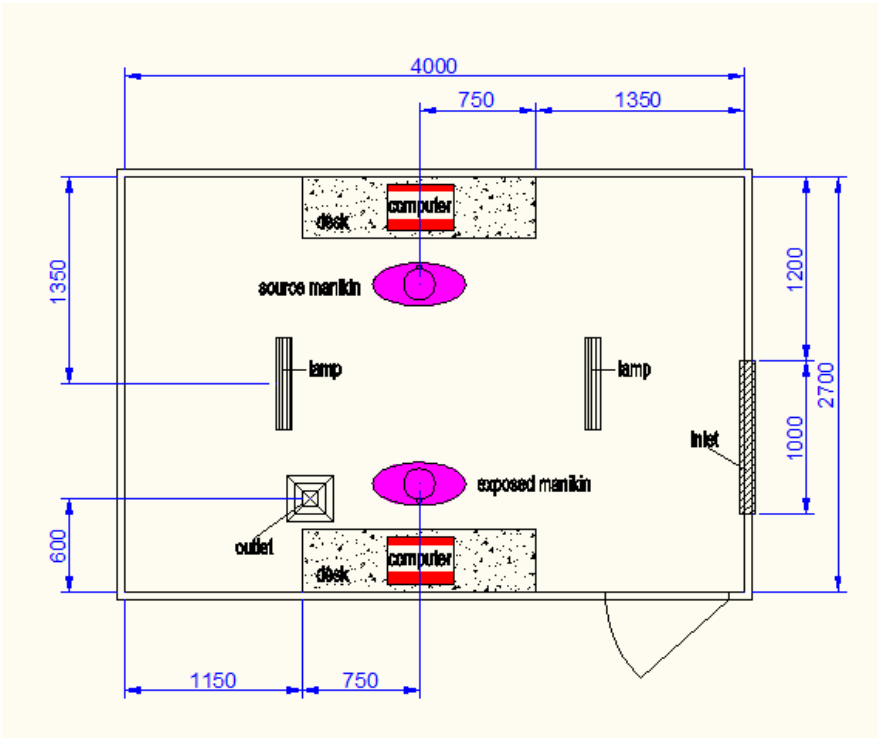


Figure 3.1 Schematic drawing of the experimental chamber

Particle experiment is conducted with the two people sitting face-to-face with a roughly 1.5 m distance between their nose-tips in order to simulate a discussion scenario (Figure 3.2) in view of the previous findings of tracer gas experiments (Bjørn and Nielsen 2002, Olmedo et al. 2012, Qian et al. 2006) and numerical simulations (Gao et al. 2008, Zhu et al. 2006) that highest personal exposure can be induced in this face-to-face situation. Heat sources in the chamber include two

manikins, two sets of computers, and two lamps. The total heat loads are 440 W, and the heat loads of for each manikin, computer, and lamp are 80 W, 120 W and 20 W respectively. All the walls are well insulated and can be considered as adiabatic surfaces.

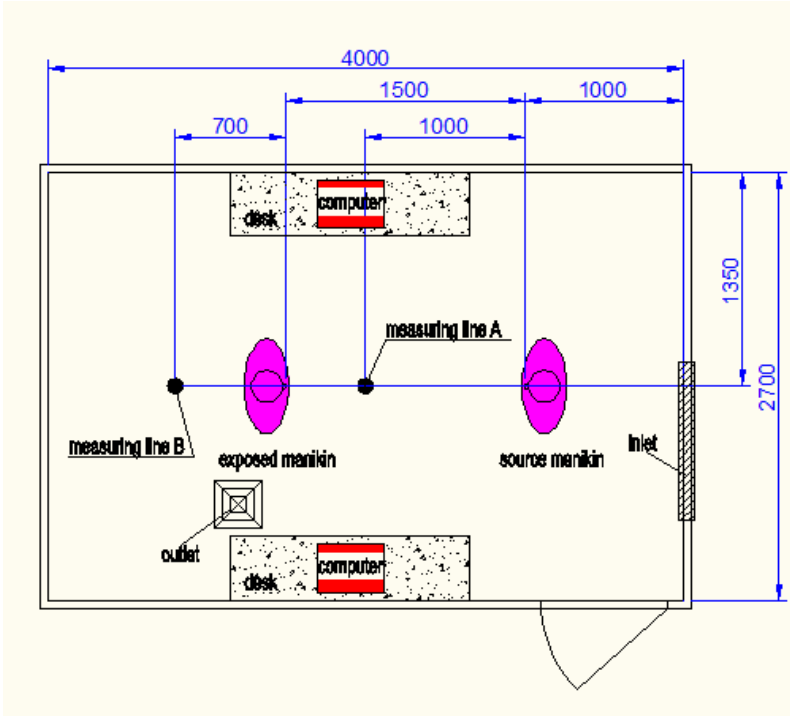


Figure 3.2 Arrangements during particle experiment

**3.2.2 Experimental equipments**

*3.2.2.1 Particle generation system.*

An assembled particle generation system, as shown in Figure 3.3, can generate poly-dispersed particles in the size range from 0.1 μm to 10 μm with an average diameter about 2 μm, based on the collision type atomizer for atomizing liquids and suspensions. In the atomizer, compressed air is used to aspirate the contained liquid into a sonic velocity gas jet in which it is sheared into droplets. The solution used

for particle generation is Di-Ethyl-Hexyl-Sebacat (DEHS) which is a non-soluble liquid with a density of  $912 \text{ kg/m}^3$  and low evaporation rate. As depicted in Figure 3.3, the compressed air is first filtered and gauged, and then injected to the atomizer in which the solution is contained. The particles from the atomizer are then introduced to a Nafion dryer to be dried, and neutralized by the following electrical neutralizer. Finally, these neutralized particles are diluted by compressed gas in the mixing bottle to achieve the intended concentration, and imparted to the experimental chamber.



Figure 3.3 Particle generation system

#### *3.2.2.2 Particle concentration measurement instruments*

A Grimm portable aerosol spectrometer (Model 1.108, Grimm Aerosol Technik GmbH & Co. KG, Germany) is used to continuously monitor particle concentration at a height of 1.2 m and a distance of 1 m away from the source, in order to ensure that the particle generation system operates stably during the measuring process.

This instrument can detect particles in the size range of 0.3 - 20  $\mu\text{m}$  in 15 size channels in real time. An optical particle sizer spectrometer (Model 3330, TSI Incorporated, USA) is employed to measure particle distribution and exposure of the exposed person point by point, with a sampling airflow rate of 1.0 L/min  $\pm$  5%.

### 3.2.2.3 Thermal manikin

The two thermal manikins are made of hard plastic human body wound with low-voltage electrical wire and then wrapped with tinfoil all over the body surfaces (Figure 3.4). The two manikins are dressed to a clothing level of approximately 1.0 clo as that for a typical office environment. Each manikin generates a sensible heat of 80 W with 15 controlled segments as seen in Table 3.1. The breathing level lies at a height of about 1.2 m above the floor at a seated position while 1.8 m for a standing position.



Figure 3.4 Picture of the two employed manikins

Table 3.1 Heat loads for each segment of the manikin

Segment	Heat load (W)	Segment	Heat load (W)
Head	18.4	Right hand	0.42
Neck	0.43	Left thigh	4.02
Trunk	47.6	Right thigh	4.02
Left fore-arm	1.74	Left leg	2.37
Left upper-arm	1.18	Right leg	2.37
Right fore-arm	1.74	Left foot	0.6
Right upper-arm	1.18	Right foot	0.6
Left hand	0.42		

### 3.2.3 Experimental design

All the experiments are conducted in a full-scale DV ventilated chamber with two thermal manikins sitting face to face with a roughly 1.5 m distance between their nose-tips as displayed in Figure 3.2. During the experiment period, conditioned air is constantly supplied at a flow rate of 80 l/s which correspond to an air change rate of nine times per hour. The conditioned air supplying temperature varies with the total heat loads indoors, while the average air temperature in the breathing level is maintained around 23.5°C. Compressed air carrying the generated droplets enters the experimental chamber through a tygon tube at a flow rate of 5 l/min and an average velocity of 1 m/s. This total air flow rate of compressed air carrying the generated particles is well controlled during the entire experimental process, while

the compressed air flow rate for particle atomizing, drying and dilution may vary slightly case by case. Therefore, the generated droplet size distribution profiles will be different for each case. A normalized data will then be employed to account for this difference in order to make comparisons between cases. The exit outlet of the tygon tube is attached on the polluting manikin and positioned 45° downward to simulate a nose breathing process and horizontal for mouth breathing. The compressed air can be heated up to  $32 \pm 0.5^{\circ}\text{C}$  representing a real breathing airflow (Höppe 1981).

The experimental study consists of six cases as summarized in Table 3.2 to investigate the effects of breathing mode, temperature of breathing air, and body heat of occupant on the spatial distribution of droplet residuals in exhaled air. The performances of these parameters on personal exposure of the co-occupant are also evaluated for the six cases when the co-occupant is facing to or backing to the face of the polluting source.

Air temperatures in the vertical directions of two locations, A and B as depicted in Figure 3.2, are constantly recorded at the heights of 0.1 m, 0.6 m, 1.1 m, 1.7 m, and 2.1 m. Particle concentration is measured point by point vertically at the two positions using TSI 3330 instrument. The measuring period for each point lasts 30 min and around 60 data will be obtained. An average value of these data is used to represent the particle concentration for each size bin at this point. The GRIMM 1.108 instrument is used to continuously monitor particle concentration at a fixed

point to ensure that particles at each size bin are stably generated throughout each experimental case. To evaluate the exposure level of the exposed person, particle concentration is measured at a point right in front of the exposed person's nose (Pantelic et al. 2009).

Table 3.2 Description of the six experimental cases

Case No.	Power of source manikin (W)	Power of exposed manikin (W)	Temperature of released airflow (°C)	Exhalation mode of source manikin	Facing orientation
1	80	80	32	Nose breathing	Face-to-face
2	80	80	32	Mouth breathing	
3	80	80	25	Nose breathing	/
4	80	80	25	Mouth breathing	Back-to-face
5	0	80	32	Nose breathing	
6	80	0	32	Nose breathing	

### 3.3 Results

#### 3.3.1 Air temperature distribution

To ensure that a steady or quasi-steady air condition is maintained in the experimental chamber during particle experiments, the wall surface temperatures and air temperatures in the two vertical lines at A and B (Figure 3.2) are constantly

monitored. It is found that a stable indoor environment can be achieved around three to four hours after the ventilation system is turned on.

Air temperature variations along the two vertical lines, A and B, are displayed in Figure 3.5 for case 1, case 5, and case 6 in which conditioned air is supplied at 17.5 °C, 18°C, and 18°C respectively. The temperature distribution in line A remains almost the same in all the three cases. Slight temperature differences in the lower space can be noticed in line B due to the different cooling loads in the room. The temperature distribution profiles well represent the airflow patterns for a typical DV ventilated room.

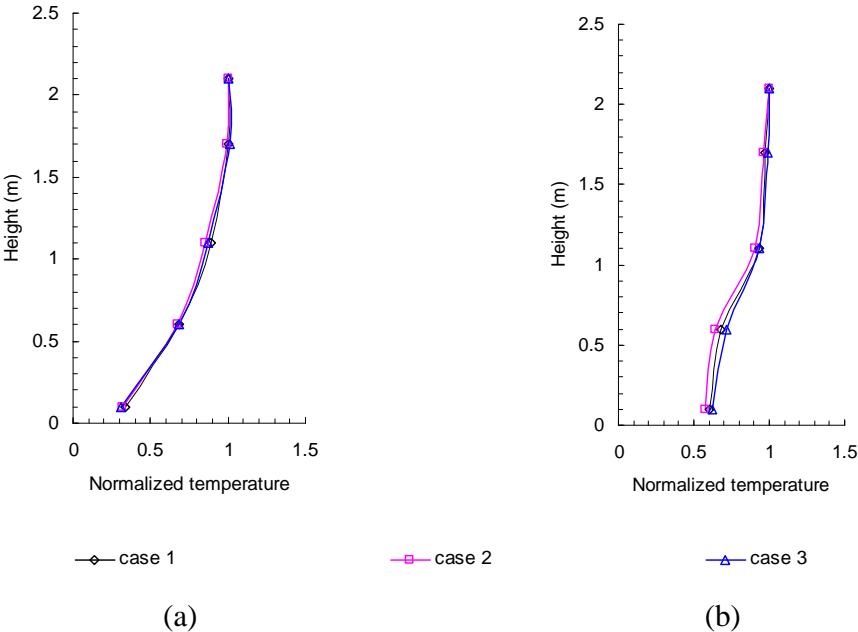


Figure 3.5 Normalized air temperature distribution in line A (a) and line B (b) ( $T_{norm} = (T_{local} - T_{in}) / (T_{out} - T_{in})$ )

### **3.3.2 Background particle concentrations**

A HEPA filter is installed in the air-supplying duct to provide a clean indoor environment. Background concentration of suspended particles in the chamber is continuously measured for several hours in different time of different days. It is found that there are small variations in the background concentration for all particle size bins. The background fine particles concentrations are about two orders of magnitude below the generated concentration. No large particles are detected during the background particle concentration measurements.

### **3.3.3 Horizontal dispersion of released particles**

The flow rate for particle carrying air is 5 l/min, which is an average breathing flow rate of a person. The particles-laden air enters the room horizontally at a velocity of 1 m/s and a height of 1.2 m from the end wall, as shown in Figure 3.6. Particle concentration at nine points, as shown in Figure 3.7, at the breathing height of 1.2 m is measured point by point using GRIMM 1.108.

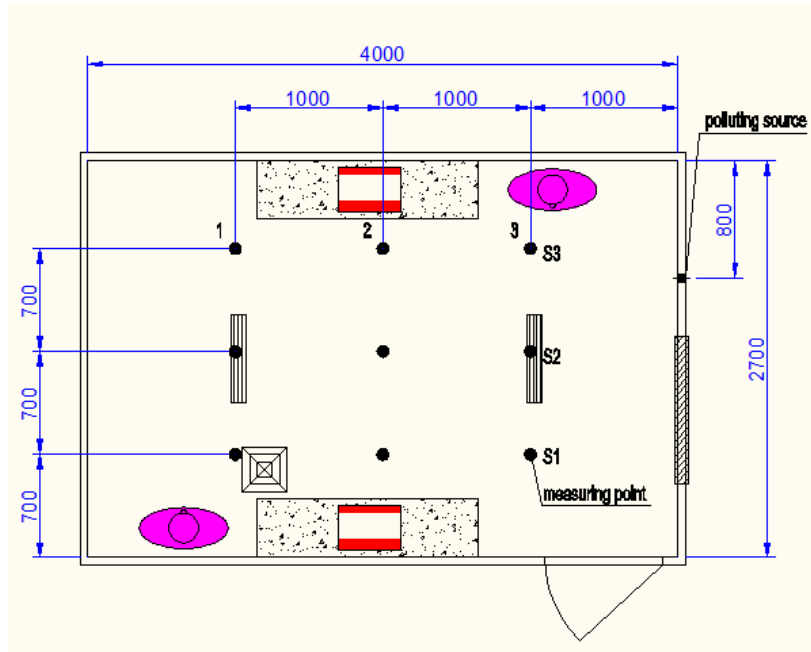


Figure 3.6 Measuring points for particle horizontal dispersion

Assuming particle concentration at point (3, S3) is unit for all size bins, Figure 3.7 presents the normalized concentration distribution for particles of different diameters in the breathing level.

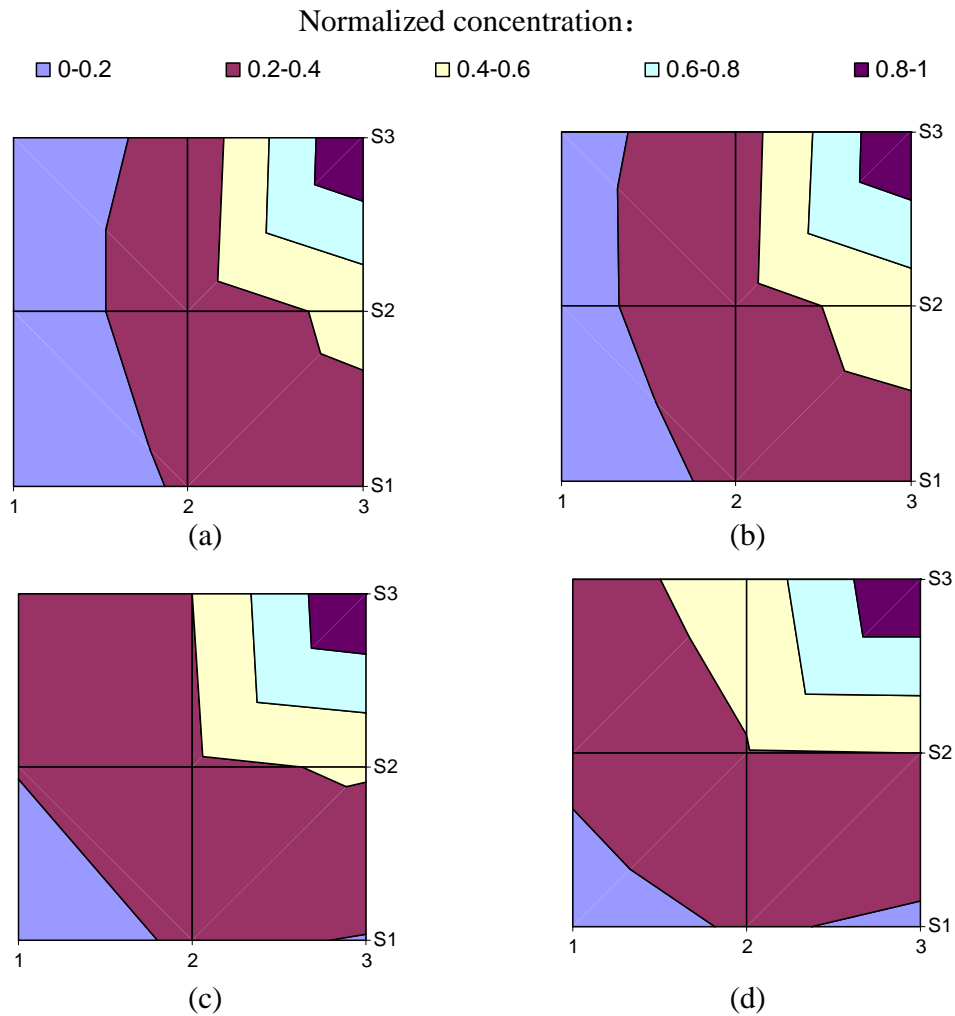


Figure 3.7 Horizontal distribution of particles with  $D_p \leq 1.0 \mu\text{m}$  (a),  $1.0 \mu\text{m} < D_p \leq 3.0 \mu\text{m}$  (b),  $3.0 \mu\text{m} < D_p \leq 5.0 \mu\text{m}$  (c),  $5.0 \mu\text{m} < D_p \leq 10.0 \mu\text{m}$  (d) (Particle concentration in point (3, S3) is denoted as 1.0 for all size bins)

Particle concentration decreases with the increasing distance to the polluting source for all size bins. There are still some differences in the distribution profiles. Larger particles in the size range of  $5 \mu\text{m} \sim 10 \mu\text{m}$  can travel a farther distance away from the polluting source than smaller particles in the size range below  $3.0 \mu\text{m}$ . The

possible reason is that smaller droplets can be easily driven to the upper space, while larger droplets with higher gravitational forces can largely remain in the occupied zone and be horizontally transported to the region far away from the source by air turbulence.

### **3.3.4 Vertical distribution of particles**

#### *3.3.4.1 Effects of exhalation mode*

Figure 3.8 presents the vertical particle distributions along the two measuring lines when breathing via nose (Case 1) and breathing through mouth (Case 2). Particle concentration is normalized by the value measured at the height of 1.2 m in line A for each case. Since the upward airflow of DV may impede the downward movement of nose breathing air, the breathing air is decelerated and driven to the upper zone. This results in a peak concentration in the height of 1.7 m for fine particles in line A, and in the breathing height for particles of all sizes in line B. Regarding larger particles, the peak concentration occurs at the breathing height of 1.2 m, presumably because their higher gravitational forces tend to balance with the upward drag forces, resulting the trapping effects in the breathing level. Meanwhile, air turbulence can significantly disperse these suspended particles to a longer distance away from the source as presented in Figure 3.7.

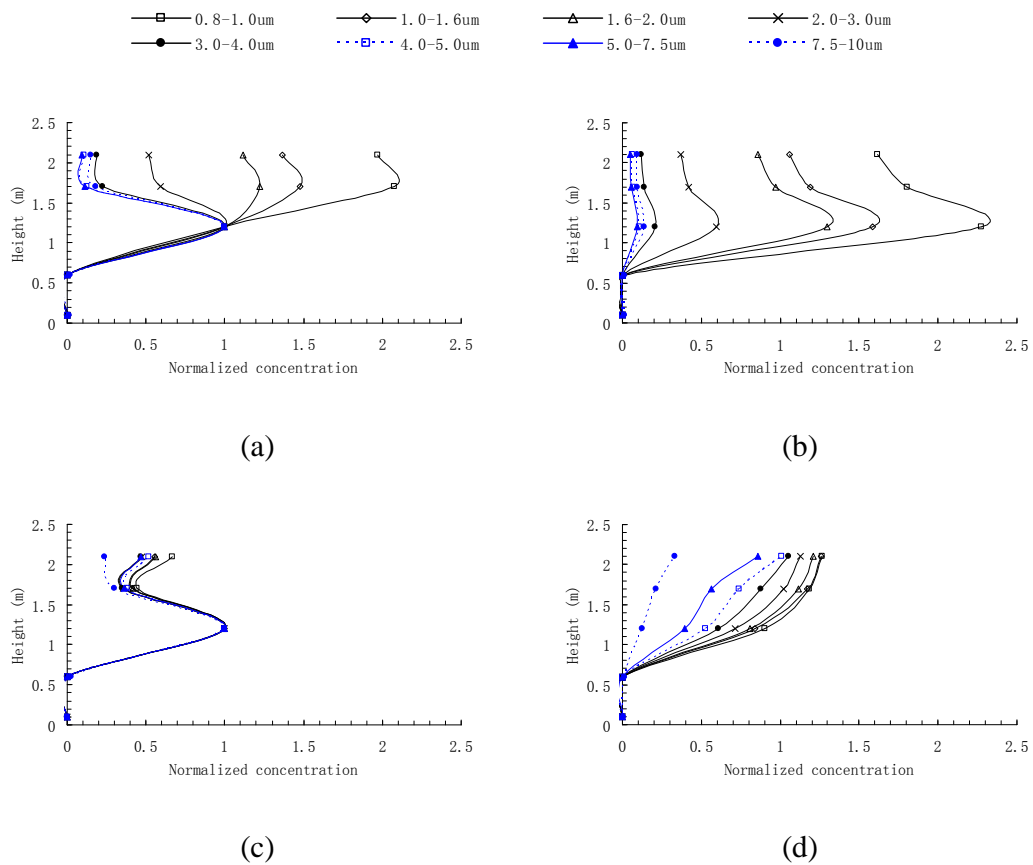


Figure 3.8 Particle distributions with breathing air heated to 32°C (line A (a) and line B (b) for Case 1 breathing through nose, and line A (c) and line B (d) for Case 2 breathing through mouth. Particle concentration at 1.2 m height of line A is denoted as 1.0).

Breathing through mouth, on the other hand, generates quite different indoor particle distribution patterns, especially along line B farther away from the source. Particles released at a horizontal direction can travel a longer distance horizontally (Qian et al. 2006), which results in a peak particle concentration at breathing height along line A. Particle concentration along line B increases with the height for all the size bins and the concentration at breathing height is lower than that along line A. These findings

suggest that exhalation through nose, compared with mouth breathing, can affect a larger region in a room and the personal exposure of the susceptible person that sits/stands at a distance farther away from the source.

Particle distributions when the particle-carrier air is delivered at a room temperature of 25°C are displayed in Figure 3.9 for Case 3 breathing through nose and Case 4 breathing via mouth. The distribution profiles are quite similar with Case 1 and Case 2 when the breathing air temperature is 32°C. Nose breathing generates the maximum particle concentration at the height of 2.1 m in line A for fine particles, but leads to the maximum concentration at the breathing height for particles larger than 2µm. Differently, breathing through mouth leads to the higher contaminant concentration at the upper zone of line B.

The possible reason is that particle-carrier air released at a temperature close to room temperature has more chances to stay in the breathing height. The upward air movement of DV may disperse more particles released at a 45° downward orientation to the breathing height at a 1.0 m distance from the source such as line A, resulting in a relatively lower particle concentration in line B farther away from the source. On the other hand, particles released horizontally can be more readily driven upward and result in higher particle concentration in the upper zone of line B due to air turbulence.

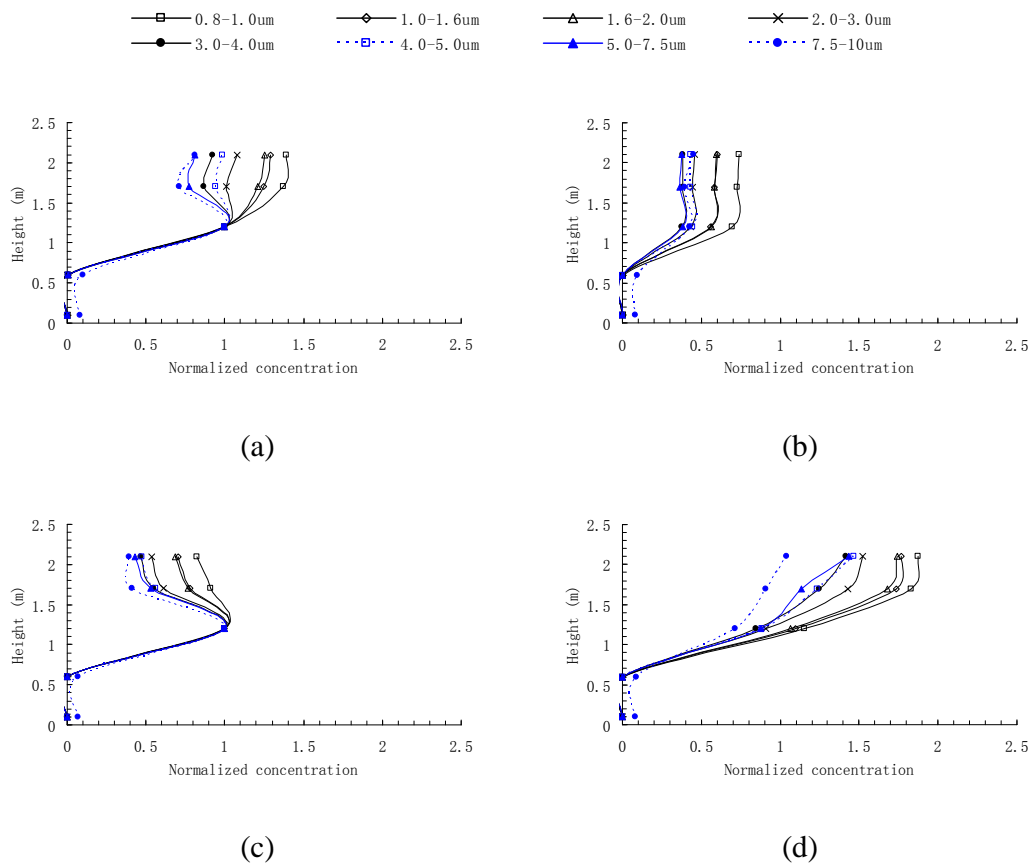


Figure 3.9 Particle distributions with breathing air delivered at a temperature of 25°C (line A (a) and line B (b) for Case 3 breathing through nose, and line A (c) and line B (d) for Case 4 breathing through mouth. Particle concentration at 1.2 m height of line A is denoted as 1.0).

#### 3.3.4.2 Effects of breathing air temperature

The effects of breathing air temperature on indoor particle distribution are presented in Figure 3.10 when the polluting person breathes through nose at a face-to-face orientation with the co-occupant. Breathing at a higher temperature can facilitate the upward movement of exhaled air because of the larger temperature difference between the breathing air and ambient air, resulting in higher concentration for fine

particles in the upper region, but higher concentration in the breathing height for larger particles due to the higher gravitational effects. Breathing at a relatively lower temperature presents quite different particle distribution patterns. The generated particles are more uniformly distributed. In the higher space of the room, normalized concentration is reduced for fine particles but increased for larger particles. Meanwhile, higher normalized concentration was found in the region below the breathing level for larger particles.

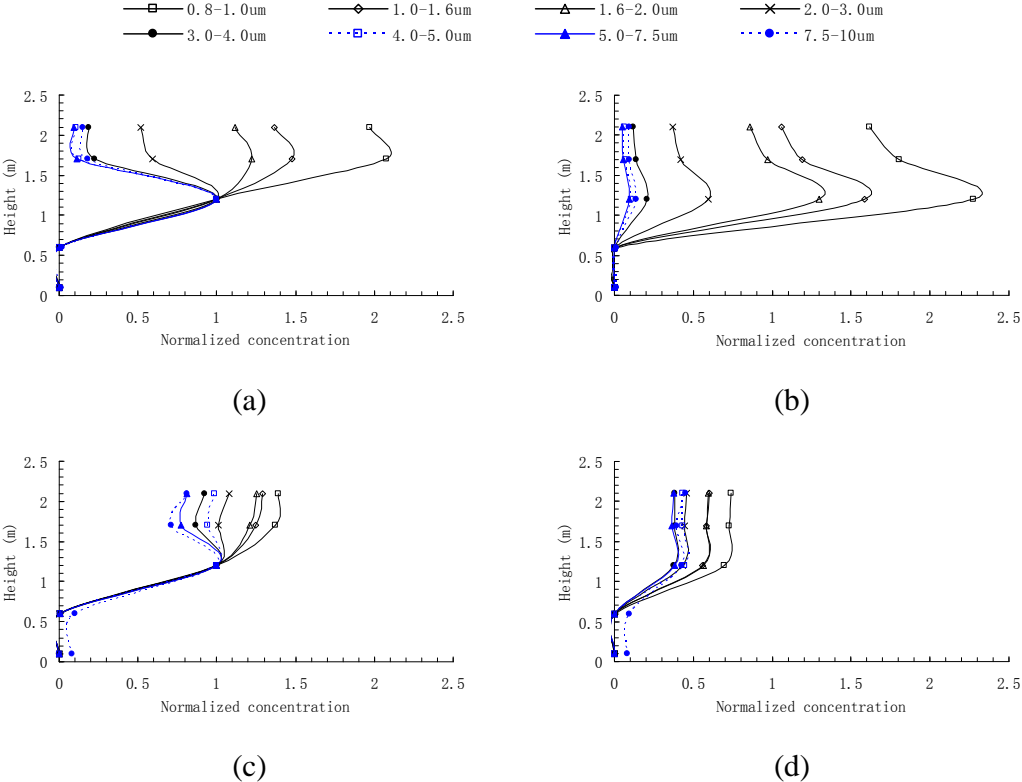


Figure 3.10 Particle distributions when breathing through nose (line A (a) and line B (b) for Case 1 at a breathing air temperature of 32°C, and line A (c) and line B (d) for Case 3 of 25°C. Particle concentration at 1.2 m height of line A is denoted as 1.0).

The influences of the breathing air temperature when exhaling through mouth are compared in Figure 3.11. Particle distribution profiles are quite similar for the two measuring lines, while the normalized particle concentration is obviously higher in line B for all the size bins at a lower breathing air temperature. This is different from nose breathing process in which lower particle concentration is induced in line B farther away from the source.

#### *3.3.4.3 Effects of body heats from the polluting person and the exposed person*

Figure 3.12 displays particle distributions with and without body heats for the two manikins at a face-to-face orientation. Since the same amount of conditioned air is supplied into the experimental chamber, temperature gradient in the occupied zone will be reduced with the decreasing of indoor heat loads. It can then be expected that particles are more uniformly distributed in the entire room. Highest normalized particle concentration in line A occurs at the height of 1.7 m for fine particles in Case 1 and Case 5, while for Case 6 the highest particle concentration happens at the breathing level for all particles. This may be attributed to the different heat loads for the exposed person. For a lower heat load in Case 6, generated particles can travel a longer horizontal distance since there is no convective airflow around the exposed person.

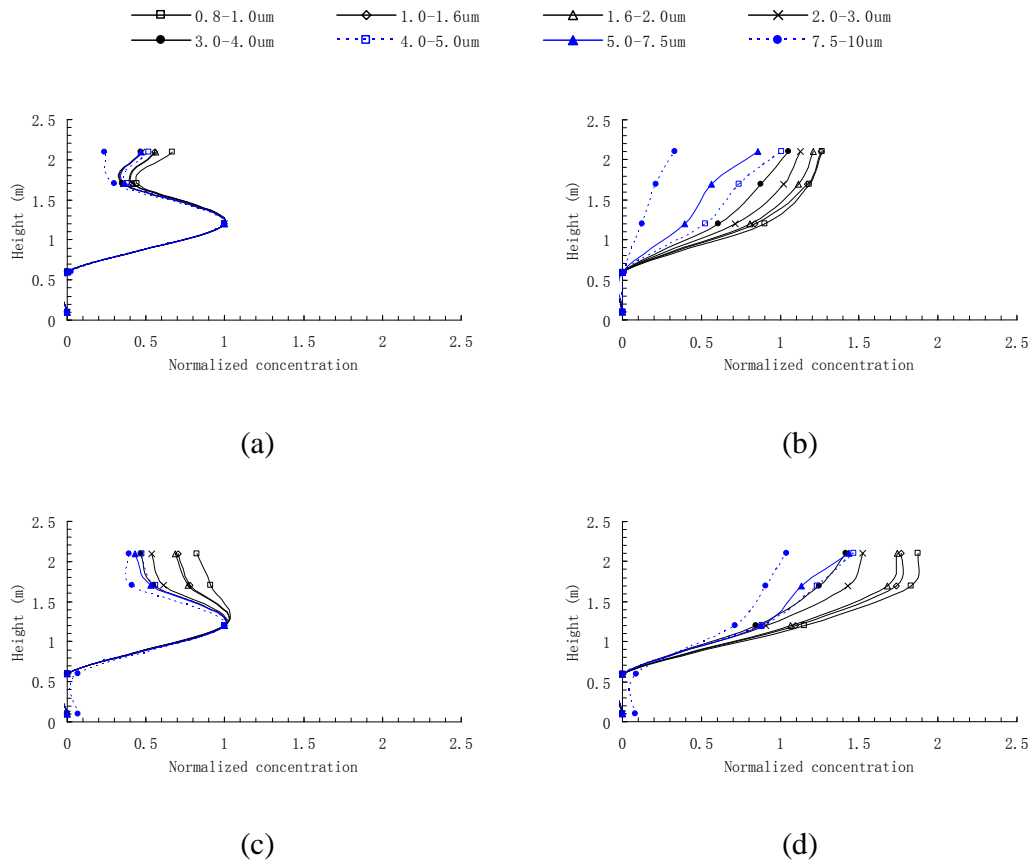
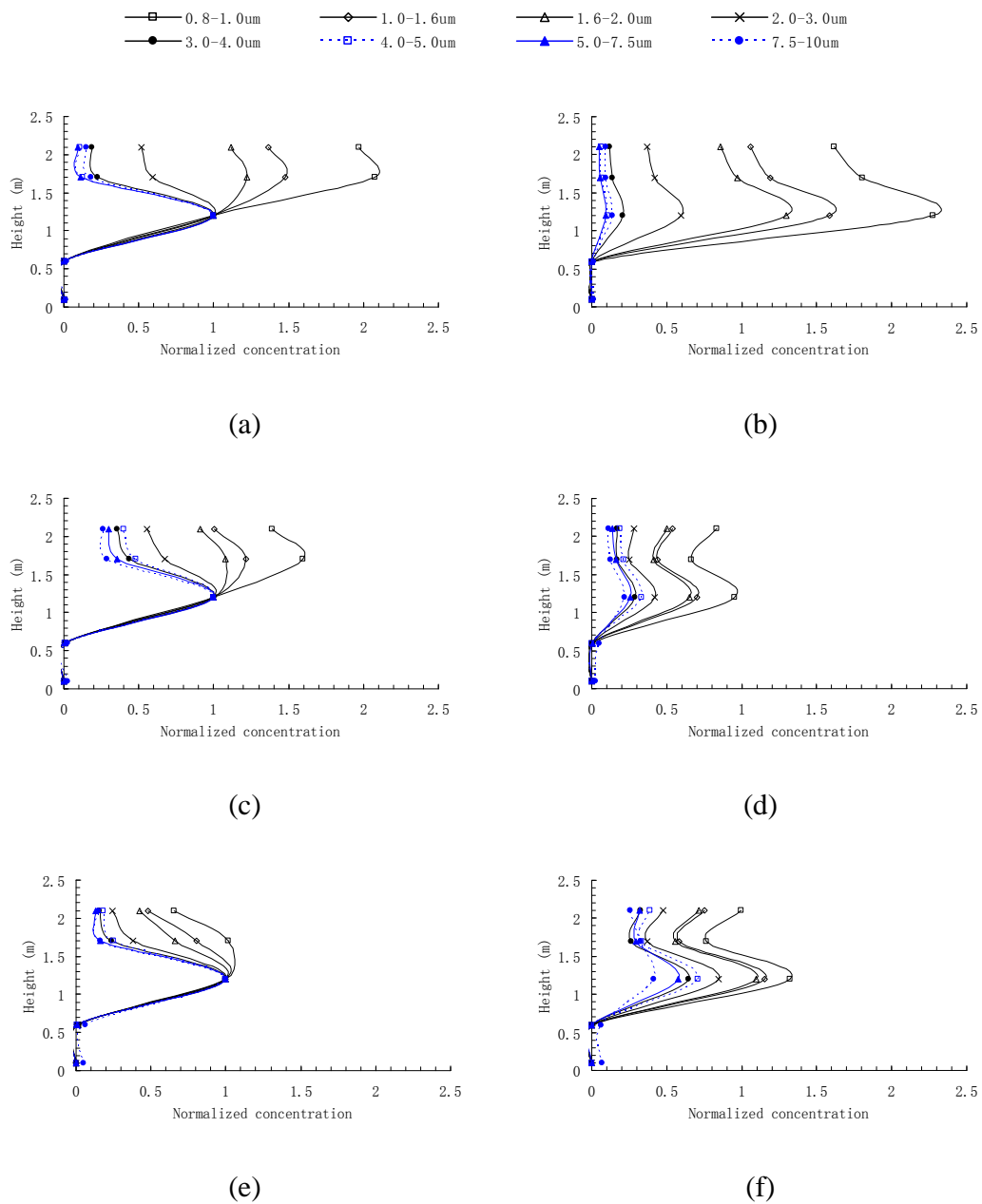


Figure 3.11 Particle distributions when breathing through mouth (line A (a) and line B (b) for Case 1 at a breathing air temperature of 32°C, and line A (c) and line B (d) for Case 3 of 25°C. Particle concentration at 1.2 m height of line A is denoted as 1.0).



### **3.3.5 Personal exposure for the co-occupant**

#### *3.3.5.1 Exposure level at a face-to-face orientation*

Figure 3.13 compares the personal exposure of the co-occupant under different exhalation modes and exhaling air temperatures at a face-to-face orientation with the polluting person. The detected particle concentration in the exposed manikin's breathing zone for Case 1 is denoted as 1.0. Compared to the exposure level when the polluting person breathes through nose, mouth exhalation results in a relatively lower personal exposure. This may be attributed to the reason that particles released horizontally can be more easily driven to the higher space by the upward air movement of DV. The effects of exhaled air temperature show that a lower breathing air temperature may induce higher personal exposure for the co-occupant, since generated particles with small buoyancy effect be largely dispersed in the occupied zone as displayed in Figure 3.10. This demonstrates that simulating a proper exhalation temperature is essential when using thermal manikins.

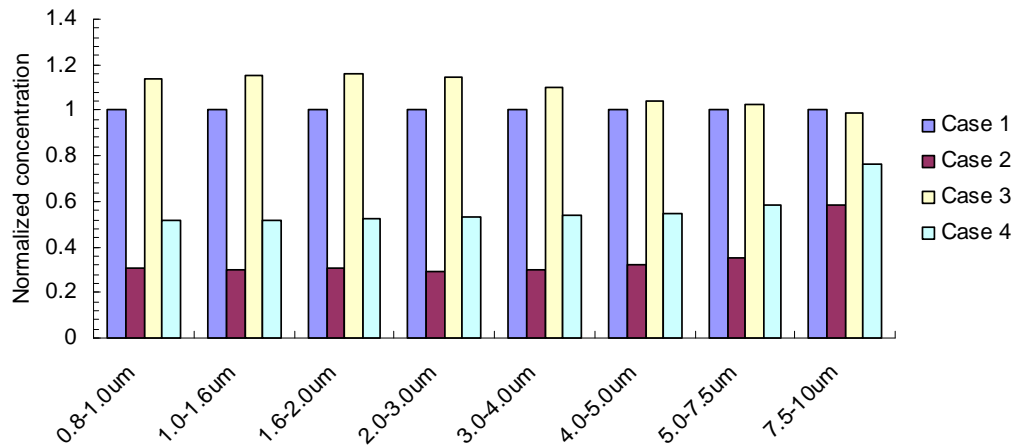


Figure 3.13 Personal exposure of the co-occupant at a face-to-face orientation with the polluting person (personal exposure for Case 1 is denoted as 1.0)

The influences of human body heat on personal exposure are illustrated in Figure 3.14, with particle concentration in the breathing zone of the exposed person in Case 1 being denoted as 1.0 for all size bins. Zero heat of the polluting person leads to the lowest personal exposure for the co-occupant. Highest exposure level is induced in Case 6 with zero heat from the co-occupant. It should be noted that one important advantage of DV in mitigating infection transmission is the formation of thermal plumes around occupants, which can drive the cleaner and cooler room air in the lower space to the breathing zone and protect occupants from the contaminants in breathing height. A zero heat for the co-occupant will weaken the effects of this protecting thermal plume and facilitate the dispersion of generated particles to the co-occupant's breathing zone.

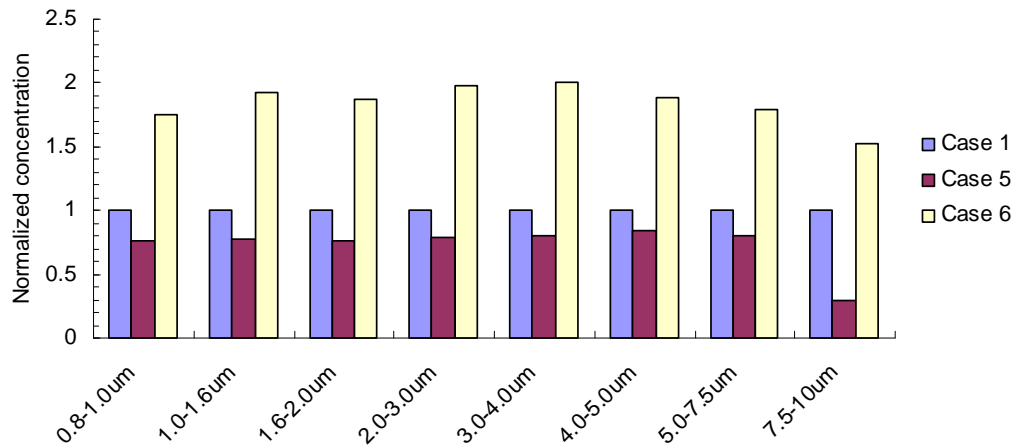
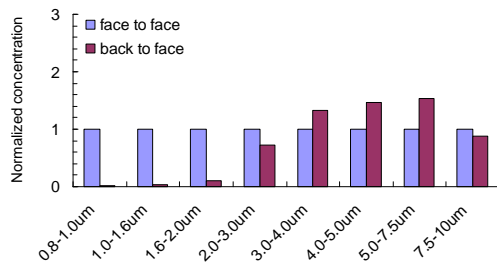


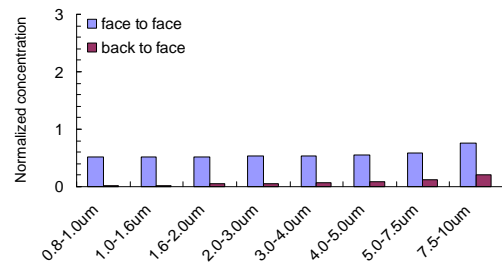
Figure 3.14 Personal exposure of the co-occupant with and without body heats  
(personal exposure for Case 1 is denoted as 1.0)

### 3.3.5.2 Personal exposure at different facing orientations

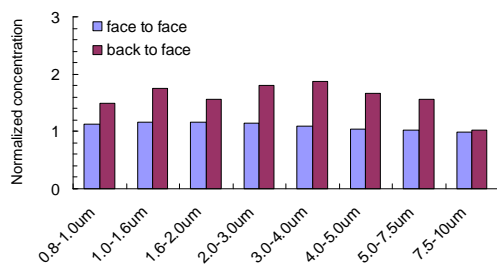
The personal exposure at different facing orientations is displayed in Figure 3.15, in which the back-to-face orientation implies that the co-occupant is back to the face of the polluting person. It is clear that lower personal exposure can generally be achieved at a back-to-face orientation since the body of the co-occupant may block the transportation of generated particle to the breathing zone, with the exceptions for Case 1 and Case 3. The possible reason may be that particles delivered through nose may have more chances being suspended in the breathing height and dispersed to a farther distance, as shown in Figure 3.8. This may increase the possibilities that more particles are delivered to the breathing zone of the co-occupant at a back-to-face orientation with the polluting person.



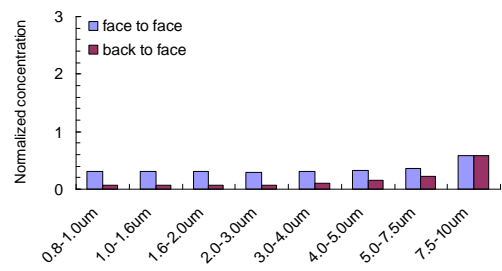
(a)



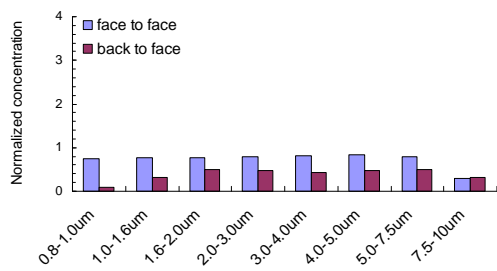
(b)



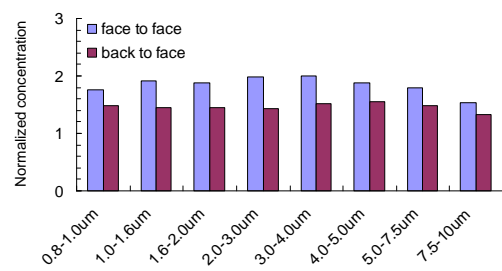
(c)



(d)



(e)



(f)

Figure 3.15 Personal exposure at different facing orientations for Case 1 (a), Case 2 (b), Case 3 (c), Case 4 (d), Case 5 (e), and Case 6 (f) (personal exposure for Case 1 at a face-to-face orientation is denoted as 1.0)

### 3.4 Summary

This chapter introduces the experimental investigation of human respiratory droplets in a DV ventilated environment. It is found that particles larger than  $5\mu\text{m}$  can travel a farther horizontal distance in the breathing height, and may pose higher personal exposure for the co-occupant. Breathing mode possesses apparent influences on the spatial distribution of generated particles. Nose breathing may induce a more uniform particle distribution pattern, while large variations in vertical distribution can be introduced by mouth breathing. The evaluation of personal exposure finds that nose breathing may lead to higher exposure level for the co-occupant since particles can be dispersed to a farther distance from the source. The effects of breathing air temperature show that particles carried in a lower temperature breathing air may be more likely to be delivered to the breathing zone of the co-occupant and lead to a higher exposure level. The heat of a human body also presents great influences on the spatial distribution of generated particles and occupant's exposure.

Still, there are some limits in particle experiments. During particle generation process, the airflow rates for drying and dilution vary slightly case by case, although the total airflow rate for particle-carrier air is well controlled. This may result in quite different initial particle size distribution profiles. Meanwhile, it is very hard to collect the particle concentration for each size bin right at the mouth/nose opening because particle concentration at this point is significantly higher than the instruments' measuring limits. These may make it difficult to directly compare the

spatial distributions of particles at different scenarios and then fully evaluate the effects of these parameters.

## **Chapter 4**

### **Numerical Studies of the Dispersion of Droplets Released during Nose-breathing and Coughing Processes**

Respiratory droplets generated by the infected person contain infectious agents which may cause infection once they reach the respiratory system or mucous membrane of a susceptible person. Although a normal breathing process expels less and smaller droplets, its continuous happening accounts for a significant fraction of droplets released over a day. On the other hand, a cough can generate a large amount of droplets in seconds and will pose higher health risk for occupants' well-being during a short-term exposure period. The understanding of the transmission of pathogen-laden droplets generated during normal breathing and coughing processes is therefore of great importance in the mitigation of infectious diseases spread in built environments.

#### **4.1 Validation of numerical models**

For the entire simulation studies, the renormalization group (RNG)  $k - \varepsilon$  model (Choudhury 1993) is employed to simulate the indoor air movement, and all the parameters are from literatures validated by research. Standard logarithmic law wall functions (Launder 1974) are adopted to bridge the solution variables at the near-wall cells and the corresponding quantities on the adjacent wall. Boussinesq

assumption is chosen in the momentum equations to account for the change of air density due to temperature variation. The SIMPLE algorithm is employed to couple the pressure and velocity fields. The one-way coupling drift-flux model is adopted to calculate the dispersion of respiratory droplets. The influences of Brownian motion, turbulent diffusion, and gravitational settling effect are all considered. To account for droplet deposition onto indoor surfaces, a semi-empirical model (Lai and Nazaroff 2000) is adopted for surfaces with low friction velocity with the assumption that the deposition flux is one-dimensional and constant in the concentration boundary layer. As to surfaces with higher friction velocity, an empirical equation (Papavergos and Hedley 1984), which can estimate the dimensionless particle deposition velocities in the diffusion-impaction regime, is then employed to estimate droplets deposition rate. The more detailed descriptions of each model have been given in Chapter 2.

The experimental data obtained in Chapter 3 will not be used to validate the numerical models due to some uncertainties. The exhaust outlet is located above the ceiling, and polluted air is extracted from the ceiling gaps or through the ceiling-mounted lamps. It is impossible to properly estimate the airflow patterns through these gaps. Meanwhile, the unsure airflow rates through the return grille and exhaust diffuser will also add some difficulties in setting the boundary conditions. Therefore, two sets of experimental data in the literature, a small-scale isothermal chamber and a full-scale non-isothermal room, will be used for the validation of numerical models before they are used to predict indoor particle dispersion.

#### 4.1.1 Isothermal condition with an average particle size of 10 $\mu\text{m}$

Lai et al. (2008) studied the dispersion of particles with an average diameter equal to 10  $\mu\text{m}$  in a two-zone chamber as depicted in Figure 4.1. This two-zone chamber is 0.8 m (length)  $\times$  0.4 m (width)  $\times$  0.4 m (height), with a partition wall located at the center of the room and a large opening in this partition wall. The opening is set in the middle of partition wall with a dimension of 0.08 m (width)  $\times$  0.24 m (Height). The inlet and outlet are arranged in the middle of room width, both with a distance of 2 cm from the ceiling and floor separately and the dimensions are 0.04 m (width)  $\times$  0.04 m (height).

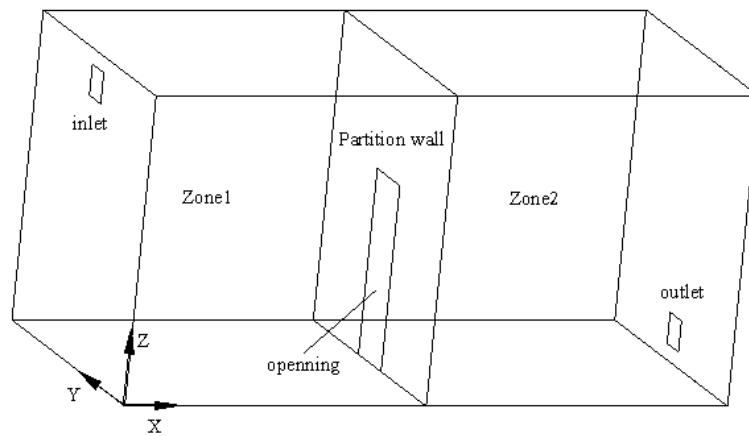


Figure 4.1 Geometry of the scaled chamber

In the experiment conducted by Lai et al. (2008), the particle distribution under two different inlet velocities, 0.225 m/s and 0.45 m/s, are investigated. Here, only the data when inlet velocity equals to 0.225 m/s are used to validate our numerical

model. Figure 4.2 and Figure 4.3 show the data comparison between the experiment and numerical simulation about the x-direction velocity and the particle concentration in four vertical lines, located at the center plane of the room with distances of 0.1 m, 0.3 m, 0.5 m, 0.7 m away from the inlet. For the x-direction velocity, numerical data agree with experimental values very well. As far as the particle concentration is concerned, similar trends between numerical simulation and experiment can be observed, but apparent discrepancies can be observed for some points.

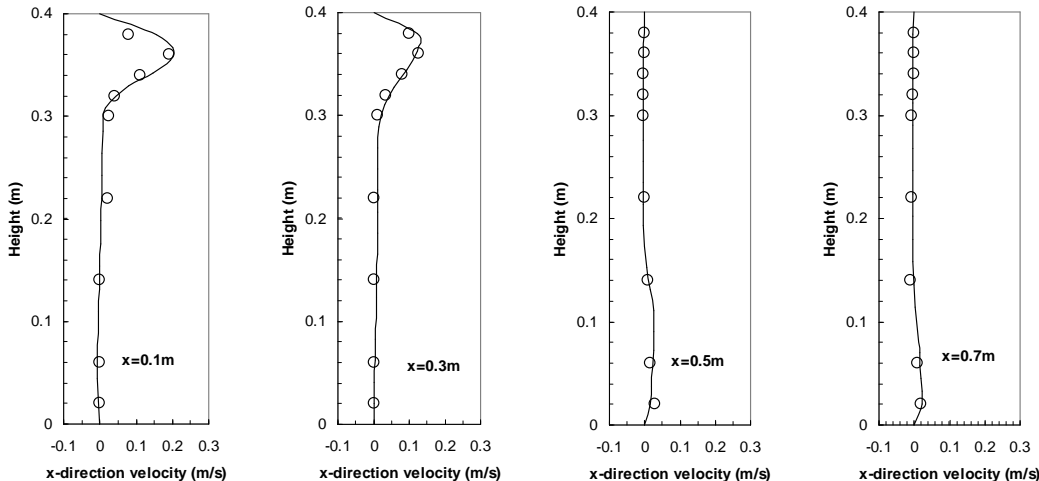


Figure 4.2 Comparison of simulated and measured x-direction velocity (Legends:experiment: o, simulation: —)

There are many reasons for this disagreement. The major reason might be that the deposition model used here is for the smooth surfaces. Some other mechanisms will also influence the particles dispersion, including electrostatic force once the released

particles are not completely neutralized in experiments, anisotropic turbulence near walls, and particle re-suspension from internal surfaces. Meanwhile, the experiment particles are not mono-dispersed. They are poly-dispersed particles with an average diameter equal to  $10\ \mu\text{m}$ , and their nominal diameters range between  $2\ \mu\text{m}$  and  $20\ \mu\text{m}$ . This may also raise uncertainties for the data comparison.

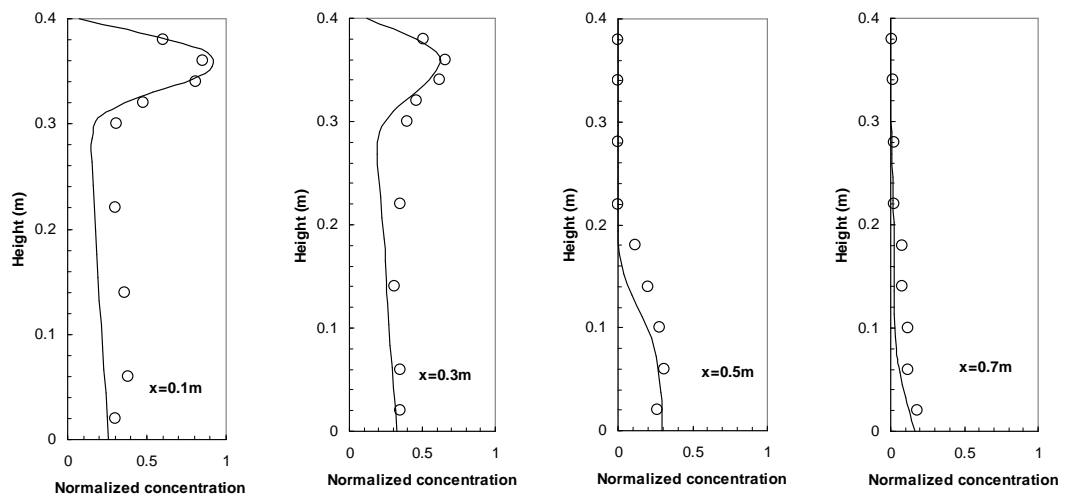


Figure 4.3 Comparison of simulated and measured normalized particle concentration (Particle concentration in the inlet air is denoted as 1.0; Legends: experiment:  $\circ$ , simulation:  $\text{—}$ )

#### 4.1.2 Non-isothermal condition with a mean particle size of $0.7\ \mu\text{m}$

The previous section shows these numerical models can reasonably present large particle dispersion in a small-scale isothermal chamber. Since buoyancy effects and temperature differences may significantly influence indoor airflow patterns and

hence particle dispersion, the applications of these numerical models are then tested in a more actual full-scale environment with UFAD, as shown in Figure 4.4 (Zhang and Chen 2008).

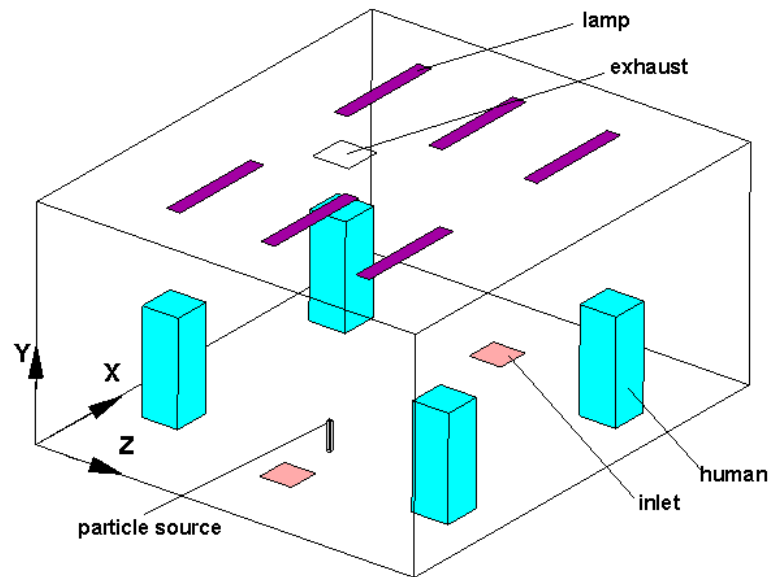


Figure 4.4 Configuration of the non-isothermal environmental chamber

The dimensions of this room are 4.91 m, 2.44 m, and 4.31 m in x, y, z direction, respectively. Conditioned air is supplied from the two inlet openings on the floor at a total airflow rate of  $0.0944 \text{ m}^3/\text{s}$ , and warm and contaminated air is extracted from the exhaust outlet on the ceiling. Four heated manikins and six lamps are arranged to simulate heat sources in a real room. Liquid droplets with low evaporation rate are introduced into the room by nitrogen at a flow rate of  $7 \times 10^{-5} \text{ m}^3/\text{s}$  at a point 0.3 m above the floor ( $X = 1.6 \text{ m}$ ,  $Y = 0.3 \text{ m}$ ,  $Z = 2.2 \text{ m}$ ). The droplet density is  $912 \text{ kg}/\text{m}^3$  and the average diameter is  $0.7 \text{ }\mu\text{m}$ . Air velocity is monitored in seven vertical lines,

with the dimensions of 0.4 m, 1.6 m, 2.05 m, 2.5 m, 2.95 m, 3.4 m, 4.6 m in X axis for vertical lines V1, V2, V2, V4, V5, V6 and V7 respectively and a Z axial value of 2.2 m for all lines. Droplet concentration is recorded in six vertical lines. The values of X axis are 4.3 m, 3.7 m, 3.1 m, 1.9 m, 1.3 m, 0.7 m for vertical lines P1, P2, P3, P4, P5 and P6 separately, and an axial value of 3.11 m in Z direction for all lines. These data are used to validate the simulated results.

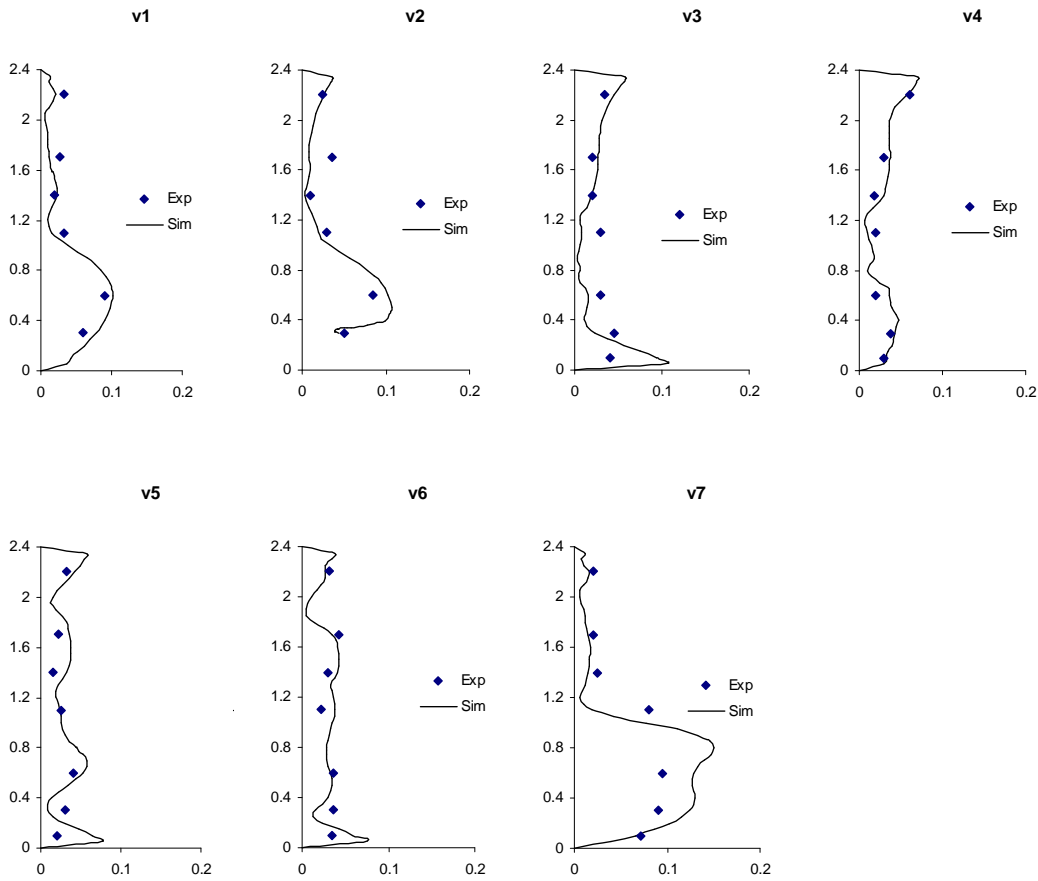


Figure 4.5 Comparison of simulated and measured air velocity

Figure 4.5 presents a comparison of simulated and measured air velocity in seven vertical lines, and the comparison of droplet concentration is displayed in Figure 4.6 with the droplet concentration at outlet being denoted as 1.0. It can be observed that the simulated data match with the experimental values well for both indoor air movement and droplet dispersion. The larger difference for droplet concentration appears in the lower level at P4 and P5. This may be attributed to the droplet generator which may introduce strong flow fluctuations in the region close to the source, as explained by Zhang and Chen (2006).

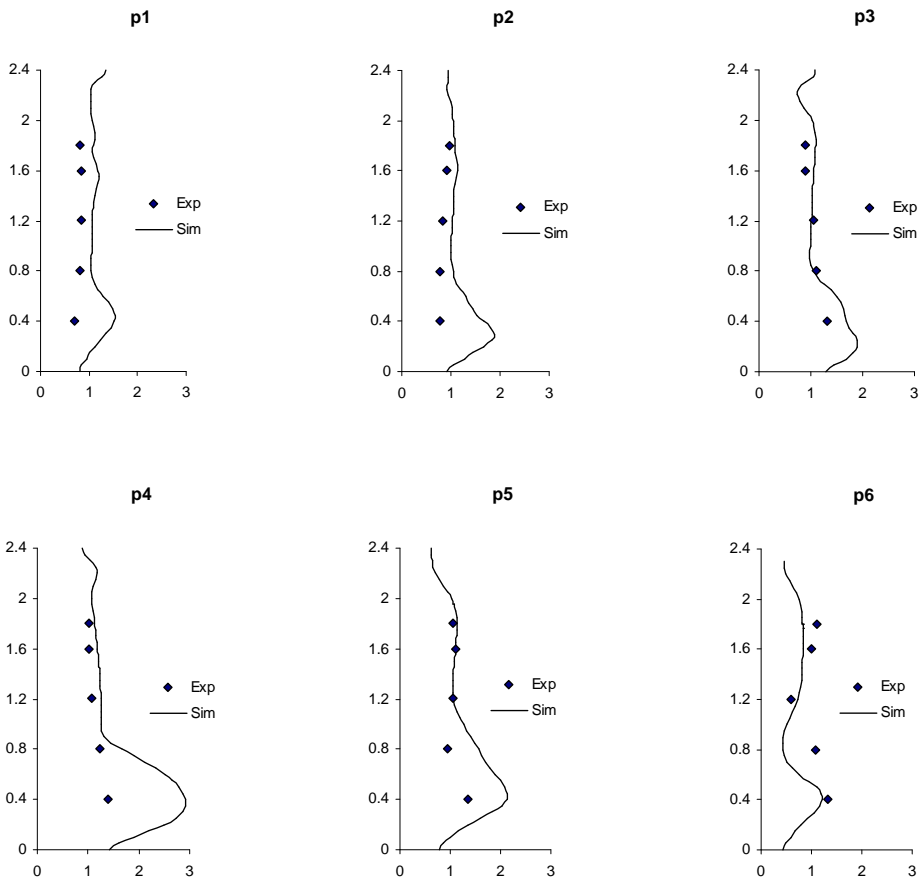


Figure 4.6. Comparison of simulated and measured droplet concentration

The comparison results in this section imply that the adopted numerical models can predict indoor air movement and particle dispersion reasonably, and can be applied for the predictions of droplet distribution and personal exposure of occupants.

## **4.2 Modeling of nose-breathing process**

### **4.2.1 Introduction**

Experimental studies (Edwards et al. 2004; Papineni et al. 1997) found that normal breathing can produce respiratory droplets. The majority of them is less than 1  $\mu\text{m}$  while some may be as large as several microns. Although coughing or sneezing can generate more droplets in each activity, normal breathing can account for a significant fraction of the droplets exhaled over the course of a day since it is continuously happening (Fiegel et al. 2006). Meanwhile, it has been concluded that ventilation system possesses strong relationship with the transmission of some respiratory diseases (Li et al. 2007). Different personal exposure may be induced in a room with different ventilation schemes. Furthermore, it will be more reliable to include an exposed person in the research domain when studying the possible exposure of the co-occupant. The geometry of this exposed person is also especially important since the thermal plume around human body can be influenced by the selected geometry. A detailed geometry can provide more realistic results when attention is primarily focused on the inhalation of the exposed person. Hence, in this section, two manikins with detailed geometries are arranged in the simulated room to investigate the co-occupant's exposure when the infected person breathes through

nose under different ventilation systems. Since smaller droplets can slip through the edges of the face masks (Fabin et al. 2007; Tang et al. 2009), reach the alveolar region of the respiratory system, and cause severe damages (Guha 2009), droplet residuals in the size range of 1  $\mu\text{m}$  to 10  $\mu\text{m}$  are selected to represent fine droplets and  $\text{CO}_2$  for tracer gas.

#### **4.2.2 Case description**

Figure 4.7 presents the configuration of the simulated room, with a dimension of 4.0 m (length)  $\times$  3.0 m (width)  $\times$  2.7 m (height). There are two people working there sitting face to face with a 1.5 m distance between their nose-tips. The one on the right is assumed to be an infected person who emits pathogen-laden droplets and the other is a susceptible person called the co-occupant.

Three ventilation methods, including MV, UFAD and DV, are investigated. The temperature of inlet air flow is set to be 16  $^\circ\text{C}$ , 20  $^\circ\text{C}$  and 20  $^\circ\text{C}$  for MV, UFAD, and DV respectively with the same air change rate equal to 6.4 times per hour. The heat flux released from window and computers are 200 W and 120 W, individually. The convective heat from the infected person and the co-occupant is 60 W respectively.

The inlet diffuser for MV is arranged at the upper level of one side wall and the outlet is at the lower level of the same side wall. For DV, a large wall-mounted diffuser is located at the floor level to supply cool air at a low speed while the exhaust is at the higher level of the opposite side wall. And about UFAD, two

swirling diffusers are mounted on the floor and each is simulated by nine small square cells, using a tangential velocity profile as proposed by Kobayashi and Chen (2008).

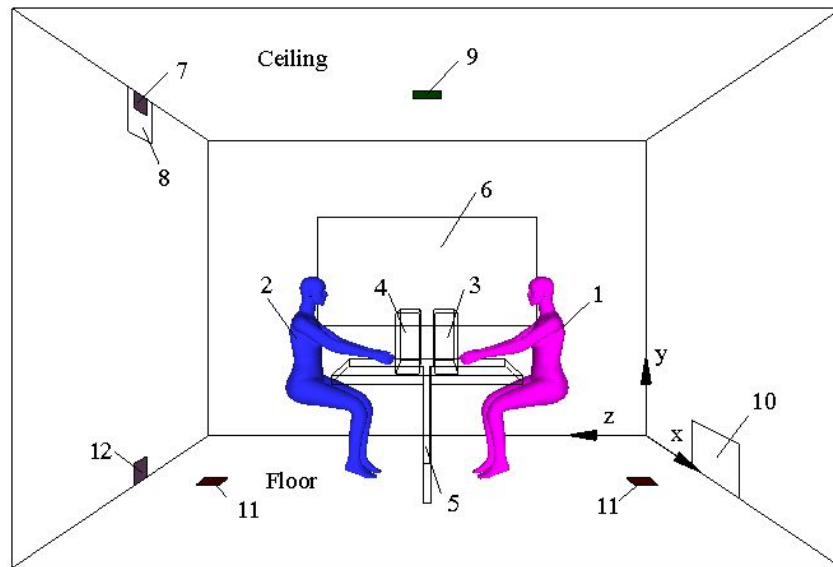


Figure 4.7 Configuration of the simulated room (room length (Z) 4 m, width (X) 3 m, Height (Y) 2.7 m; 1-infected person; 2-co-occupant; 3, 4-computer; 5-desk; 6-window; 7-MV inlet 0.2 m × 0.12 m; 8-DV outlet 0.4 m × 0.3 m; 9-UFAD outlet 0.2 m × 0.2 m; 10-DV inlet 0.8 m × 0.35 m; 11-UFAD inlet 0.165 m × 0.165 m; 12-MV outlet 0.2 m × 0.15 m)

A normal respiration process follows a sinusoidal cycle. However, a steady exhalation is assumed to simulate the nose-breathing process for the infected person, and continuous inhalation for the co-occupant. The breathing rate is 8.4 l/min (Huang 1997) through nostrils, and the direction of exhaled jet is 45° downward

while the orientation for inhalation is 45° upward. The temperature of the expelled air is set to be 35°C.

Before the simulation of droplet dispersion in the room, grid independence tests are performed by using grid convergence index (GCI), which is based on Richardson extrapolation method (Richardson 1910) and has been suggested by Roache (Roache 1994), for three conditions when the office is ventilated by MV, UFAD and DV respectively.

$$GCI(u) = F_s \frac{\mathcal{E}_{rms}}{r^p - 1} \quad (4-1)$$

where  $F_s = 3$ ,  $p = 2$ , and  $r$  is the ratio of the number of fine grids to that of coarse grids. The grids number for coarse meshes are 1,532,283 for MV, 1,655,349 for UFAD and 1,553,883 for DV, while the number for fine grids are 2,865,835, 2,959,224 and 2,914,640 respectively.  $\mathcal{E}_{rms}$  is calculated by:

$$\mathcal{E}_{rms} = \left( \frac{\sum_{i=1}^n \mathcal{E}_{i,u}^2}{n} \right)^{\frac{1}{2}} \quad (4-2)$$

where  $\mathcal{E}_{i,u} = \frac{u_{i,coarse} - u_{i,fine}}{u_{i,fine}}$  and  $u$  is velocity magnitude.

A total number of 48 points evenly distributed in the simulated room is chosen in coarse and fine grid cases to check the grid independence. The values of  $GCI(u)$

are 3.2% for MV, 3.6% for UFAD and 3.4% for DV, which demonstrate that the coarse meshes can be selected in this research.

#### **4.2.3 Airflow fields**

The airflow patterns and temperature distribution profiles under different ventilation systems are presented in Figure 4.8, as well as the inhaled air path-lines of the co-occupant under DV. The conditioned air is delivered at a higher velocity under MV to promote the well-mixing of air and heat, and the average temperature is maintained around 24 °C. Under DV, fresh air is supplied at a lower velocity near the floor level, and thermal plumes developed over the heat sources play the major role in driving the room air upward and being extracted. This buoyancy-driven airflow produces a well stratified temperature distribution pattern. Although thermal stratification phenomenon can also be observed under UFAD, the relatively well-mixed lower region induced by the two swirling diffusers lessens the temperature gradient in this zone. As to the temperature distribution, the average temperature in the middle height of the room is maintained around 24 °C under both UFAD and DV to guarantee the comparison basis of the three ventilation methods.

The well-mixed airflow under MV can promote the dispersion of exhaled droplets and then increase the infection possibilities for occupants, while the mainly upward-driven airflow may facilitate the extraction of contaminants under UFAD and DV. However, UFAD would result in different contaminant distribution profiles from DV because of the relatively mixed airflow in the lower region of the room.

Meanwhile, it can be observed in Figure 4.8 that the inhaled air of the co-occupant under DV comes from the lower level of the room because of the thermal plumes around human body. Therefore, it is essential to include the detailed body geometry of the co-occupant in the computation domain to realistically assess the exposure.

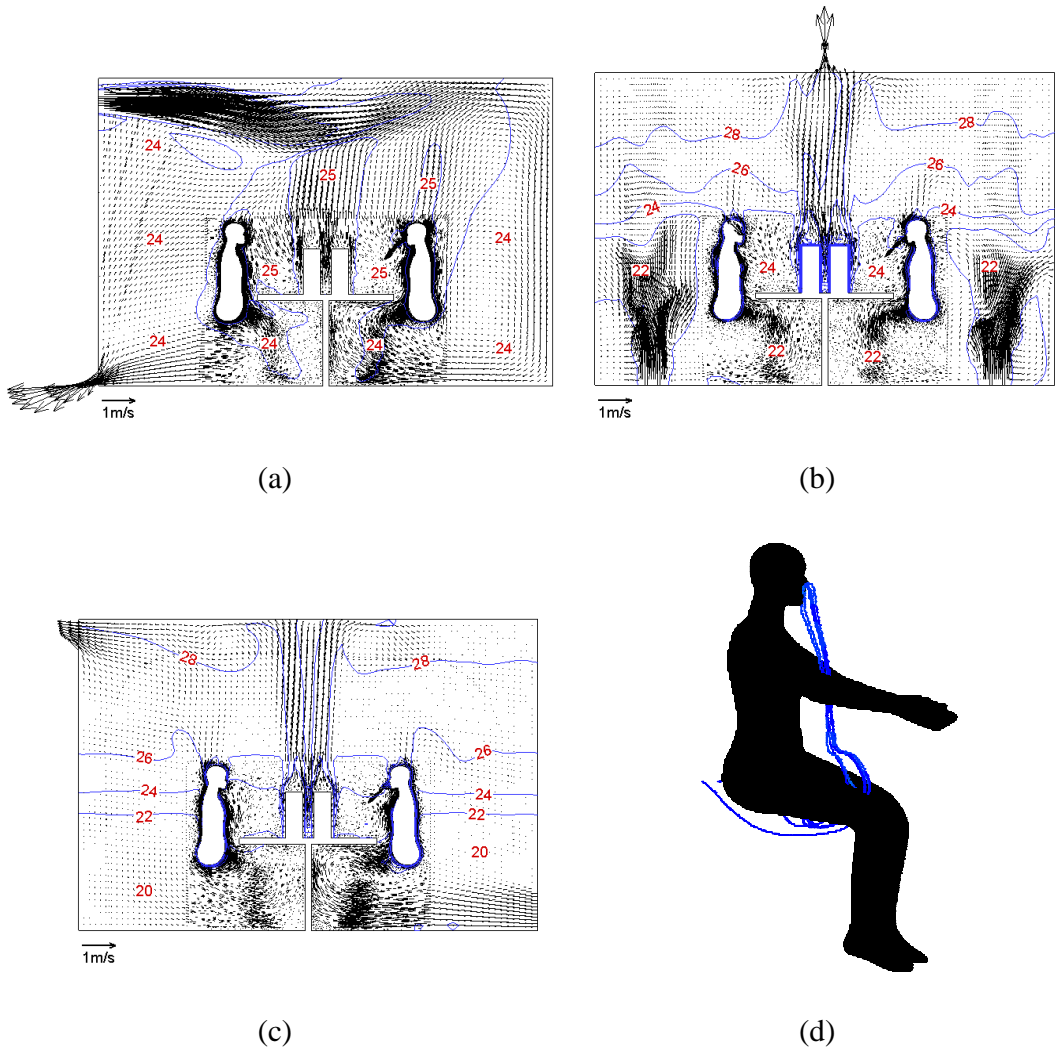


Figure 4.8 Airflow patterns and temperature distribution in the middle section ( $X=1.5\text{m}$ ) of the simulated room under MV (a), UFAD (b), DV (c), and the inhaled air path-line of the co-occupant under DV (d).

#### 4.2.4 Droplet dispersion

Figure 4.9 illustrates the normalized concentration distribution of 10  $\mu\text{m}$  droplets in the middle vertical plane of the simulated room, and the average normalized concentration in horizontal planes at different heights is shown in Figure 4.10.

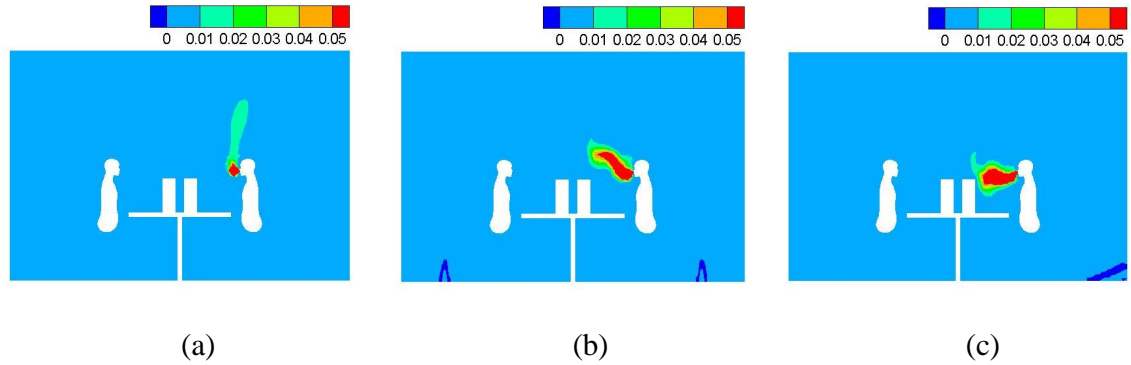


Figure 4.9 Normalized concentration distribution of 10  $\mu\text{m}$  droplets on the middle plane ( $X = 1.5 \text{ m}$ ) under MV (a), UFAD (b), and DV (c) (droplet concentration in the exhaled air is denoted as 1.0)

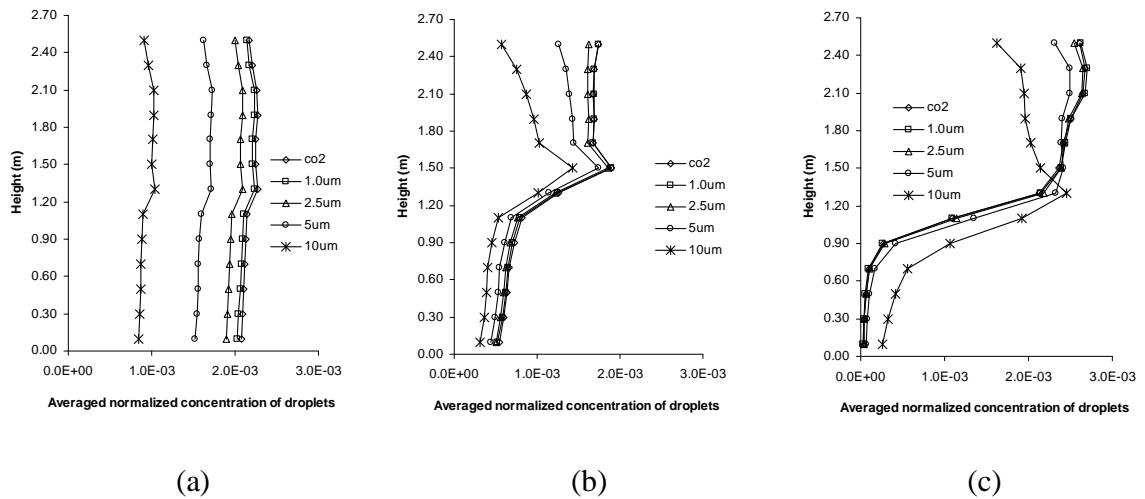


Figure 4.10 Average normalized concentration in the horizontal planes at different heights under MV (a), UFAD (b), and DV (c) (droplet concentration in the exhaled air is denoted as 1.0)

In line with the findings of Qian et al. (2006) and Gao et al. (2008), the exhaled air travels a longer distance horizontally under UFAD and DV because of thermal stratification, while it is driven upward directly under MV. As shown in Figure 4.10, the exhaled droplets are quite evenly dispersed under MV, whilst concentration stratification exists under UFAD and DV. The spatial concentration decreases with droplet size under MV and UFAD. However, DV presents a quite different distribution profile. In the space below the breathing level, larger droplets present higher concentration, while it decreases with droplet size in the region above the breathing level. The average concentration in breathing height is highest under DV, compared with MV and UFAD. This highest concentration can be associated with the trapping phenomenon of exhaled droplets in the breathing zone of the infected person, see Figure 4.9. Therefore, the higher concentration in the breathing level does not necessarily imply higher personal exposure for the co-occupant.

#### **4.2.5 co-occupant's exposure**

The inhaled fraction (*IF*) of the co-occupant is displayed in Figure 4.11 to accurately assess the exposure level.

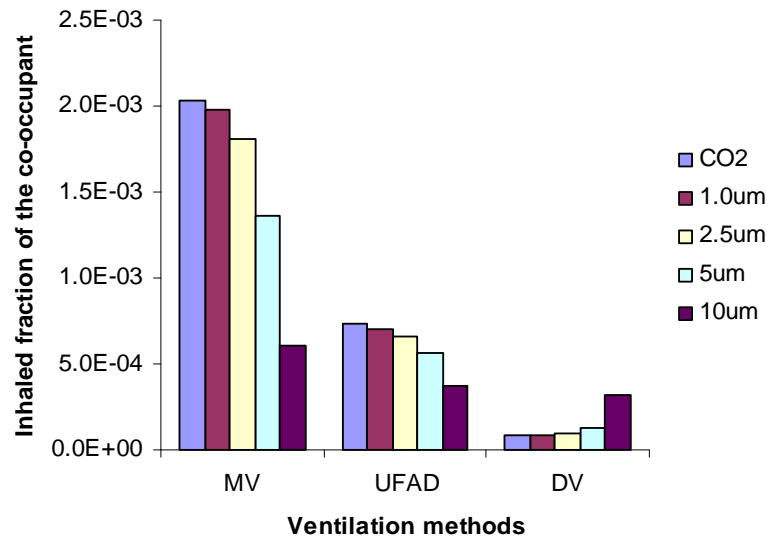


Figure 4.11 Inhaled fraction ( $IF$ ) of the co-occupant under different ventilation methods

It can be observed that for all the droplets, the inhaled fraction is highest under MV and lowest under DV. This means that most of the exhaled droplets are distributed to the upper region of the room before they reach the breathing zone of the co-occupant under UFAD and DV, though the exhaled air can penetrate longer distance horizontally. Compared with the experimental data of Qian et al. (2006), this finding implies that keeping the co-occupant a certain distance away from the infected person can avoid higher health risk under UFAD and DV, which is consistent with the results of Nielsen et al. (2008).

Since other occupants may also stay in this simulated room, Figure 4.12 presents the concentration distribution of 10  $\mu\text{m}$  droplets on the horizontal plane at breathing height ( $Y = 1.3 \text{ m}$ ). As shown in this figure, generally, the contaminant

concentration is highest under DV because thermal stratification can promote the horizontal distribution of exhaled droplets, while the relatively lower concentration under UFAD may be attributed to the reason that the exhaled air is driven to the upper region, as seen in Figure 4.9. Although it seems that the contaminant concentration at breathing height is higher under DV, the actual exposed concentration may remain at a lower level because the thermal plume around human body can bring the lower fresh air to the co-occupant's breathing zone.

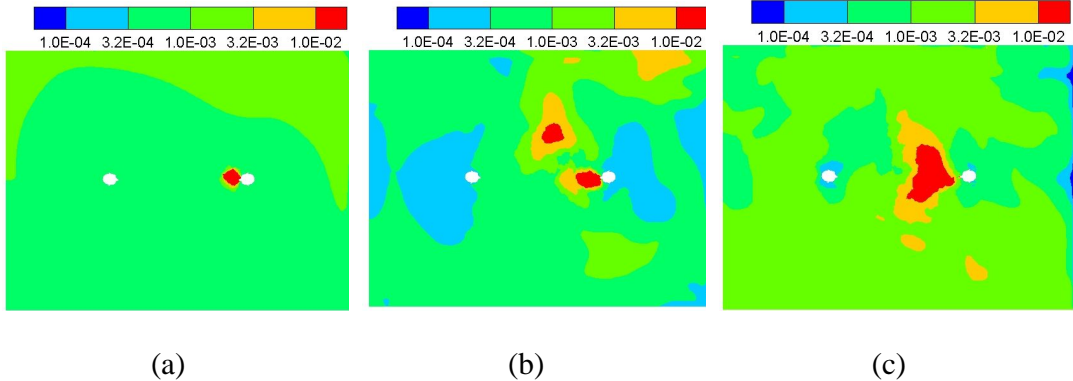


Figure 4.12 Normalized concentration of 10  $\mu\text{m}$  droplets on the horizontal plane at breathing height ( $Y = 1.3 \text{ m}$ ) under MV (a), UFAD (b), and DV (c) (droplet concentration in the exhaled air is denoted as 1.0)

Since droplets deposited onto indoor surfaces may cause infectious diseases transmission through direct contact route, Figure 4.13 presents the deposition rates of exhaled droplets with varying diameters. The deposition rate is highest under MV for all the droplets studied, lowest under DV for droplets less than 10  $\mu\text{m}$ , and comparable under UFAD and DV for 10  $\mu\text{m}$  droplets. Among the total deposited droplets, almost two-third of them under MV and UFAD, and around half under DV,

deposits onto the floor. While desk, the infected person, and the co-occupant become the next three higher particle deposition sites and each of them may account for around five percent. As to the co-occupant, less than ten percent of droplets among the total deposition rate on the body are deposited onto the head.

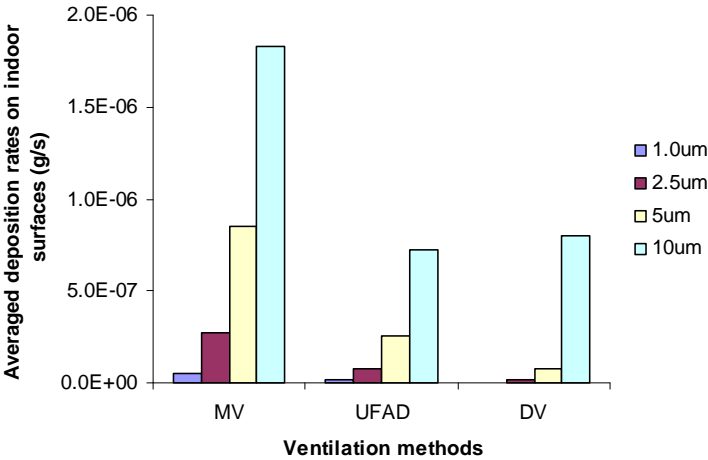


Figure 4.13 Deposition rates on indoor surfaces (droplet concentration in the exhaled air is 0.05 g/m<sup>3</sup> for all the size range)

The relatively stronger bulk airflow of MV widely disperses the exhaled droplets in the entire room once they are released, leading to a higher personal exposure for the co-occupant. Since the gravitational settling force increases with the droplet size, a higher percentage of larger droplets deposit onto indoor surfaces which results in the lower inhaled concentration. Different from MV and UFAD, smaller droplets under DV are driven upward by the weak unidirectional airflow and convective flows of the indoor heat sources, and then exhausted directly, which may explain the lower inhaled concentration and deposition rate. Larger particles, on the other hand, can

remain suspended in the breathing zone due to the combined effects of droplet gravitational force and the upward air movement, and deposit onto indoor surfaces because of the larger gravitational settling force. All of these lead to lower inhalation and deposition for smaller droplets, and higher inhaled mass and deposition rate for larger droplets under DV.

#### **4.2.6 Summary**

The research of nose-breathing process under different ventilation methods finds that the personal exposure of the co-occupant via airborne transmission is lower under UFAD and lowest under DV for all the droplets investigated, although the average concentration at the breathing level is higher than MV. This demonstrates the importance of including the co-occupant in the computation domain in order to achieve a more reliable and actual exposure level. The average pollutant concentration in the breathing height may only indicate the general distribution of the exhaled droplets and is difficult to embody the health impact to the co-occupant. Regarding both airborne transmission and physical contact transmission, the exposure level for the co-occupant is the least under DV, and highest under MV. Although the exhaled air can penetrate a longer distance horizontally under DV which will induce higher personal exposure when the co-occupant stands close to the infected person, a certain distance away from the infected person can assure the lowest inhaled fraction during the normal breathing process.

## **4.3 CFD study of the dispersion of droplets released at different coughing velocities**

### **4.3.1 Introduction**

Although coughing or sneezing does not happen frequently, these processes have been often investigated since they can generate a large amount of droplets in seconds and pose higher health risk for a short-term exposure. The droplet number released in a cough is less than a sneeze, while its deeper origin from the lungs can introduce droplets carrying more contagious agents (Qian et al. 2006). Many experimental studies have been conducted to investigate the characteristics for a cough (Chao et al. 2009, Gupta et al. 2009, Zhu et al. 2006). Because of the variation of investigating subjects and experimental methods, different parameters have been obtained. Zhu et al. (2006) detected coughing velocities in the range from 6 to 22 m/s with the most value being around 10 m/s using a digital PIV. Employing the same method, Chao et al. (2009) measured a maximum coughing velocity of 13.2 m/s for male and 10.2 m/s for female, with an average velocity of 11.7 m/s. Different from Zhu et al. (2006) and Chao et al. (2009), Gupta et al. (2009) characterized a cough by mouth opening area, airflow rate, and direction of expelled air. The cough peak flow rate changed from 3 to 8.5 l/s for male and 1.6 to 6 l/s for female. The expired volume during one cough lied in the range of 400-1600 ml for male and 250-1250 ml for female. These varieties in human respiration activities may induce different dispersion profiles of respiratory droplets and personal exposure of the co-occupant. Therefore, the impacts of coughing velocity on co-occupant's exposure are investigated under MV, UFAD, and DV.

### **4.3.2 Research method**

The configuration of the simulated room is the same as the one in section 4.2. The only difference is the boundary condition for the infected person. Regarding the infected person, both a minimum coughing velocity (6 m/s) and a maximum velocity (22 m/s) (Zhu et al. 2006) are simulated under MV, UFAD, and DV to investigate the influences of coughing velocities on the co-occupant's inhalation. This horizontal pulsating jet lasts 0.5 seconds to simulate several consecutive coughs. To ensure the comparison basis for the co-occupant's exposure to different coughing velocities, it is assumed that the same amounts of droplets are released.

### **4.3.3 Distribution of droplets generated at a higher coughing velocity of 22 m/s**

#### ***4.3.3.1 Droplet dispersion***

Figure 4.14 illustrates the dispersion of CO<sub>2</sub> at the 0.5<sup>th</sup>, 1.5<sup>th</sup> and 5<sup>th</sup> second. It can be observed that the coughed air travels fastest under MV and slowest under DV. The exhaled air under MV can enter into the micro-environment of the co-occupant within a half second, and the highly concentrated droplet cloud approaches the co-occupant at the 1.5<sup>th</sup> second.

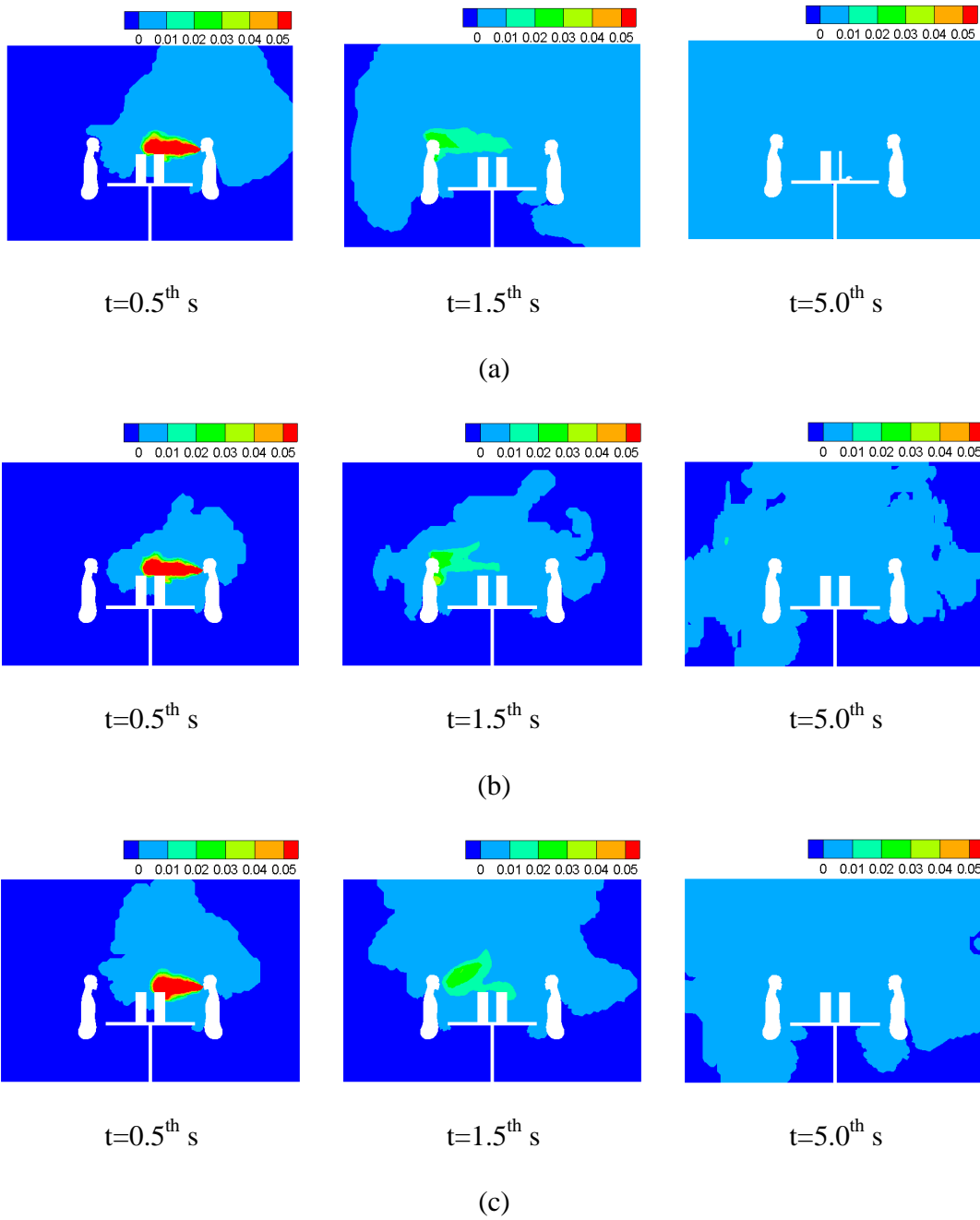
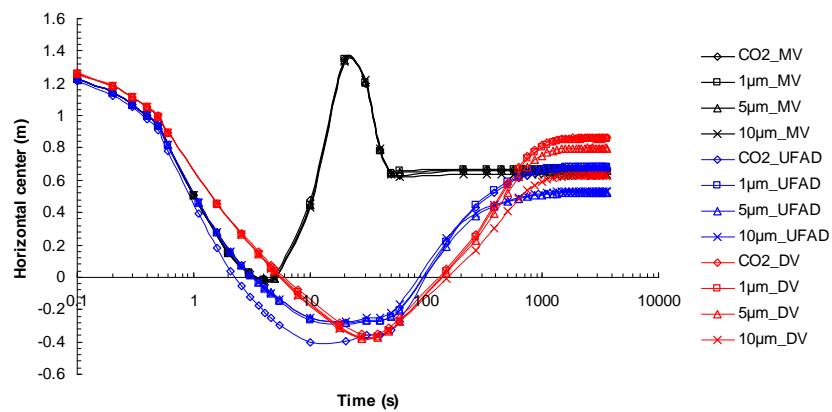


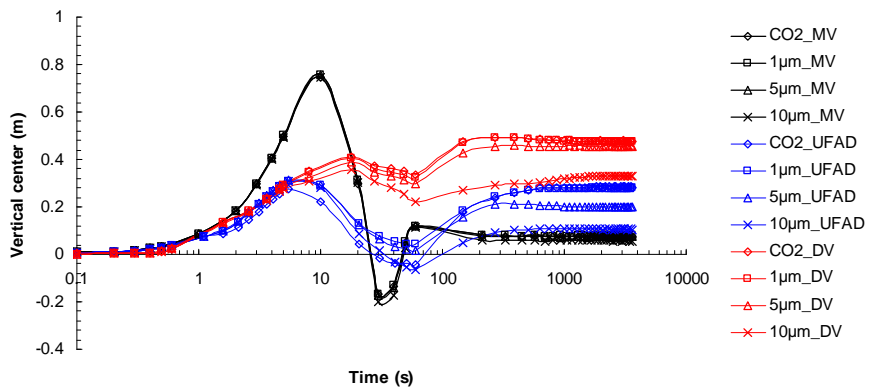
Figure 4.14 Distribution of CO<sub>2</sub> in the center plane of the room at the 0.5<sup>th</sup>, 1.5<sup>th</sup> and 5<sup>th</sup> second under MV (a), UFAD (b) and DV (c). (CO<sub>2</sub> concentration in the instantaneous coughed air is denoted as 1.0)

The exhaled air under UFAD, however, moves slower than MV for the reason that the mainly upward air movement hinders the horizontal transportation, while faster than DV because of the air mixing in the lower space of the room. At the 5<sup>th</sup> second, CO<sub>2</sub> is already dispersed to the entire room under MV while only partly occupies the space in UFAD and DV.

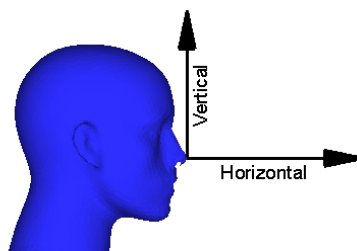
To explore the dispersion history of respiratory droplets and account for the co-occupant's exposure during the whole process, Figure 4.15 shows the vertical and horizontal center of droplet clouds varying with time. The nose-tip of the co-occupant is denoted as zero point, and a farther distance may imply a relatively lower exposure. It can be observed that the coughed air penetrates much slower under DV than MV and UFAD during the first 5 seconds because the upward air movement of DV will hamper the horizontal transportation. The horizontal and vertical dispersion history of exhaled droplets presents similar trends under UFAD and DV because of their mainly upward air movement. The exhaled air in UFAD and DV ventilated room approaches the co-occupant horizontally at first due to the high momentum coughing jet and then ascends vertically because of the upward airflow and thermal plumes of heat sources.



(a)



(b)



(c)

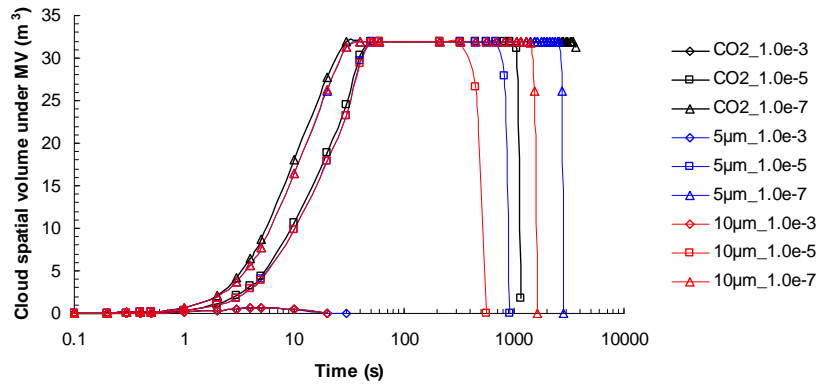
Figure 4.15 Horizontal center (a) and vertical center (b) of droplet clouds varying with time under MV, UFAD, and DV (The nose-tip of the co-occupant is denoted as zero point (c))

With the time elapsing, the coughing jet dissipates gradually and ventilation system becomes the main force to distribute the exhaled droplets. The exhaled droplets

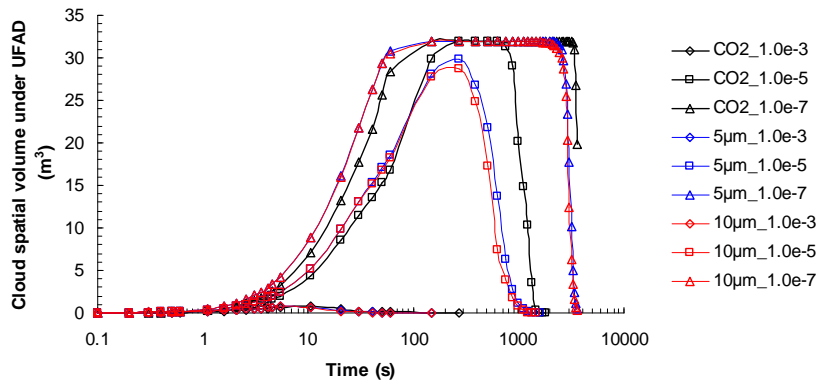
which are transported to the region close to the co-occupant are driven by air movement to be slowly dispersed in the entire room and extracted at the same time. The ultimate location of the horizontal center is right in the room center, i.e. about 0.7 m away from the co-occupant. The final vertical center is higher for smaller droplets and lower for larger droplets because of gravitation. Meanwhile, the vertical center under DV is highest for all the droplets simulated. This might be attributed to the reason that the air mixing of UFAD in the lower space of room deteriorates the upward transportation of exhaled droplets to the higher level.

As to MV, a quite different profile can be observed. Due to its higher air velocity and well-mixed property, the coughing jet is dissipated most quickly and the exhaled droplets are dispersed fastest as shown in Figure 4.14. The released droplets are fully distributed indoors at about the 50<sup>th</sup> second under MV, while it is at around the 1000<sup>th</sup> second for UFAD and DV. In MV, the exhaled air is firstly transported to the co-occupant by the high-momentum coughing jet, then delivered far away by air movement, and at last fully dispersed in the room.

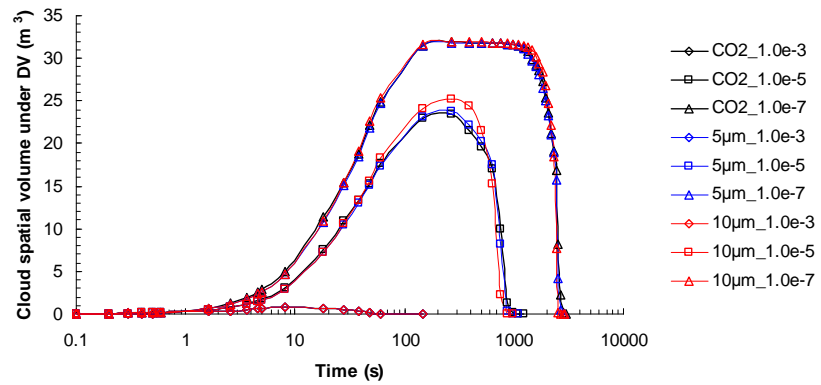
Another parameter to evaluate the dispersion of droplets is cloud spatial volume (CSV). Figure 4.16 displays the cloud spatial volume for CO<sub>2</sub>, 5 μm, and 10 μm droplets under MV, UFAD, and DV to illustrate the dispersion history of droplets with different diameters for each ventilation system. The more detailed description of droplet clouds during the first 10 seconds is shown in Figure 4.17.



(a)

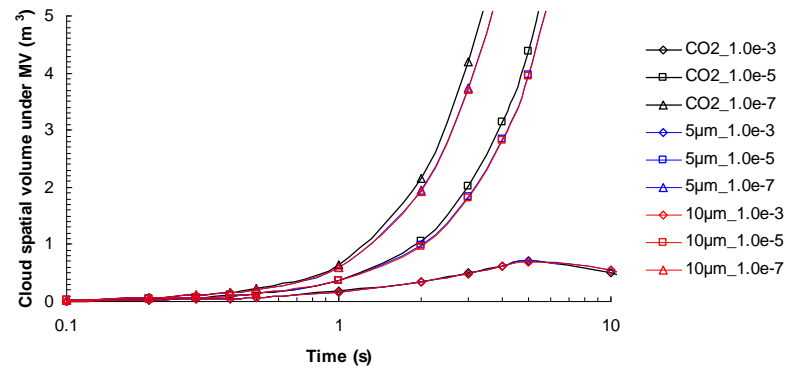


(b)

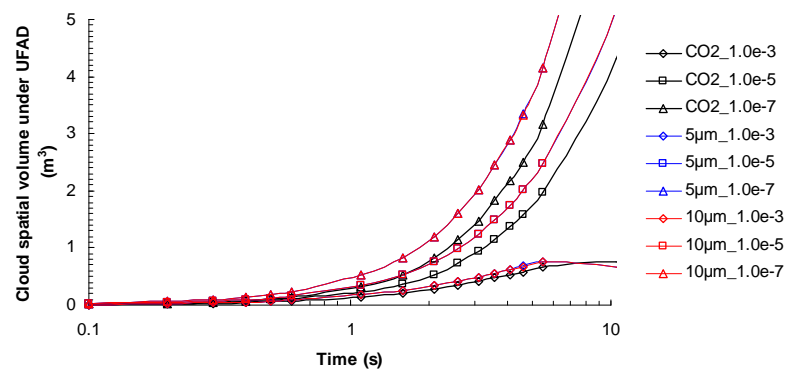


(c)

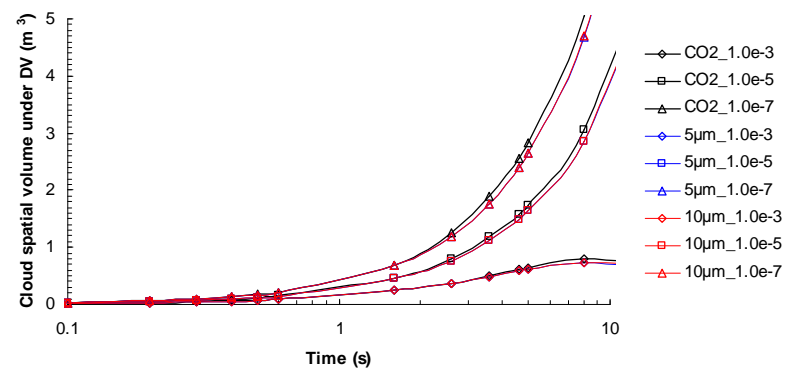
Figure 4.16 Cloud spatial volume of CO<sub>2</sub>, 5  $\mu m$  and 10  $\mu m$  droplets varying with time under MV (a), UFAD (b) and DV (c) (MV\_1.0e-3 means the volume of the space in which normalized concentration of CO<sub>2</sub> is never less than 1.0e-3 under MV)



(a)



(b)

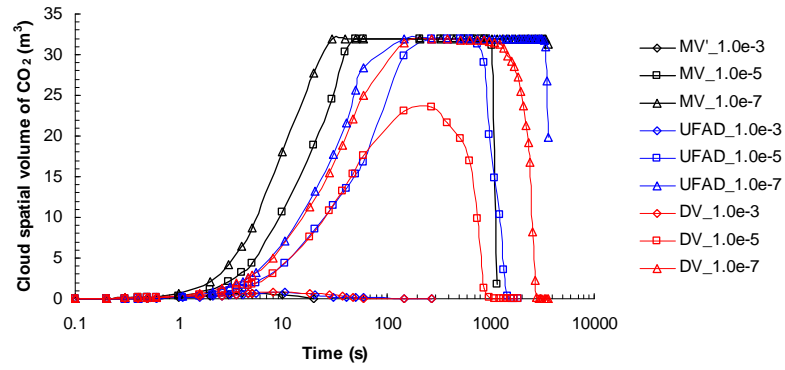


(c)

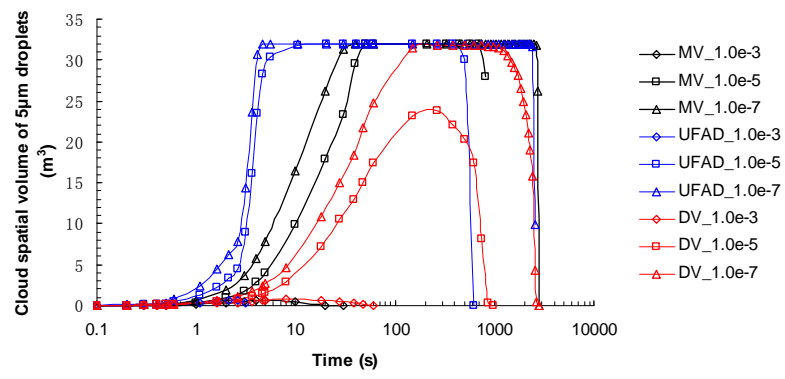
Figure 4.17 Cloud spatial volume of CO<sub>2</sub>, 5 μm and 10 μm droplets under MV (a), UFAD (b) and DV (c) during the first 10 seconds (MV\_1.0e-3 means the volume of the space in which normalized concentration of CO<sub>2</sub> is never less than 1.0e-3 under MV)

For MV, droplets less than 10  $\mu\text{m}$  have the same cloud volume before the 200<sup>th</sup> second. Smaller droplets disperse faster since their lower inertia makes it much easier for indoor air movement to change their moving direction and enhance their dispersion. During the later period, the spatial volume for larger droplets decreases faster due to their higher deposition rate. Different phenomena can be observed under UFAD because of its specific airflow patterns. 5  $\mu\text{m}$  and 10  $\mu\text{m}$  droplets have the same cloud volume for the whole investigated period. Their spatial volume is larger than that for fine droplets at the first 200 seconds and then becomes smaller because of higher gravitational force. It is interesting to find that all the droplets present almost the same volume variation under DV. This may be related to the reason that its upward air movement can facilitate the extraction of smaller droplets with lower deposition rate and hamper the deposition of larger droplets with higher deposition rate. The balance between the convective and gravitational forces induces the similar dispersion profiles for all the droplets in DV ventilated environment.

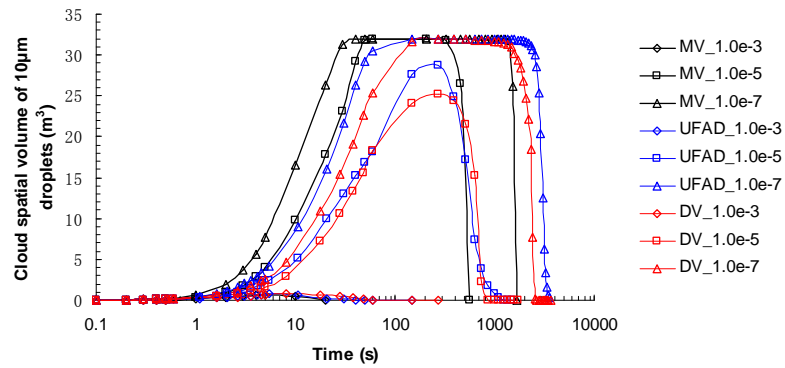
Comparison is made in Figure 4.18 for cloud spatial volume of  $\text{CO}_2$ , 5  $\mu\text{m}$  and 10  $\mu\text{m}$  droplets under MV, UFAD, and DV to investigate the influences of ventilation system on the dispersion of respiratory droplets.



(a)



(b)



(c)

Figure 4.18 Comparison of Cloud spatial volume for CO<sub>2</sub> (a), 5 µm (b) and 10 µm (c) droplets changing with time under MV, UFAD and DV (MV\_1.0e-3 means the volume of the space in which normalized concentration of CO<sub>2</sub> is never less than 1.0e-3 under MV)

CO<sub>2</sub> and 10 μm droplets disperse fastest under MV during the first 100 seconds, while 5 μm droplets are diluted the most quickly under UFAD. The quick dilution of exhaled droplets in MV is due to the well-mixed air movement. Fast dispersion of 5 μm droplets in UFAD may be related to the total effects of the upward air movement, gravitational force of droplets, and the strong air mixing in the lower space induced by the two swirling diffusers. All the droplets are the most slowly diluted under DV because of its lower air velocity. At the second stage, the spatial volume for CO<sub>2</sub> and 5 μm droplets decreases fastest under DV and faster under UFAD due to the upward extraction by ventilation system. The higher deposition rate for 10 μm droplets in MV ventilated room results in the quickest decrease of the cloud volume.

#### ***4.3.3.2 Co-occupant's exposure***

Figure 4.19 presents the normalized inhaled concentration of the co-occupant when the infected person coughs at a velocity of 22 m/s, and the inhaled dose is displayed in Figure 4.20. The exposed concentration reaches its highest level faster under MV and UFAD, but a short delay can be observed in DV. This is consistent with the transportation profile of the exhaled air shown in Figure 4.14 in which the coughed air approaches the co-occupant much earlier in MV and UFAD. Because of the delayed exposure to the highly concentrated coughing jet under DV, the maximum exposed concentration is only half of that under MV and UFAD. This lower peak value can be attributed to the reason that the droplets in the coughing jet are more dispersed when the highly concentrated droplet cloud approaches the co-occupant.

As shown in Figure 4.21, the maximum inhaled concentration happens at about the 1<sup>st</sup> second under MV and the spatial volume for concentration no less than  $1.0 \times 10^{-3}$  is  $0.174 \text{ m}^3$  at this moment, while it is around the 2<sup>nd</sup> second that the exposed concentration reaches its highest level under DV and the corresponding cloud volume is  $0.295 \text{ m}^3$ . Since the same amounts of droplets are released, the larger occupied volume implies lower concentration. Meanwhile, a decay curve of  $\text{CO}_2$  in a well-mixed environment is displayed in Figure 4.19 assuming the exhaled contaminants are fully and evenly dispersed in the room at the 200<sup>th</sup> second. The decay curve rightly overlaps with the normalized inhaled concentration lines for  $\text{CO}_2$  and  $1 \mu\text{m}$  droplets under MV. This indicates that the simulation results are reasonable.

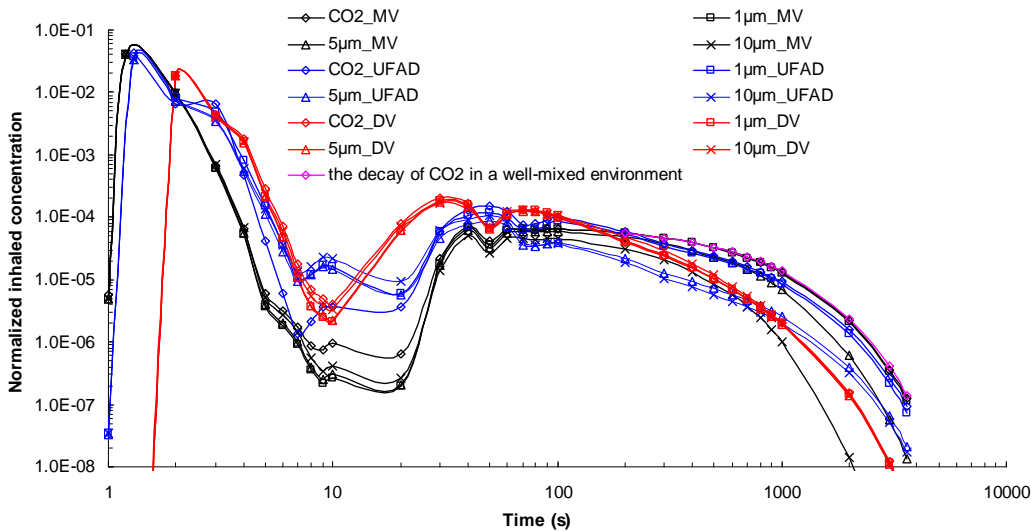


Figure 4.19 Normalized inhaled concentration of the co-occupant under MV, UFAD, and DV (the concentration in the instantaneous coughed air is denoted as 1.0)

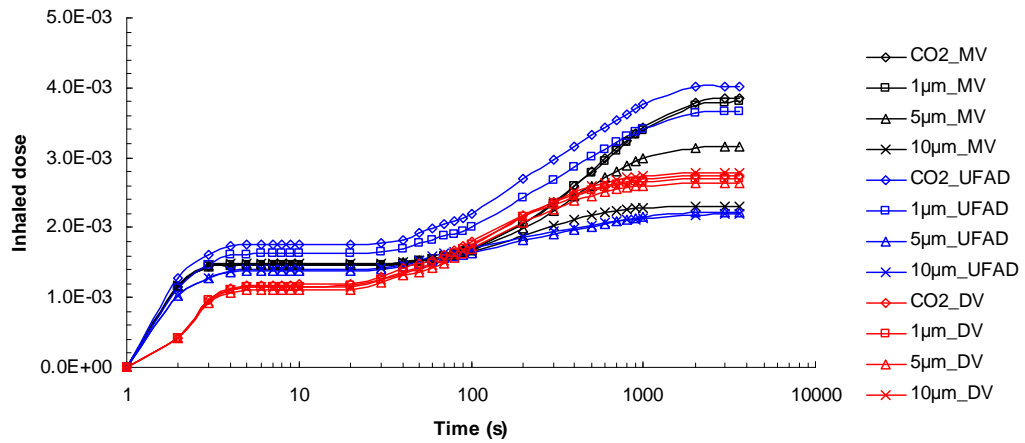


Figure 4.20 Inhaled dose of the co-occupant under MV, UFAD, and DV

With the passage of time, the effect of coughing jet dissipates and the dispersion of droplets is affected by indoor air movement more significantly during the later period. As shown in Figure 4.19, there is a second inhaled concentration peak. This peak value is about two to three orders of magnitude lower than that in the first 10 seconds. Because of the continuous extraction and deposition of those coughed droplets, the exposed concentration decreases gradually. Though the inhaled fraction is much lower at this stage, the inhaled dose can still be comparable with the quantity inhaled during the first process because of its longer exposure period.

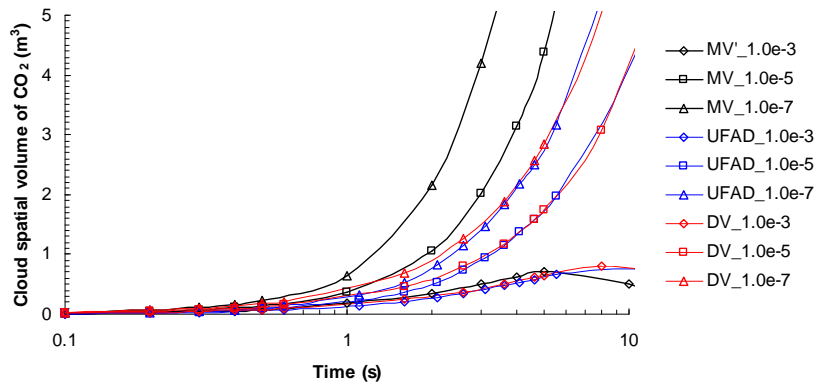


Figure 4.21 Cloud spatial volume of CO<sub>2</sub> under MV, UFAD, and DV during the first 10 seconds (MV\_1.0e-3 means the volume of the space in which normalized concentration of CO<sub>2</sub> is never less than 1.0e-3 under MV)

It can be seen from Figure 4.19 and Figure 4.20 that droplet diameter exhibits strong influence on the co-occupant's exposure under MV and UFAD. The inhaled dose for 10 µm droplets is about half of the amount that for CO<sub>2</sub>. Different phenomena can be observed under DV. There are no significant differences in the inhaled dose for all the droplets investigated. The inhaled dose remains almost in the same level under MV and UFAD for CO<sub>2</sub>, 1 µm and 10 µm droplets separately, while obvious differences can be observed for 5 µm droplets and the inhaled mass is higher for MV. The inhaled dose is lowest under DV for droplets less than 5 µm whilst interestingly highest for 10 µm droplets.

Table 4.1 lists the co-occupant's inhaled dose in the first 10 seconds and the later period. The inhaled dose during the first period is lowest under DV for all the droplets, while it is highest under MV for larger droplets and UFAD for smaller

droplets. At the second stage, ventilation system gradually disperses those exhaled droplets to be largely distributed in the room. The higher deposition rate of larger droplets can enhance their deposition under MV and UFAD and then results in a lower inhalation for the co-occupant, while the widely dispersed smaller droplets can remain suspended for a longer period and lead to higher exposure. The inhaled dose under DV however is about the same for all the droplets. Although larger droplets show higher tendencies to deposit onto indoor surfaces, the upward air flow of DV tends to suspend the larger droplets around the breathing height. Smaller droplets are more likely to be extracted by the ventilation system, but the lower deposition rate means that more are dispersed in the room air. The balance of these mechanisms including gravitation settling, upward air movement, and ventilation extraction leads to the same level of exposure for all the droplets under DV.

Table 4.1 Inhaled dose of the co-occupant during the two stages

Droplets type	The first stage			The second stage		
	MV	UFAD	DV	MV	UFAD	DV
CO <sub>2</sub>	1.46e-3	1.75e-3	1.18e-3	2.40e-3	2.27e-3	1.55e-3
1 μm	1.46e-3	1.63e-3	1.16e-3	2.34e-3	2.02e-3	1.55e-3
5 μm	1.47e-3	1.38e-3	1.11e-3	1.69e-3	0.84e-3	1.53e-3
10 μm	1.48e-3	1.40e-3	1.15e-3	0.81e-3	0.79e-3	1.64e-3

It is also interesting to be noted that the inhaled dose since the 10<sup>th</sup> second as illustrated in Figure 4.22 exhibits almost the same trends as that for the normalized inhaled concentration during the steady nose-breathing process as shown in Figure 4.11. The inhaled dose is reversely proportional to the droplet size under MV and

UFAD, while a slight increase with droplet diameter can be observed under DV. The co-occupant's exposure during the first several seconds is affected by the coughing jet. As the effect of this coughing jet dies out gradually, the ventilation system may play almost the same role on the exposure level of the co-occupant for both the steady respiratory process and the transient coughing process.

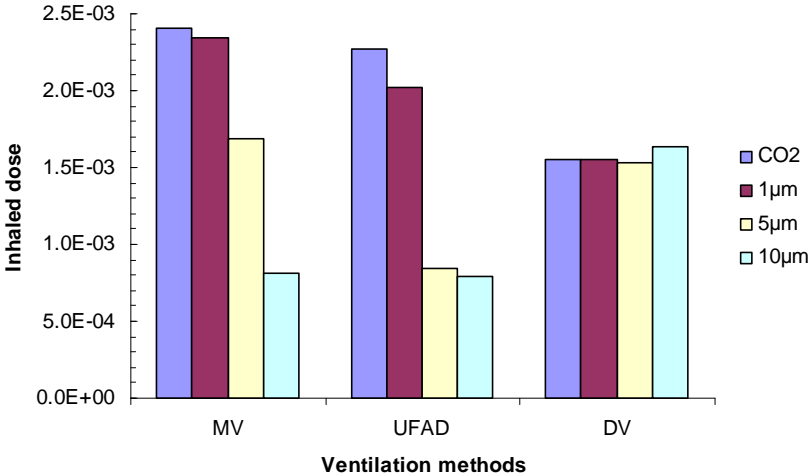


Figure 4.22 Inhaled dose since the 10<sup>th</sup> second

**4.3.4 Simulation of the distribution of droplets coughed at a low velocity of 6 m/s**

**4.3.4.1 Droplet dispersion**

Figure 4.23 presents the dispersion of 10 µm droplets released at a velocity of 6 m/s under MV, UFAD, and DV. When the infected person coughs at a low velocity, the coughing jet can not bring the pathogen-laden droplets to the breathing zone of the co-occupant directly at a distance of 1.5 m from the infected person. The exhaled

droplets are first diluted by the ventilation system and largely distributed in the room. This means that the direct exposure to the coughing jet can be avoided and the total inhaled dose may be decreased greatly.

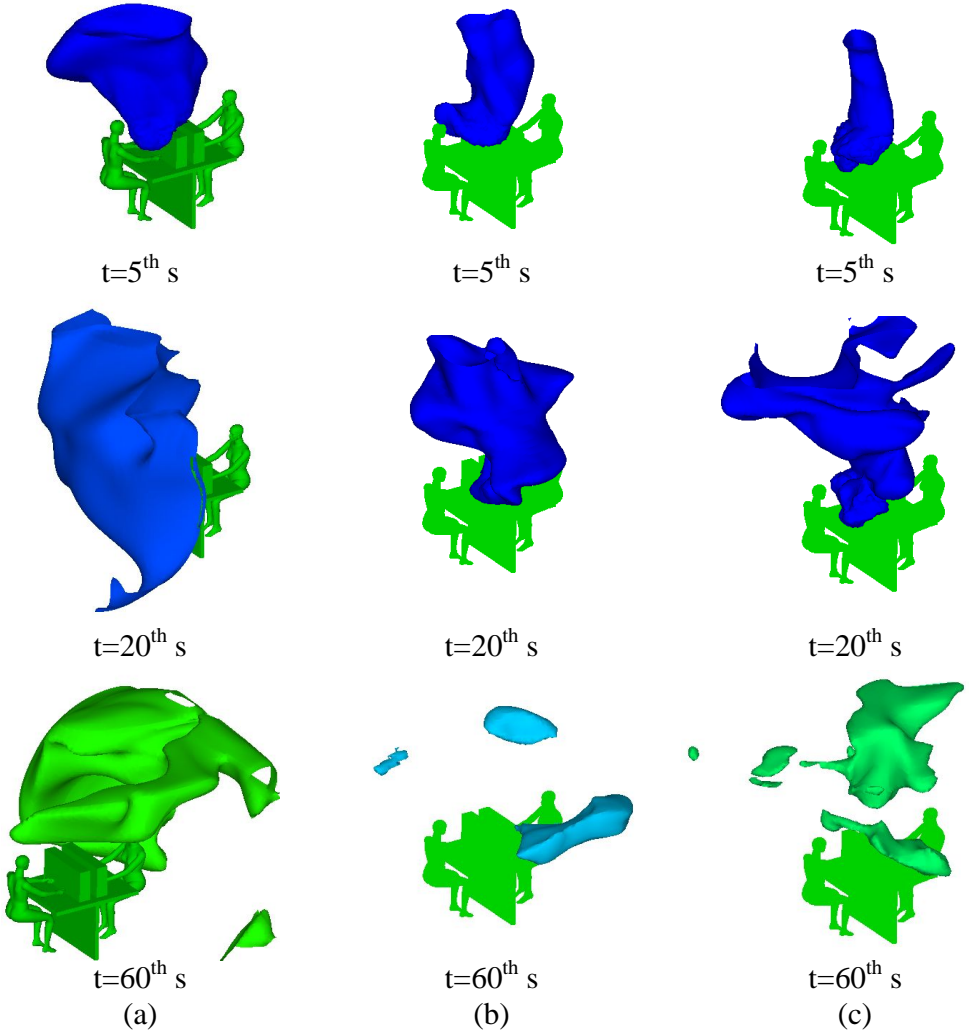
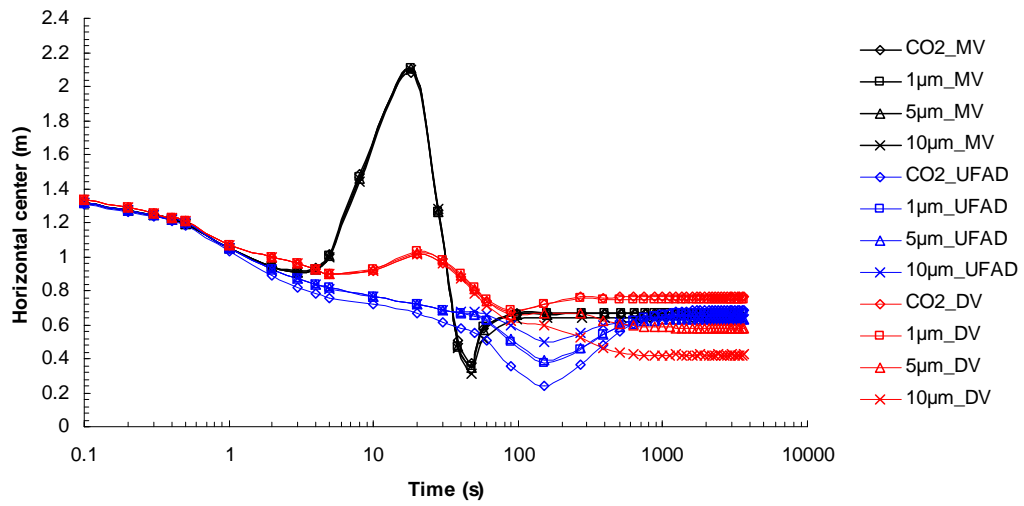


Figure 4.23 Dispersion of exhaled  $10\ \mu\text{m}$  droplets under MV (a), UFAD (b), and DV (c) when the infected person coughs at a low velocity of  $6\ \text{m/s}$  (the normalized concentration is not less than  $0.0001$  while the concentration in the instantaneous coughed air is denoted as  $1.0$ ).

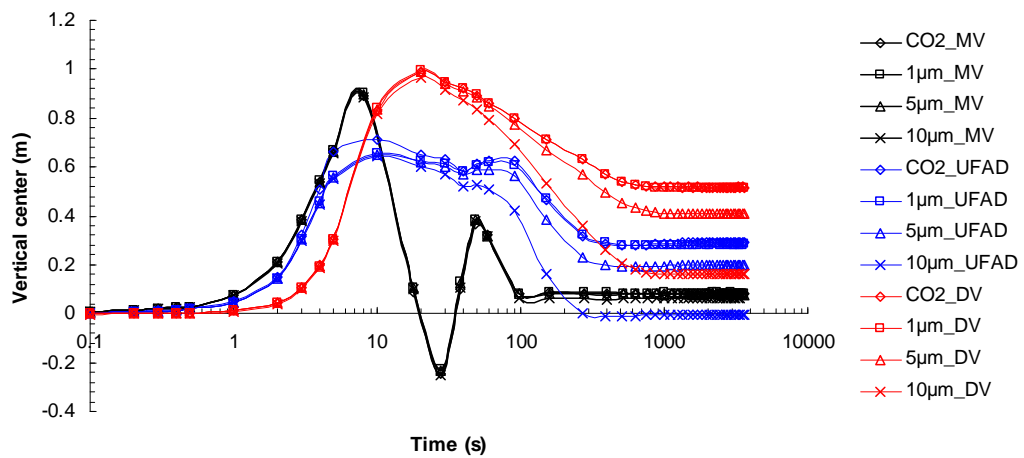
As to the dispersion of exhaled droplets under different ventilation systems, MV can quickly and widely disperse the released droplets which may induce a relatively higher inhaled concentration during the earlier period. The exhaled droplets under UFAD and DV, on the other hand, are first driven to a higher level by the thermal plume of heat sources and the upward air movement, and then gradually distributed mainly in the upper space. This may induce a later lower exposed concentration.

To analyze the dispersion history of the exhaled droplets during the whole research period, Figure 4.24 displays the traveling trajectories of the droplet clouds in the form of the transition of their horizontal and vertical center. Since the respiratory droplets are released at a relatively lower velocity, the horizontal center of droplet clouds is always certain distance away from the co-occupant under all the three ventilation schemes. The horizontal center under UFAD and DV changes quite smoothly while sharp curve can be observed under MV during a short period because of its enhanced air mixing. As to the vertical center of droplet clouds, the changing profiles are quite similar for UFAD and DV due to their alike upward air movement. The exhaled air is driven upward by the thermal plumes of heat sources and upward air movement at first. With the continuous extraction of exhaled droplets, the vertical center varies toward the middle height of the room. It can be observed that the exhaled air travels slowest vertically in DV during the first several seconds for the reason that the higher temperature gradient in the breathing level hampers its upward transportation. Meanwhile, the weaker air turbulence in DV will

also hinder the transportation of exhaled air to the lower region of the room. This may result in the highest vertical center under DV for the remaining period.



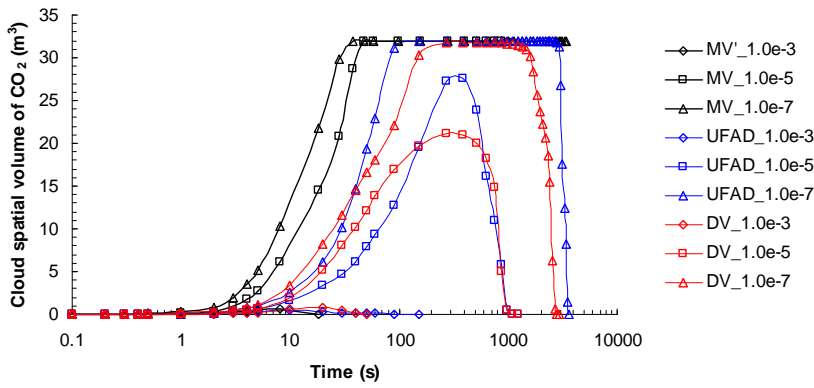
(a)



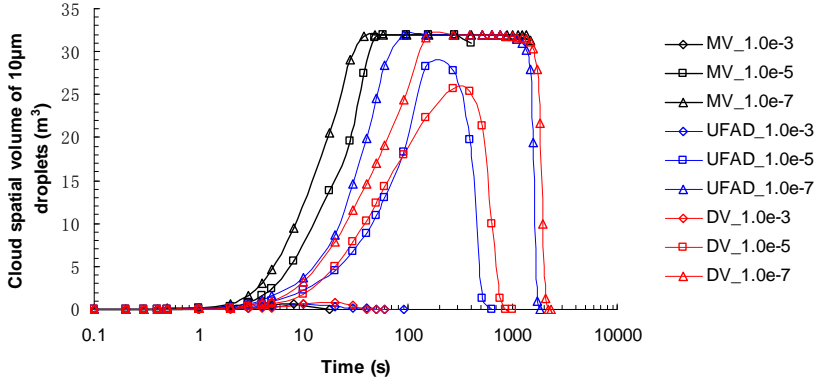
(b)

Figure 4.24 Horizontal center (a) and vertical center (b) of droplet clouds varying with time under MV, UFAD, and DV

Figure 4.25 presents the variation of spatial cloud volume for CO<sub>2</sub> and 10 μm droplets with time under the three ventilation systems. For all the droplets investigated, MV can distribute them to be the most largely dispersed due to its stronger air movement. Even during the later period, the cloud volume decreases slowest. This may induce a longer-term exposure for the co-occupant in MV ventilated environment.



(a)



(b)

Figure 4.25 Cloud spatial volume of CO<sub>2</sub> (a) and 10 μm (b) droplets varying with time under MV, UFAD, and DV when the infected person coughs at 6 m/s (MV\_1.0e-3 means the volume of the space in which normalized concentration of CO<sub>2</sub> is never less than 1.0e-3 under MV)

Compared with UFAD, smaller droplets are diluted faster in DV during the first 100 seconds, and the occupied volume decreases more quickly during the later remaining period. The possible reason is that smaller droplets can be more easily dispersed and extracted by the upward airflow of DV while it is much difficult for larger droplets. The cloud spatial volume for larger droplets declines more quickly under UFAD since the air mixing induced by the two swirling diffusers can facilitate the deposition of larger droplets.

#### ***4.3.4.2 Co-occupant's exposure***

Figure 4.26 illustrates the normalized inhaled concentration of the co-occupant when the infected person coughs at a velocity of 6 m/s. The contaminant inhalation in the first 20 seconds is too low to cause severe damage to the co-occupant. During the later period, on the other hand, ventilation system distributes the exhaled droplets to be widely dispersed in the room and then results in a long-term exposure. The exhaled droplets disperse fastest under MV due to its well-mixed airflow, and the exposed concentration is the highest during the first 200 seconds. The inhaled concentration profile under UFAD is quite similar with MV, while the concentration value is much lower because of the relatively weaker air mixing abilities. For the co-occupant's exposure under DV, a sharp decline at about the 50<sup>th</sup> second in the inhaled concentration can be observed. As shown in Figure 4.27, the exhaled droplets in DV are first driven to the higher region of the room by thermal plumes of heat sources and upward air movement. Later, air turbulence gradually disperses the

exhaled droplets to be largely dispersed in the room. During the transition between the coughing jet and indoor air movement which are the two major forces influencing the transportation of exhaled droplets, an apparent decrease of inhaled concentration will be induced by the conflicts among the upward air movement of DV, convective airflow around heat sources, and air turbulence.

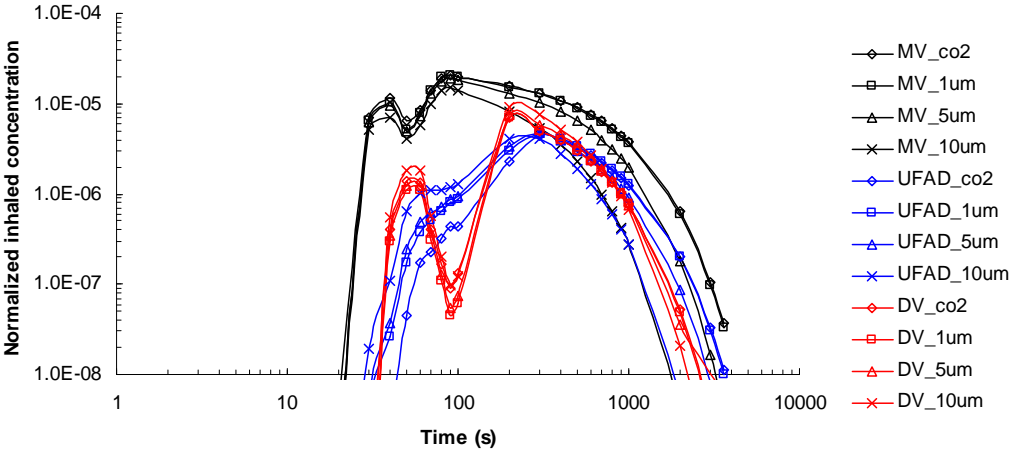


Figure 4.26 Normalized inhaled concentration of the co-occupant under different ventilation methods when the infected person coughs at a velocity of 6 m/s (droplet concentration in the instantaneous coughed air is denoted as 1.0).

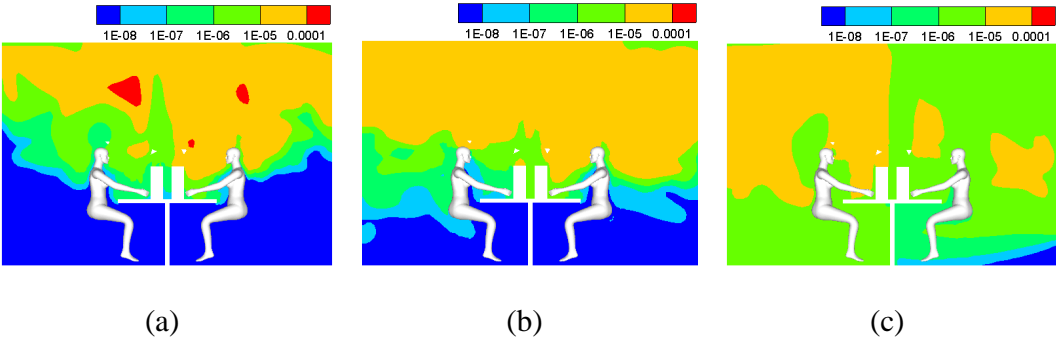


Figure 4.27 Distribution of exhaled 10 μm droplets at the 50<sup>th</sup> second (a), 100<sup>th</sup> second (b), and 270<sup>th</sup> second (c) under DV

Figure 4.28 displays the inhaled dose of the co-occupant under different ventilation systems. It is clear that a short-term exposure to the coughed air can be eliminated when the infected person coughs a lower velocity. For a long-term exposure process, the inhaled dose is highest under MV for all the investigated droplets since the exhaled droplets can be quickly and widely dispersed indoors. Nevertheless, the mainly upward airflow of UFAD and DV can transport the expelled air to the higher region as seen in Figure 4.23, which may hamper the dispersion of exhaled droplets to the co-occupant's breathing zone. For this reason, the inhaled dose is quite lower than MV, especially for smaller droplets. UFAD achieves the lowest inhalation for 10  $\mu\text{m}$  droplets since its quite strong air mixing in the lower region may facilitate the deposition of larger droplets when compared with DV.

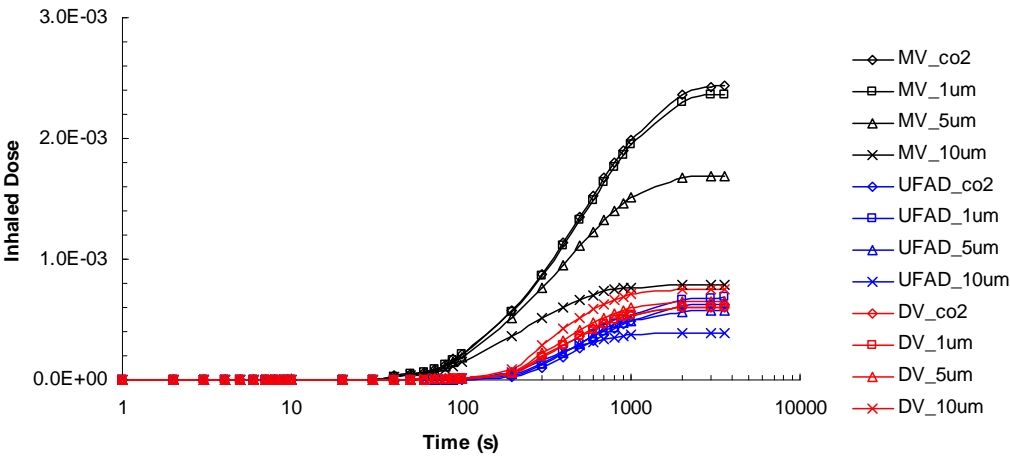


Figure 4.28 Inhaled dose of the co-occupant under different ventilation methods when the infected person coughs at a velocity of 6 m/s

### **4.3.5 Comparison of co-occupant's exposure at different coughing velocities**

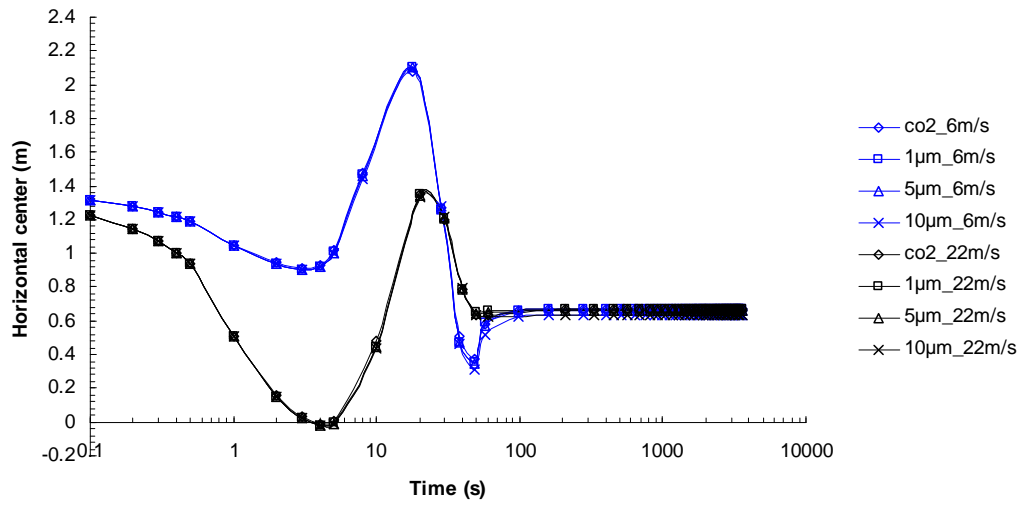
#### ***4.3.5.1 Personal exposure at different coughing velocities under MV***

It has been stated that, at a sitting distance of 1.5 m between the infected person and the co-occupant, coughed air released at a velocity of 22 m/s can deliver the exhaled droplets to the co-occupant's breathing zone directly and result in a higher short-term direct exposure, while a 6 m/s coughing jet has dissipated before approaching the co-occupant and the direct exposure can be eliminated. This is consistent with the numerical finding of Xie et al. (2007) that the traveling distance of the exhaled air was mainly associated with the initial expelling velocity. For a typical sitting/standing distance between the infected person and the co-occupant, the co-occupant's exposure is strongly influenced by the respiratory characteristics of the infected person. The study of the two extreme velocities demonstrates that a certain distance away from the infected person can safely avoid the direct impact from the highly pathogen-laden breathing airflow, even when the co-occupant is in a face-to-face orientation with the infected person.

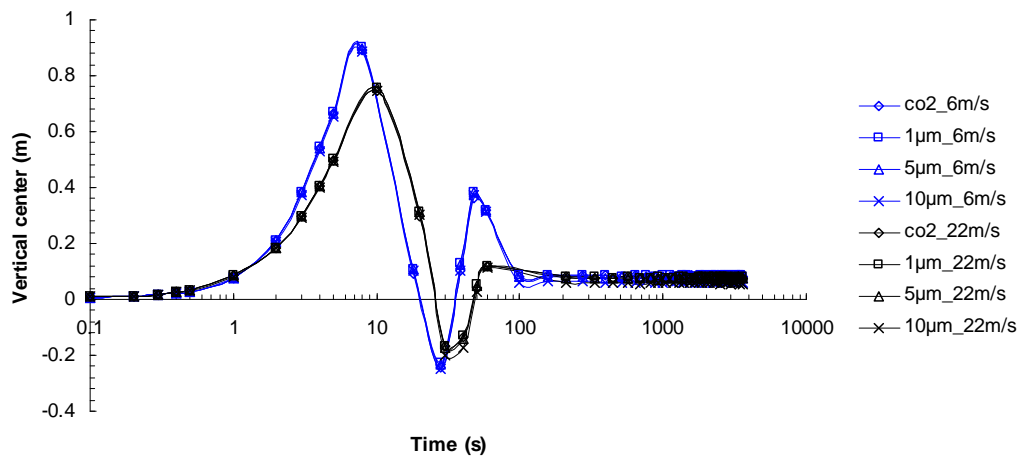
The traveling profiles of exhaled droplets under MV are presented in Figure 4.29 to evaluate their dispersion processes. The same variation trends can be observed when the infected person coughs at different velocities. The main difference is that a higher coughing velocity can transport the expelled droplets farther to the breathing zone of the co-occupant and lead to higher inhaled concentration. When the infected person coughs at a lower velocity of 6 m/s, this low momentum coughing jet can

only transport the exhaled droplets to the region in the middle of the two occupants where the thermal plume of heat sources will drive these droplets upward and then being dispersed. This will induce a relatively higher and earlier maximum vertical value. At about the 100<sup>th</sup> second, MV can distribute all the exhaled droplets being widely dispersed in the room no matter at what a velocity those droplets are released.

Figure 4.30 illustrates the variations of cloud spatial volume for CO<sub>2</sub> and 10 μm droplets under MV at different coughing velocities. It can be observed that all the droplets are dispersed at the same speed during the whole period. The transportation and dilution processes of exhaled droplets demonstrate that MV can quickly and largely disperse the exhaled droplets generated at different velocities. The mainly difference is induced by the coughing jet during the first one minute according to Figure 4.29. This implies that the same inhaled dose at the later period is expected to be resulted in since air movement is the main force to distribute the exhaled droplets at that moment, while the inhalation at the first stage will vary with the coughing velocity. Once the direct impact from the coughing jet is avoided, the same exposure level will be achieved without apparent relations with the releasing velocity and location of polluting source.

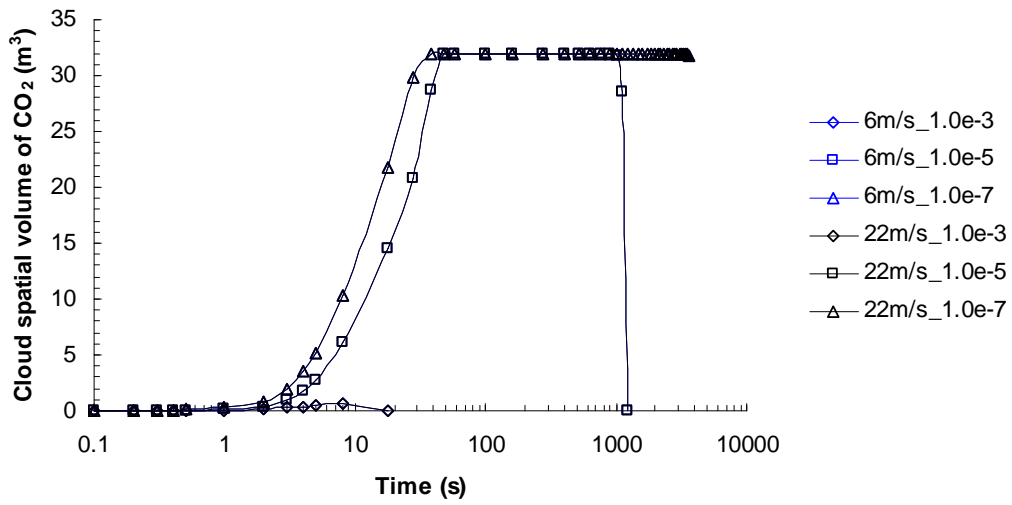


(a)

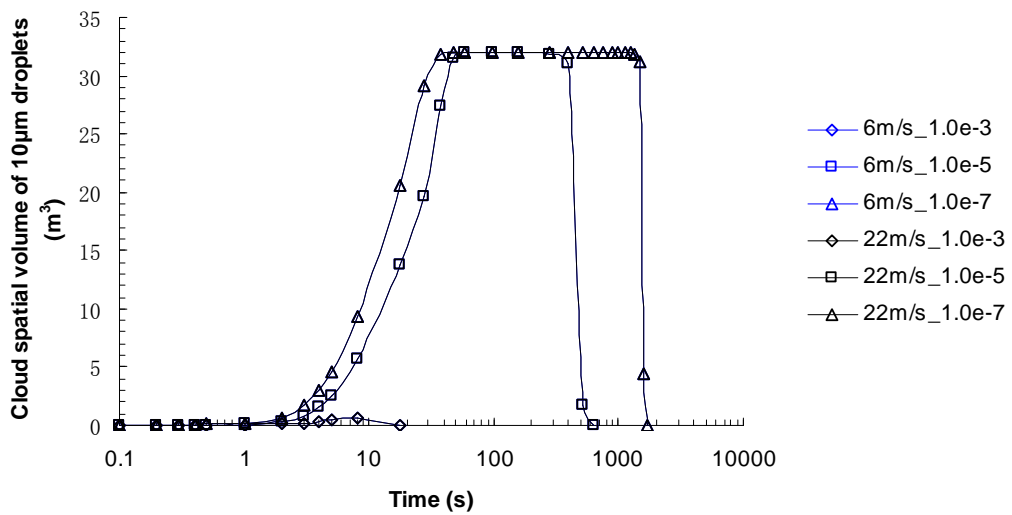


(b)

Figure 4.29 Horizontal center (a) and vertical center (b) of droplet clouds varying with time under MV when the infected person coughs at different velocities



(a)



(b)

Figure 4.30 Cloud spatial volume of CO<sub>2</sub> (a) and 10 µm droplets (b) varying with time under MV when the infected person coughs at different velocities (6 m/s\_1.0e-3 means the volume of the space in which normalized concentration of CO<sub>2</sub> is never less than 1.0e-3 at a coughing velocity of 6 m/s)

Figure 4.31 displays the normalized inhaled concentration of the co-occupant at different exhaled air releasing velocities, and the co-occupant's inhaled dose is presented in Figure 4.32. It can be observed clearly that, in the first 10 seconds, the direct exposure to the coughed air is completely avoided at a distance of around 1.5 m from the infected person with a coughing velocity of 6 m/s. During the later period, the co-occupant's exposed concentration shows almost the same patterns for the two respiration velocities. To further analyze the co-occupant's exposure, Figure 4.33 presents a comparison of the inhaled dose at different exposure periods. The total inhaled dose indicates the co-occupant's exposure level during the whole process, while the indirect inhaled dose only counts the co-occupant's inhalation since the 10<sup>th</sup> second in which the co-occupant's exposure is caused by the indirect air-borne transmission of exhaled droplets. Since the coughing jet at a velocity of 6 m/s can not bring the virus-laden droplets to the co-occupant directly, as seen in Figure 4.29, the co-occupant's inhaled dose due to direct exposure is extremely small and the total inhaled dose equals the indirect inhaled dose. Assuming that the same amount of droplets is released, the total inhaled dose is reduced apparently at a lower coughing velocity because of the avoidance of the direct impact from the coughing jet. However, the inhalation at the second stage, in which the exhaled droplets are distributed to the breathing zone of the co-occupant by ventilation airflows, not by the high momentum coughing jet, remains nearly in the same level.

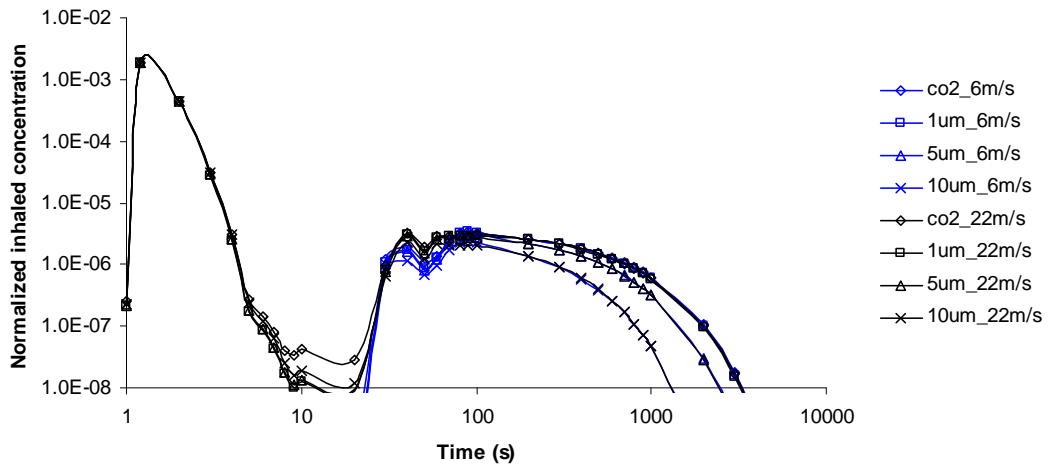


Figure 4.31 Normalized inhaled concentration of the co-occupant when the infected person coughs at 6 m/s and 22 m/s under MV (The initial droplet concentration in the exhaled air is denoted as 1.0)

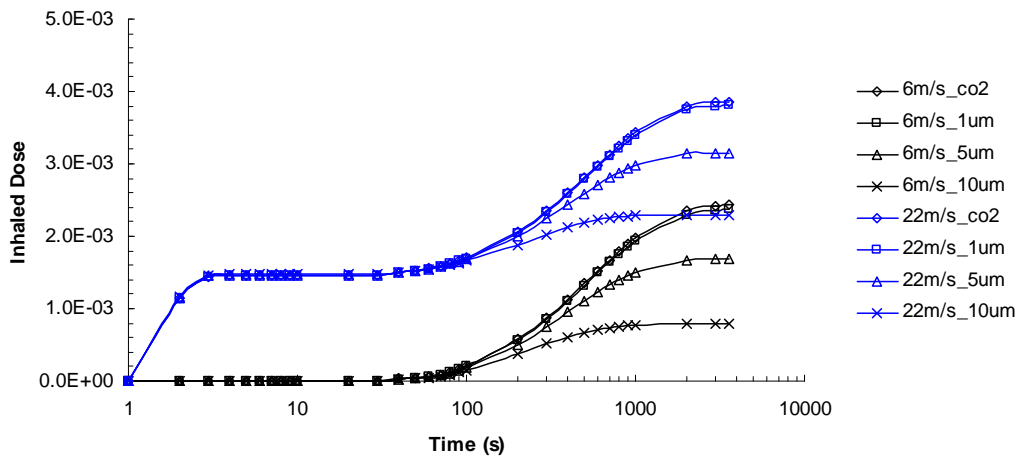


Figure 4.32 Inhaled dose (*ID*) of the co-occupant when the infected person coughs at 6 m/s and 22 m/s under MV

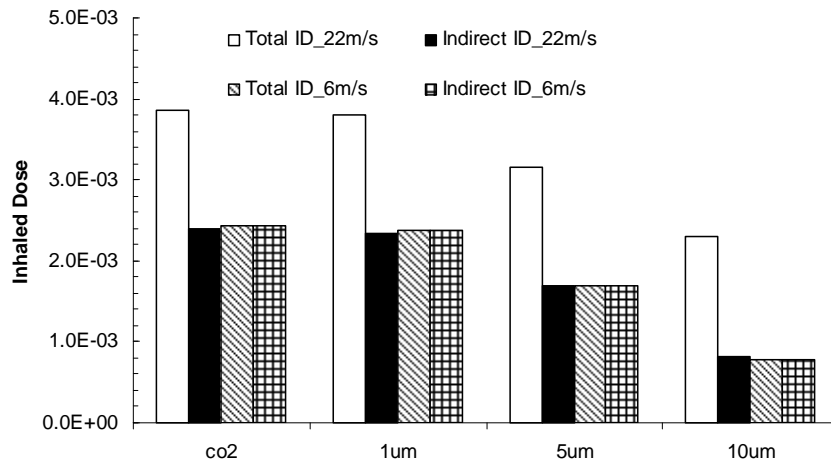
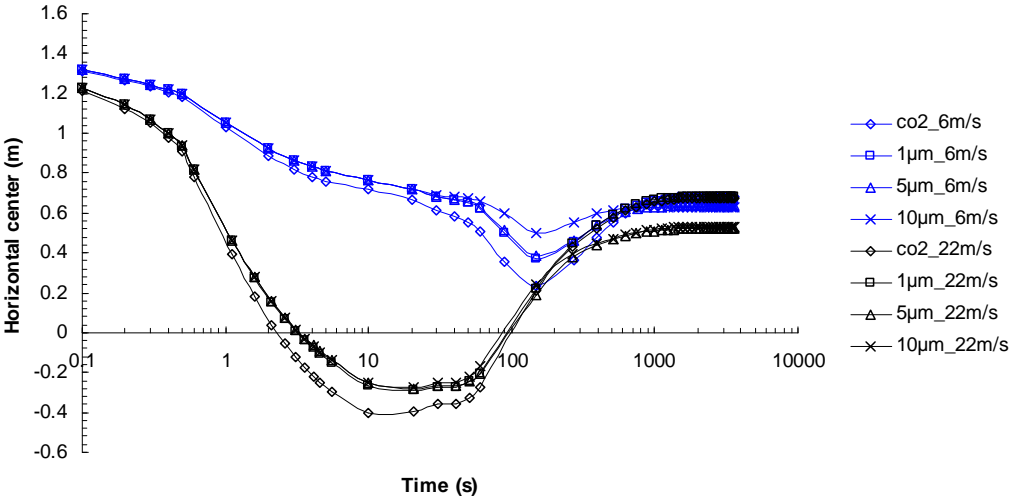


Figure 4.33 Comparison of the inhaled dose (*ID*) of the co-occupant at coughing velocities of 6m/s and 22m/s under MV (Indirect inhaled dose refers to the co-occupant’s inhalation since the 10<sup>th</sup> second)

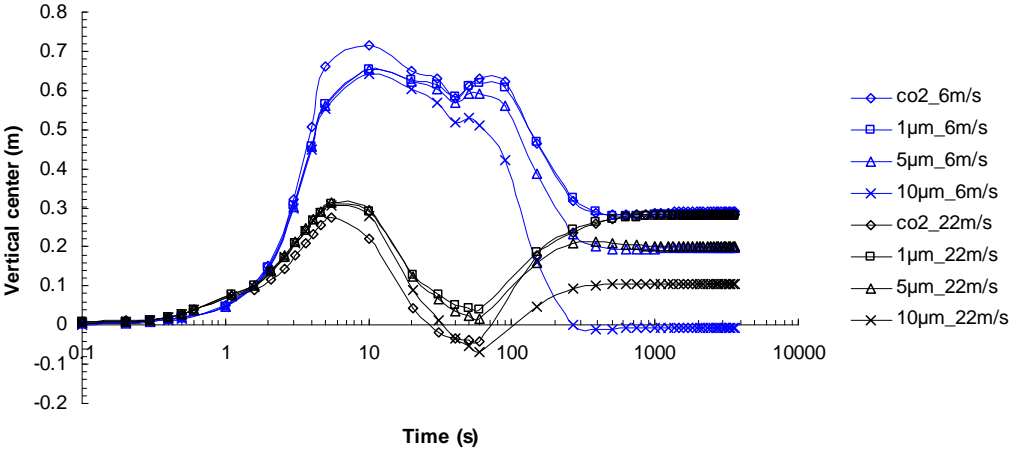
#### 4.3.5.2 Personal exposure at different coughing velocities under UFAD

Figure 4.34 presents the traveling profiles of exhaled droplets shown as the variations of the horizontal and vertical center of droplet clouds, and the cloud spatial volume is displayed in Figure 4.35. Same as MV, coughing at a low velocity under UFAD can not transport the exhaled droplets to the co-occupant’s breathing zone directly. The differences are that the traveling history of exhaled droplets under UFAD varies with the expelling velocity during the whole research period. Exhaled droplets generated at a low velocity are first transported toward the co-occupant by the coughing jet, and upward by the thermal plumes of heat sources and upward air movement. With the continuous functions of extraction, deposition, and air turbulence, the horizontal and vertical centers vary to the center of the room gradually. Differently, coughed airflow at a higher velocity of 22 m/s can deliver the

exhaled droplets to the co-occupant directly with a slight rise of the vertical center of droplet clouds. Since the exhaled droplets are transported to the upper space of one swirling diffuser, the strong air mixing movement can enhance the dispersion of droplets in the occupied zone. This may explain the decrease in the vertical center of droplet clouds since the 10<sup>th</sup> second.



(a)

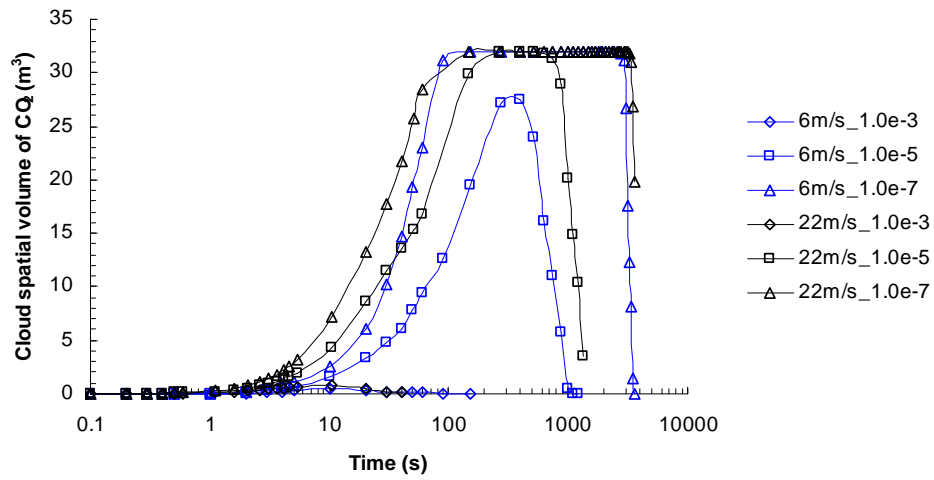


(b)

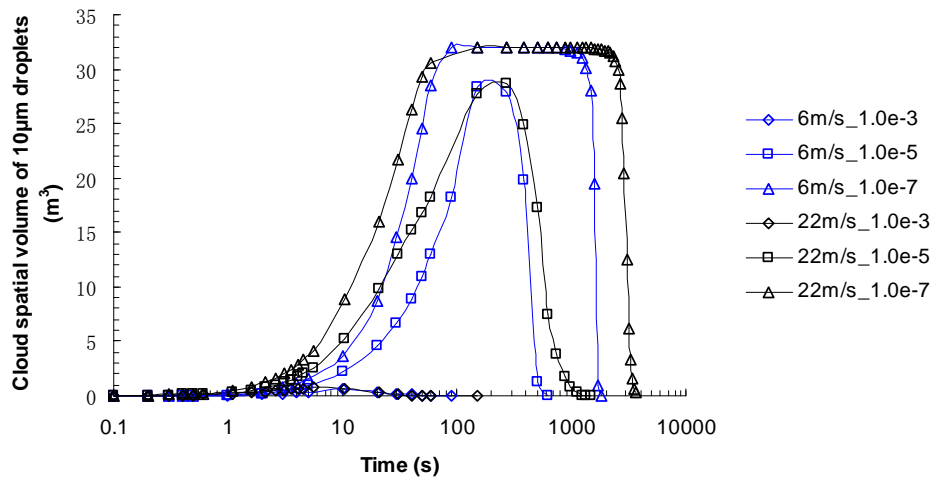
Figure 4.34 Horizontal center (a) and vertical center (b) of droplet clouds varying with time under UFAD when the infected person coughs at different velocities

As to the spatial volume of the exhaled droplets at different coughing velocities, it can be noticed in Figure 4.35 that droplets expelled at a higher velocity disperse faster and are more difficult to be extracted. The possible reason is that a higher coughing velocity can transport the exhaled droplets farther, and the continuous interaction with room air during this process can facilitate the dilution and dispersion of exhaled droplets. The quicker decrease of droplet cloud volume at a lower coughing velocity during the later period may be attributed to the reason that the upward air movement of UFAD and convective flow around heat sources can transport the exhaled droplets to the higher space of the room and being extracted.

Figure 4.36 shows the normalized inhaled concentration of the co-occupant when the infected person coughs at a higher velocity of 22 m/s and a lower velocity of 6 m/s, and the inhaled dose is presented in Figure 4.37. When the infected person coughs at a higher velocity, the expelled droplets can reach the co-occupant directly and pose higher short-term exposure. The inhaled concentration during the later period is also higher since exhaled droplets are transported to the region close to the co-occupant by the high momentum coughing jet during the earlier period. Nevertheless, droplets released at a lower velocity can not reach the co-occupant directly and the upward air movement of UFAD can distribute these droplets to region above the breathing level. This may hamper the dispersion of these droplets to the breathing zone of the co-occupant and reduce the exposure level.



(a)



(b)

Figure 4.35 Cloud spatial volume of CO<sub>2</sub> (a) and 10 µm droplets (b) varying with time under UFAD when the infected person coughs at different velocities (6 m/s\_1.0e-3 means the volume of the space in which normalized concentration of CO<sub>2</sub> is never less than 1.0e-3 at a coughing velocity of 6 m/s)

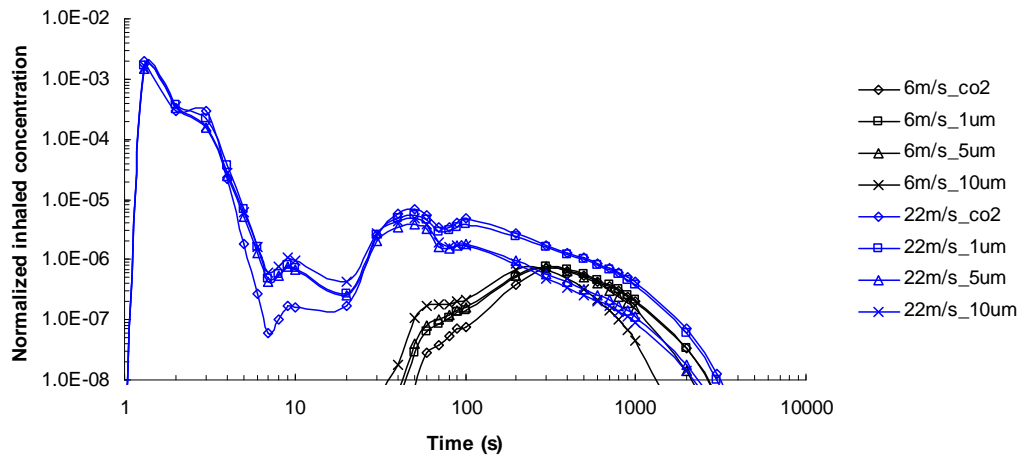


Figure 4.36 Normalized inhaled concentration of the co-occupant when the infected person coughs at 6 m/s and 22 m/s under UFAD (The initial droplet concentration in the exhaled air is denoted as 1.0)

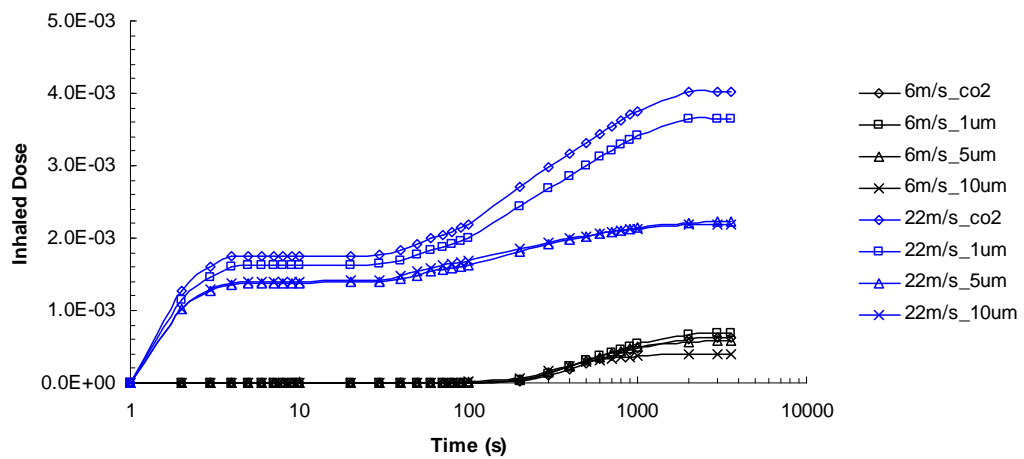


Figure 4.37 Inhaled dose (*ID*) of the co-occupant when the infected person coughs at 6 m/s and 22 m/s under UFAD

Figure 4.38 presents a comparison of the co-occupant's inhaled dose at different coughing velocities. The total inhaled dose is reduced substantially when the infected person coughs at a lower velocity, mainly because of the elimination of the direct exposure to the coughed airflow. Great reduction of inhalation during the later period for a 6 m/s coughing velocity, especially for smaller droplets, can also be achieved since the upward airflow of UFAD system can move the exhaled pathogen-laden droplets to the higher region of the room.

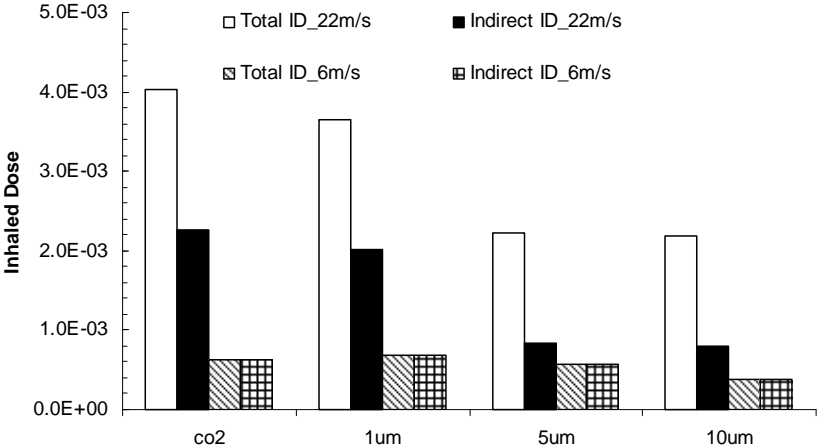
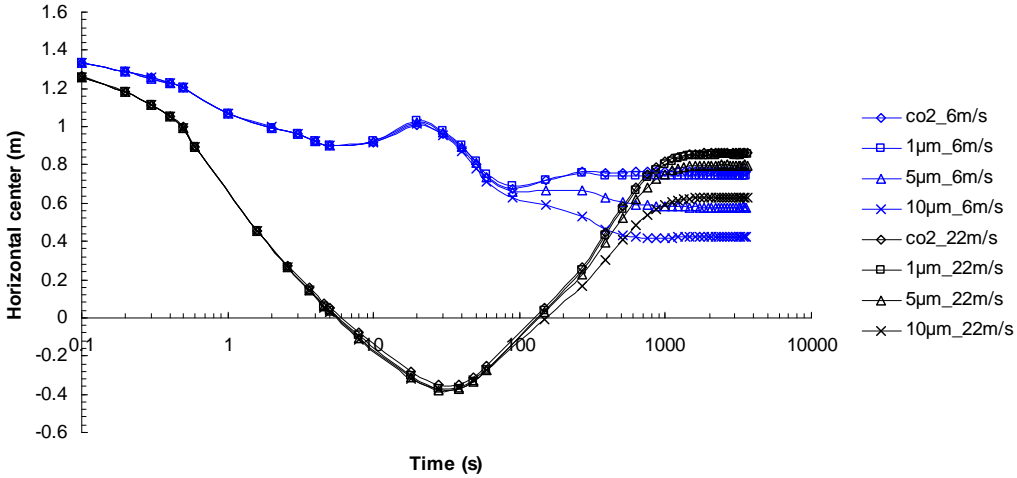


Figure 4.38 Comparison of the inhaled dose (*ID*) of the co-occupant at coughing velocities of 6m/s and 22m/s under UFAD (Indirect inhaled dose refers to the co-occupant's inhalation since the 10<sup>th</sup> second)

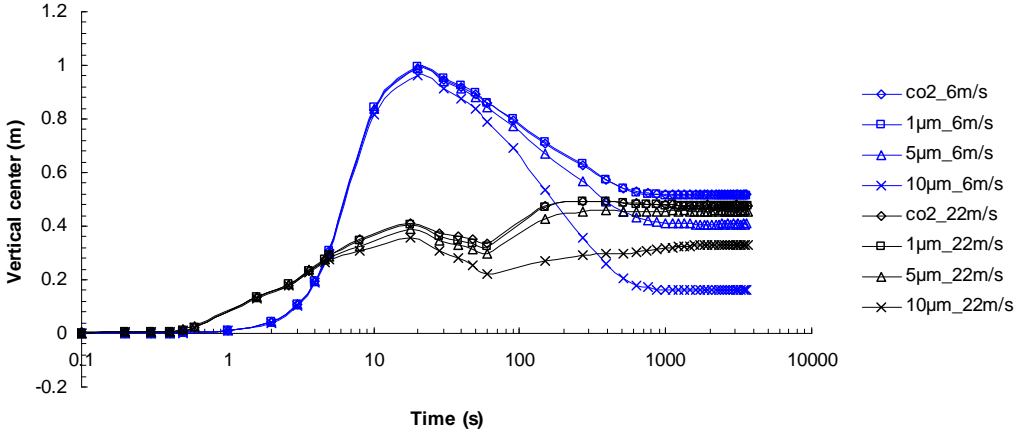
**4.3.5.3 Personal exposure at different coughing velocities under DV**

As seen in Figure 4.39 and Figure 4.40, the variations of droplet dispersion and dilution at different coughing velocities under DV are quite similar with UFAD since both the two ventilation schemes share some features in common. A major

difference between UFAD and DV lies in the dispersion profile of smaller droplets. It can be observed in Figure 4.40 (a) that smaller droplets can all be efficiently extracted during the later period in a DV ventilated environment because of its uni-directional upward air movement.

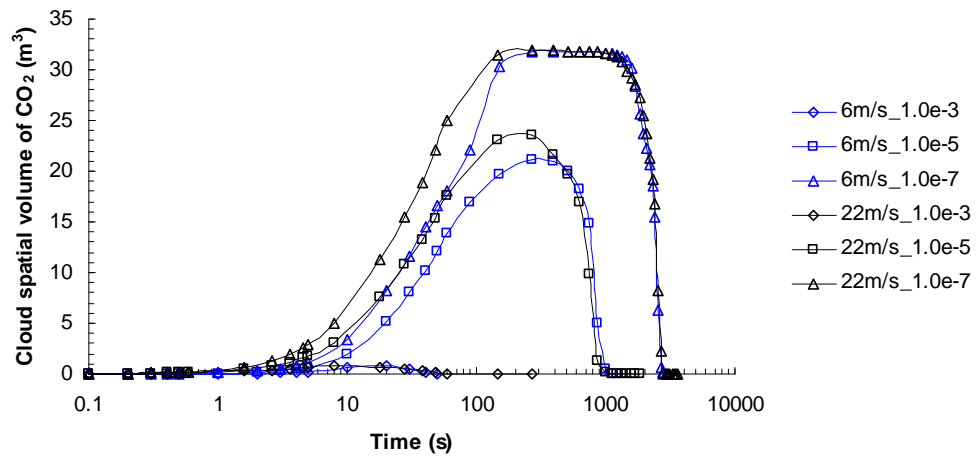


(a)

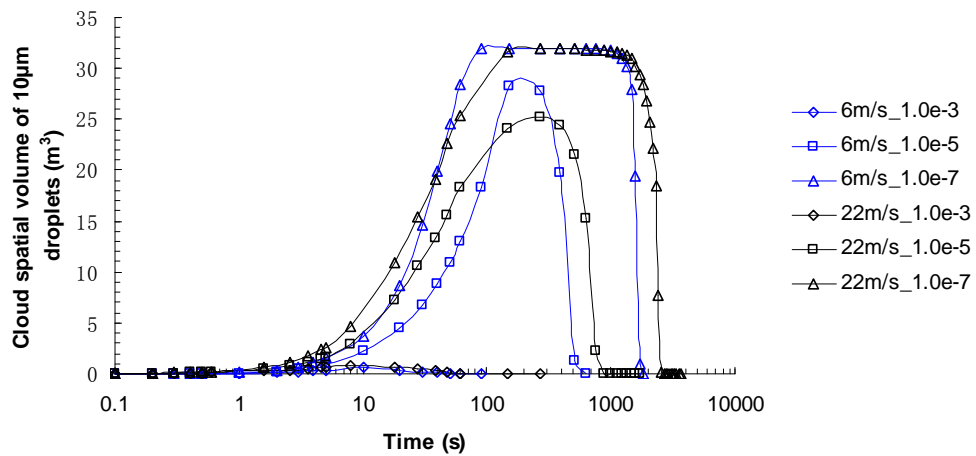


(b)

Figure 4.39 Horizontal center (a) and vertical center (b) of droplet clouds varying with time under DV when the infected person coughs at different velocities



(a)



(b)

Figure 4.40 Cloud spatial volume of CO<sub>2</sub> (a) and 10 µm droplets (b) varying with time under DV when the infected person coughs at different velocities (6 m/s\_1.0e-3 means the volume of the space in which normalized concentration of CO<sub>2</sub> is never less than 1.0e-3 at a coughing velocity of 6 m/s)

Figure 4.41 illustrates the normalized inhaled concentration of the co-occupant at different coughing velocities under DV, and the inhaled dose is presented in Figure 4.42. Same as UFAD, a lower coughing velocity can not only eliminate the direct exposure of the co-occupant to the highly contagious coughing jet but also reduce the inhaled concentration during the later period.

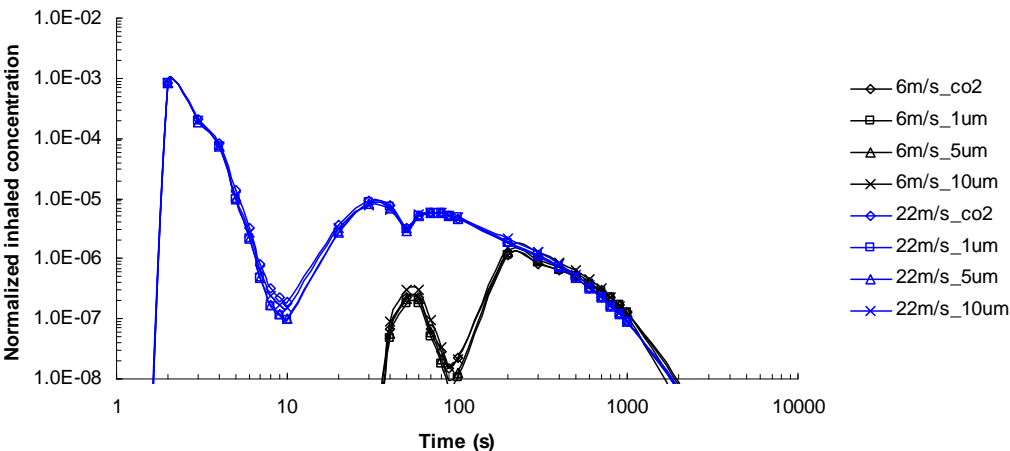


Figure 4.41 Normalized inhaled concentration of the co-occupant when the infected person coughs at 6 m/s and 22 m/s under DV (The initial droplet concentration in the exhaled air is denoted as 1.0)

The comparison of inhaled dose at different coughing velocities under DV is presented in Figure 4.43. Because of the avoidance of the direct exposure to the coughed airflow expelled at a lower velocity, the total inhaled dose is reduced remarkably, and a large decrease of the inhalation during the later period can also be achieved. This may be explained by the transportation of exhaled droplets during the whole period in which the coughed droplets are first delivered to the region between

the two occupants, and then moved to the upper space by indoor air movement and the convective airflow of heat sources.

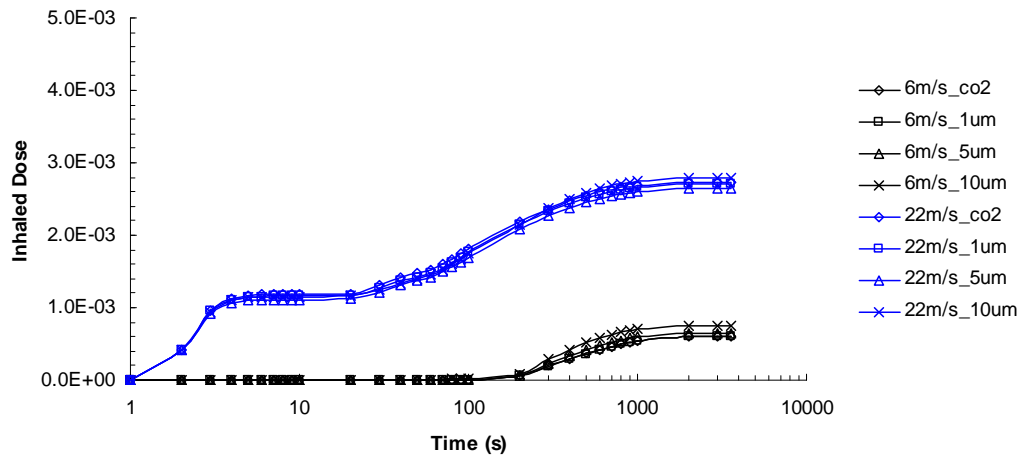


Figure 4.42 Inhaled dose (*ID*) of the co-occupant when the infected person coughs at 6 m/s and 22 m/s under DV

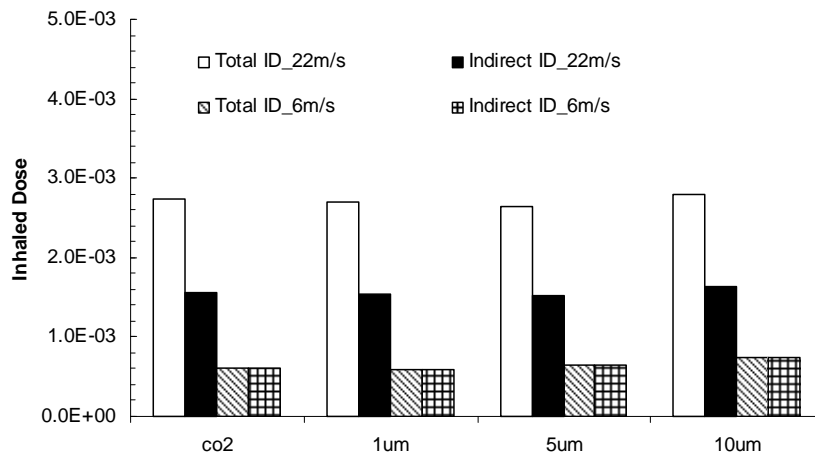


Figure 4.43 Comparison of the inhaled dose (*ID*) of the co-occupant at coughing velocities of 6m/s and 22m/s under DV (Indirect inhaled dose refers to the co-occupant's inhalation since the 10<sup>th</sup> second)

#### 4.3.6 Summary

In this section, the simulation of transient coughing process with a coughing velocity of 22 m/s illustrates much clearly that there are two distinctive stages of exposure for the co-occupant during the whole airborne transmission, a direct exposure due to coughing jet at the first stage and an indirect exposure caused by indoor air movement at the second stage. Though the inhaled concentration at the second stage is about two to three orders of magnitude lower than that at the first stage, the inhaled dose during this period can still pose higher health risk to the co-occupant. As to the co-occupant's total inhaled dose, it is found that stratified ventilation system can not always assure a better inhaled air quality for the co-occupant. Highest inhaled dose may be induced by UFAD for smaller droplets and DV for 10  $\mu\text{m}$  droplets, although DV can provide a better indoor environment for the co-occupant when the droplets smaller than 5  $\mu\text{m}$  are the major concern. UFAD can achieve the lowest inhaled dose for droplets larger than 5  $\mu\text{m}$ .

When the respiratory droplets are released at a lower velocity of 6 m/s, the inhaled dose are reduced apparently mainly because of the avoidance of the direct exposure to the coughed airflow. At a coughing velocity of 6 m/s, the total inhaled dose is highest under MV for all the droplets, while comparable lower personal exposure can be achieved under UFAD and DV. Compared with DV, UFAD achieves the lower inhalation for 10  $\mu\text{m}$  droplets since its quite strong air mixing movement in the lower region can facilitate the deposition of larger droplets.

The comparison of the co-occupant's exposure indicates that the personal exposure during the first stage can be eliminated under all the three ventilation systems at a lower coughing velocity. The inhaled dose during the second indirect exposure stage, on the other hand, exhibits quite differently. Almost the same exposure level during the second stage is induced under MV at different coughing velocities because of its well-mixed air movement. Nevertheless, lower inhalation at this stage is resulted in under UFAD and DV when the infected person coughs at a lower velocity. The results demonstrate that certain distance away from the infected person can safely avoid the direct impact from the coughed airflow even when the two occupants are in the face-to-face orientation. Meanwhile, stratified ventilation system shows better performance at a lower coughing velocity, since its upward air movement can drive the exhaled droplets upward to the higher region and being extracted, and reduce the co-occupant's inhaled dose substantially not only for the whole exposure process but also for the second indirect exposure stage.

## **Chapter 5**

### **Effects of Coughing Orientations and Physical Blockings on Co-occupant's Exposure**

Numerical studies in Chapter 4 reveal that higher personal exposure can be induced in seconds if the infected person coughs at a face-to-face orientation with the susceptible person. Although a certain distance away from the polluting source can safely avoid this short-term direct exposure, the variation of expelling velocities due to human varieties makes it much difficult to ascertain the travelling distance of the exhaled droplets generated by the target infected person. Hence, this chapter aims to numerically investigate the exposure level of the co-occupant when the infected person coughs at different orientations under the three ventilation schemes, and the performances of two types of physical blockings are also studied to evaluate their effects in mitigating infectious diseases transmission.

#### **5.1 Numerical studies of droplet distribution at different coughing orientations**

##### **5.1.1 Introduction**

The transportation of droplets released during coughing or sneezing are highly directional. For a face-to-face orientation with the infected person, direct exposure will happen if the co-occupant lies in the traveling distance of the exhaled droplets

(Xie et al. 2006). Once this direct exposure to the coughed air is avoided, it is found that great reduction of inhaled dose can be obtained not only for the whole exposure period but also for the second indirect exposure stage. Due to the individual preferences among peoples, however, it is difficult to ascertain the safe distance from the infected person. This section therefore aims to investigate the personal exposure of the co-occupant if the infected person coughs at different directions in order to protect the co-occupant from the direct exposure to the coughed droplets.

### **5.1.2 Case description**

The configuration of the simulated room is presented in Figure 5.1. The dimensions of the room, the arrangements of the heat sources, the inlet and outlet diffusers are all the same as those in Chapter 4. The only difference is the facing direction of the infected person when he/she coughs and the corresponding coughing orientation. It is assumed that the infected person is in the face-to-face orientation with the co-occupant at first. During a cough process, the infected person will either bend the head  $45^\circ$  down, or turn around to face one inner wall as displayed in Figure 5.1. The coughed droplets are assumed to be released at a velocity of 22 m/s (Zhu et al. 2006), and the coughing orientation is  $45^\circ$  downward for bending the head scenario and horizontal for turning around. The temperature of the expelled air is set to be  $35^\circ\text{C}$  (Höppe, 1981). As to the co-occupant, continuous inhalation is assumed and the breathing rate is 8.4 l/min (Huang 1997) through nostrils with a direction of  $45^\circ$  upward.

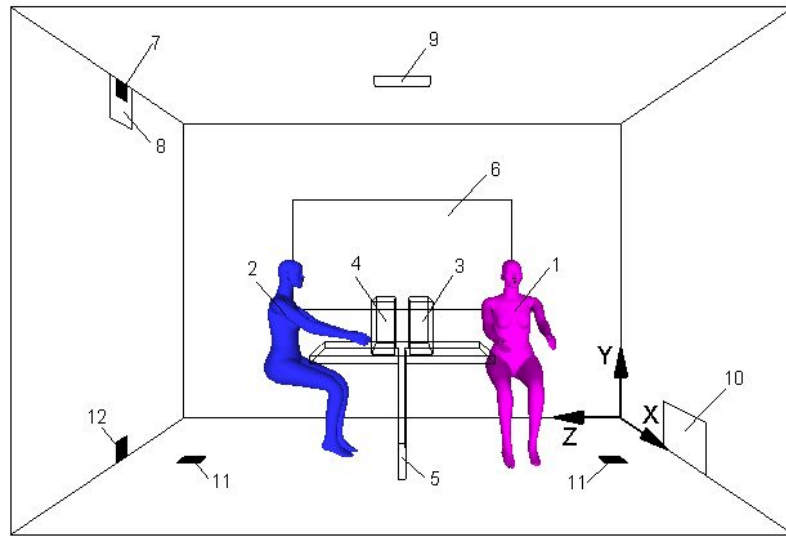


Figure 5.1 Configuration of the simulated room (room length (Z) 4 m, width (X) 3 m, Height (Y) 2.7 m; 1-infected person; 2-co-occupant; 3, 4-computer; 5-desk; 6-window; 7-MV inlet 0.2 m × 0.12 m; 8-DV outlet 0.4 m × 0.3 m; 9-UFAD outlet 0.2 m × 0.2 m; 10-DV inlet 0.8 m × 0.35 m; 11-UFAD inlet 0.165 m × 0.165 m; 12-MV outlet 0.2 m × 0.15 m)

### **5.1.3 Co-occupant’s exposure when the infected person coughs with the head bending down**

#### ***5.1.3.1 Droplet dispersion***

Figure 5.2 displays the distribution of 10  $\mu\text{m}$  droplets at the 2<sup>nd</sup>, and 10<sup>th</sup> second when the infected person coughs with the head bending down under different ventilation systems. The exhaled air is blocked by the arrangements in the desk at first, such as computers in this case, and then distributed by air distribution system. The exhaled droplets disperse fastest horizontally under MV due to the strong air mixing properties. The upward air movement of UFAD and DV can transport the

coughed air to the higher space of the room, which may hamper the dispersion of exhaled droplets to the breathing zone of the co-occupant.

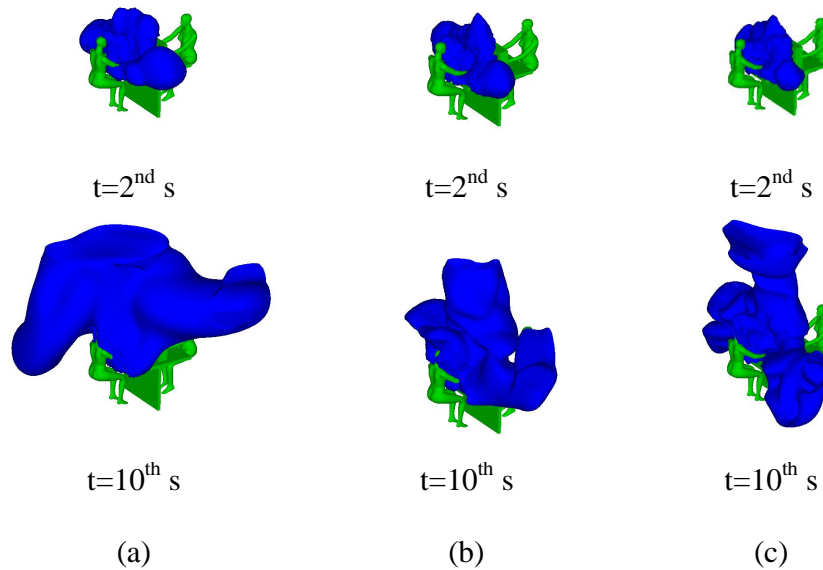
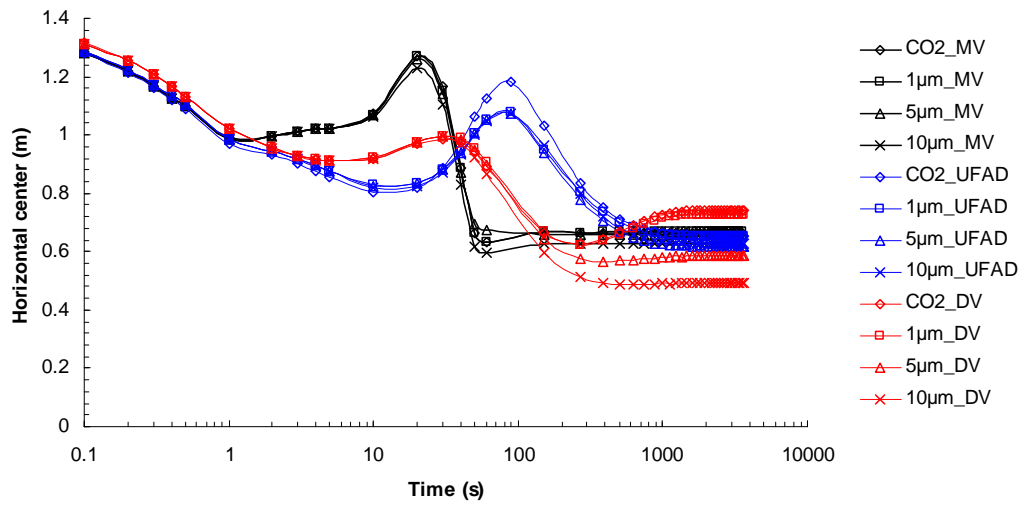


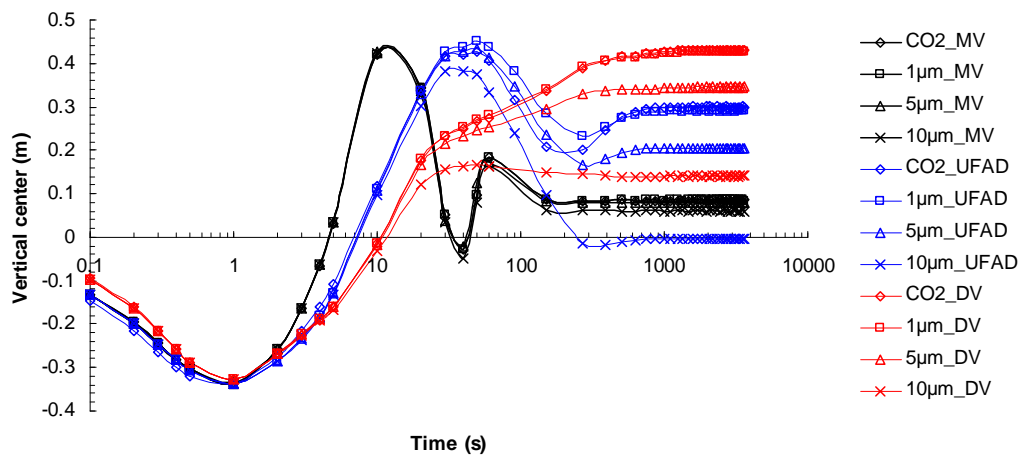
Figure 5.2 Distribution of exhaled  $10\ \mu\text{m}$  droplets in the first 10 seconds under MV (a), UFAD (b), and DV (c) when the infected person coughs with the head bending down (the normalized concentration is not less than 0.0001 with the droplet concentration in the initial coughed air being denoted as 1.0)

The transportation of exhaled droplets is shown in Figure 5.3 in the form of the variations of the horizontal and vertical center of droplet clouds. Due to the interruption by the arrangements in the desk, the coughed air approaching the co-occupant is deflected to the region close to the infected person. With the dissipation of this high momentum coughing jet, ventilation system then gradually distributes

the exhaled droplets to be widely dispersed indoors with the cloud center varying to the center of the room.

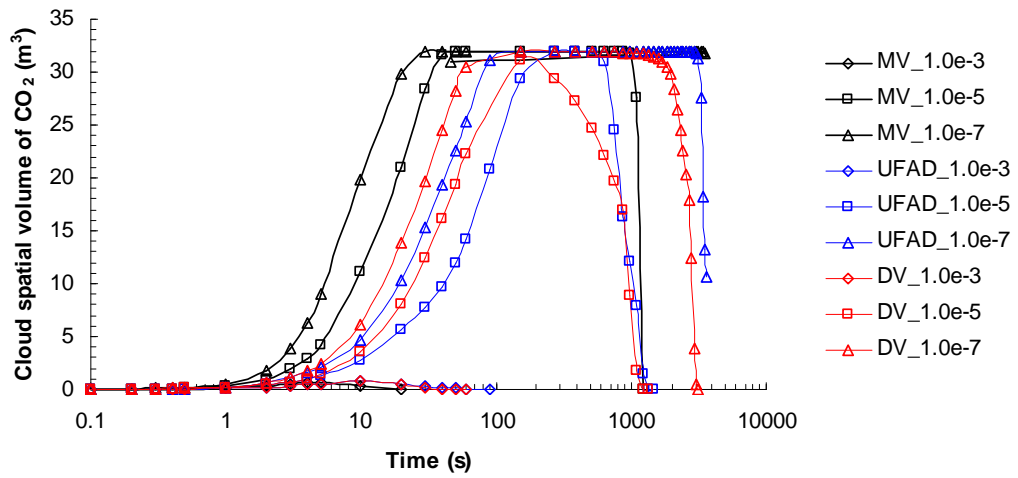


(a)

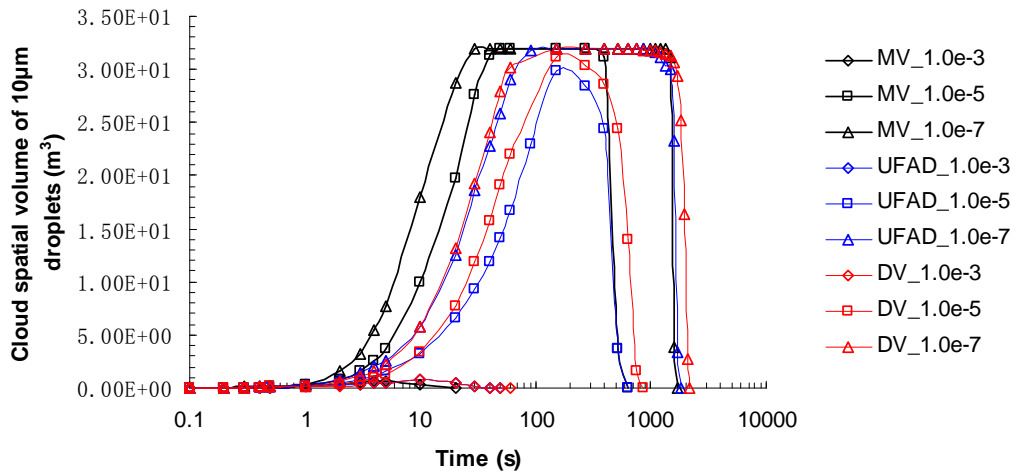


(b)

Figure 5.3 Horizontal center (a) and vertical center (b) of droplet clouds varying with time under MV, UFAD, and DV when the infected person coughs with the head bending down



(a)



(b)

Figure 5.4 Cloud spatial volume of CO<sub>2</sub> (a) and 10 µm droplets (b) under MV, UFAD, and DV when the infected person coughs with the head bending down (MV\_1.0e-3 means the volume of the space in which normalized concentration of CO<sub>2</sub> is never less than 1.0e-3 under MV)

The cloud spatial volume is displayed in Figure 5.4 to present the dilution process of the exhaled droplets under each ventilation scheme. The exhaled droplets are the

most quickly dispersed under MV, while faster in DV for smaller droplets because of its uni-directional upward air movement. No apparent differences for larger droplets can be observed between UFAD and DV. The cloud volume of smaller droplets decreases fastest under DV due to its higher contaminant extraction effectiveness, while slowest for larger droplets since its upward airflow can interact with the gravitational settling forces of droplets and suspend them in the occupied zone.

#### ***5.1.3.2 Co-occupant's exposure***

Figure 5.5 presents the normalized inhaled concentration of the co-occupant under MV, UFAD, and DV when the infected person coughs with the head bending down, and the inhaled dose is displayed in Figure 5.6. Because of the fastest dispersion of exhaled droplets in MV ventilated room, the exposed concentration is highest in the first 10 seconds, while highest exposure is induced under UFAD from the 10<sup>th</sup> to the 40<sup>th</sup> second since the highly concentrated droplet clouds are much closer to the co-occupant, as seen in Figure 5.3 (a). The inhaled concentration is lowest under DV because its upward air movement and the convective airflow around heat sources forward the exhaled droplets to the higher region of the room. During the later period, the exposed concentration for 10  $\mu\text{m}$  droplets is lowest under MV because of the higher droplet deposition rate, while highest for droplets less than 10  $\mu\text{m}$  due to its well-mixed air movement. The low deposition rate of DV results in the highest inhaled concentration for 10  $\mu\text{m}$  droplets since about the 200<sup>th</sup> second.

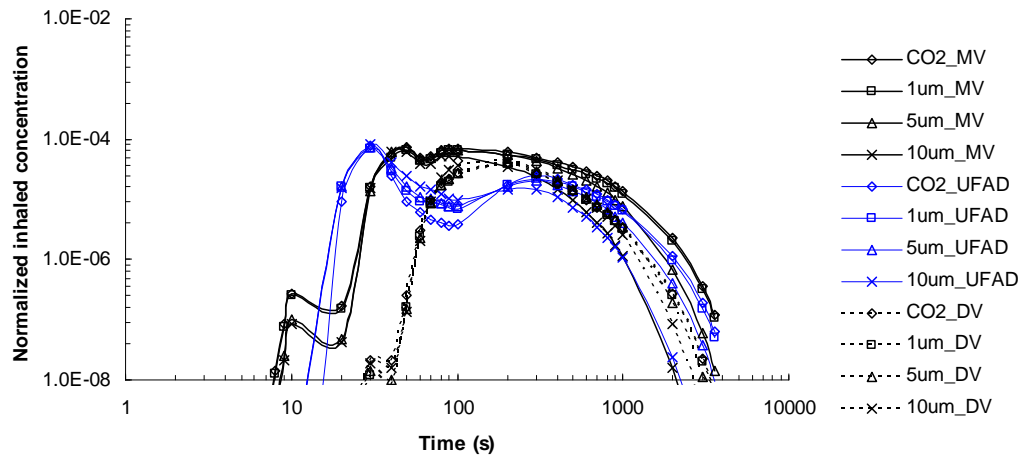


Figure 5.5 Normalized inhaled concentration of the co-occupant under different ventilation systems when the infected person coughs with the head bending down

As shown in Figure 5.6, the inhaled dose of 10  $\mu\text{m}$  droplets is highest under DV because its upward air movement can suspend more large droplets in the breathing level, while highest under MV for droplets less than 10  $\mu\text{m}$  since the well-mixed air movement can distribute the exhaled droplets being largely dispersed in the occupied zone. It is interesting to find that the lowest exposure can be achieved by UFAD for all the droplets investigated. The primary reason is that the coughed air is blocked to the region close to the infected person where the strong air mixing of UFAD can facilitate the deposition of larger droplets and the mainly upward air movement will enhance the extraction of smaller droplets as what DV does.

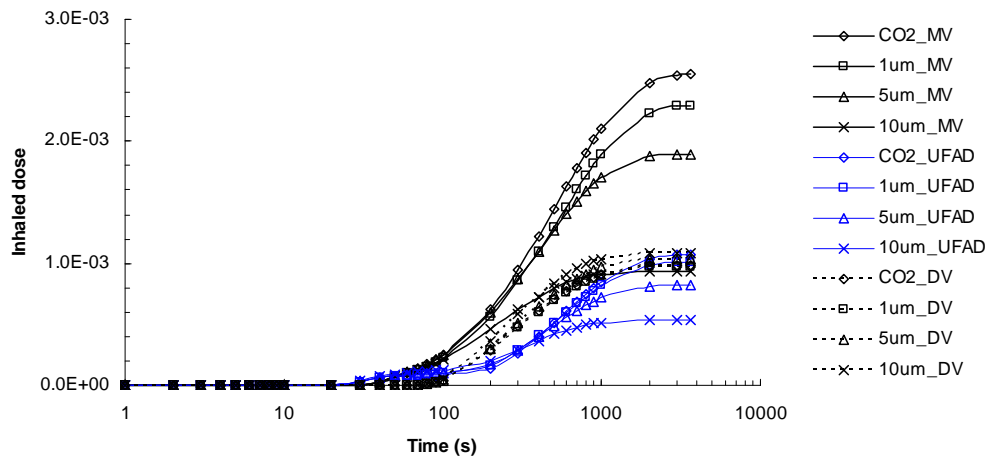


Figure 5.6 Inhaled dose of the co-occupant under different ventilation systems when the infected person coughs with the head bending down

#### 5.1.4 Co-occupant's exposure when the infected person coughs with body turning around

##### 5.1.4.1 Droplet dispersion

Figure 5.7 presents the distribution of exhaled 10  $\mu\text{m}$  droplets in the 10<sup>th</sup> and 40<sup>th</sup> second under different air distribution methods. The coughed air first impacts on the wall and are then redirected toward the infected person with the dissipation of the high momentum coughing jet. Air distribution system then gradually distributes the exhaled droplets to be dispersed in the room. The coughed droplets are the most quickly dispersed in the MV ventilated room, while they are mainly distributed in the region close to the infected person under UFAD and DV because their upward air movements can not efficiently transport the exhaled droplets to be largely dispersed indoors.

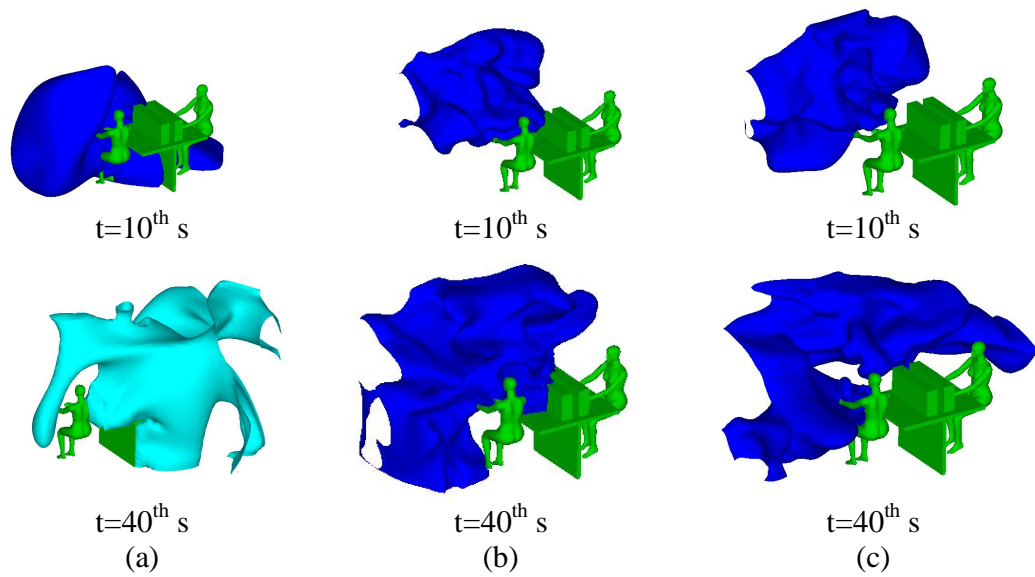
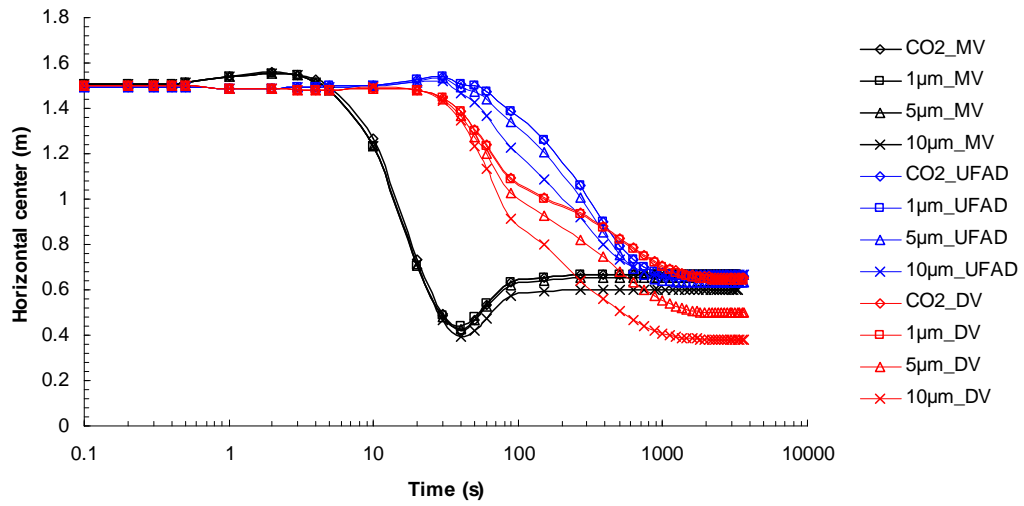


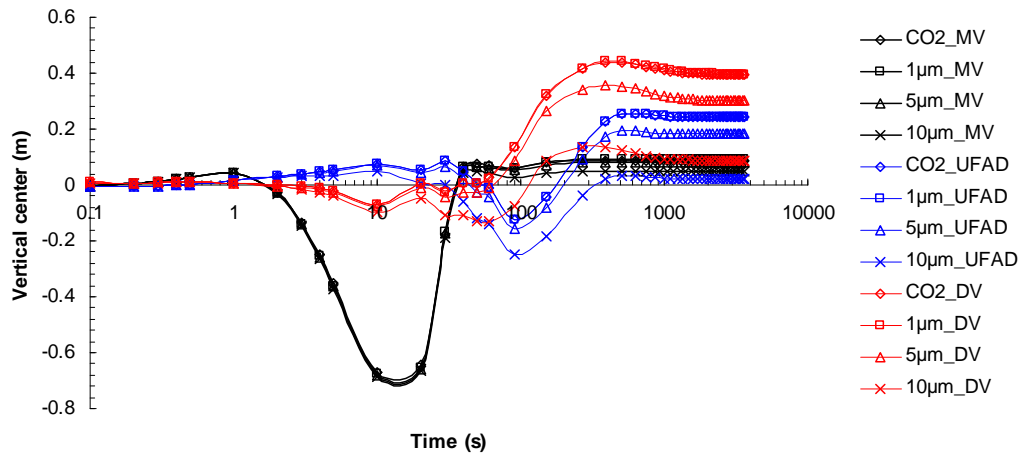
Figure 5.7 Dispersion of exhaled  $10\ \mu\text{m}$  droplets in the first 40 seconds under MV (a), UFAD (b), and DV (c) when the infected person coughs with the body turning around (the normalized concentration is not less than 0.0001 with the droplet concentration in the initial coughed air being denoted as 1.0)

The traveling history of the exhaled droplets is illustrated in Figure 5.8 in the form of the horizontal and vertical center of droplet clouds. Since the coughed droplets are released horizontally toward the facing wall, the horizontal center of exhaled droplets remains in the same level during the first 10 seconds. Later, ventilation system slowly distributes those droplets to be widely dispersed and extracted with the final droplet center locating at the center of the room. The vertical center of droplet clouds varies quite smooth under UFAD and DV because the exhaled air is reflected to the region between the infected person and the facing wall where the

weak air movement can not efficiently distribute the droplets. On the other hand, large variation can be observed under MV because of its well-mixed airflow.

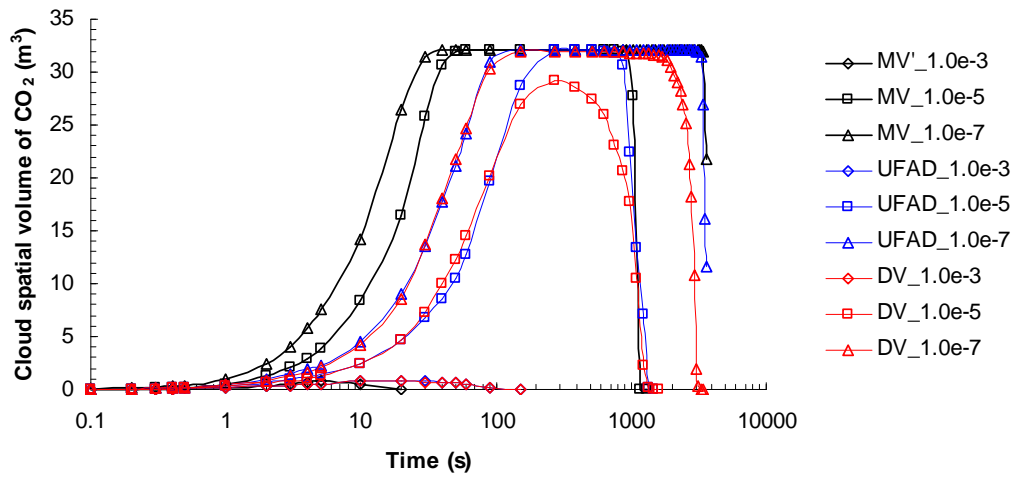


(a)

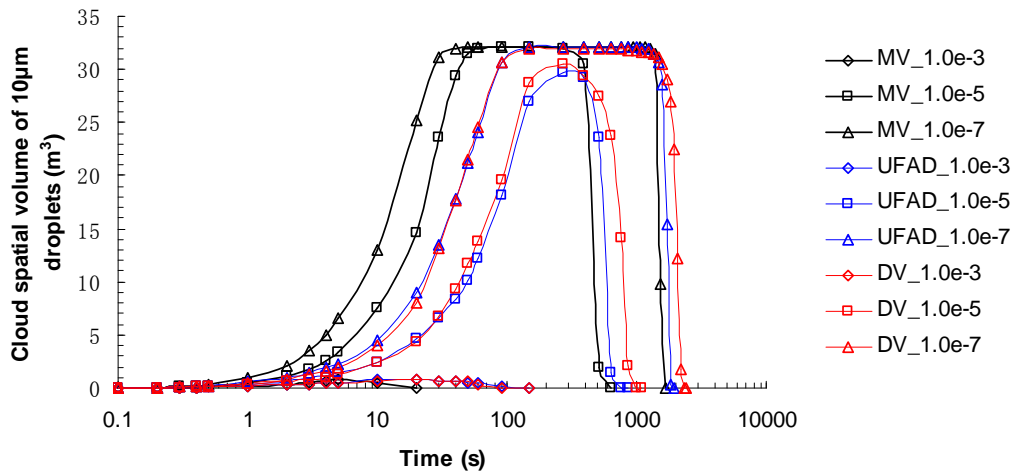


(b)

Figure 5.8 Horizontal center (a) and vertical center (b) of droplet clouds under MV, UFAD, and DV when the infected person coughs with the body turning around



(a)



(b)

Figure 5.9 Cloud spatial volume of CO<sub>2</sub> (a) and 10 µm droplets (b) under MV, UFAD, and DV when the infected person coughs with the body turning around (MV\_1.0e-3 means the volume of the space in which normalized concentration of CO<sub>2</sub> is never less than 1.0e-3 under MV)

Figure 5.9 presents the cloud spatial volume of exhaled droplets under MV, UFAD, and DV. The exhaled droplets are the most quickly dispersed under MV at first, while larger droplets are eliminated fastest due to the higher deposition rate. The

same cloud spatial volume profiles can be observed under UFAD and DV during the first 100 seconds since the exhaled droplets are reflected to the region between the infected person and the facing wall where the swirling diffuser of UFAD exhibits no apparent influences on the dispersion of those droplets. The cloud spatial volume of larger droplets decreases the most slowly in DV ventilated room since the uni-directional upward air movement can interact with the gravitational settling effects and suspend those droplets in the occupied zone.

#### ***5.1.4.2 Co-occupant's exposure***

The normalized inhaled concentration of the co-occupant is illustrated in Figure 5.10 when the infected person coughs with the body turning around, and the inhaled dose is presented in Figure 5.11. The exposed concentration is the highest under MV for the first about 70 seconds since the coughed droplets are the most quickly dispersed in the room. Due to the lower dispersion rate of exhaled droplets under UFAD and DV, the exposed concentration is much lower at first. Since about the 300<sup>th</sup> second, the inhaled concentration of 10  $\mu\text{m}$  droplets is lowest under MV because of the higher deposition rate, while DV presents the highest exposure since the upward air movement can suspend those larger droplets in the breathing level. As to smaller droplets, the lowest inhaled concentration is induced under DV because its uni-directional upward air movement can efficiently transport those droplets to the higher space of the room and being extracted.

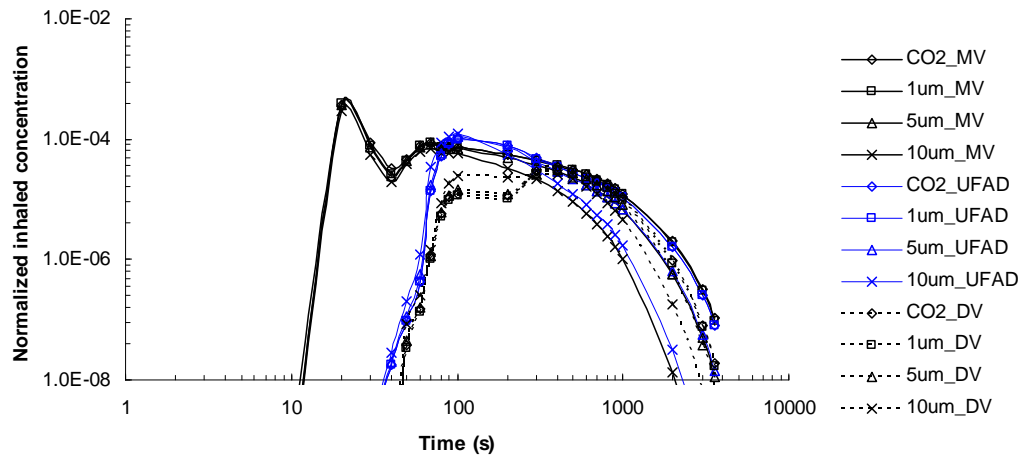


Figure 5.10 Normalized inhaled concentration of the co-occupant under different ventilation systems when the infected person coughs with the body turning around

As shown in Figure 5.11, the inhaled dose is lowest under DV for all the droplets investigated. This can be attributed to the reason that the coughed droplets are released to the region far away from the co-occupant and the low air turbulence of DV can not largely disperse those droplets to the co-occupant's breathing zone. The inhaled dose for droplets smaller than 10  $\mu\text{m}$  is highest under MV because its well-mixed air movement can quickly disperse the exhaled droplets to the breathing zone of the co-occupant. On the other hand, the highest inhaled dose for 10  $\mu\text{m}$  droplets is induced in UFAD since the mainly upward air movement can support larger droplets being suspended in the breathing level, although the strong air mixing in the lower space of the room can facilitate droplet deposition.

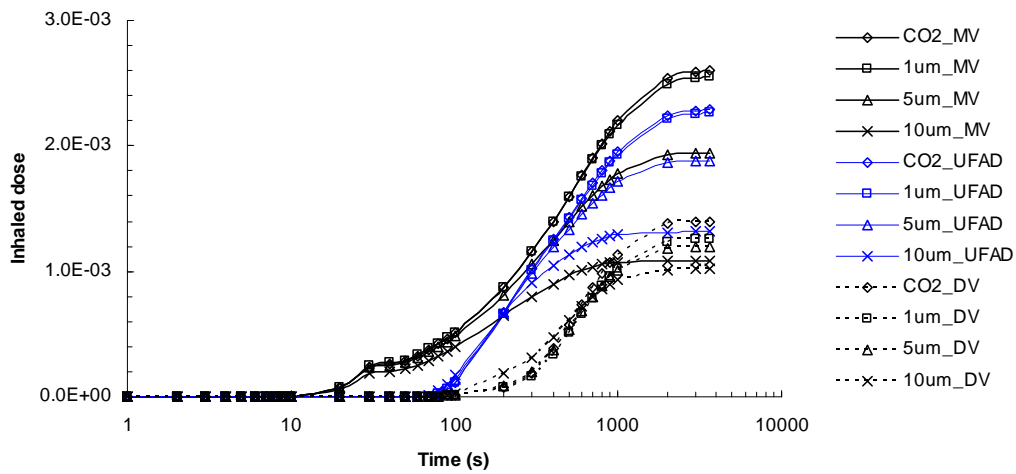


Figure 5.11 Inhaled dose of the co-occupant under different ventilation systems when the infected person coughs with the body turning around

### 5.1.5 Comparison of the co-occupant's exposure when the infected person coughs at different orientations

Figure 5.12 compares the co-occupant's inhaled dose at two coughing orientations, coughing directly to the co-occupant and bending the head down when coughing. It can be noticed that the total inhaled dose is reduced remarkably if the infected person coughs with the head bending down. The primary reason is the elimination of the first stage direct exposure by avoiding the horizontal transportation of the exhaled droplets to the co-occupant's breathing zone. Although higher inhalation may be induced for stratified ventilation system at a face-to-face orientation, bending the head down when coughing can ensure the lower exposure level, especially under UFAD. This can be associated with the position where the coughed droplets are transported to by the high momentum coughing jet. When the infected

person coughs directly, exhaled droplets are delivered to the region close to the co-occupant in seconds. The existence of one swirling diffuser there for UFAD system can facilitate the dispersion of exhaled droplets and enhance the deposition of larger droplets. The total effects of droplet dispersion and deposition lead to higher inhaled dose for smaller droplets and lowest inhalation for larger droplets. Once the infected person bends the head when coughing, the exhaled air is blocked by the arrangements on the desk where the convective flow around heat sources can promote the transportation of exhaled droplets to the higher region of the room for stratified ventilation system. The continuous extraction of coughed droplets can ensure less of them are dispersed to the breathing zone of the co-occupant and reduce the inhaled dose.

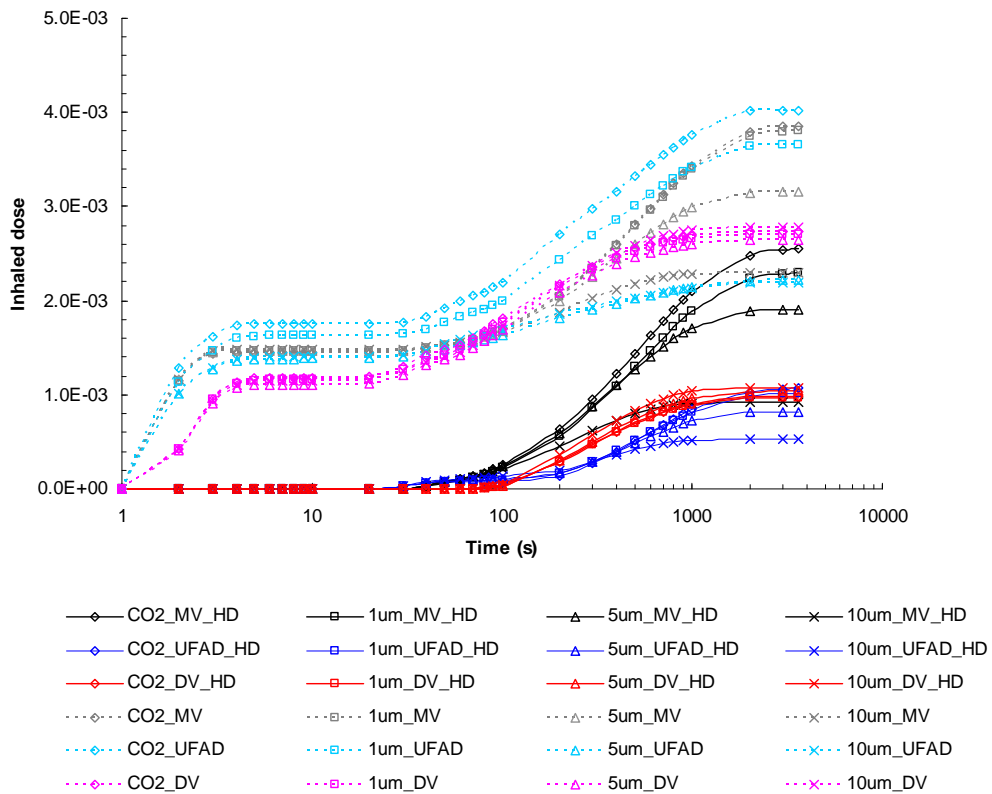


Figure 5.12 Comparison of the co-occupant’s inhaled dose when the infected person coughs directly or with the head bending down (The legend ‘10µm\_MV\_HD’ represents the co-occupant’s inhaled dose for 10 µm droplets under MV when the infected person coughs with the head bending down, while ‘10µm\_MV’ for inhalation under MV when the infected person coughs directly at a face-to-face orientation with the co-occupant)

Another comparison of inhaled dose is made in Figure 5.13 between two coughing directions, coughing directly at face-to-face orientation and turning the body around. The total inhaled dose can also be reduced substantially when coughing with the body turning around by protecting the co-occupant from the direct exposure to the

coughed airflow. However, a quite higher personal exposure can still be induced under UFAD.

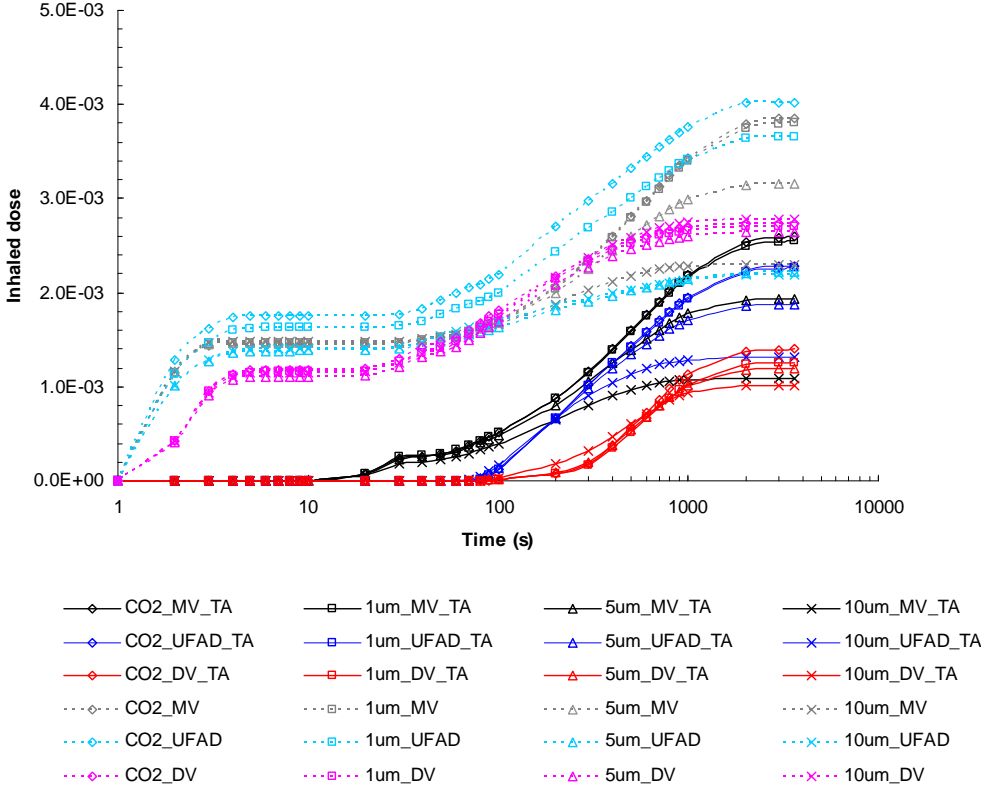


Figure 5.13 Comparison of the co-occupant’s inhaled dose when the infected person coughs directly or with the body turning around (The legend ‘10um\_MV\_TA’ represents the co-occupant’s inhaled dose for 10 μm droplets under MV when the infected person coughs with the body turning around, while ‘10um\_MV’ for inhalation under MV when the infected person coughs directly at a face-to-face orientation with the co-occupant)

It is clear that coughing with the head bending down or with the body turning around can reduce the co-occupant's inhaled dose mainly because of the elimination of the first stage direct exposure. Since the coughing jet is highly directional and can be avoided easily, it will be necessary to know the personal exposure during the later indirect exposure stage at different coughing scenarios. Figure 5.14, 5.15 and 5.16 then present the comparison of the co-occupant's inhaled dose during the second stage under different ventilation systems.

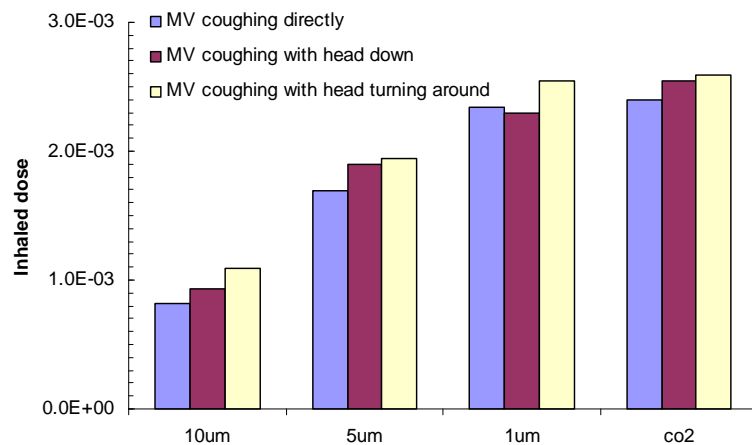


Figure 5.14 Comparison of the co-occupant's inhaled dose at the second indirect exposure stage under MV when the infected person coughs directly, with the head bending down, and with the body turning around

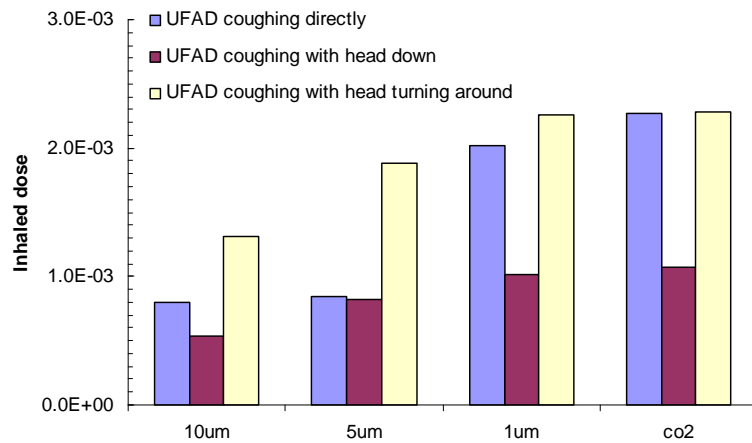


Figure 5.15 Comparison of the co-occupant's inhaled dose at the second indirect exposure stage under UFAD when the infected person coughs directly, with the head bending down, and with the body turning around

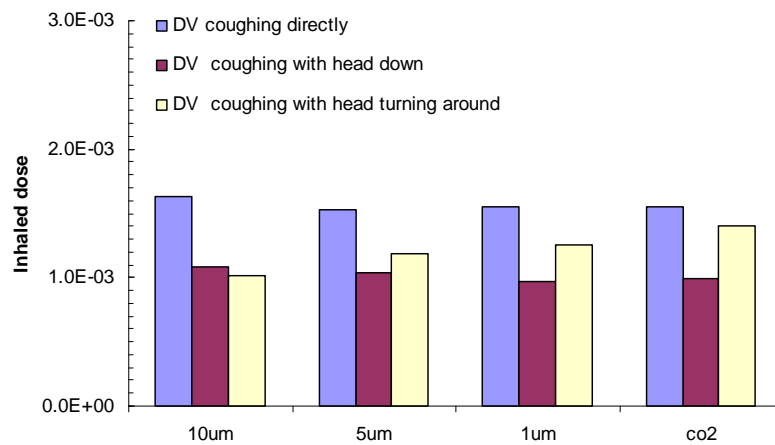


Figure 5.16 Comparison of the co-occupant's inhaled dose at the second indirect exposure stage under DV when the infected person coughs directly, with the head bending down, and with the body turning around

The inhaled dose at the second stage is almost the same for all the coughing orientations under MV since the well-mixed airflow can quickly disperse the exhaled droplets being evenly distributed in the room. Coughing with the head bending down can induce the lowest exposure under UFAD because the convective airflow around the heat sources located between the two occupants can assist the upward movement of exhaled droplets. Coughing with the body turning around, on the other hand, results in comparable inhalation with the case when the infected person coughs directly for smaller droplets, while great discrepancies exist for larger droplets. The inhaled dose is lower when the infected person coughs directly because the exhaled air travels to the space right over one swirling diffuser of UFAD which can enhance the deposition of larger droplets. As to the co-occupant's inhalation during the later stage under DV, coughing directly induces the highest inhaled dose since the coughed air is first transported to the region close to the co-occupant by the high momentum coughing jet. It will then be much easier for the weak air turbulence of DV to deliver the exhaled droplets to the co-occupant's breathing zone.

### **5.1.6 Summary**

This section investigates the co-occupant's exposure under different ventilation systems when the infected person coughs at two kinds of orientations. It is found that the total inhaled dose can be reduced remarkably if the infected person coughs with the head bending down or turning the body around, while the performance of ventilation system varies with the infected person's coughing orientation. When the

infected person coughs directly to the co-occupant, the inhaled dose is highest under DV for 10  $\mu\text{m}$  droplets and UFAD for  $\text{CO}_2$ . Meanwhile, higher personal exposure for larger droplets can also be induced under UFAD when the infected person coughs with the body turning around. However, coughing with the head down can obtain the lower contaminant inhalation under UFAD and DV for all the droplets investigated. The comparison of the co-occupant's inhaled dose during the second indirect exposure stage reveals that the intake under MV is almost the same for all the coughing orientations since the well-mixed air movement can quickly disperse the exhaled droplet being evenly distributed in the room. On the other hand, different inhaled dose can be induced under UFAD. Coughing with the head bending down can obtain the lowest personal exposure, while highest inhaled dose may be resulted in when the infected person coughs with the body turning around. It is cheering to find that the co-occupant's intake during the second stage under DV can be reduced either by coughing with the head bending down or turning the body around. This implies that the avoidance of coughing direct to the co-occupant can not only eliminate the direct exposure but also reduce the personal exposure during the second stage.

## **5.2 Simulation of the performances of physical blockings on co-occupant's exposure**

### **5.2.1 Introduction**

During the campaign with epidemic and pandemic viral infections, antiviral drugs and vaccines are believed to be the mainstay (WHO 2009). But they might be

limited or not available at the beginning of the outbreaks. Non-pharmaceutical measures, on the other hand, are simple and cost-effective interventions, and can effectively reduce the transmission of epidemic respiratory viruses (Jefferson et al. 2009). Mouth covering and desk partition are two effective approaches in mitigating the transmission of infectious diseases and are widely employed. However, their performances under different ventilation systems have been less studied. In this section, numerical simulations are conducted to investigate the effects of mouth covering and desk partition on the co-occupant's exposure under MV, UFAD and DV when the infected person coughs at 22 m/s (Zhu et al. 2007).

### **5.2.2 Case description**

Figure 5.17 displays the configuration of the simulated room. Room dimensions are the same as the one in Chapter 4, which is 4.0 m in length, 3.0 m wide and 2.7 m in height. The distance of the two occupants is about 1.5 m between their nose-tips. The one on the right is the infected person, and the left one is the co-occupant. The boundary conditions in this section are similar with those set in Chapter 4, except the inclusion of two physical blockings. In front of the infected person, a rectangular slab (0.20 m (Length)  $\times$  0.12 m (Height)) is set to represent mouth covering, the normally used surgical mask, located at about 0.03 m ahead of the mouth. There are desk partitions in the middle of the two people to build a private environment for each and the upper level of the partitions is 1.5 m above the floor. Mouth covering and desk partition in between are both treated as adiabatic walls.

Since the coughed air approaches the mouth covering at a higher velocity, droplet deposition on this covering is calculated according to an empirical equation proposed by Papavergos and Hedley (1984) which can correctly estimate the particle deposition in diffusion-impaction regime with higher friction velocity on the covering surface. The deposition model for other indoor surfaces still adopts the one developed by Lai and Nazaroff (2000).

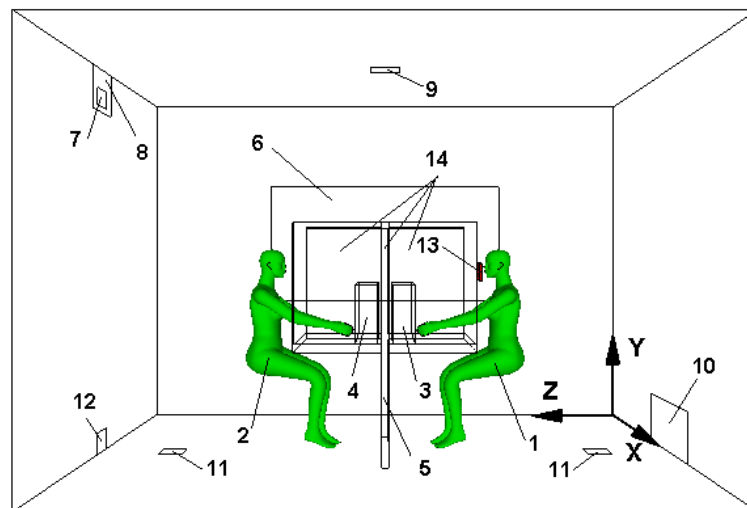


Figure 5.17 Configuration of the simulated room with physical blockings (room length (Z) 4 m, width (X) 3 m, Height (Y) 2.7 m; 1-infected person; 2-co-occupant; 3, 4-computer; 5-desk; 6-window; 7-MV inlet; 8-DV outlet; 9-UFAD outlet; 10-DV inlet; 11-UFAD inlet; 12-MV outlet; 13-mouth covering; 14-desk partition)

### 5.2.3 Effects of mouth covering

#### 5.2.3.1 Droplet dispersion

Figure 5.18 displays the dispersion of exhaled droplets in the first 10 seconds when the infected person coughs directly or with the mouth covered. The coughed air can travel to the co-occupant's breathing zone and pose higher short-term exposure when the infected person coughs directly. Using mouth covering, on the other hand, can interrupt the horizontal transportation of exhaled air and protect the co-occupant from the direct exposure.

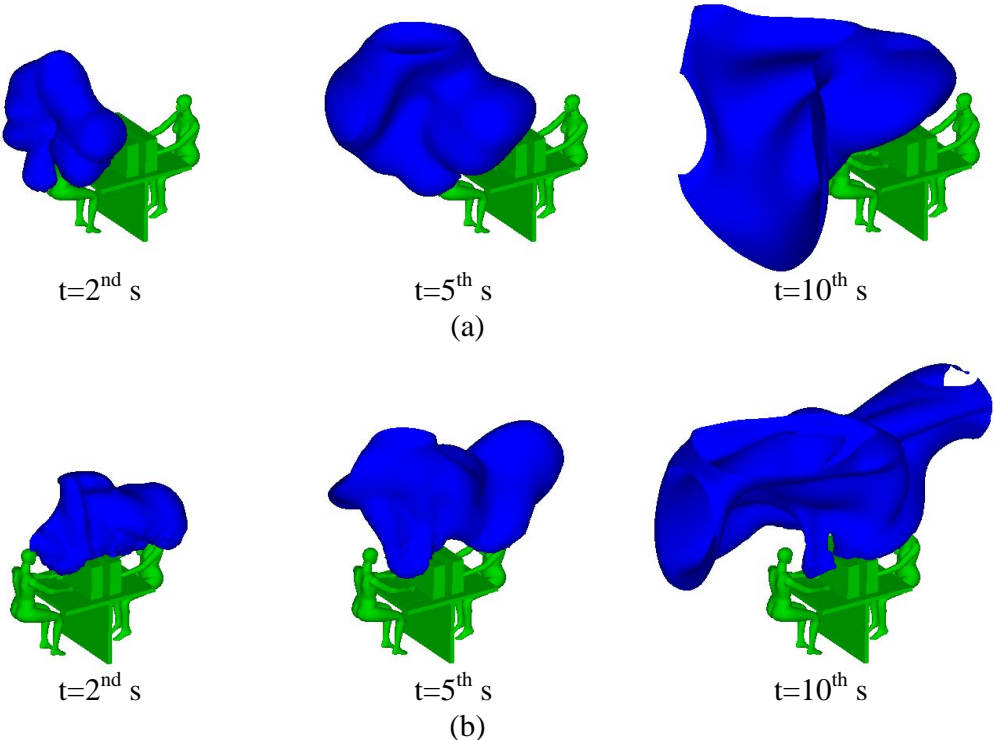


Figure 5.18 Dispersion of exhaled 10  $\mu\text{m}$  droplets during the first 10 seconds under MV when the infected person coughs with (a) and without (b) mouth covering (the normalized concentration is not less than 0.0001 with the droplet concentration in the initial coughed air being denoted as 1.0)

The dispersion of exhaled 10  $\mu\text{m}$  droplets is displayed in Figure 5.19 to analyze the influences of ventilation system on droplets' transportation when the infected person

coughs with mouth covering. The coughed droplets blocked by mouth covering are the most quickly diluted under MV which may induce an earlier and higher exposure for the co-occupant. Slower dispersion of droplets can be observed under both UFAD and DV. However, the uni-directional upward air movement of DV mainly delivers exhaled droplets being dispersed in the region close to the infected person, while the strong air mixing in the lower space of UFAD ventilated room can more widely disperse those droplets in the occupied zone.

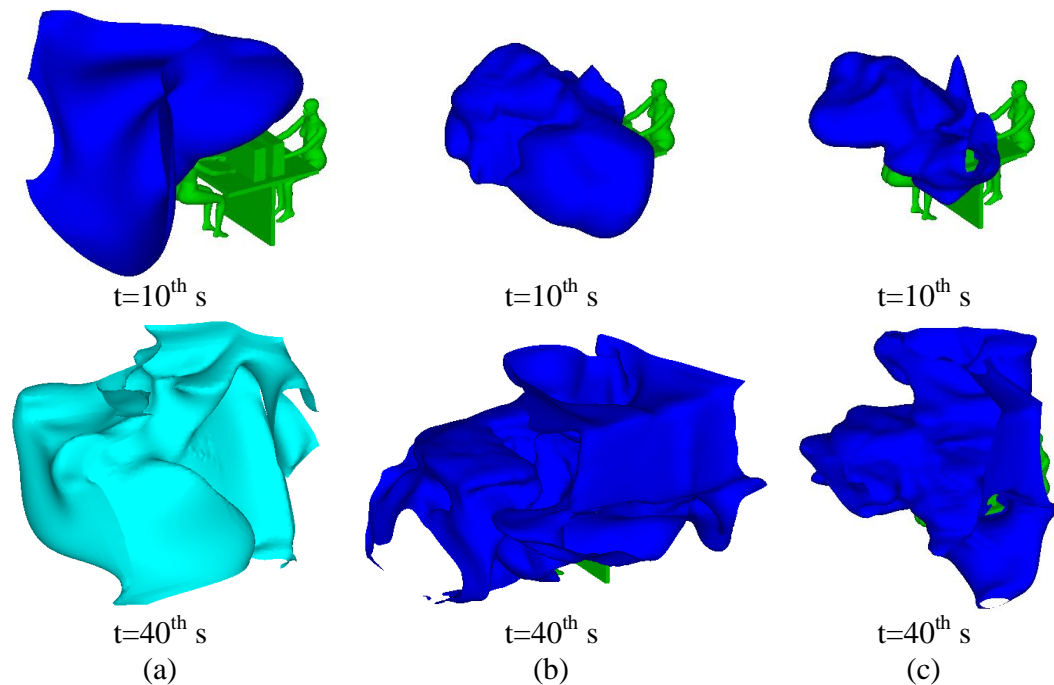
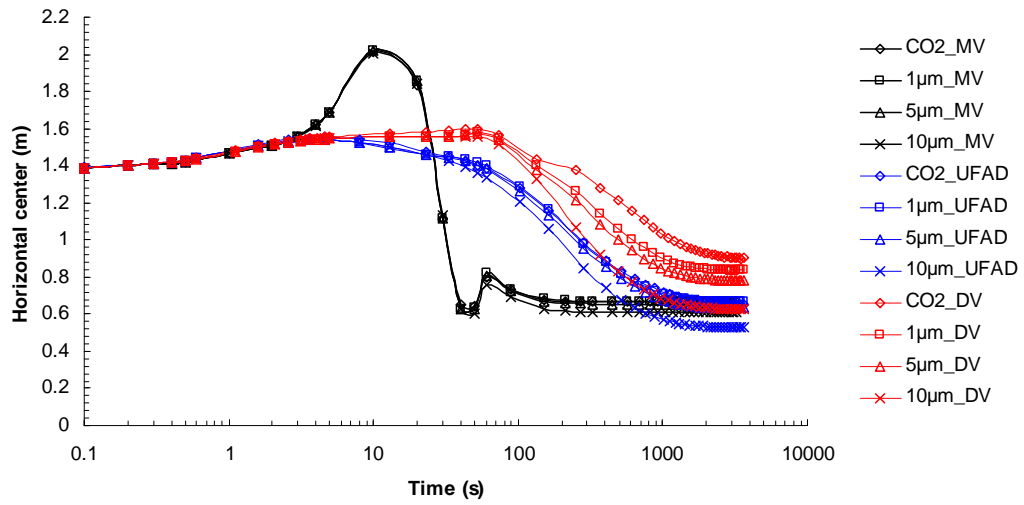


Figure 5.19 Dispersion of exhaled  $10\ \mu\text{m}$  droplets under MV (a), UFAD (b), and DV (c) when the infected person coughs with mouth covering (the normalized concentration is not less than 0.0001 with the droplet concentration in the initial coughed air being denoted as 1.0)

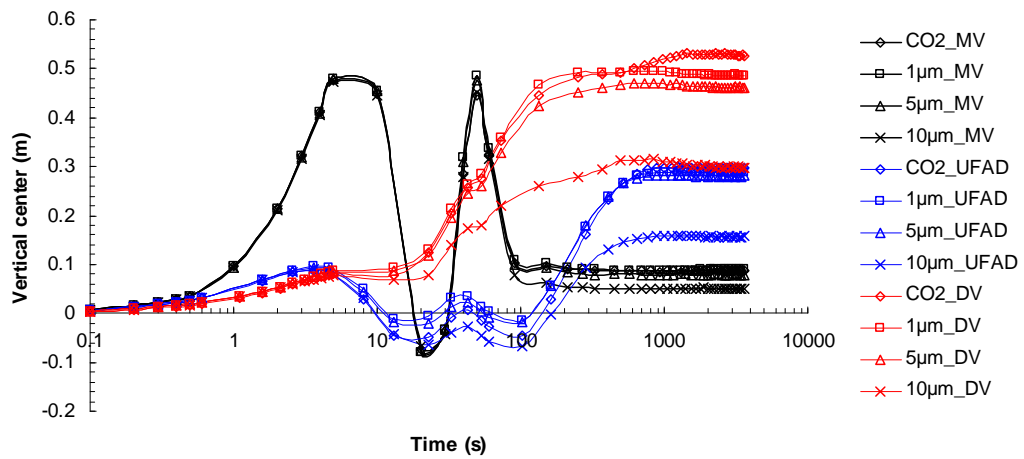
Figure 5.20 presents the transportation of exhaled droplets in the form of the variation of the droplet cloud center. Since the horizontal travelling of exhaled air is

interrupted by the mouth covering, the coughed droplets locate at a farther distance from the co-occupant during the first 10 seconds. Later, ventilation system gradually drives those reflected droplets to be continuously dispersed in the room and delivered to the co-occupant's breathing zone. This may result in a relatively lower exposure level compared with the co-occupant's inhaled dose when the infected person coughs directly, since the pathogen-laden droplets will be largely dispersed when they approach the co-occupant. It can be noticed that the vertical center of droplet clouds under DV is much higher than UFAD. The possible reason is that the coughed droplets are mainly reflected into the micro-environment of the infected person in which the thermal plume around the human body can assist the upward air movement of DV in transporting those droplets to the higher space, as shown in Figure 5.19. This may result in a quite lower personal exposure for the co-occupant in DV ventilated room.

The dilution of exhaled droplets under different ventilation systems is displayed in Figure 5.21. The generated droplets are the most quickly dispersed under MV because of its well-mixed air movement, and faster diluted under UFAD because the exhaled droplets are reflected to the region right over one swirling diffuser. Since the weak air turbulence of DV can not widely disperse the exhaled droplets in the room, the cloud spatial volume decreases quite slowly during the second stage for all the droplets.

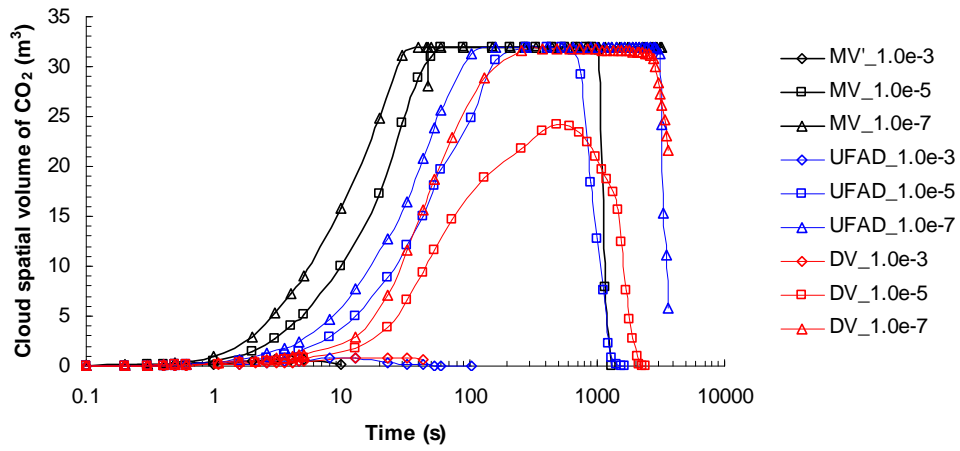


(a)

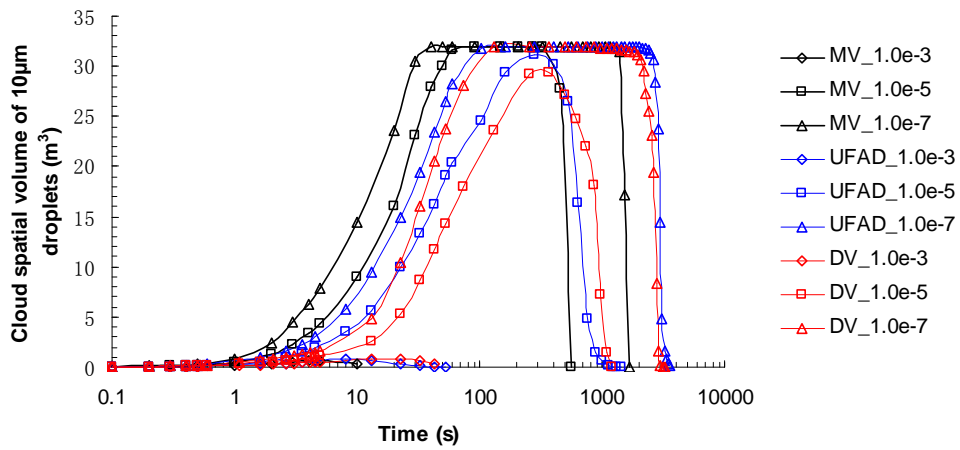


(b)

Figure 5.20 Horizontal center (a) and vertical center (b) of droplet clouds under MV, UFAD, and DV when the infected person coughs with mouth covering



(a)



(b)

Figure 5.21 Cloud spatial volume of CO<sub>2</sub> (a) and 10 µm droplets (b) under MV, UFAD, and DV when the infected person coughs with mouth covering (MV\_1.0e-3 means the volume of the space in which normalized concentration of CO<sub>2</sub> is never less than 1.0e-3 under MV)

**5.2.3.2 Co-occupant's exposure**

Figure 5.22 and Figure 5.23 illustrate the normalized inhaled concentration of the co-occupant for CO<sub>2</sub> and 10 μm droplets respectively, when the infected person coughs with and without mouth covering. Since the horizontal transportation of coughed droplets is interrupted by the covering, direct exposure during the first stage can be avoided and lower inhalation can be induced for all the three ventilation systems. As presented in Figure 5.19, exhaled droplets are more quickly dispersed under MV and UFAD, while they are mainly distributed in the space around the infected person under DV when the mouth covering is employed. Therefore, higher inhaled concentration is induced in MV and UFAD ventilated room during the first 200 seconds.

Compared with the co-occupant's exposure under DV when the infected person coughs directly, the inhaled concentration is obviously higher since about the 200<sup>th</sup> second when a covering is adopted. The possible reason is that the exhaled droplets are mainly redirected to the micro-environment of the infected person in which the convective airflow around the human body can facilitate the upward movement of those droplets and hamper their dispersion in the occupied zone. Meanwhile, the weak air turbulence of DV can not efficiently dilute the exhaled droplets in the room with the highest spatial cloud volume during the later period, as seen in Figure 5.21. All of these may result in a quite higher exposed concentration at the second stage under DV when coughing with the mouth covered. Higher exposure is also induced in UFAD for larger droplets since the coughed air is thwarted to the region right over one swirling diffuser which can hamper the deposition of the exhaled droplets.

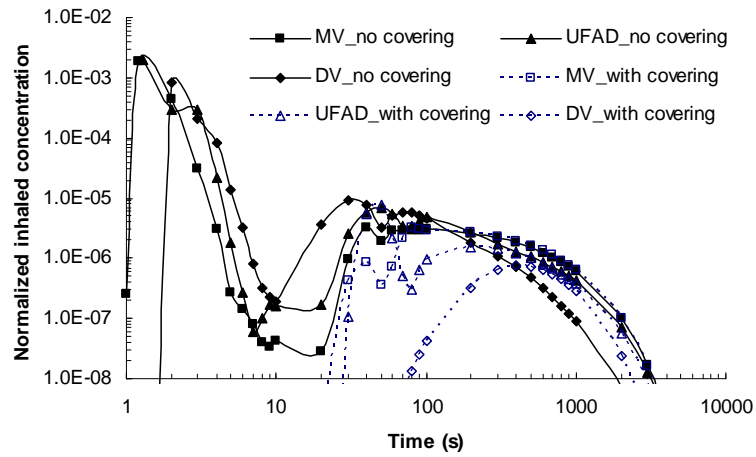


Figure 5.22 Normalized inhaled concentration of CO<sub>2</sub> under MV, UFAD and DV when the infected person coughs with and without mouth covering

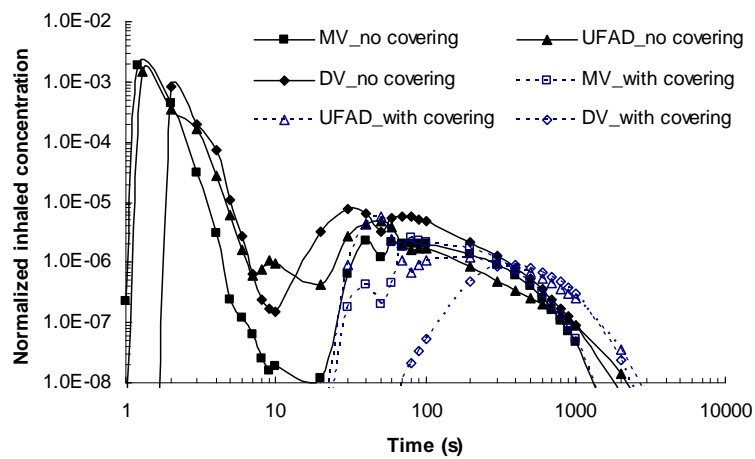


Figure 5.23 Normalized inhaled concentration of 10 μm droplets under MV, UFAD and DV when the infected person coughs with and without mouth covering

The inhaled dose is displayed in Figure 5.24 to compare the co-occupant's exposure level when the infected person coughs with and without mouth covering. The contaminant inhalation is reduced remarkably by wearing a mouth covering for all the three ventilation systems, mainly because of the elimination of the first stage direct exposure. The total inhaled dose under MV can be reduced by about 40% for fine droplets and 60% for 10  $\mu\text{m}$  droplets by using mouth-covering, about 60% for fine droplets and 40% for 5  $\mu\text{m}$  and 10  $\mu\text{m}$  droplets under UFAD, and more than 70% under DV for all the droplets. It can also be observed that DV can not ensure the lowest exposure for all the droplets investigated when the infected person coughs directly to the co-occupant, while lowest inhalation can be achieved when the infected person coughs with a covering. Furthermore, using a covering under UFAD can also obtain smaller inhalation than MV for fine droplets, while UFAD achieves the highest inhaled dose for 10  $\mu\text{m}$  droplets because of its lower deposition rate.

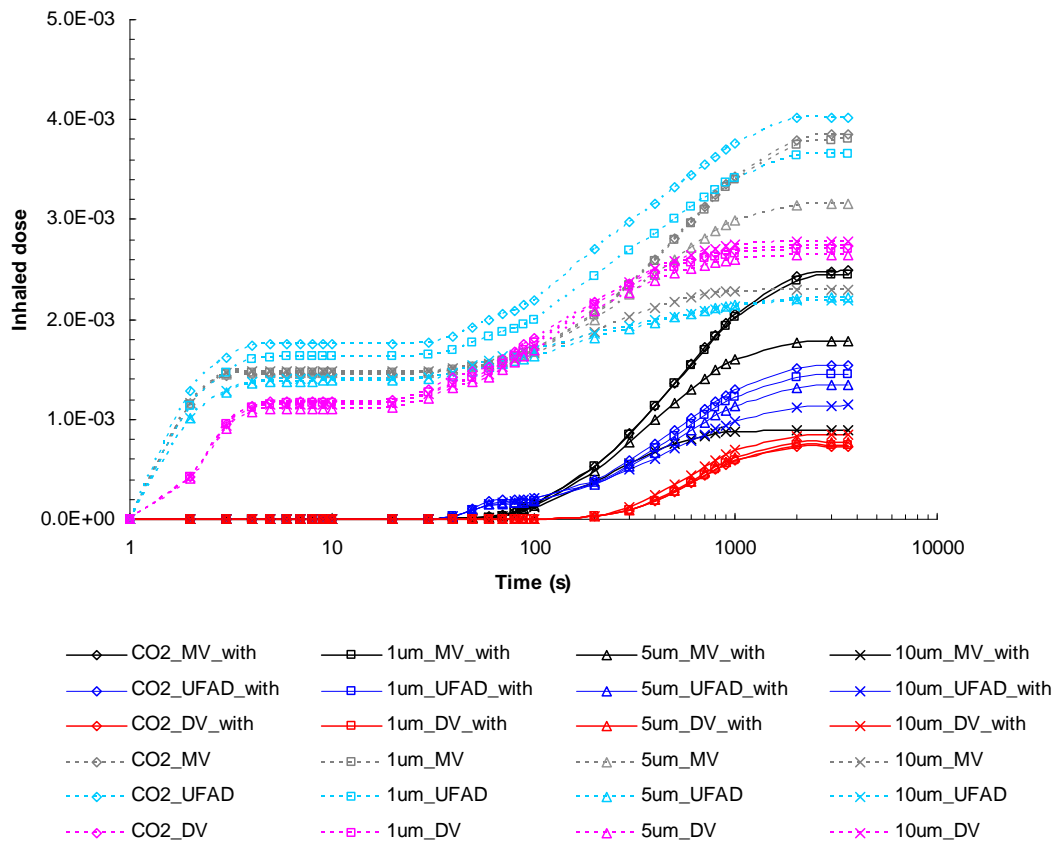


Figure 5.24 Inhaled dose of the co-occupant when the infected person coughs with and without mouth covering under MV, UFAD and DV (The legend ‘10um\_MV\_with’ represents the co-occupant’s inhaled dose for 10 μm droplets with mouth covering under MV, while ‘10um\_MV’ for inhalation without mouth covering under MV)

The personal exposure during the second indirect exposure stage is compared in Figure 5.25, Figure 5.26, and Figure 5.27 for MV, UFAD, and DV respectively to evaluate the possible exposure of occupants locating at a position away from the shedding area of coughed droplets. It is clear that using mouth covering exhibit no apparent differences on the inhalation during the second stage under MV. UFAD

system, on the other hand, induces higher personal exposure for larger droplets and lower inhalation for smaller droplets. The possible reason is that the exhaled air is reflected by the covering to the space right over one swirling diffuser in which the strong air movement can assist the extraction of smaller droplets while hamper the deposition of larger droplets. As to DV, the inhaled dose during the second stage is reduced apparently by the mouth covering for all the droplets investigated. Different from some reports (Bjørn and Nielsen 2002; Gao et al. 2008; Qian et al. 2006) in which it is reported that the trapping phenomenon under DV may leads to higher personal exposure for the co-occupant, using a mouth covering can confine the exhaled air being mainly distributed in the micro-environment of the infected person where the thermal plume around the human body can facilitate the extraction of coughed droplets and then reduce their dispersion to the co-occupant's breathing zone.

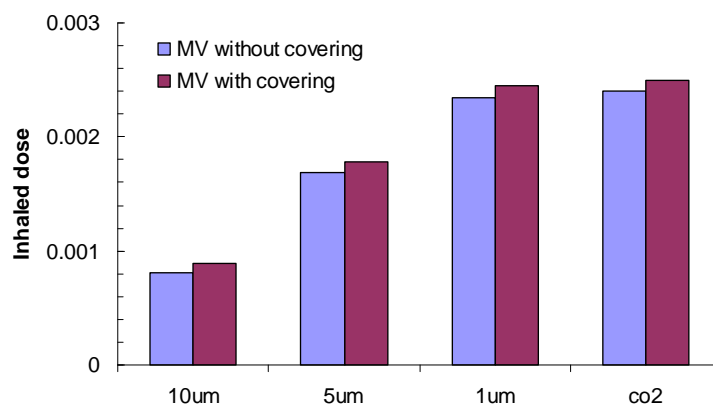


Figure 5.25 Comparison of the inhaled dose during the second stage (since the 10<sup>th</sup> second) under MV when the infected person coughs with and without mouth covering

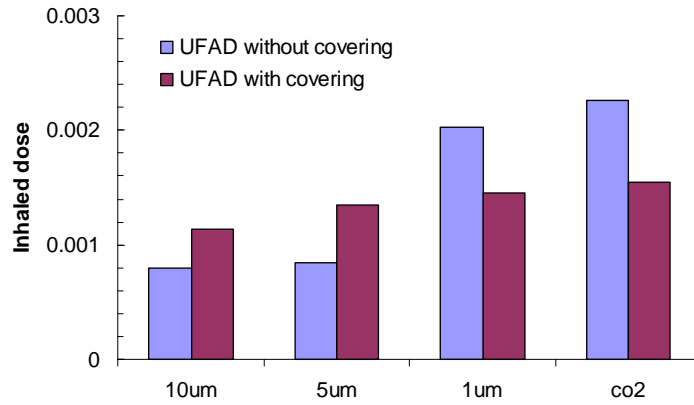


Figure 5.26 Comparison of the inhaled dose during the second stage under UFAD when the infected person coughs with and without mouth covering

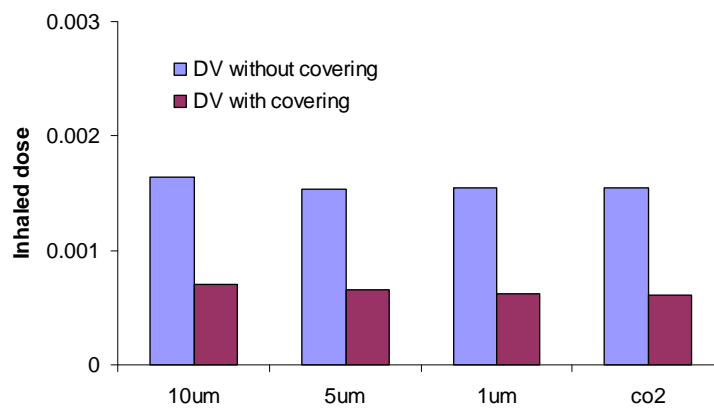


Figure 5.27 Comparison of the inhaled dose during the second stage under DV when the infected person coughs with and without mouth covering

## 5.2.4 Effects of desk partition in between

### 5.2.4.1 Droplet dispersion

Figure 5.28 presents the dispersion of exhaled  $10\ \mu\text{m}$  droplets in the first 10 seconds when the infected person coughs with and without desk partition in between. Arranging a desk partition in the middle of the two occupants can interrupt the horizontal transportation of exhaled air and redirect the coughed droplets to the region close to the infected person, while the coughed droplets can travel to the breathing zone of the co-occupant directly and cause higher direct exposure without this partition.

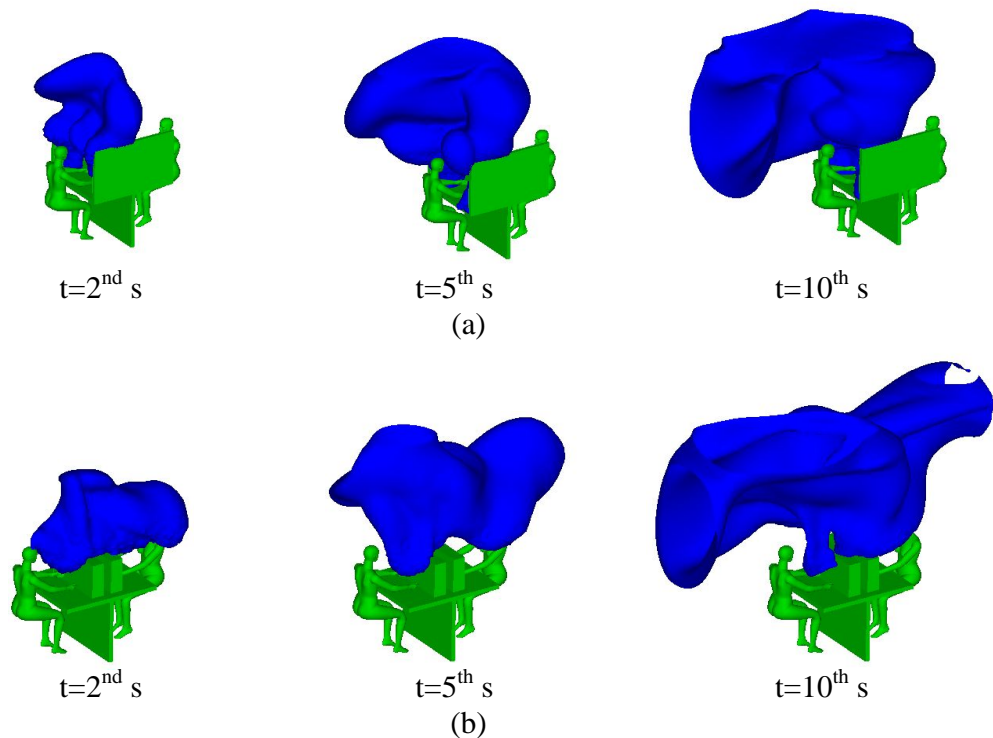


Figure 5.28 Dispersion of exhaled  $10\ \mu\text{m}$  droplets during the first 10 seconds under MV when the infected person coughs with (a) and without (b) desk partition in between (the normalized concentration is not less than 0.0001 with the droplet concentration in the initial coughed air being denoted as 1.0)

The dispersion of exhaled  $10\ \mu\text{m}$  droplets under the three ventilation systems is presented in Figure 5.29 for comparison. Although the released droplets can be blocked by the desk partition under all the air distribution methods, differences exist in the dispersion of exhaled droplets due to the specific characteristics of each system. The coughed droplets are the most largely distributed and quickly diluted in MV ventilated room, while upward air movement of UFAD and DV transport those droplets to the higher space. This will result in a relatively earlier and higher inhaled concentration for the co-occupant under MV, and slightly later for UFAD and DV.

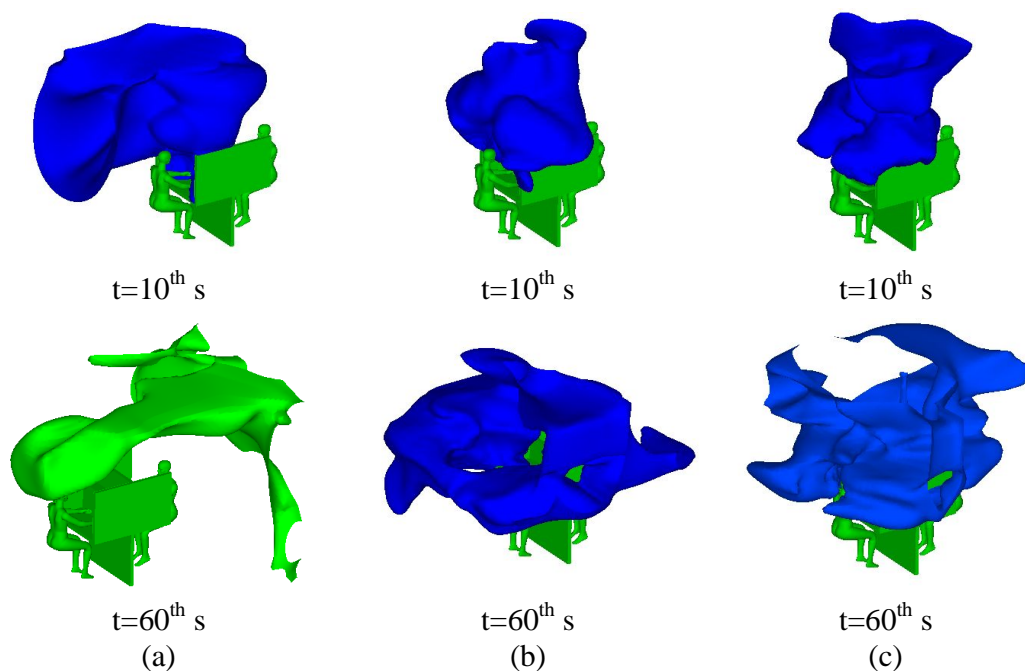
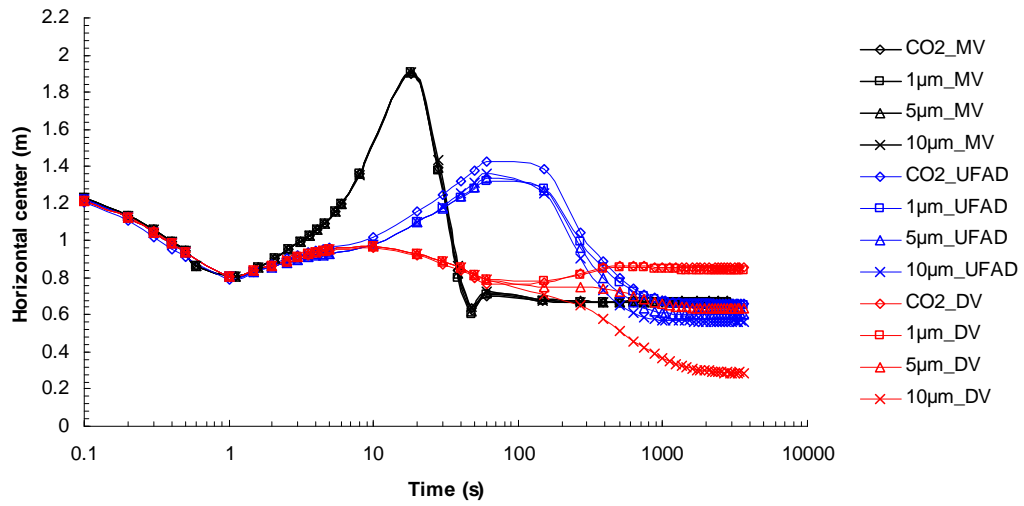


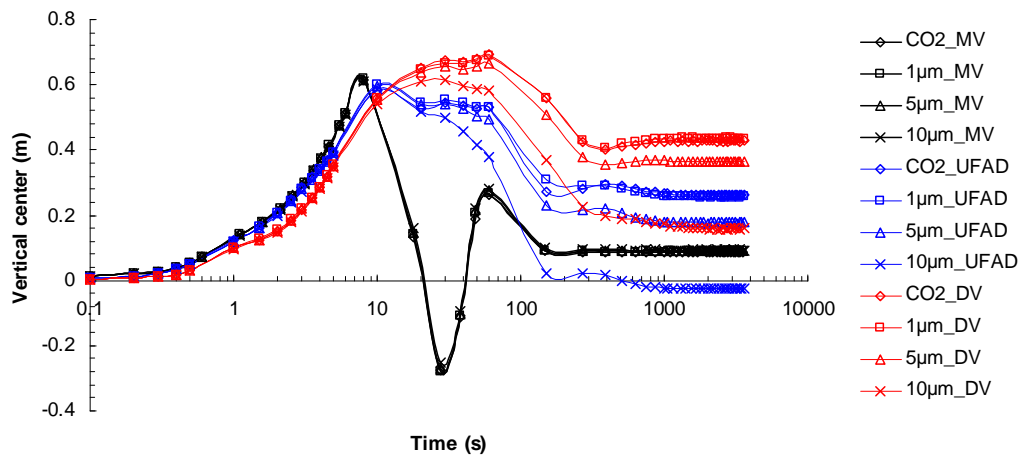
Figure 5.29 Dispersion of exhaled  $10\ \mu\text{m}$  droplets under MV (a), UFAD (b), and DV (c) when the infected person coughs with desk partition in between (the normalized concentration is not less than 0.0001 with the droplet concentration in the initial coughed air being denoted as 1.0)

To trace the dispersion of exhaled droplets during the whole research period, Figure 5.30 illustrates the variation of the horizontal and vertical center of droplet clouds. Since the coughed droplets are redirected by the desk partition toward the infected person, the cloud center remains at a certain distance away from the infected person during the first 10 seconds with the ascending of the vertical center because the thermal plumes of heat sources can drive the exhaled air to the higher space of the room. Ventilation system then distributes the coughed droplets to be gradually dispersed and extracted. Exhaled droplets are the most quickly and evenly distributed in MV ventilated room with the cloud center locating at the center of the room at the 200<sup>th</sup> second. The upward air movement of UFAD and DV can deliver the coughed droplets to the higher region and facilitate their extraction with the cloud center varying to the middle height of the room.

Figure 5.31 presents the dilution process of released droplets under different ventilation systems. As being discussed before, the coughed droplets are the most quickly dispersed and diluted under MV. There are no apparent differences for larger droplets under UFAD and DV during the first 20 seconds, while smaller droplets are faster diluted under DV because its uni-directional upward air movement can easily drive the smaller droplets to a higher level and being dispersed. During the later period, the cloud volume for smaller droplets decreases the most quickly under DV due to its higher contaminant extraction effectiveness, while slowly under MV because of the stronger air movement.

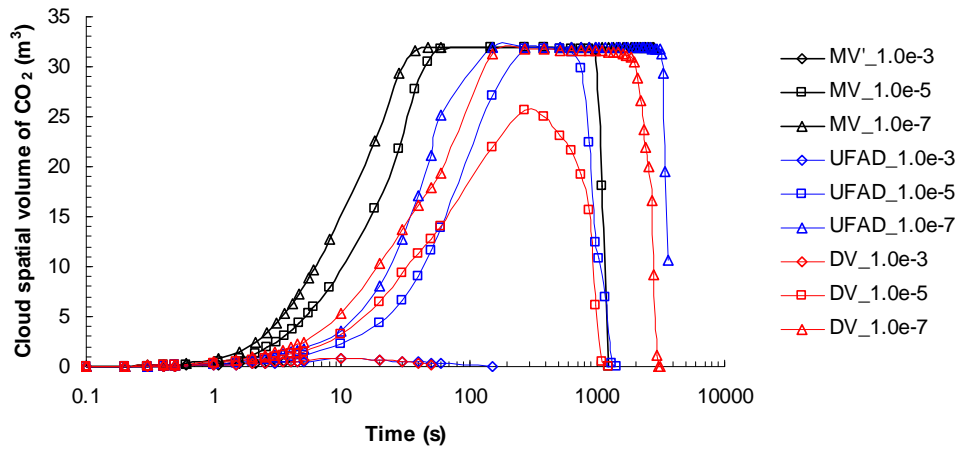


(a)

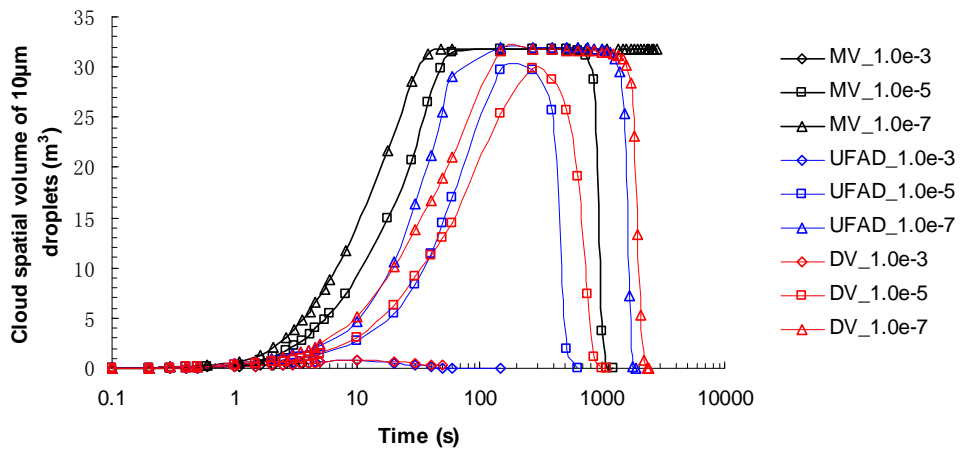


(b)

Figure 5.30 Horizontal center (a) and vertical center (b) of droplet cloud under MV, UFAD, and DV when the infected person coughs with desk partition in between



(a)



(b)

Figure 5.31 Cloud spatial volume of CO<sub>2</sub> (a) and 10 µm droplets (b) under MV, UFAD, and DV when the infected person coughs with desk partition in between (MV\_1.0e-3 means the volume of the space in which normalized concentration of CO<sub>2</sub> is never less than 1.0e-3 under MV)

**5.2.4.2 Co-occupant's exposure**

The normalized inhaled concentration of the co-occupant is presented in Figure 5.32 for CO<sub>2</sub> and Figure 5.33 for 10 μm droplets under MV, UFAD, and DV. Due to the interruption of the horizontal transportation of exhaled droplets by desk partition, the exposed concentration during the first direct exposure stage is too low to cause any risk for the co-occupant under all three ventilation systems. Since the upward air movement of UFAD and DV can deliver the exhaled droplets to the region above the breathing level, these droplets can not be efficiently dispersed to the breathing zone of the co-occupant, which then leads to lower exposed concentration at first.

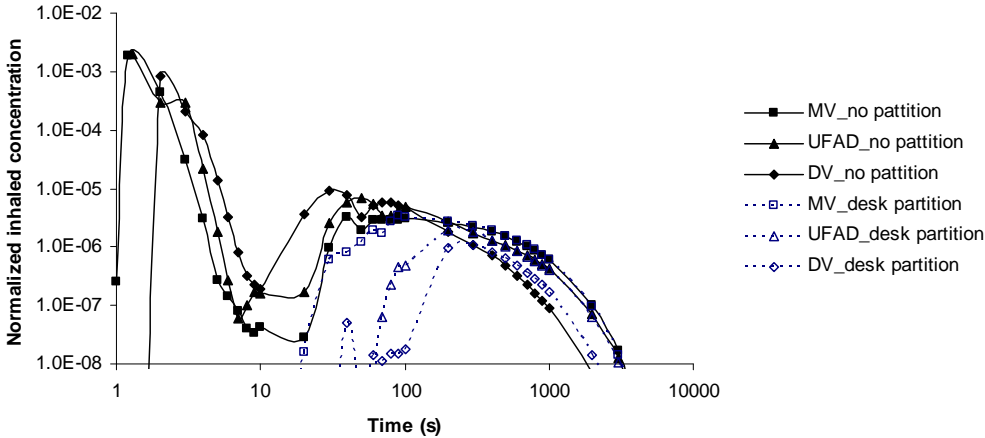


Figure 5.32 Normalized inhaled concentration for CO<sub>2</sub> under MV, UFAD and DV when the infected person coughs with desk partition in between

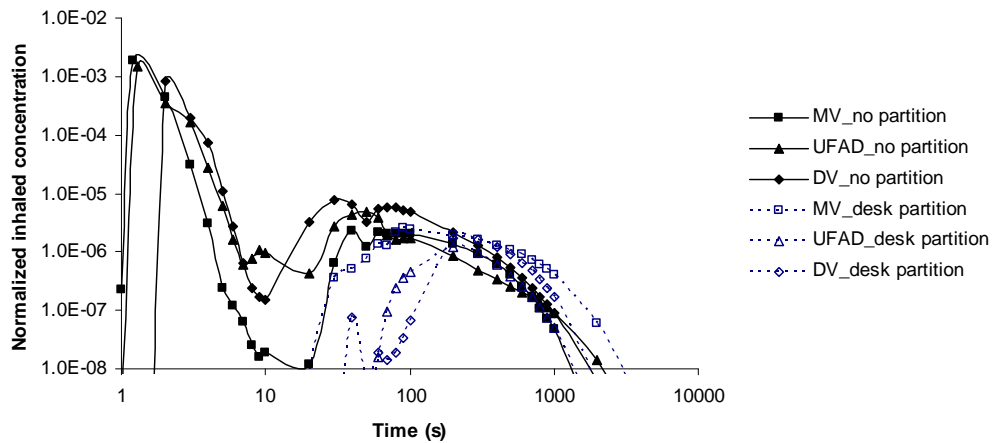


Figure 5.33 Normalized inhaled concentration for 10  $\mu\text{m}$  droplets under MV, UFAD and DV when the infected person coughs with desk partition in between

The co-occupant's inhaled dose is presented in Figure 5.34 to evaluate the general performances of the arranged desk partition. The co-occupant's exposure level can be reduced remarkably by using desk partition to interrupt the horizontal transportation of coughed droplets to the co-occupant's breathing zone. However, different exposure profiles are induced by this partition for the three ventilation systems. The inhaled dose is highest under UFAD for  $\text{CO}_2$  and DV for 10  $\mu\text{m}$  droplets when there is no partition, while stratified ventilation system can obtain the lower personal exposure for all the droplets studied by arranging desk partition. DV achieves the lowest exposure for droplets less than 10  $\mu\text{m}$  and the inhaled dose is lowest under UFAD for 10  $\mu\text{m}$  droplets. The primary reason is that the coughed droplets are redirected to the space away from the co-occupant at first by the partition where the upward air movement of UFAD and DV can distribute the

exhaled droplets to the upper region of the room and hinder their dispersion to the breathing zone of the co-occupant.

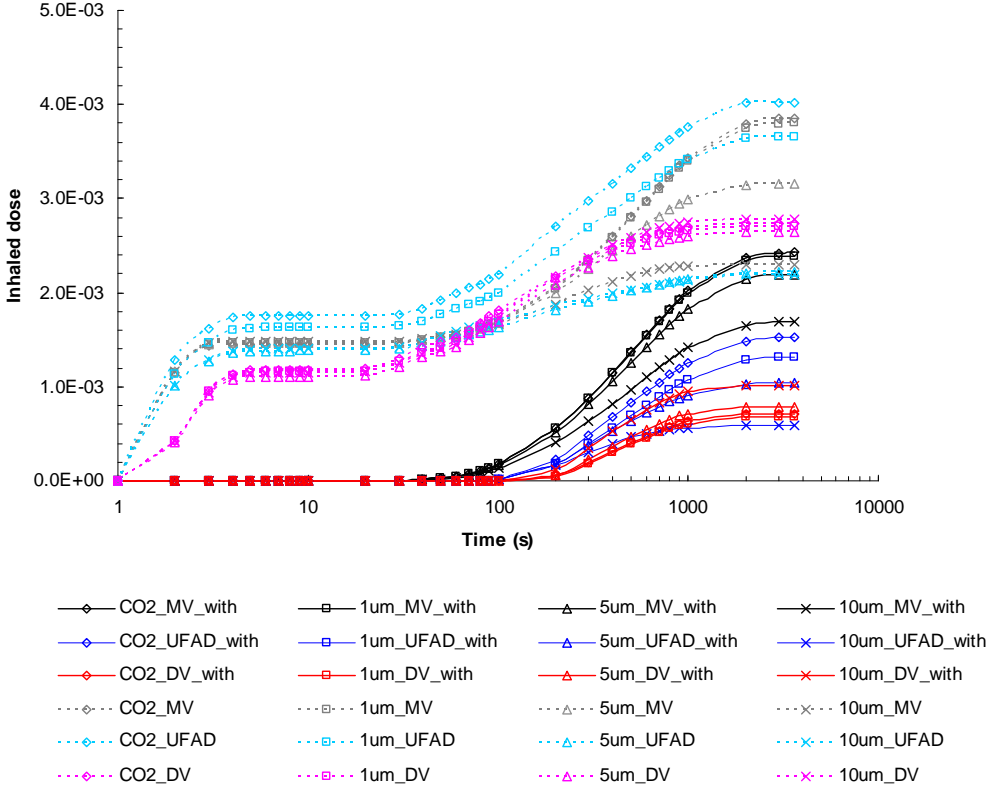


Figure 5.34 Inhaled dose of the co-occupant when the infected person coughs with and without desk partition in between under MV, UFAD and DV (The legend ‘10um\_MV\_with’ represents the co-occupant’s inhaled dose for 10 μm droplets with desk partition under MV, while ‘10um\_MV’ for inhalation without desk partition under MV)

The comparison of the co-occupant’s inhaled dose during the second stage is presented in Figure 5.35, Figure 5.36, and Figure 5.37 for MV, UFAD, and DV

respectively, when the infected person coughs with and without desk partition in between. Employing desk partition under MV can block the exhaled air to the recirculation region between the two occupants, as seen in Figure 5.29, which may reduce the deposition of larger droplets and lead to higher personal exposure. Apparent differences of inhalation for larger droplets can be observed under UFAD. The inhaled dose can be decreased by arranging desk partition between the two occupants since the coughed droplets are blocked to the space where the two swirling diffusers preserve limited influences on the dispersion, and the upward air movement and thermal plumes of heat sources can facilitate the extraction. As to DV, great reduction can be achieved for all the droplets by employing desk partition.

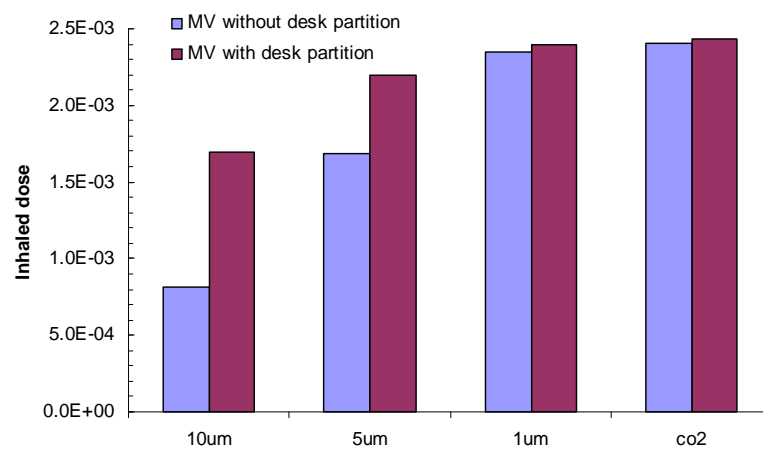


Figure 5.35 Comparison of the inhaled dose during the second stage (since the 10<sup>th</sup> second) under MV when the infected person coughs with and without desk partition in between

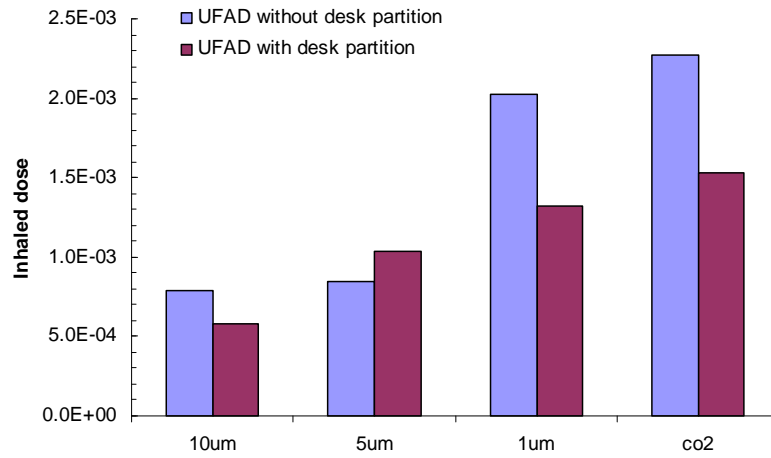


Figure 5.36 Comparison of the inhaled dose during the second stage under UFAD when the infected person coughs with and without desk partition in between

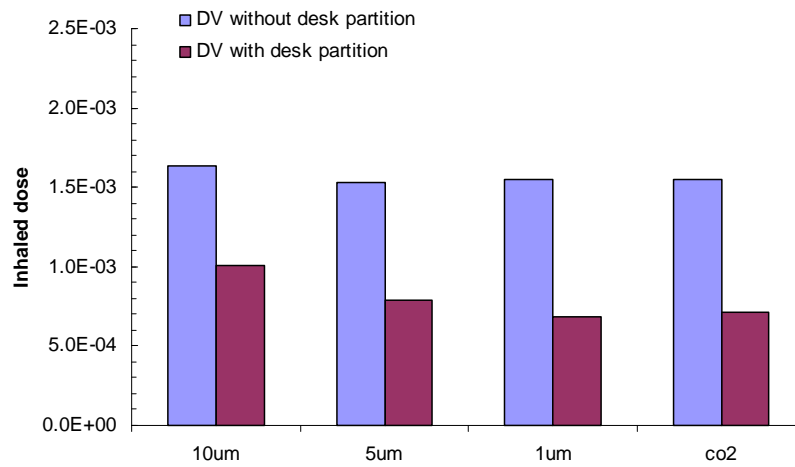


Figure 5.37 Comparison of the inhaled dose during the second stage under DV when the infected person coughs with and without desk partition in between

### 5.2.5 Comparison of co-occupant's exposure with different physical interventions

The effects of mouth covering and desk partition in mitigating the infectious diseases transmission are compared in Figure 5.38 for MV, Figure 5.39 for UFAD, and Figure 5.40 for DV. It can be observed that the two interventions obtain almost the same inhalation for smaller droplets under all the three air conditioning systems, while different personal exposures are induced for larger droplets. Better inhaled air quality can be achieved by using mouth covering under MV and DV, and through arranging desk partition for UFAD system. The primary reason is that the coughed droplets are redirected to the space surrounding the infected person by mouth covering. For larger droplets within this region, the main air movement of MV can facilitate their deposition, and the upward airflow of DV can assist the thermal plume around the infected person in driving the exhaled droplets to the higher level to reduce the co-occupant's exposure. Nevertheless, desk partition thwarts coughed droplets in the space between the two occupants where the swirling diffuser of UFAD exhibits limited effects on the dispersion of these droplets and the gravitational force can promote the deposition of larger droplets.

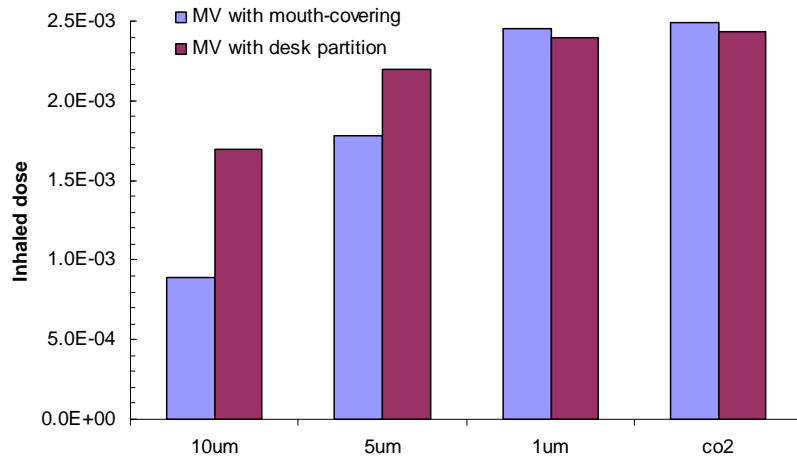


Figure 5.38 Comparison of the co-occupant's total inhaled dose under MV when the infected person coughs with mouth covering and desk partition in between

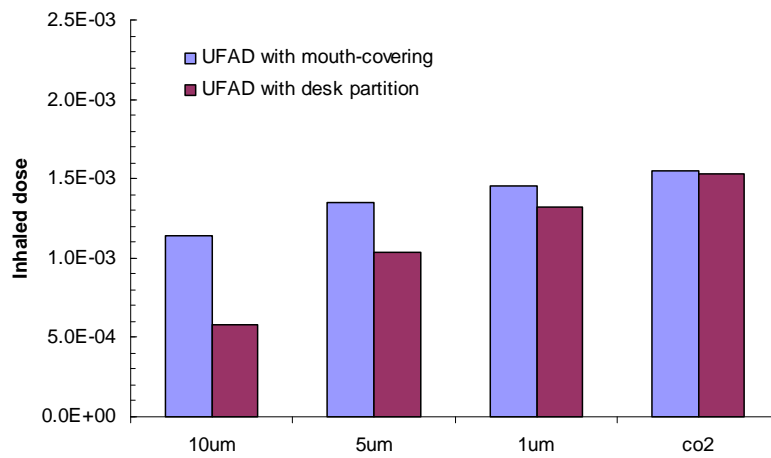


Figure 5.39 Comparison of the co-occupant's total inhaled dose under UFAD when the infected person coughs with mouth covering and desk partition in between

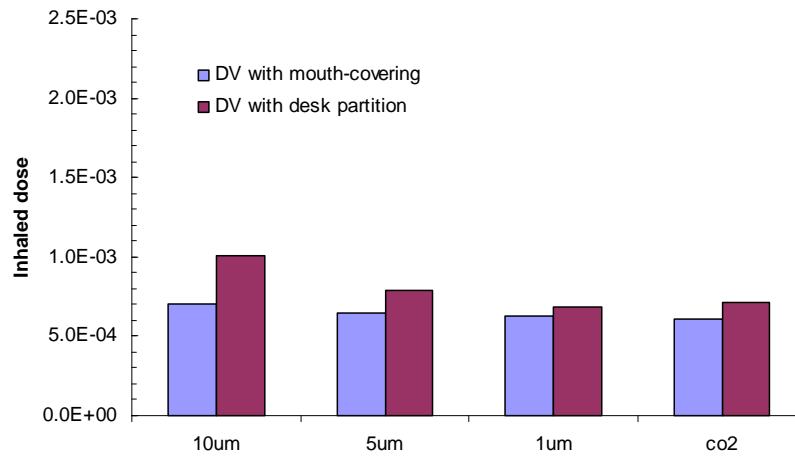


Figure 5.40 Comparison of the co-occupant’s total inhaled dose under DV when the infected person coughs with mouth covering and desk partition in between

### 5.2.6 Summary

This section numerically investigates the effects of two physical interventions, namely mouth covering and desk partition, on the mitigation of infectious diseases transmission. It is found that both physical blockings can efficiently protect the co-occupant from direct exposure to the coughed droplets and reduce the exposure level. When the infected person coughs with mouth covering, the total inhaled dose under MV can be reduced by about 40% for fine droplets and 60% for 10  $\mu\text{m}$  droplets by using mouth-covering, about 60% for fine droplets and 40% for 5  $\mu\text{m}$  and 10  $\mu\text{m}$  droplets under UFAD, and more than 70% under DV for all the droplets investigated. Arranging desk partition can also reduce the inhaled dose by about 30% under MV, and more than 60% under UFAD and DV for all the droplets investigated. However, different inhaled dose may be induced during the second stage. Compared with the contaminant inhalation when the infected person coughs

directly, covering the mouth may result in higher exposure for larger droplets under UFAD during the second indirect exposure period. However, it achieves lower inhaled dose under DV for all the droplets investigated and exhibits no apparent differences under MV. Desk partition, on the other hand, can ensure lower exposure for the two stratified ventilation systems, whilst increase the co-occupant's inhalation for larger droplets under MV. The comparison of the two interventions reveals that almost the same inhaled dose is induced for smaller droplets under all the three air conditioning systems, while different personal exposures can be achieved for larger droplets

## **Chapter 6**

# **Airborne transmission with two types of personalized ventilation strategies under mixing and displacement ventilation schemes**

### **6.1 Introduction**

Personalized ventilation (PV), as one complementary ventilation system to the total air conditioning schemes, including MV and DV, can deliver conditioned fresh air to the occupants' breathing zone directly and offers an opportunity for each occupant to adjust the flow rate and direction of conditioned air supply to satisfy each individual's requirements. However, there are still some worries about whether the protecting PV devices, on the other hand, facilitate the dispersion of infectious agents generated by the PV user. This study therefore investigates the performances of two types of PV systems, including a desk-mounted PV and one chair-based PV, with the conditioned fresh air supplied in the same direction with the convective airflow around the human body, in mitigating the infectious diseases transmission under MV and UFAD with varying PV using conditions. A detailed introduction of PV system has been presented in Chapter 2.

### **6.2 Cases description**

Figure 6.1 illustrates the configuration of the simulated room, with the same dimensions as the experimental chamber used by Faulkner et al. (2004). The room is 4 m long, 2.4 m wide and 3 m high. The performances of two types of PV systems are investigated under MV and DV. One is the chair-based PV proposed by Niu et al. (2007), and the other is a desk-mounted PV experimentally studied by Faulkner et al. (2004). The chair-based PV is located right below the chin of the user with a diameter of round fresh air inlet equal to 80 mm. The supplied airflow rates are 0.8 l/s and 1.6 l/s separately according to the experimental study of Niu et al. (2007). For the desk-based PV, a slot with a size of 3.8 cm  $\times$  30.5 cm is employed to deliver fresh air to the breathing zone of the user. The personalized air flow rates are 3.5 l/s and 6.5 l/s respectively, and the air flow direction is 45° upward.

The inlet of DV (0.57 m  $\times$  0.5 m) is located at the floor level of the side wall and the outlet is arranged in the upper level of the same wall with a dimension of 0.5 m  $\times$  0.2 m. The inlet and outlet of MV both locate at the higher level of the side wall. The size of inlet is 0.2 m  $\times$  0.1 m, and 0.2 m  $\times$  0.15 m for outlet. The total supplied airflow rate is 57 l/s for the two systems which equals 7.6 air change rate per hour. For different personalized airflow rates served to the occupants, Table 6.1 lists all the cases investigated with detailed airflow rates supplied by the total ventilation system and PV system. The inlet air temperature is 20 °C for DV and 18 °C for MV to ensure the same average temperature in the middle height of the room. The temperature of fresh air delivered by PV is maintained at 20 °C for all the cases.

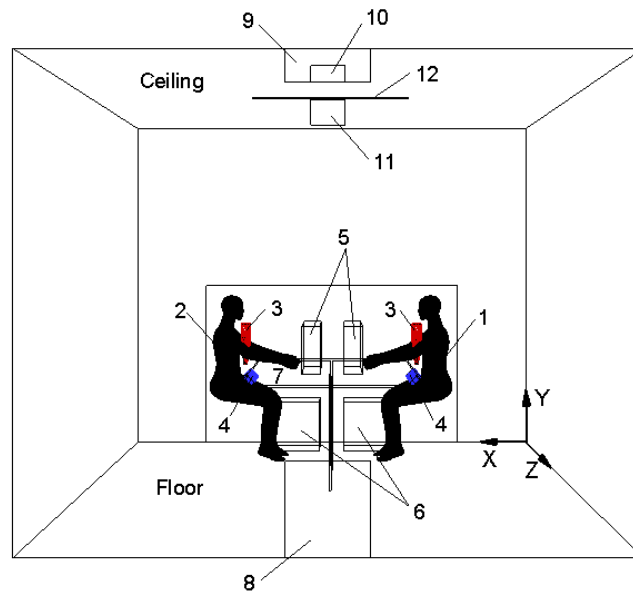


Figure 6.1 Configuration of the simulated room (length - X (4 m); Width - Z (2.4 m); Height - Y (3 m); 1 - infected person; 2 - co-occupant; 3 - chair-based PV device; 4 - desk-mounted PV device; 5 - PC monitor; 6 - PC; 7 - desk; 8 - DV inlet; 9 - DV outlet; 10 - MV inlet; 11 - MV outlet; 12 - light)

There are two people working in this room with a distance about 2 m. The person on the right side as shown in Figure 6.1 is the infected person who generates pathogen-laden droplets and the other one is the co-occupant exposed to the infectious droplets. The heat flux released from the thermal manikin, personal computer, monitor, and light are 60 W, 50 W, 62 W, and 29 W, respectively. Although a normal respiration process follows a sinusoidal cycle, steady exhalation for the infected person and continuous inhalation for the co-occupant are assumed in this simulation. The breathing rate is 8.4 l/min (Huang 1977) through nostrils, and the direction of exhaled jet is 45° downward while the orientation for inhalation is 45° upward. The exhaled air temperature is set to be 35 °C (Höppe 1981).

Table 6.1 Airflow rates served in different cases (PVi refers to the personalized airflow rate supplied to the infected person, and PVc represents the personalized air delivered to the co-occupant)

Cases		MV	DV	PVi	PVc	PV system
Case 1	DV57/PVi0/PVc0		57 l/s	0 l/s	0 l/s	Chair-based PV system
Case 2	DV55.4/PVi0.8/PVc0.8		55.4 l/s	0.8 l/s	0.8 l/s	
Case 3	DV53.8/PVi1.6/PVc1.6		53.8 l/s	1.6 l/s	1.6 l/s	
Case 4	DV55.4/PVi0/PVc1.6		55.4 l/s	0 l/s	1.6 l/s	
Case 5	DV56.2/PVi0.8/PVc0		56.2 l/s	0.8 l/s	0 l/s	
Case 6	DV55.4/PVi1.6/PVc0		55.4 l/s	1.6 l/s	0 l/s	
Case 7	DV57/PVi0/PVc0		57 l/s	0 l/s	0 l/s	Desk-mounted PV system
Case 8	DV50/PVi3.5/PVc3.5		50 l/s	3.5 l/s	3.5 l/s	
Case 9	DV44/PVi6.5/PVc6.5		44 l/s	6.5 l/s	6.5 l/s	
Case 10	DV50.5/PVi0/PVc6.5		50.5 l/s	0 l/s	6.5 l/s	
Case 11	DV53.5/PVi3.5/PVc0		53.5 l/s	3.5 l/s	0 l/s	
Case 12	DV50.5/PVi6.5/PVc0		50.5 l/s	6.5 l/s	0 l/s	
Case 13	MV57/PVi0/PVc0	57 l/s		0 l/s	0 l/s	Chair-based PV system
Case 14	MV55.4/PVi0.8/PVc0.8	55.4 l/s		0.8 l/s	0.8 l/s	
Case 15	MV53.8/PVi1.6/PVc1.6	53.8 l/s		1.6 l/s	1.6 l/s	
Case 16	MV55.4/PVi0/PVc1.6	55.4 l/s		0 l/s	1.6 l/s	
Case 17	MV56.2/PVi0.8/PVc0	56.2 l/s		0.8 l/s	0 l/s	
Case 18	MV55.4/PVi1.6/PVc0	55.4 l/s		1.6 l/s	0 l/s	

Case 19	MV57/PVi0/PVc0	57 l/s		0 l/s	0 l/s	Desk- mounted PV system
Case 20	MV50/PVi3.5/PVc3.5	50 l/s		3.5 l/s	3.5 l/s	
Case 21	MV44/PVi6.5/PVc6.5	44 l/s		6.5 l/s	6.5 l/s	
Case 22	MV50.5/PVi0/PVc6.5	50.5 l/s		0 l/s	6.5 l/s	
Case 23	MV53.5/PVi3.5/PVc0	53.5 l/s		3.5 l/s	0 l/s	
Case 24	MV50.5/PVi6.5/PVc0	50.5 l/s		6.5 l/s	0 l/s	

### 6.3 Airflow fields

Figure 6.2 presents the airflow patterns and temperature distribution for MV and DV. The stronger air mixing of MV induces an uniform temperature distribution, about 23 °C, in the occupied zone. Temperature stratification with enhanced thermal plume around the two occupants can be observed under DV. The average temperature in the horizontal plane at the middle height of the DV ventilated room is maintained at around 23 °C to ensure the comparison basis with MV.

The well-mixed airflow under MV can promote the dispersion of exhaled droplets and may result in evenly distributed contaminant concentration profiles with varying source locations and releasing velocities (Gao and Niu 2007, Gao et al. 2008, He et al. 2011, Li et al. 2011). It can then be expected that the PV system employed by the infected person may not have significant impact on the co-occupant's exposure. Differently, DV system can facilitate the extraction of exhaled droplets by its upward airflow while may induce a relatively higher exposure for the co-occupant located close to the infected person because of its temperature stratification

phenomenon (Bjorn and Nielsen 2002; Qian et al. 2006). The co-occupant's inhalation is then strongly associated with the source location including its height and horizontal distance to the co-occupant. Large differences in co-occupant's exposure can therefore be anticipated under DV when the infected person does or does not adopt personalized fresh air.

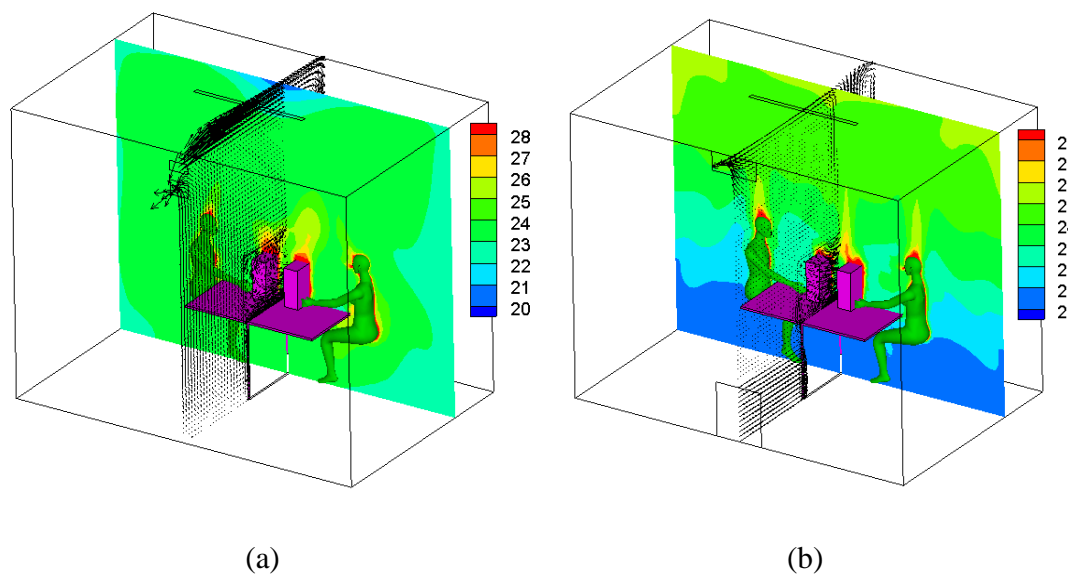
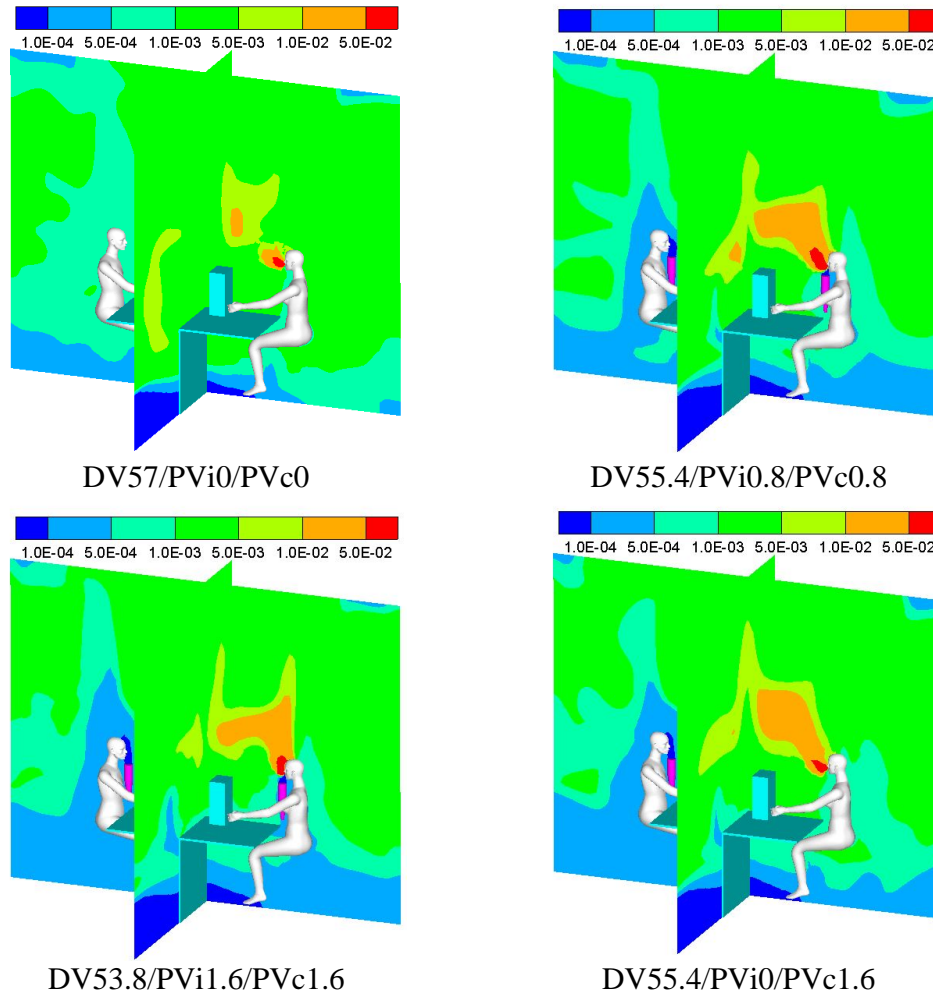


Figure 6.2 Airflow patterns at  $X = 2$  m and temperature distribution at  $Z = 0.65$  m under MV (a) and DV (b)

## 6.4 Co-occupant's exposure under DV when the chair-based or the desk-mounted PV is employed

### 6.4.1 Droplet dispersion

Figure 6.3 displays the normalized concentration distribution of 10  $\mu\text{m}$  droplets when the chair-based PV is employed, with the droplet concentration in the exhaled air of the infected person being denoted as 1.0.



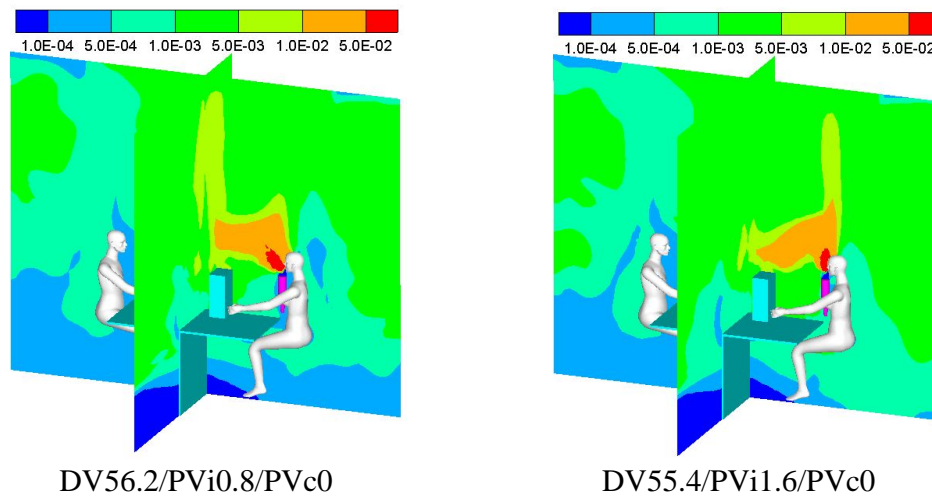
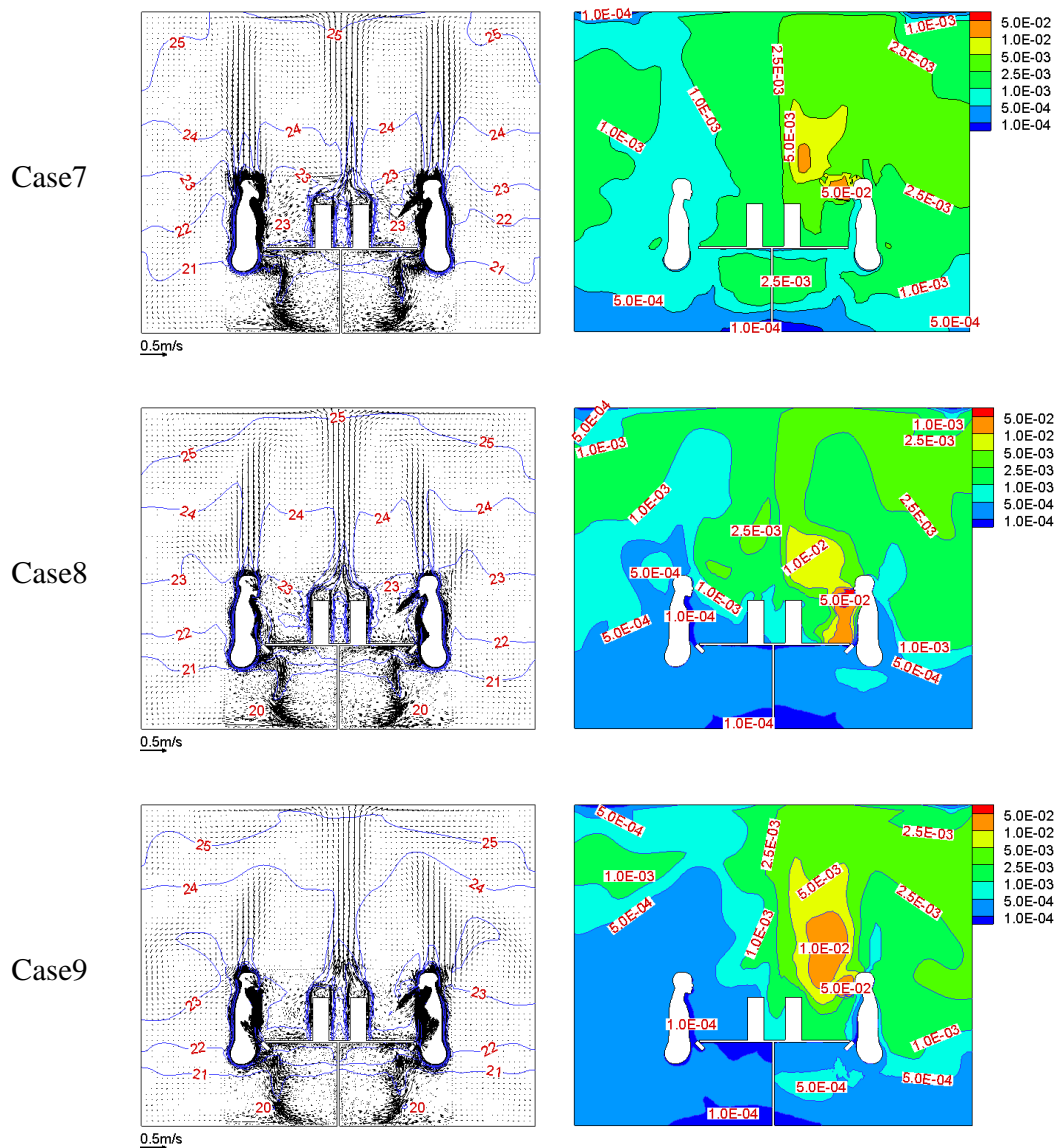


Figure 6.3 Concentration distribution profiles of 10  $\mu\text{m}$  droplets under DV when using the chair-based PV (The droplet concentration in the exhaled air is denoted as 1.0)

The distribution of 10  $\mu\text{m}$  droplets in the vertical plane of  $X = 0.65$  m is presented in Figure 6.4 when the desk-mounted PV is used, as well as the temperature contour and velocity vector since the higher airflow rate served by the desk-mounted PV will influence air movement in the entire room. It is clear that employing PV system by either the infected person or the co-occupant under DV can diminish the horizontal dispersion of exhaled droplets to the co-occupant's breathing zone in comparison with the condition of a sole DV system. Serving personalized fresh air to the co-occupant alone can definitely improve the inhaled air quality and achieve the lowest exposure. If only the infected person employs the PV supplied fresh air, a relatively polluted micro-environment can be resulted in for the co-occupant when compared with cases in which fresh air is delivered directly to the breathing zone of

the co-occupant. However, a better inhaled air quality can still be achieved in contrast to the co-occupant's exposure with sole DV system because of the diminished horizontal dispersion of exhaled droplets by the PV system employed by the infected person.



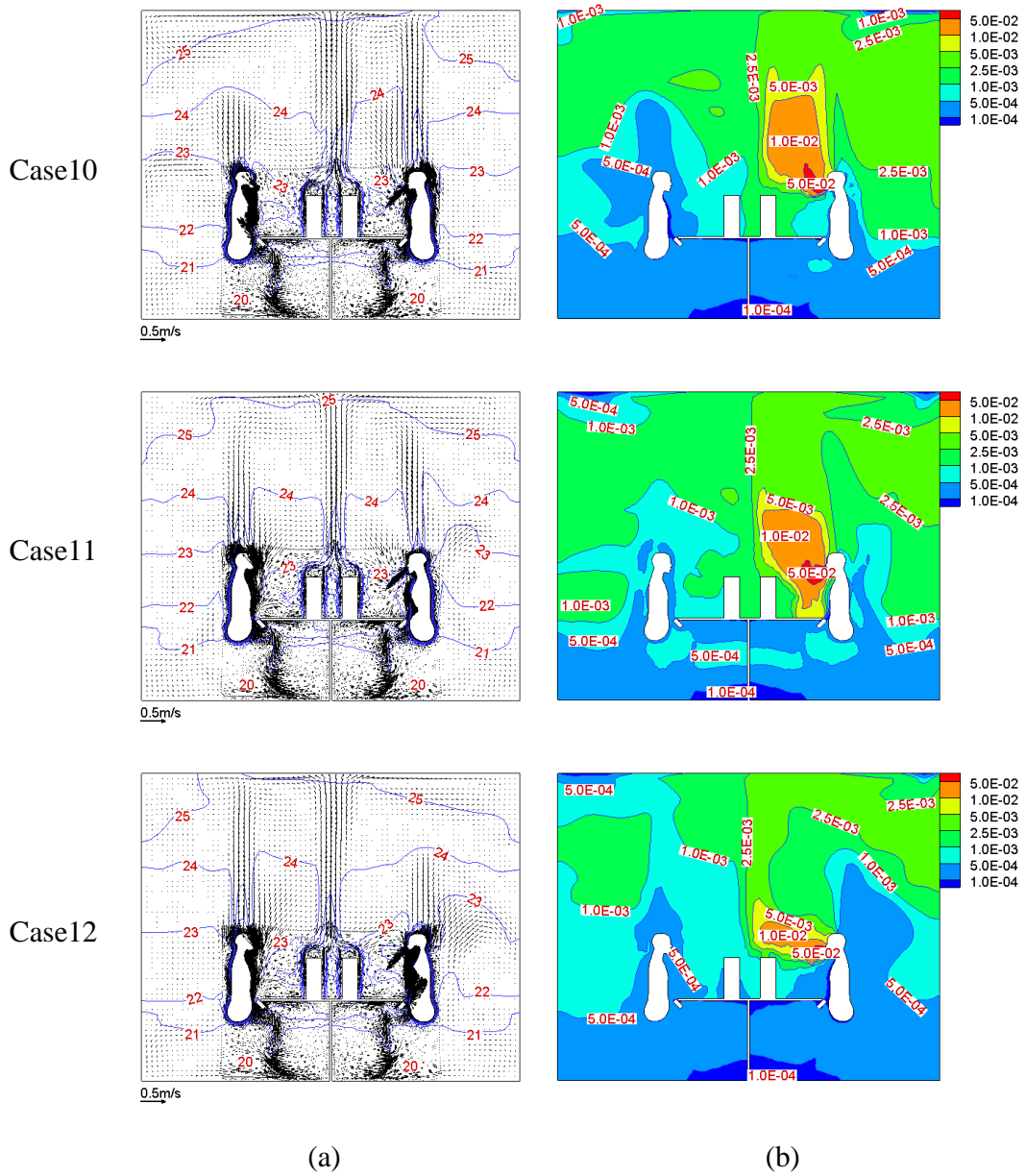


Figure 6.4 Temperature contour and velocity vector (a), and concentration distribution profiles of 10  $\mu\text{m}$  droplets (b) at the vertical plane of  $X = 0.65$  m under DV when using the desk-mounted PV (The droplet concentration in the exhaled air is denoted as 1.0)

#### 6.4.2 Co-occupant's exposure

To compare the impacts of PV systems on the co-occupant's exposure, the inhaled fraction of the co-occupant is compared in Figure 6.5 when using the chair-based PV, and Figure 6.6 presents the co-occupant's exposure when the desk-mounted PV is adopted.

The co-occupant's inhalation increases with the droplet size under DV for all the cases with different PV airflow rates, which is consistent with the findings in Chapter 4. The reason is that the upward airflow of DV can move the exhaled smaller droplets upward and being extracted, and result in lower exposure for the co-occupant, while it may hamper the deposition of larger droplets and then lead to a relatively higher exposure. Furthermore, both PV systems present the same trends in decreasing the co-occupant's exposure because of their parallel airflow patterns to the DV system.

Delivering personalized fresh air to both the occupants can reduce the co-occupant's exposure apparently, especially when the chair-based PV is employed as shown in Figure 6.5 and Figure 6.6. The primary reason is that the PV served fresh air can dilute the concentration of exhaled droplets in the breathing zone of the co-occupant. With the increase of PV airflow rates, a further decrease of the co-occupant's exposure can be achieved by serving a stream of fresh air in higher velocity to penetrate the thermal plume around the human body. For the same PV supplied airflow rate to the co-occupant, a slightly higher exposure will be induced for all the droplets investigated if the infected person breathes directly without using the PV

system. Meanwhile, adopting PV system by the infected person alone can also result in an increasing exposure for the co-occupant when compared with the situation that both of them employ PV supplied fresh air. An interesting result is that a higher PV airflow rate for the infected person can always mitigate the co-occupant's exposure under DV. This might be for the reason that the airflow of these two investigated PV systems can enhance the upward-driven force of the thermal plume around the infected person to extract the exhaled pathogen-laden droplets.

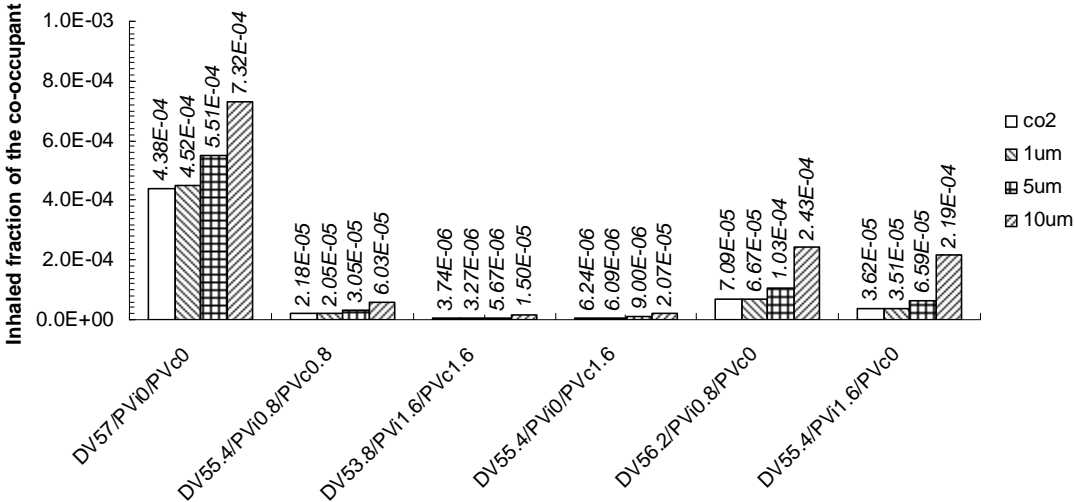


Figure 6.5 Inhaled fraction of the co-occupant under DV using chair-based PV

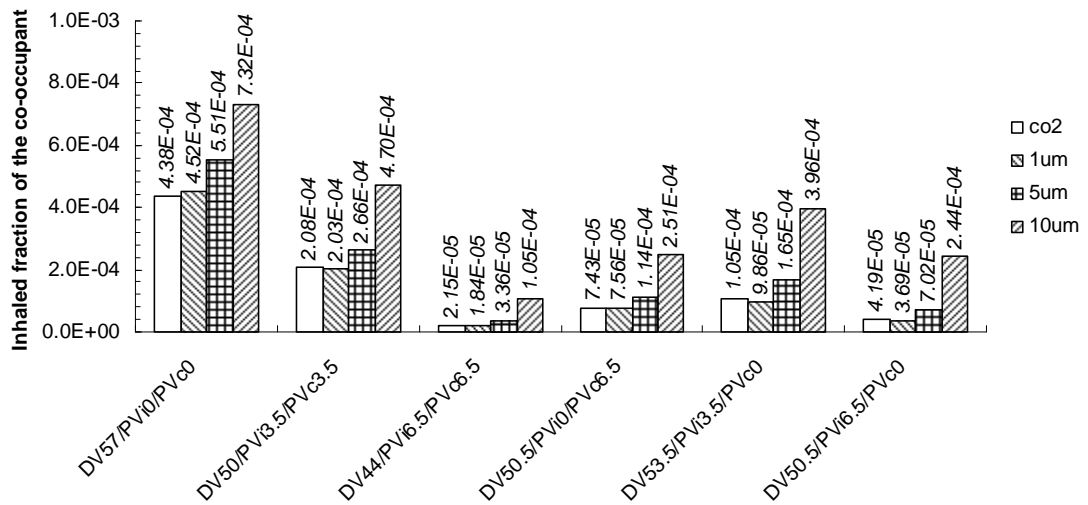


Figure 6.6 Inhaled fraction of the co-occupant under DV using desk-mounted PV

The performances of the two types of PV systems under DV show a cheering picture that the co-occupant's exposure can always be reduced by these complementary personalized air supplying devices even when the infected person alone employs the PV system. This conclusion is quite different from the findings of He et al. (2011) in which round movable panel mounted above the occupant's head level is used to deliver fresh air. Although researches found that exhaled air could travel a long distance under DV which might result in higher exposure when the co-occupant sited/stood close to the infected person (Nielsen et al. 2002; Qian et al. 2006), a lower exposure can still be achieved because the upward-driven airflow of DV can forward the exhaled air to a higher level and being extracted. For this reason, a head level mounted round movable panel with a transverse airflow to DV system may diminish the advantages of DV system and accelerate the mixing of exhaled air with room air in the breathing level. This will lead to a higher exposure for the co-

occupant when the infected person adopts PV system alone. The chair-based or desk-mounted PV, however, delivers an upward air flow which is in consistency with the main airflow patterns of DV and can preserve the positive effects of DV in extracting respiratory droplets effectively. This may explain the better performances of the investigated chair-based and desk-mounted PV systems than the head-level arranged movable panel device.

## **6.5 Co-occupant's exposure under MV when the chair-based or the desk-mounted PV is employed**

### **6.5.1 Droplet dispersion**

Figure 6.7 displays the concentration distribution of 10  $\mu\text{m}$  droplets at different PV supplied airflow rates under MV when the chair-based PV is employed, and the droplets distribution when using the desk-mounted PV is presented in Figure 6.8.

It can be observed that delivering PV fresh air to the co-occupant's breathing zone can definitely improve the inhaled air quality and reduce contaminant inhalation, because of the dilution of exhaled droplets in the micro-environment of the co-occupant. Compared with the situation with a sole MV system, no apparent differences on the contaminant distribution in the co-occupant's breathing zone can be observed when only the infected person adopts PV. This may be attributed to the reason that the well-mixed air movement of MV can quite evenly distribute the generated contaminants with no regards to their final location influenced by PV

devices, and the low airflow rate delivered by the chair-based PV can not exert much influence on the airflow rate supplied by MV.

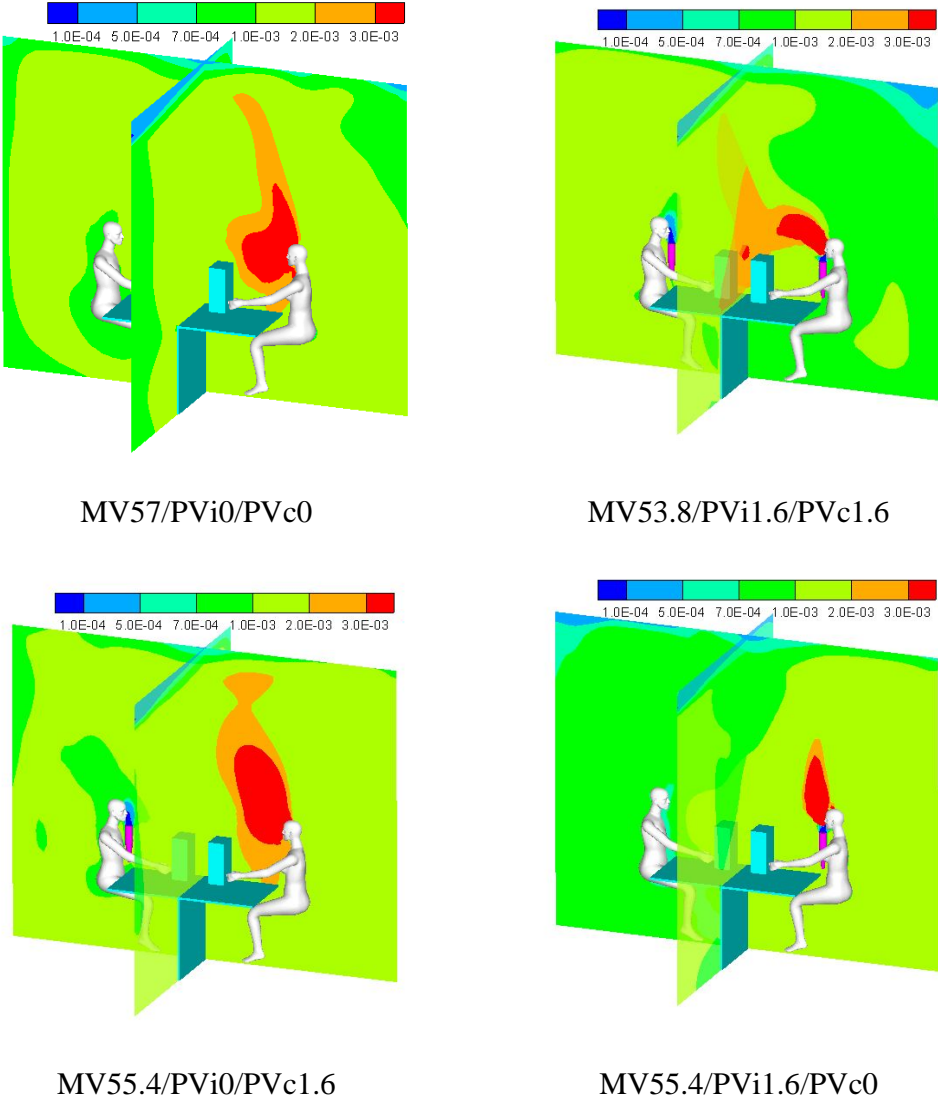
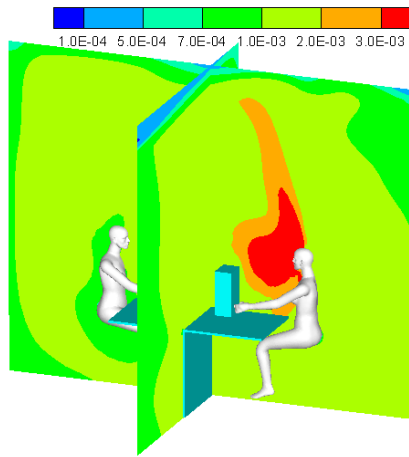
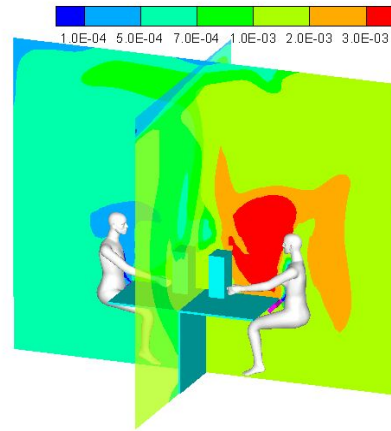


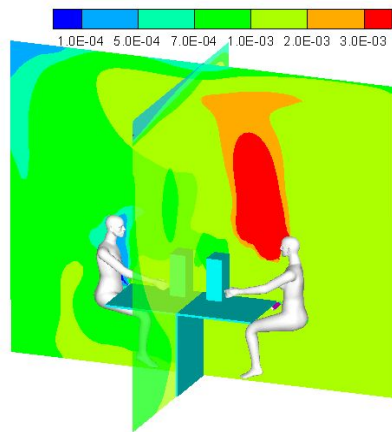
Figure 6.7 Concentration distribution profiles of 10 μm droplets under MV when using the chair-based PV (The droplet concentration in the exhaled air is denoted as 1.0)



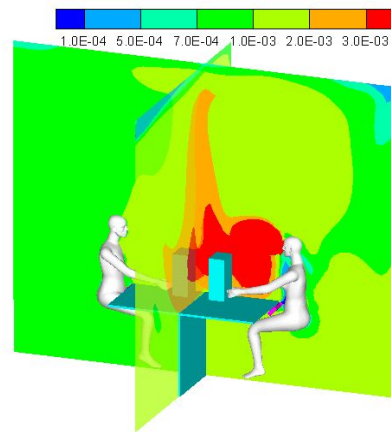
MV57/PVi0/PVc0



MV44/PVi6.5/PVc6.5



MV50.5/PVi0/PVc6.5



MV50.5/PVi6.5/PVc0

Figure 6.8 Concentration distribution profiles of 10  $\mu\text{m}$  droplets under MV when using the desk-mounted PV (The droplet concentration in the exhaled air is denoted as 1.0)

On the other hand, using the chair-based PV by the infected person alone can result in a much longer traveling distance of exhaled droplets, when compared with a sole

MV system. This can be explained by the decreased airflow rate delivered by MV which may slow down the dilution and dispersion of exhaled droplets in the occupied zone, and the higher temperature difference in the breathing level induced by the PV supplied air can facilitate the horizontal dispersion of the expelled droplets.

### **6.5.2 Co-occupant's exposure**

Figure 6.9 and Figure 6.10 present the co-occupant's inhaled fraction under MV using the chair-based and the desk-mounted PV, respectively. The co-occupant's inhalation decreases with the droplet size under MV for all the cases with different PV airflow rates, which is also in consistency with the findings in Chapter 4. The reason is that larger droplets with higher gravitational force preserve greater deposition rates in a well-mixed environment like MV, which may result in a lower inhaled fraction of the co-occupant for larger droplets. Just like their performances under DV, the two PV systems also present almost the same trends in the co-occupant's exposure.

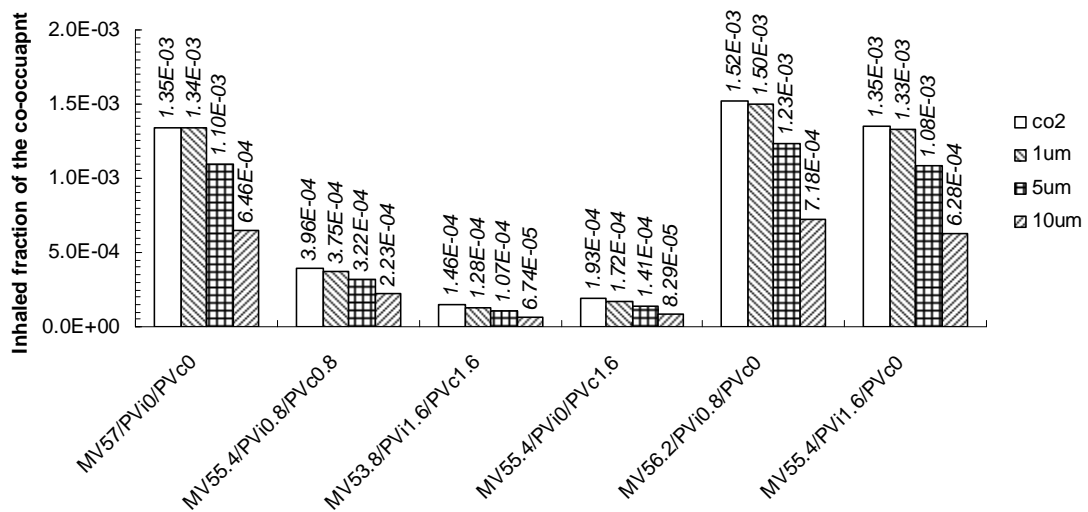


Figure 6.9 Inhaled fraction of the co-occupant under MV when using chair-based PV

Serving fresh air via PV systems to both occupants can reduce the co-occupant's exposure under MV since the PV supplied air can reach the co-occupant directly and dilute the contaminant concentration in the breathing zone. A further dilution can be achieved by a higher PV airflow rate to result in a better inhaled air quality for the co-occupant. For the same personalized airflow rate supplied to the co-occupant, almost the same inhaled fraction is resulted in no matter the infected person does or does not employ PV system. This may be attributed to the reason that a well-mixed environment of MV can largely promote the dispersion of exhaled droplets without obvious impact from the location of the pollutants. Unlike the co-occupant's exposure under DV, the inhaled fraction of respiratory droplets increases apparently if only the infected person employs PV system under MV. The inhaled air quality may be even worse than the situation when no PV system is used at all. The possible

reason is that the relatively smaller airflow rate supplied by MV system may decelerate the dilution of exhaled droplets in the occupied zone and induce higher exposure for the co-occupant correspondingly. The small differences between the two PV systems under MV are that the inhaled fraction increases with the personalized airflow rate served to the infected person if using the desk-based PV while decreases slightly if using the chair-based PV system when no fresh air is delivered to the co-occupant. This phenomenon may be related to their specific functions.

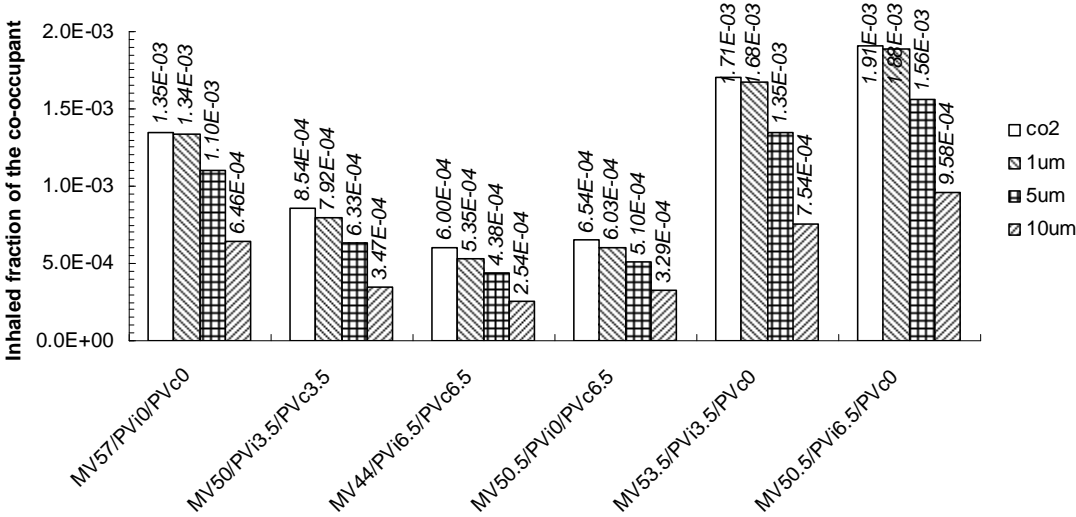


Figure 6.10 Inhaled fraction of the co-occupant under MV when using desk-mounted PV

The performances of the two PV systems under MV are quite in line with the findings of He et al. (2011). It might be concluded that, different from DV, the

designing of PV system under MV is more flexible since different types of PV systems may exhibit roughly the same exposure profiles for the co-occupant.

## **6.6 Summary**

This chapter investigates the performances of two types of PV systems with the conditioned air supplied in an upward direction in MV and DV ventilated environments under various possible PV use scenarios. It is found that better inhaled air quality for the co-occupant can always be ensured under different total ventilation systems as long as personalized fresh air is served directly to his/her breathing zone. Delivering PV fresh air to the infected person alone under MV may lead to slightly higher exposure than the inhalation with a sole total ventilation system. The co-occupant's exposure under DV, on the other hand, can always be reduced when either the infected person or the co-occupant employs the PV supplied fresh air, when compared with the co-occupant's inhalation under a sole DV system. PV systems which deliver fresh air in the same orientation with the main airflow of DV and the free convection airflow around the human body can always improve the inhaled air quality of the co-occupant even when only the infected person alone uses his/her PV. However, personalized air delivered in a transverse direction to the upward airflow of DV may enhance the mixing of the exhaled droplets with room air in the breathing level and then result in a higher exposure for the co-occupant. It can then be concluded that the PV outlet plays an important role on the reduction of infectious diseases transmission in DV ventilated

room, while the type of PV system has no apparent influences on the co-occupant's exposure under MV.

## **Chapter 7**

### **Conclusions**

#### **7.1 Conclusions**

The distributions of human respiratory droplets in office settings with the three commonly employed ventilation systems, namely MV, UFAD, and DV, are investigated experimentally and numerically, and co-occupant's exposure level is also evaluated in different scenarios. It is found that the personal exposure to coughed droplets can be separated as two stages, a first direct exposure stage and a second indirect exposure stage. Although the exposed concentration at the second stage is much lower, higher personal exposure can still be induced and more attentions should be paid on infection control in this area. It is also found that a lower personal exposure can be achieved generally by stratified ventilation system, especially DV, when direct exposure to the exhaled droplets can be avoided. As to PV system, the results demonstrate that the type of PV device preserves apparent influences on indoor infection transmission. More detailed descriptions of the conclusions are given as follows.

The experimental study in a full-scale DV ventilated room reveals that the heat load of a human body, breathing air temperature, and breathing mode all have apparent effects on the indoor dispersion of exhaled droplets and occupant's exposure. It is

therefore important to employ detailed manikins in the simulation zone when attention is paid on studying indoor infection transmission. For all the simulation work in this research, manikins with detailed geometries are used to fully and reasonably assess the dispersion of exhaled droplets and the co-occupant's exposure. Meanwhile, compared with nose-breathing process, it is found that mouth breathing of an infected person can impose a lower personal exposure for the co-occupant when the DV conditioned air is supplied from the region close to the infected person.

There are two distinctive stages of exposure in the whole airborne transmission process for the co-occupant when exposed directly to a cough, a first direct-exposure stage induced by the high momentum coughing jet and a second indirect-exposure stage caused by indoor air movement. Though the inhaled concentration at the second stage is about two to three orders of magnitude lower than that at the first stage, the inhaled dose during the second period can still pose a comparable health risk to the co-occupant. Therefore, more attentions should be paid on infection control in this stage.

The investigations on the effects of ventilation systems show that the personal exposure under stratified ventilation system, especially DV, is generally lower than MV due to its mainly upward air movement in driving the respiratory droplets upward and being extracted, when occupant's direct exposure to the exhaled air can be avoided. Using physical blockings, such as mouth covering and desk partition, can interrupt the horizontal transportation of exhaled contaminants to be transported

to the co-occupant's breathing zone directly. Turning the body around or bending the head down when coughing or sneezing can also protect the other occupant's from direct exposure to the exhaled droplets. These are all feasible measures in reducing the exposure level of indoor occupants. They can reduce not only the total inhaled dose during the whole exposure process for all the ventilation systems, but also the second stage indirect exposure for stratified ventilation system, especially for DV.

Even when the infected person breathes directly in a face-to-face orientation with the co-occupant, personal exposure can still be reduced as long as the co-occupant stands/sits at a distance farther than the travelling distance of the breathing airflow, no matter for a normal breathing process or a coughing process with high initial coughing velocity. However, it may be difficult for the susceptible person in ensuring a safe distance from the infected person in the real world, especially for coughing or sneezing activities with higher initial velocities. Physical blockings or the infected person's effective actions will be more reliable in the reduction of the co-occupant's exposure to the respiratory droplets.

What if the co-occupant turns around to avoid the direct exposure? The total inhaled dose at this condition can definitely be reduced when compared to a face-to-face orientation with the infected person. However, personal exposure during the second stage can not be decreased effectively since the breathing jet will bring the carried droplets to the region close to the co-occupant. Indoor air movement can quite easily

disperse these contaminants to the breathing zone and being inhaled. This action of the co-occupant may be useful for MV because its well-mixed air movement can induce almost the same personal exposure at the second stage no matter where the contaminants are released. However, personal exposure under DV will be quite different.

Since stratified ventilation can generally achieve lower exposure for the co-occupant, will the employment of PV system enhance the dispersion of exhaled contaminants and then increase the exposure level for the co-occupant? This research finds that the type of PV system plays an important role in infection control. PV device delivering conditioned air in an upward direction can enhance the effects of thermal plumes around human body in transporting the exhaled contaminants to the region above the breathing level. Personal exposure under DV can always be reduced either the PV supplied air is used by the infected person or the co-occupant, while slightly higher exposure may be induced for MV.

## **7.2 Limitations and future work**

It is found that DV can always provide a cleaner and healthier micro-environment for the co-occupant when the first-stage direct exposure is avoided. Although the upward air movement of UFAD can drive the exhaled droplets upward to reduce the co-occupant's exposure, which is the same as DV, higher personal exposure can be resulted in since its higher velocity of supply air may enhance the dispersion of respiratory droplets in the breathing level. Meanwhile, the relative positions of

occupants and the inlet diffuser may also preserve strong influences on the transportation of exhaled droplets and the co-occupant's exposure. Further investigations are therefore needed to study the effects of different types and arrangements of fresh air supplying diffuser on the indoor distribution of exhaled droplets and the corresponding exposure of the co-occupant.

The investigation of two types of PV system reveals that a better inhaled air quality can always be ensured under DV even when the infected person alone is using a PV system. Since other expiratory events with higher expelling velocities, including talking, coughing, and sneezing, can all generate pathogen-laden droplets, it will be important to evaluate the co-occupant's inhaled air quality under these scenarios in order to fully assess the applicability of PV systems in infection control.

Also, the whole studies are conducted in mechanically ventilated indoor environments. The relative humidity here is well controlled and mainly lies in the range of 40% to 60%. For a naturally ventilated room with higher humidity, however, the evaporation speed for exhaled droplets will be reduced and the equilibrium diameter will be increased. Droplets may have more chances to deposit onto indoor surfaces. But, the air movement for natural ventilation can not be well controlled. Besides indoor arrangements, personal exposure of occupants through airborne transmission may also be influenced by the openings on facades and outdoor environments. Detailed analysis should be conducted when evaluating occupant's exposure in a naturally ventilated room.

## References

Agah R, Cherry J D, Garakian A J, and Chapin M (1987) Respiratory syncytial virus (RSV) infection rate in personnel caring for children with RSV infections, Routine isolation procedure vs routine procedure supplemented by use of masks and goggles, *Am. J. Dis. Child*, 141: 695-697.

Aiello A E, Murray G F, Perez V, Coulborn R M, Davis B M, and Uddin M (2010) Mask use, hand hygiene, and seasonal influenza-like illness among young adults: a randomized intervention trial, *J. Infect. Dis.*, 201: 494-498

Akimoto T, Nobe, T, Tanabe S. and Kimura K (1999) Floor-supply displacement air-conditioning: laboratory experiments, *ASHRAE Transaction*, 105: 739-751.

Altman P L, and Dittmer D S (1971) *Respiration and Circulation*, Federation of American Societies for Experimental Biology, Bethesda, Maryland.

Araujo G A L, Freire R C S, Silva J F, Oliveira A, and Jaguaribe E F (2004) Breathing flow measurement with constant temperature hot-wire anemometer for forced oscillation technique, *Instrumentation and measurement technology conference, Italy*, 730-733.

ASHRAE (2001) *ASHRAE Handbook of Fundamentals*, American Society of Heating, Refrigerating and Air Conditioning Engineers, Atlanta.

Baldwin E D, Cournand A, and Richards D W (1948) Pulmonary insufficiency: I. Physiological classification, clinical methods of analysis, standard values in normal subjects, *Medicine (Baltimore)*, 27: 243-278.

Bean B, Moore B M, Sterner B, Peterson L R, Gerding D N, and Balfour H H (1982) Survival of influenza viruses on environmental surfaces, *J. Infect. Dis.*, 146: 47-51.

Behr M A, Warren S A, Salamon H, Hopewell P C, Ponce de L A, Daley C L, Small P M (1999) Transmission of *Mycobacterium tuberculosis* from patients smear-negative for acid-fast bacilli, *Lancet*, 353(9151): 444–449.

Bjorn E, and Nielsen P V (2002) Dispersal of exhaled air and personal exposure in displacement ventilated rooms, *Indoor Air*, 12: 147-164.

Bolashikov Z, Nikolaev L, Melikov A K, Kaczmarczyk J, and Fanger P O (2003) Personalized ventilation: air terminal devices with high efficiency, *Proceedings of Healthy Buildings 2003*, Singapore, 850-855.

Bonne S A, and Gerba C P (2007) Significance of fomites in the spread of respiratory and enteric viral disease, *Appl. Environ. Microbiol.*, 73: 1687-1696.

Brankston G, Gitterman L, Hirji Z, Lemieux C, Gardam M (2007) Transmission of influenza A in human beings, *Lancet Infect. Dis.*, 7: 257–265.

Brohus H, and Nielsen P V (1996) Personal exposure in displacement ventilated rooms, *Indoor Air*, 6: 157-167.

Caroline B H (2007) The spread of influenza and other respiratory viruses: complexities and conjectures, *Clin. Infect. Dis.*, 45: 353-359.

CDC (1996) Guidelines for Isolation Precautions in Hospitals Hospital Infection Control Advisory Committee, USA, U.S. Department of health and human services centers for disease control and prevention (CDC).

CDC (2003) Use of quarantine to prevent transmission of severe acute respiratory syndrome-Taiwan, USA, U.S. Department of health and human services centers for disease control and prevention (CDC).

CDC (2005) Guidelines for preventing the transmission of Mycobacterium tuberculosis in health-care Settings, USA, U.S. Department of health and human services centers for disease control and prevention (CDC).

CDC (2011) Smallpox disease Overview, Centers for Disease Control and Prevention.

<http://www.bt.cdc.gov/agent/smallpox/overview/disease-facts.asp>.

Cermak R, Melikov A K, Forejt L, and Kovar O (2006) Performance of personalized ventilation in conjunction with mixing and displacement ventilation, HVAC&R Research, 12:295-311.

Cermak R, and Melikov A K (2007) Protection of occupants from exhaled infectious agents and floor material emissions in rooms with personalized and underfloor ventilation, HVAC&R Research, 13:23-38.

Chao C Y H, and Wan M P (2004) Experimental study of ventilation performance and contaminant distribution of underfloor ventilation systems vs traditional ceiling-based ventilation system, Indoor Air, 14: 306-316.

Chao C Y H, Wan M P, Morawska L, Johnson G R, Ristovski Z D, Hargreaves M, Mengersen K, Corbett S, Li Y, Xie X, and Katoshevski D (2009) Characterization of expiration air jets and droplet size distributions immediately at the mouth opening, Aerosol Sci., 40: 122-133.

Chapin C V (1910) The sources and modes of infection, John Wiley, New York.

Cole E C, and Cook C E (1998) Characterization of infectious aerosols in health care facilities: An aid to effective engineering controls and preventive strategies, *Am. J. Infect. Control*, 26: 453–464.

Collins F M (1971) Relative susceptibility of acid-fast and non-acid-fast bacteria to ultraviolet light, *Appl. Microbiol.*, 21: 411-413.

Cox C S (1987) *The aerobiological pathway of microorganisms*, John Wiley & Sons, Chichester (UK).

Del Valle S Y, Tellier R, Settles G S, and Tang J W (2010) Can we reduce the spread of influenza in schools with face masks? *AJIC*, 38: 676-677.

Dubochet J, Adrian M, Richter K, Garces J, and Wittek R (1994) Structure of intracellular mature vaccinia virus observed by cryoelectron microscopy, *J. Virol.*, 68: 1935–1941.

Duguid J F (1945) The numbers and the sites of origin of the droplets expelled during expiratory activities, *Edinburg Med. J.*, 52: 385–390.

Duguid J F (1946) The size and the duration of air-carriage of respiratory droplets and droplet-nuclei, *J. Hyg.*, 4: 471-480.

Edwards D A, Man J C, Brand P, Katstra J P, Sommerer K, Stone H A, Nardell E, and Scheuch G (2004) Inhaling to mitigate exhaled bioaerosols, *PNAS*, 101: 17383-17388.

Effros R M, Wahlen K, Bosbous M, Castillo D, Foss B, Dunnin M, Gare M, Lin W, and Sun F (2002) Dilution of respiratory solutes in exhaled condensates, *Am. J. Resp. Crit. Care. Med.*, 165: 663-669.

Fairchild C I, and Stamper J F (1987) Particle concentration in exhaled breath, *Am. Ind. Hyg. Assoc. J.*, 48: 948 - 949.

Faulkner D, Fisk W J, Sullivan D P, and Wyon D P (1999) Ventilation efficiency of desk-mounted task/ambient conditioning systems, *Indoor Air*, 9: 273-281.

Fennelly K P, Martyny J W, Fulton K E, Orme I M, Cave D M, and Heifets L B (2004) Cough-generated aerosols of *Mycobacterium tuberculosis*: a new method to study infectiousness, *Am. J. Resp. Crit. Care Med.*, 169: 604-609.

Fiegel J, Clarke R, and Edwards D A (2006) Airborne infectious disease and the suppression of pulmonary bioaerosols, *DDT*, 11: 51-57.

Friberg B, Friberg S, Burman L G, Lundholm R, Östensson R (1996) Inefficiency of upward displacement operating theatre ventilation. *J. Hosp. Infect.*, 33:263-272.

Garner J S (1996) Guideline for isolation precautions in hospitals, *Am. J. Infect. Control*, 24: 24-52.

Gao N P, and Niu J L (2007) Modeling particle dispersion and deposition in indoor environments, *Atmos. Environ.*, 41: 3862-3876.

Gao N P, and Niu J L (2008) Personalized ventilation for commercial aircraft cabins, *J. Aircraft*, 45: 508-512.

Gao N P, Niu J L, and Morawska L (2008) Distribution of respiratory droplets in enclosed environments under different air distribution methods, *Build. Simulation*, 1: 326-335.

Gao N P, He Q B, and Niu J L (2012) Numerical study of the lock-up phenomenon of human exhaled droplets under a displacement ventilated room, *Build. Simulation*, 5: 51-60.

Griese M, Noss J, and Bredow C (2002) Protein pattern of exhaled breath condensate and saliva, *Protemics*, 2: 690-699.

Griese G (2004) Exhaled breath condensate, *Pediatr. Pulm.*, 37: 14-15.

Grivel F, and Candas V (1991) Ambient temperatures preferred by young European males and females at rest, *Ergon.*, 34: 365 - 378.

Gupta J K, Lin C H, and Chen Q Y (2009) Flow dynamics and characterization of a cough, *Indoor Air*, 19: 517-525.

Gupta J K, Lin C H, and Chen Q Y (2010) Characterizing exhaled airflow from breathing and talking, *Indoor Air*, 20: 31-39.

Hall C B, Geiman J M, Douglas R G (1980) Possible transmission by fomites of respiratory syncytial virus, *J. Infect. Dis.*, 141: 98-102.

Hall C B (2007) The spread of influenza and other respiratory viruses: complexities and conjectures, *Clin. Infect. Dis.*, 45: 353-359.

Handbook of Physiology (1986) Mechanics and breathing, American Physiology Society, Bethesda, Maryland.

Harper G J (1961) Airborne micro-organisms: survival tests with four viruses, *J. Hyg. Camb.*, 59: 479-486.

Hickey A J (1996) Inhalation aerosols: physical and biological basis for therapy,

Lung biology in health and disease, Marcel Dekker Inc.

Hillerbrant B, and Ljungqvist B (1990) Comparison between three air distribution systems for operating rooms, *Swiss Contamination Control*, 4a: 336-339.

Hiwatashi K, Akabayashi S, Morikawa Y, and Sakaguchi J (2000) Numerical study of a new ventilation tower system for fresh air supply in an air conditioned room, *Proceedings of ROOMVENT2000*, UK, 1: 565-570.

Höppe P (1981) Temperatures of expired air under varying climatic conditions, *Int. J. Biometeor*, 25: 127-132.

Huang D Y (1977) *Physical diagnostics*, China Commerce Publishing Co., China.

IESNA (2000) *The IESNA lighting handbook—reference and application*, Illuminating Engineering Society of North America, New York.

Ijaz M K, Brunner A H, Sattar S A, Nair R C, and Lussenburg C M (1985) Survival characteristics of airborne human coronavirus 229E, *J. Gen. Virol.*, 66: 2743-2748.

ISO (2007) *Space Environment (Natural and Artificial) Process for Determining Solar 17 Irradiances*, International standard 21348.

James C (2001) *Control of communicable disease manual*, American Public Health Association.

Jefferson T, Del Mar C, Dooley L, Ferroni E, Al-Ansary L A, Bawazeer G A, Driel M L, Foxlee R, and Rivetti A (2009) Physical interventions to interrupt or reduce the spread of respiratory viruses: systematic review, *BMJ*, 339: b3675.

Jenkins P L, Philips T J, Mulberg E J, and Hui S P (1992) Activity patterns of

Californians: Use of and proximity to indoor pollutant sources, *Atmos. Environ.*, 26A: 2141-2148.

Jennison M W (1942a) The dynamics of sneezing - studies by high-speed photography, *Scientific Monthly*, 52: 24-33.

Jeong K (2003) Thermal characteristics of a partition air supply system at a personal task area, *Proceedings of Healthy Buildings 2003*, Singapore, 86-91.

Jeremy H, Norman B, Julius W, Iain B, Ralf R (2001) *Communicable disease control handbook*, Blackwell publishing, USA.

Kethley T W, and Branch K (1972) Ultraviolet lamps for room air disinfection - Effect of sampling location and particle size of bacterial aerosol, *Arc. Environ. Health*, 25:205-14.

Kitamura T, Satomura K, Kawamura T, Yamada S, Takashima K, and Suganuma N (2007) Can we prevent influenza – like illness by gargling? *Intern. Med.*, 46: 1623-1624.

Klepeis N E, Neilson W C, Ott W R, Robison J P, Tsang A M, Switzer P, Behar J V, Hern S C, and Englemann W H (2001) The national human activity pattern survey (NHAPS): a resource for assessing exposure to environmental pollutants, *J. Exp. Sci. Environ. Epidemiol.*, 11: 231-252.

Ko G, First M W, and Burge H A (2000) Influence of relative humidity on particle size and UV sensitivity of *Serratia marcescens* and *Mycobacterium bovis* BCG aerosols, *Tubercle Lung Dis.*, 80:217-28.

Ko G, First MW, Burge H A (2002) The characterization of upper-room ultraviolet germicidal irradiation in inactivating airborne microorganisms, *Environ. Health*

Persp., 110:95–101.

Kobayashi N, and Chen Q (2008) Floor-supply displacement ventilation in a small office, *Indoor Built Environ.*, 12: 281-291.

Li X P, Niu J L, and Gao N P (2011) Spatial distribution of human respiratory droplet residuals and exposure risk for the co-occupant under different ventilation methods, *HVAC&R Research*, 17: 432-445.

Li Y, Leung G M, Tang J W, Yang X, Chao C Y H, Lin J Z, Lu J W, Nielsen P V, Niu J L, Qian H, Sleigh A C, Su H J J, Sundell J, Wong T W, and Yuen P L (2007) Role of ventilation in airborne transmission of infectious agents in the built environment – a multidisciplinary systematic review, *Indoor Air*, 17: 2-18.

Loudon R G, and Roberts R M (1967) Droplet expulsion from the respiratory tract, *Am. Rev. Resp. Dis.*, 95: 435 - 442.

Manolis A (1983) The diagnostic potential of breath analysis, *Clin. Chem.*, 29: 5–15.

Mathi B, Fieland V P, Walter M, and Seidler R J (1990) Survival of bacteria during aerosolization, *Appl. Environ. Microb.*, 56: 3463-3467.

Matsunawa K, Iizuka H, and Tanabe S (1995) Development and application of an underfloor air-conditioning system with improved outlets for a “smart” building in Tokyo, *ASHRAE Transaction*, 101: 2053-2067.

Melikov A K, Arakelian R S, Halkjaer L, and Fanger P O (1994) Spot cooling – part 2: Recommendations for design of spot cooling systems, *ASHRAE Transactions*, 100: 500 - 510.

Melikov A K, Cermak R, and Mayer M (2002) Personalized ventilation: Evaluation

of different air terminal devices, *Energ. Buildings*, 34: 829 - 836.

Melikov A K, Cermak R, Kovar O, and Forejt L (2003) Impact of airflow interaction on inhaled air quality and transport of contaminant in rooms with personalised and total volume ventilation, *Proceedings of Healthy Building 2003*, Singapore, 2: 592 - 597.

Melikov A K (2004) Personalized ventilation, *Indoor Air*, 14: 157-167.

Melikov A K, Pitchurov G, Naydenov K, and Langkilde G (2004) Field study on occupant comfort and the office thermal environment in rooms with displacement ventilation, *Indoor Air*, 15:205-214.

Miller S, and Artenstein M S (1967) Aerosol stability of three acute respiratory disease viruses, *Proc. Soc. Exp. Biol. Med.*, 125: 222-227.

Miller S L, and Macher J M (2000) Evaluation of a methodology for quantifying the effect of room air ultraviolet germicidal irradiation on airborne bacteria, *Aerosol Sci. Tech.*, 33:274-295.

Naydenov K, Pitchurov G, Langkilde G, and Melikov A (2002) Performance of displacement ventilation in practice, *Proceedings of Roomvent 2002*, Copenhagen, Denmark and DANVAK, 483-486.

Nicas M, Nazaroff W W, and Hubbard A (2005) Toward understanding the risk of secondary airborne infection: emission of respirable pathogens, *J. Occup. Environ. Hyg.*, 2: 143-154.

Nicholls J M, Chan R W, Russell R J, Air G M, and Peiris J S (2008) Evolving complexities of influenza virus and its receptors, *Trends Microbiol.*, 16: 149-157.

Nielsen P V, Winther F V, Buus M, and Thilageswaran M (2008) Contaminant flow in the microenvironment between people under different ventilation conditions, *ASHRAE Transaction*, 114: 632-638.

Niu J L (2005) Indoor ventilation system with personalized ventilation device and its method of usage, United States Patent No.: US6, 910, 921B2 (Application No. 10/664,317, filed Sept.17, 2003).

Nobe T, Tanabe S, and Tomioka Y (2003) Task AC unit operating rate prediction in office, *Proceedings of Healthy Buildings 2003, Singapore*, 725-730.

Olmedo I, Nielsen P V, Ruiz de Adana M, Jensen R L, and Grzelecki P (2012) Distribution of exhaled contaminants and personal exposure in a room using three different air distribution strategies, *INDOOR AIR*, 22: 64-76.

Pantelic J, Sze-To G N, Tham K W, Chao C Y H, and Khoo Y C M (2009) Personalized ventilation as a control measure for airborne transmissible disease spread, *J. R. Soc. Interface*, 6: S715-S726.

Papinen R S, and Rosenthal F S (1997) The size distribution of droplets in the exhaled breath of healthy human subjects, *J. Aerosol Med.*, 10: 105-116.

Peccia J, Werth H M, Miller S, and Hernandez M (2001) Effects of relative humidity on the ultraviolet induced inactivation of airborne bacteria, *Aerosol Sci. Tech.*, 35:728-740.

Poutanen S M, Low D E, and Henry B (2003) Identification of severe acute respiratory syndrome in Canada, *N. Engl. J. Med.*, 348: 1995-2005.

Qian H, Li Y, Nielsen P V, Hyldgaard C E, Wong T W, and Chwang A T Y (2006) Dispersion of exhaled droplets nuclei in a two-bed hospital ward with three different

ventilation systems, *Indoor Air*, 16:111-128.

Qian H, Li Y, Nielsen P V, and Hyldgaard C E (2008) Dispersion of exhalation pollutants in a two-bed hospital ward with a downward ventilation system, *Build. Environ.*, 43: 344-354.

Qian H, and Li Y (2010) Removal of exhaled particles by ventilation and deposition in a multi-bed airborne infection isolation room, *Indoor Air*, 20:284-297.

Qu J M, Dun Z, Li Q, Qin A L, Zeng G (2003) Efficiency of the quarantine system during the epidemic of severe acute respiratory syndrome in Beijing, *Chinese J. Epidemiol.*, 24: 1093-1095.

Riley R L, and O'Grady F (1961) *Airborne infection: transmission and control*, MacMillan, New York.

Riley R L, and Permutt S (1971) Room air disinfection by ultraviolet irradiation of upper air - Air mixing and germicidal effectiveness. *Arch. Environ. Health*, 22: 208-219.

Riley R L, and Kaufman J E (1971) Air disinfection in corridors by upper air irradiation with ultraviolet, *Arch. Environ. Health*, 22: 551-553.

Riley R L, and Kaufman J E (1972) Effect of relative humidity on the inactivation of airborne *Serratia marcescens* by ultraviolet radiation, *Appl. Microbiol.*, 23: 1113-1120.

Riley R L, Knight M, and Middlebrook G (1976) Ultraviolet susceptibility of BCG and virulent tubercle bacilli, *Am. Rev. Respir. Dis.*, 113: 413-418.

Robinson J, and Nelson W C (1995) National human activity pattern survey data

base, USEPA, Research Triangle Park, NC.

Robinson S (1938) Experimental studies of physical fitness in relation to age, *Eur. J. Appl. Physiol.*,10: 251-323.

Satomura K, Kitamura T, Kawamura T, Shimbo T, Watanabe M, and Kamei M (2005) Prevention of upper respiratory tract infections by gargling: a randomized trial, *Am. J. Prev. Med.*, 29: 302-307.

Sattar S A, and Iljaz M K (1987) Spread of viral infections by aerosols, *Crit. Rev. Env. Contr.*, 17: 89-131.

Sattar S A, Springthorpe V S, Tetro J, Vashon R, and Keswick B (2002) Hygienic hand antiseptics: should they not have activity and label claims against viruses? *Am. J. Infect. Control*, 30: 355-372.

Shaffer F L, Soergel M E, and Straube D C (1976) Survival of airborne influenza virus: effects of propagating host, relative humidity and composition of spray fluids, *Arch. Virol.*, 51: 263-273.

Sharp D G (1937) A Quantitative Method of Determining the Lethal Effect of Ultraviolet Light on Bacteria Suspended in Air, *Journal of Bacteriology* provided courtesy of American Society for Microbiology (ASM), 589-599.

Shinya K, Ebina M, Yamada S, Ono M, Kasai N, and Kawaoka Y (2006) Avian flu: influenza virus receptors in the human airway, *Nature*, 440: 435-436.

Spengler J D, and Sexton K (1983) Indoor Air Pollution: A Public Health Perspective, *Science*, 221: 9-17.

Tang J W, Liebner T J, Craven B A, and Settles G S (2009) A Schlieren optical

study of the human cough with and without wearing masks for aerosol infection control, *J. R. Soc. Interface*, 6: S727-S736.

Tellier R (2006) Review of aerosol transmission of influenza A virus, *Emerging Infect. Dis.*, 12: 1657-1662.

Thiel V (2007) *Coronaviruses: Molecular and Cellular Biology*, Caister Academic Press, ISBN.

Thomas Y, Vogel G, Wunderli W, Suter P, Witschi M, and Koch D (2008) Survival of influenza virus on banknotes, *Appl. Environ. Microbiol.*, 74: 3002-3007.

Twu S J, Chen T J, and Chen C J (2003) Control measures for severe acute respiratory syndrome (SARS) in Taiwan, *Emerg. Infect. Dis.*, 9: 718-720.

van Riel D, Munster V J, and de Wit E (2006) H5N1 Virus Attachment to Lower Respiratory Tract, *Science*, 312: 399.

van Riel D, Munster VJ, and de Wit E (2007) Human and avian influenza viruses target different cells in the lower respiratory tract of humans and other mammals, *Am. J. Pathol.*, 171: 1215-1223.

Weber T P, and Stilianakis N I (2008) Inactivation of influenza A viruses in the environment and modes of transmission: a critical review, *J. Infect.*, 57: 361-373.

Weber T P, and Stilianakis N I (2009) Inactivation of influenza A viruses in the environment and modes of transmission: A critical review, *J. infect.*, 57: 361-373.

Wells W F, and Brown H W (1936) Recovery of influenza virus suspended in air and its destruction by ultraviolet radiation, *Am. J. Hyg.*, 24:407-413.

Wells W F (1934) On air-borne infection Study II: Droplets and droplet nuclei, *Am. J. Hyg.*, 20: 611-618.

WHO (2009) Pandemic influenza preparedness and response: a WHO guidance document, Geneva.

Wood M J (2000), History of Varicella Zoster Virus. *Herpes*, 7: 60–65.

Xie X, Li Y, Chwang A T Y, Ho P L, and Seto W H (2007) How far droplets can move in indoor environments - revisiting the Wells evaporation - falling curve, *Indoor Air*, 17: 211-225.

Yang J H, Kato S, and Chikamoto T (2004) Air flow measurement around human body with wide-cover personal air conditioning, Proceedings of ROOMVENT 2004, Coimbra, Portugal.

Yang S, Lee G W M, Chen C M, Wu C C, and Yu K P (2007) The size and concentration of droplets generated by coughing in human subjects, *J. Aerosol Med.*, 20: 484-494.

Yin Y, Xu W, Gupta J K, Guity A, Marmion P, Manning A, Gulick B, Zhang X, and Chen Q (2009) Experimental study on displacement and mixing ventilation systems for a patient ward, *HVAC&R Research*, 15:1175-1191.

Yu I T S, Li Y, and Wong T W (2004) Evidence of airborne transmission of the severe acute respiratory syndrome virus, *N. Engl. J. Med.*, 350: 1731-1739.

Zentner R J (1966) Physical and chemical stresses of aerosolization, *Bacteriological Reviews*, 30: 551-557.

Zhu S W, Kato S, and Yang J H (2006) Study on transport characteristics of saliva

droplets produced by coughing in a calm indoor environment, *Build. Environ.*, 41: 1691-1702.